

ACCURACY OF ORIGINAL GAS IN PLACE ESTIMATION BY MATERIAL BALANCE IN RADIAL
WATER-DRIVE DRY-GAS RESERVOIRS

Miss Chonlada Jungjaroensin



จุฬาลงกรณ์มหาวิทยาลัย

CHULALONGKORN UNIVERSITY

บทคัดย่อและแฟ้มข้อมูลฉบับเต็มของวิทยานิพนธ์ตั้งแต่ปีการศึกษา 2554 ที่ให้บริการในคลังปัญญาจุฬาฯ (CUIR)
เป็นแฟ้มข้อมูลของนิสิตเจ้าของวิทยานิพนธ์ ที่ส่งผ่านทางบัณฑิตวิทยาลัย

The abstract and full text of theses from the academic year 2011 in Chulalongkorn University Intellectual Repository (CUIR)
are the thesis authors' files submitted through the University Graduate School.

A Thesis Submitted in Partial Fulfillment of the Requirements
for the Degree of Master of Engineering Program in Petroleum Engineering
Department of Mining and Petroleum Engineering
Faculty of Engineering
Chulalongkorn University
Academic Year 2014

Copyright of Chulalongkorn University

ความแม่นยำของการประมาณปริมาณก๊าซเริ่มแรกด้วยสมการสมดุลมวลสารในแหล่งกักเก็บก๊าซที่มี
ชั้นน้ำโอบล้อม



วิทยานิพนธ์นี้เป็นส่วนหนึ่งของการศึกษาตามหลักสูตรปริญญาวิศวกรรมศาสตรมหาบัณฑิต

สาขาวิชาวิศวกรรมปิโตรเลียม ภาควิชาวิศวกรรมเหมืองแร่และปิโตรเลียม

คณะวิศวกรรมศาสตร์ จุฬาลงกรณ์มหาวิทยาลัย

ปีการศึกษา 2557

ลิขสิทธิ์ของจุฬาลงกรณ์มหาวิทยาลัย

Thesis Title	ACCURACY OF ORIGINAL GAS IN PLACE ESTIMATION BY MATERIAL BALANCE IN RADIAL WATER-DRIVE DRY-GAS RESERVOIRS
By	Miss Chonlada Jungjaroensin
Field of Study	Petroleum Engineering
Thesis Advisor	Assistant Professor Suwat Athichanagorn, Ph.D.

Accepted by the Faculty of Engineering, Chulalongkorn University in Partial
Fulfillment of the Requirements for the Master's Degree

.....Dean of the Faculty of Engineering
(Professor Bundhit Eua-arporn, Ph.D.)

THESIS COMMITTEE

.....Chairman
(Assistant Professor Jirawat Chewaroungroaj, Ph.D.)

.....Thesis Advisor
(Assistant Professor Suwat Athichanagorn, Ph.D.)

.....Examiner
(Falan Srisuriyachai, Ph.D.)

.....External Examiner
(Dalad Nattwongasem, Ph.D.)

ชลดดา จิ่งเจริญคิลป์ : ความแม่นยำของการประมาณปริมาณก๊าซเริ่มแรกด้วยสมการสมดุลมวลสารในแหล่งกักเก็บก๊าซที่มีชั้นน้ำโอบล้อม (ACCURACY OF ORIGINAL GAS IN PLACE ESTIMATION BY MATERIAL BALANCE IN RADIAL WATER-DRIVE DRY-GAS RESERVOIRS) อ.ที่ปรึกษาวิทยานิพนธ์หลัก: ผศ. ดร.สุวัฒน์ อธิษนากร, 282 หน้า.

หนึ่งในวิธีการคำนวณค่าก๊าซเริ่มแรกของแหล่งกักเก็บก๊าซที่ขับเคลื่อนด้วยน้ำที่ใช้กันอย่างแพร่หลายคือวิธีการสมดุลมวลสาร โดยการสร้างกราฟระหว่าง $(G_p B_g + W_p B_w) / (B_g - B_{gi})$ กับ $W_e / (B_g - B_{gi})$ สำหรับแหล่งกักเก็บก๊าซที่ขับเคลื่อนด้วยน้ำ หรือ กราฟความสัมพันธ์ระหว่าง p/z กับ G_p ซึ่งใช้สำหรับแหล่งกักเก็บก๊าซที่ขับเคลื่อนด้วยแรงดันก๊าซ เนื่องจากวิธีสมดุลมวลสารอ้างอิงสมมติฐานที่ว่า คุณสมบัติต่างๆของแหล่งกักเก็บและของไหลในแหล่งกักเก็บนั้นเท่ากันหมดโดยทั่วแหล่งกักเก็บ จึงทำให้เกิดความคลาดเคลื่อนในการคำนวณค่าก๊าซเริ่มแรกได้

เพื่อที่จะศึกษาผลของความซึมผ่าน ขนาดของแหล่งกักเก็บน้ำ ระยะเวลาในการปิดหลุมผลิต และปริมาณข้อมูลการผลิต ที่มีต่อความแม่นยำในการคำนวณค่าก๊าซเริ่มแรกด้วยวิธีการสมดุลมวลสารนั้น แบบจำลองแหล่งกักเก็บก๊าซได้ถูกสร้างขึ้น ข้อมูลการผลิตที่ได้จากแบบจำลองนี้จะถูกนำไปใช้สร้างกราฟความสัมพันธ์ทั้งสองแบบของวิธีการสมดุลมวลสาร โดยจะมีการประยุกต์แบบจำลองแหล่งกักเก็บน้ำทั้งสี่แบบเข้ามาใช้ได้แก่ แบบจำลอง simple aquifer, Fetkovich, van Everdingen & Hurst และ Carter & Tracy

จากผลการศึกษาพบว่ากราฟความสัมพันธ์ระหว่าง p/z กับ G_p จะมีความแม่นยำก็ต่อเมื่อขนาดของแหล่งกักเก็บน้ำไม่ใหญ่เกินสิบเท่าของแหล่งกักเก็บก๊าซ กราฟความสัมพันธ์ระหว่าง $(G_p B_g + W_p B_w) / (B_g - B_{gi})$ กับ $W_e / (B_g - B_{gi})$ หากประยุกต์ใช้กับระยะเวลาในการปิดหลุมผลิตและแบบจำลองแหล่งกักเก็บน้ำที่เหมาะสมจะมีความแม่นยำไปจนถึงกรณีที่แหล่งกักเก็บน้ำมีขนาดเป็นหนึ่งร้อยเท่าของแหล่งกักเก็บก๊าซ ความคลาดเคลื่อนจะเพิ่มขึ้นหากขนาดของแหล่งกักเก็บน้ำเพิ่มขึ้น แต่จะลดลงหากความซึมผ่านเพิ่มขึ้น เมื่อระยะเวลาในการปิดหลุมผลิตเพิ่มขึ้นความคลาดเคลื่อนในแหล่งกักเก็บก๊าซที่มีความซึมผ่านน้อยจะลดลง แต่ความคลาดเคลื่อนในแหล่งกักเก็บก๊าซที่มีความซึมผ่านมากจะไม่เปลี่ยนแปลง เรายังสามารถคำนวณค่าก๊าซเริ่มแรกได้อย่างแม่นยำในกรณีที่ไม่ทราบขนาดของแหล่งกักเก็บน้ำถ้าขนาดจริงของแหล่งกักเก็บน้ำไม่ใหญ่เกินสามสิบเท่าของขนาดแหล่งกักเก็บก๊าซสำหรับแหล่งกักเก็บก๊าซที่มีความซึมผ่านน้อยและไม่ใหญ่เกินหนึ่งร้อยเท่าของขนาดแหล่งกักเก็บก๊าซสำหรับแหล่งกักเก็บก๊าซที่มีความซึมผ่านมาก

ภาควิชา วิศวกรรมเหมืองแร่และปิโตรเลียม ลายมือชื่อนิสิต

สาขาวิชา วิศวกรรมปิโตรเลียม ลายมือชื่อ อ.ที่ปรึกษาหลัก

ปีการศึกษา 2557

5471202921 : MAJOR PETROLEUM ENGINEERING

KEYWORDS: WATER-DRIVE DRY-GAS RESERVOIR / OGIP ESTIMATION / MATERIAL BALANCE

CHONLADA JUNGJAROENSIN: ACCURACY OF ORIGINAL GAS IN PLACE ESTIMATION BY MATERIAL BALANCE IN RADIAL WATER-DRIVE DRY-GAS RESERVOIRS. ADVISOR: ASST. PROF. SUWAT ATHICHANAGORN, Ph.D., 282 pp.

One of the commonly used methods to estimate the original gas in place (OGIP) for water-drive dry-gas reservoirs is the material balance method, the $(G_p B_g + W_p B_w) / (B_g - B_{gi})$ versus $W_e / (B_g - B_{gi})$ plot (water-drive form) or the p/z versus G_p plot (depletion-drive form). Due to tank assumption of material balance, this method can lead to some errors of the estimation under certain circumstances.

In order to investigate the error of estimated OGIP from these plots for cases having different permeability, aquifer sizes, shut-in durations, and amounts of historical data, a hypothetical dry-gas reservoir was created in a reservoir simulator. Production data from the simulation were used to make plots in order to determine OGIPs using four different water influx models, namely, simple aquifer model, Fetkovich, van Everdingen & Hurst, and Carter & Tracy.

Results from this study show that p/z versus G_p plot with enough amount of historical data is still applicable if aquifer size is not larger than 10 PV. The $(G_p B_g + W_p B_w) / (B_g - B_{gi})$ versus $W_e / (B_g - B_{gi})$ plot with proper shut-in durations and water influx models is applicable for aquifer size up to 100 PV. The error increases when the aquifer size increases but decreases when the permeability increases. When shut-in duration increases, the errors in 50 mD cases decrease but the errors in 500 mD cases are not affected. If the aquifer size is unknown, OGIP can still be accurately estimated if the actual aquifer size is not larger than 30 PV in 50 mD cases and 100 PV in 500 mD cases.

Department: Mining and Petroleum Engineering Student's Signature

Advisor's Signature

Field of Study: Petroleum Engineering

Academic Year: 2014

ACKNOWLEDGEMENTS

First of all, I would like to thank Assistant Professor Dr. Suwat Athichanagorn, my thesis advisor, for guiding me technical knowledge.

I would like to thank my thesis committees for their valuable advice.

I would like to thank Mr. Danes Vesjaroon, my supervisor during 2009-2011, for encouraging me to join this Master degree program and helping me with the Chevron scholarship.

I would like to thank Mr. Minh Vo, my supervisor during 2012-2013, for managing my work load to support my study.

I would like to thank Mr. Teerawat Vaccharasiritham and Mr. Wasin Saengnumpong for training me how to use ECLIPSE 100 simulation.

I would like to thank Mr. Charat Thamcharoen for guiding me how to use E-THESIS.

I would like to thank Miss Natakarn Satjawitwisarn, Miss Kunwadee Teerakijpaiboon, Mr. Komsant Suriyawutithum and Mr. Taradon Pleanrungsi, my colleagues, for supporting my routine works during my vacation.

Last, but not least, I thank my mom and my husband for all support.

CONTENTS

	Page
THAI ABSTRACT	iv
ENGLISH ABSTRACT	v
ACKNOWLEDGEMENTS	vi
CONTENTS	vii
List of Tables	1
List of Figures.....	6
List of Abbreviations.....	19
Nomenclatures.....	20
CHAPTER 1 INTRODUCTION	22
1.1 Background.....	22
1.2 Objectives.....	23
1.3 Outline of Thesis.....	23
CHAPTER 2 LITERATURE REVIEW.....	25
2.1 Material Balance Equation in Water-drive Gas Reservoir	25
2.2 Water Influx Models.....	25
2.3 Polynomial Approach to van Everdingen-Hurst Dimensionless Variables.....	26
2.4 Material Balance Equation in Water-drive Gas Reservoir with Unknown Aquifer Properties	27
CHAPTER 3 THEORY AND CONCEPT	30
3.1 Material Balance Equations.....	30
3.1.1 Depletion-Drive Dry-Gas Reservoirs	30
3.1.2 Water-Drive Dry-Gas Reservoirs	32
3.2 Cole Plot [11]	34

	Page
3.3 Water Influx Models.....	35
3.2.1 Simple Aquifer Model	35
3.2.2 van Everdingen & Hurst Model [2].....	36
3.2.2.1 Radial Aquifer Geometry	38
3.2.2.2 Linear Aquifer Geometry	39
3.2.2.3 Bounded Aquifer.....	39
3.2.2.4 Infinite Aquifer	40
3.2.3 Fetkovich Model [3].....	42
3.2.4 Carter and Tracy Model [4].....	46
3.3 Numerical Simulation Concept	47
CHAPTER 4 THESIS METHODOLOGY.....	49
4.1 Reservoir Simulation Model Construction.....	49
4.2 ECLIPSE 100 Analytical Aquifer Method Comparison	49
4.3 Water Influx Model Comparison	50
4.4 OGIP Estimation Using a Plot of p/z versus G_p for 50 mD and 500 mD Water- drive Dry-gas Reservoir.....	50
4.5 OGIP Estimation Using a Plot of $(G_p B_g + W_p B_w)/(B_g - B_{gi})$ versus $W_e/(B_g - B_{gi})$ for 50 mD Water-drive Dry-gas Reservoir	51
4.6 OGIP Estimation Using a Plot of $(G_p B_g + W_p B_w)/(B_g - B_{gi})$ versus $W_e/(B_g - B_{gi})$ for 500 mD Water-drive Dry-gas Reservoir	52
4.7 OGIP Estimation from Unknown Aquifer Size for 50 mD and 500 mD Water- drive Dry-gas Reservoir.....	52
CHAPTER 5 RESERVOIR SIMULATION MODEL	54
5.1 Reservoir Properties	54

	Page
5.2 PVT Properties.....	56
5.3 Well Characteristics and Production Limitations	57
5.4 SCAL	58
5.5 VFP	59
CHAPTER 6 RESULTS AND DISCUSSIONS	61
6.1 ECLIPSE 100 Analytical Aquifer Method Comparison	61
6.2 Effect of Aquifer Size	67
6.2.1 Reservoir Pressure.....	68
6.2.2 Water Production Rate.....	69
6.2.3 Gas Rate	70
6.2.4 Gas Recovery Factor.....	71
6.2.5 Drawdown Pressure.....	72
6.2.6 Pressure Loss in Tubing.....	73
6.2.7 Water Influx Rate	74
6.3 Effect of Permeability.....	77
6.3.1 SBHP Build up Rate.....	77
6.3.2 Reservoir Pressure.....	79
6.3.3 Water Production Rate.....	80
6.3.4 Gas Rate and Recovery Factor	83
6.3.5 Drawdown Pressure.....	86
6.3.6 Water Influx Rate	87
6.4 Water Influx Model Comparison	90

	Page
6.5 OGIP Estimation Using p/z versus G_p Plot for 50 mD and 500 mD Water-drive Dry-gas Reservoir.....	98
6.6 OGIP Estimation Using $(G_p B_g + W_p B_w)/(B_g - B_{gi})$ versus $W_e/(B_g - B_{gi})$ Plot for 50 mD Water-drive Dry-gas Reservoir.....	113
6.7 OGIP Estimation Using $(G_p B_g + W_p B_w)/(B_g - B_{gi})$ versus $W_e/(B_g - B_{gi})$ Plot for 500 mD Water-drive Dry-gas Reservoir.....	150
6.8 Effect of the Amount of Historical Data	164
6.8.1 p/z versus G_p for 50 mD Water-drive Dry-gas Reservoir.....	167
6.8.2 p/z versus G_p for 500 mD Water-drive Dry-gas Reservoir.....	181
6.8.3 $(G_p B_g + W_p B_w)/(B_g - B_{gi})$ versus $W_e/(B_g - B_{gi})$ Plot for 50 mD Water-drive Dry-gas Reservoir	195
6.8.4 $(G_p B_g + W_p B_w)/(B_g - B_{gi})$ versus $W_e/(B_g - B_{gi})$ Plot for 500 mD Water-drive Dry-gas Reservoir	222
6.9 OGIP Estimation from Unknown Aquifer Size	246
CHAPTER 7 CONCLUSIONS AND RECOMMENDATIONS	266
7.1 Conclusion	266
7.2 Recommendation.....	268
REFERENCES	269
APPENDIX A: Reservoir Model Construction by ECLIPSE 100.....	271
APPENDIX B: PROSPER Input Data for Reservoir Model	278
VITA.....	282

List of Tables

Table 3.1 Productivity index for each flow condition and aquifer geometry [3]	45
Table 5.1 Reservoir properties	53
Table 5.2 Dry-gas PVT properties	55
Table 5.3 Water and rock properties at reference pressure 3500 psia	56
Table 5.4 Well characteristics, operating conditions and abandonment condition	57
Table 5.5 Parameters used in VFP table calculation	58
Table 6.1 Parameters to be studied on the effect of analytical aquifer methods.....	60
Table 6.2 Parameters to be studied on the accuracy of calculated W_e from different water influx models.....	90
Table 6.3 Parameters to be studied on the feasibility of OGIP estimation in water- drive dry-gas reservoir by applying p/z versus G_p plot.....	98
Table 6.4 Result of OGIP estimation for 50 mD water-drive dry-gas reservoir by p/z versus G_p plot.....	103
Table 6.5 Accuracy of OGIP estimation for 50 mD water-drive dry-gas reservoir by p/z versus G_p plot.....	104
Table 6.6 Result of OGIP estimation for 500 mD water-drive dry-gas reservoir by p/z versus G_p plot.....	110
Table 6.7 Accuracy of OGIP estimation for 500 mD water-drive dry-gas reservoir by p/z versus G_p plot.....	111
Table 6.8 Parameters to be studied on the accuracy of OGIP estimation for 50 mD water-drive dry-gas reservoir by applying $(G_p B_g + W_p B_w)/(B_g - B_{gi})$ versus $W_e/(B_g - B_{gi})$ plot	112
Table 6.9 Result of OGIP estimation at 1-PV aquifer size for 50 mD water-drive dry-gas reservoir by $(G_p B_g + W_p B_w)/(B_g - B_{gi})$ versus $W_e/(B_g - B_{gi})$ plot.....	119

Table 6.10 Result of OGIP estimation at 10-PV aquifer size for 50 mD water-drive dry-gas reservoir by $(G_p B_g + W_p B_w) / (B_g - B_{gi})$ versus $W_e / (B_g - B_{gi})$ plot.....	124
Table 6.11 Result of OGIP estimation at 30-PV aquifer size for 50 mD water-drive dry-gas reservoir by $(G_p B_g + W_p B_w) / (B_g - B_{gi})$ versus $W_e / (B_g - B_{gi})$ plot.....	129
Table 6.12 Result of OGIP estimation at 70-PV aquifer size for 50 mD water-drive dry-gas reservoir by $(G_p B_g + W_p B_w) / (B_g - B_{gi})$ versus $W_e / (B_g - B_{gi})$ plot.....	134
Table 6.13 Result of OGIP estimation at 100-PV aquifer size for 50 mD water-drive dry-gas reservoir by $(G_p B_g + W_p B_w) / (B_g - B_{gi})$ versus $W_e / (B_g - B_{gi})$ plot.....	140
Table 6.14 Result of OGIP estimation for 50 mD water-drive dry-gas reservoir by $(G_p B_g + W_p B_w) / (B_g - B_{gi})$ versus $W_e / (B_g - B_{gi})$ plot.....	142
Table 6.15 Accuracy of OGIP estimation for 50 mD water-drive dry-gas reservoir by $(G_p B_g + W_p B_w) / (B_g - B_{gi})$ versus $W_e / (B_g - B_{gi})$ plot.....	148
Table 6.16 Parameters to be studied on the accuracy of OGIP estimation for 500 mD water-drive dry-gas reservoir by applying $(G_p B_g + W_p B_w) / (B_g - B_{gi})$ versus $W_e / (B_g - B_{gi})$ plot.....	149
Table 6.17 Result of OGIP estimation at 1-PV aquifer size for 500 mD water-drive dry-gas reservoir by $(G_p B_g + W_p B_w) / (B_g - B_{gi})$ versus $W_e / (B_g - B_{gi})$ plot.....	151
Table 6.18 Result of OGIP estimation at 10-PV aquifer size for 500 mD water-drive dry-gas reservoir by $(G_p B_g + W_p B_w) / (B_g - B_{gi})$ versus $W_e / (B_g - B_{gi})$ plot.....	153
Table 6.19 Result of OGIP estimation at 30-PV aquifer size for 500 mD water-drive dry-gas reservoir by $(G_p B_g + W_p B_w) / (B_g - B_{gi})$ versus $W_e / (B_g - B_{gi})$ plot.....	155
Table 6.20 Result of OGIP estimation at 70-PV aquifer size for 500 mD water-drive dry-gas reservoir by $(G_p B_g + W_p B_w) / (B_g - B_{gi})$ versus $W_e / (B_g - B_{gi})$ plot.....	157
Table 6.21 Result of OGIP estimation at 100-PV aquifer size for 500 mD water-drive dry-gas reservoir by $(G_p B_g + W_p B_w) / (B_g - B_{gi})$ versus $W_e / (B_g - B_{gi})$ plot.....	158
Table 6.22 Result of OGIP estimation for 500 mD water-drive dry-gas reservoir by $(G_p B_g + W_p B_w) / (B_g - B_{gi})$ versus $W_e / (B_g - B_{gi})$ plot.....	160

Table 6.23 Accuracy of OGIP estimation for 500 mD water-drive dry-gas reservoir by $(G_p B_g + W_p B_w) / (B_g - B_{gi})$ versus $W_e / (B_g - B_{gi})$ plot.....	161
Table 6.24 Parameters to be studied on the effect of the amount of historical data on the feasibility and accuracy of OGIP estimation.....	163
Table 6.25 The result of OGIP estimation for 50 mD water-drive dry-gas reservoir by p/z versus G_p plot for various amounts of historical data.....	176
Table 6.26 The accuracy of OGIP estimation for 50 mD water-drive dry-gas reservoir by p/z versus G_p plot for various amounts of historical data...	180
Table 6.27 The result of OGIP estimation for 500 mD water-drive dry-gas reservoir by p/z versus G_p plot for various amounts of historical	190
Table 6.28 The accuracy of OGIP estimation for 500 mD water-drive dry-gas reservoir by p/z versus G_p plot for various amounts of historical data...	193
Table 6.29 The result of OGIP estimation at 1-PV aquifer size for 50 mD water-drive dry-gas reservoir by $(G_p B_g + W_p B_w) / (B_g - B_{gi})$ versus $W_e / (B_g - B_{gi})$ plot for various amounts of historical data	197
Table 6.30 The result of OGIP estimation at 10-PV aquifer size for 50 mD water-drive dry-gas reservoir by $(G_p B_g + W_p B_w) / (B_g - B_{gi})$ versus $W_e / (B_g - B_{gi})$ plot for various amounts of historical data	202
Table 6.31 The result of OGIP estimation at 30-PV aquifer size for 50 mD water-drive dry-gas reservoir by $(G_p B_g + W_p B_w) / (B_g - B_{gi})$ versus $W_e / (B_g - B_{gi})$ plot for various amounts of historical data	206
Table 6.32 The result of OGIP estimation at 70-PV aquifer size for 50 mD water-drive dry-gas reservoir by $(G_p B_g + W_p B_w) / (B_g - B_{gi})$ versus $W_e / (B_g - B_{gi})$ plot for various amounts of historical data	210
Table 6.33 The result of OGIP estimation at 100-PV aquifer size for 50 mD water-drive dry-gas reservoir by $(G_p B_g + W_p B_w) / (B_g - B_{gi})$ versus $W_e / (B_g - B_{gi})$ plot for various amounts of historical data	214

Table 6.34 The result of OGIP estimation for 50 mD water-drive dry-gas reservoir by $(G_p B_g + W_p B_w) / (B_g - B_{gi})$ versus $W_e / (B_g - B_{gi})$ plot for various amounts of historical data.....	216
Table 6.35 The accuracy of OGIP estimation for 50 mD water-drive dry-gas reservoir by $(G_p B_g + W_p B_w) / (B_g - B_{gi})$ versus $W_e / (B_g - B_{gi})$ plot for various amounts of historical data	219
Table 6.36 The result of OGIP estimation at 1-PV aquifer size for 500 mD water-drive dry-gas reservoir by $(G_p B_g + W_p B_w) / (B_g - B_{gi})$ versus $W_e / (B_g - B_{gi})$ plot for various amounts of historical data	224
Table 6.37 The result of OGIP estimation at 10-PV aquifer size for 500 mD water-drive dry-gas reservoir by $(G_p B_g + W_p B_w) / (B_g - B_{gi})$ versus $W_e / (B_g - B_{gi})$ plot for various amounts of historical data	228
Table 6.38 The result of OGIP estimation at 30-PV aquifer size for 500 mD water-drive dry-gas reservoir by $(G_p B_g + W_p B_w) / (B_g - B_{gi})$ versus $W_e / (B_g - B_{gi})$ plot for various amounts of historical data	232
Table 6.39 The result of OGIP estimation at 70-PV aquifer size for 500 mD water-drive dry-gas reservoir by $(G_p B_g + W_p B_w) / (B_g - B_{gi})$ versus $W_e / (B_g - B_{gi})$ plot for various amounts of historical data	236
Table 6.40 The result of OGIP estimation at 100-PV aquifer size for 500 mD water-drive dry-gas reservoir by $(G_p B_g + W_p B_w) / (B_g - B_{gi})$ versus $W_e / (B_g - B_{gi})$ plot for various amounts of historical data	240
Table 6.41 The result of OGIP estimation for 500 mD water-drive dry-gas reservoir by $(G_p B_g + W_p B_w) / (B_g - B_{gi})$ versus $W_e / (B_g - B_{gi})$ plot for various amounts of historical data.....	242
Table 6.42 The accuracy of OGIP estimation for 500 mD water-drive dry-gas reservoir by $(G_p B_g + W_p B_w) / (B_g - B_{gi})$ versus $W_e / (B_g - B_{gi})$ plot for various amounts of historical data	245

Table 6.43 Parameters to be studied on the feasibility and accuracy of OGIP estimation by $(G_p B_g + W_p B_w) / (B_g - B_{gi})$ versus $W_e / (B_g - B_{gi})$ plot with unknown aquifer size.....	246
Table 6.44 The result of OGIP estimation for 50 mD water-drive dry-gas reservoir by $(G_p B_g + W_p B_w) / (B_g - B_{gi})$ versus $W_e / (B_g - B_{gi})$ plot with unknown aquifer size	256
Table 6.45 The accuracy of OGIP estimation for 50 mD water-drive dry-gas reservoir by $(G_p B_g + W_p B_w) / (B_g - B_{gi})$ versus $W_e / (B_g - B_{gi})$ plot with unknown aquifer size.....	259
Table 6.46 The result of OGIP estimation for 500 mD water-drive dry-gas reservoir by $(G_p B_g + W_p B_w) / (B_g - B_{gi})$ versus $W_e / (B_g - B_{gi})$ plot and van Everdingen & Hurst water influx model with unknown aquifer size	263
Table 6.47 The accuracy of OGIP estimation for 500 mD water-drive dry-gas reservoir by $(G_p B_g + W_p B_w) / (B_g - B_{gi})$ versus $W_e / (B_g - B_{gi})$ plot and van Everdingen & Hurst water influx model with unknown aquifer size	264

List of Figures

Figure 3.1 Plot of p/z vs. G_p	32
Figure 3.2 Plot of $[(G_p B_g) + (W_p B_w)] / (B_g - B_{gi})$ vs. $W_e / (B_g - B_{gi})$	33
Figure 3.3 Cole plots in water-drive and depletion-drive reservoirs (after Dake [12]) .	34
Figure 3.4 Radial aquifer geometry	38
Figure 3.5 Linear aquifer geometry	39
Figure 3.6 Series of discrete pressure steps.....	41
Figure 5.1 Radial water-drive gas reservoir model.....	54
Figure 5.2 The relative permeability to gas.....	57
Figure 5.3 The relative permeability to water	58
Figure 6.1 Simulated W_e , SBHP, G_p and W_p versus %RF at 1-PV aquifer size, case 1-2.....	62
Figure 6.2 Simulated W_e , SBHP, G_p and W_p versus %RF at 10-PV aquifer size, case 3-4	63
Figure 6.3 Simulated W_e , SBHP, G_p and W_p versus %RF at 30-PV aquifer size, case 5-6	64
Figure 6.4 Simulated W_e , SBHP, G_p and W_p versus %RF at 70-PV aquifer size, case 7-8	65
Figure 6.5 Simulated W_e , SBHP, G_p and W_p versus %RF at 100-PV aquifer size, case 9-10.....	66
Figure 6.6 Simulated field pressure versus %RF for all aquifer sizes.....	67
Figure 6.7 Simulated cumulative water influx versus %RF for all aquifer sizes	67
Figure 6.8 Simulated water production rate versus %RF for all aquifer sizes	68
Figure 6.9 Simulated water saturation profile in the reservoir at water breakthrough in 100-PV case.....	69

Figure 6.10 Simulated water saturation profile in the reservoir at the abandonment condition in 1-PV case	69
Figure 6.11 Simulated gas rate versus %RF for all aquifer sizes	70
Figure 6.12 Gas recovery factor for all aquifer sizes.....	71
Figure 6.13 Simulated field pressure and flowing bottom hole pressure versus %RF at 1-PV, 30-PV and 100-PV aquifer sizes.....	72
Figure 6.14 Simulated flowing bottom hole pressure and flowing tubing head pressure versus %RF at 1-PV, 30-PV and 100-PV aquifer sizes	73
Figure 6.15 Simulated water influx rate and gas rate versus %RF at 1-PV aquifer size	74
Figure 6.16 Simulated water influx rate and gas rate versus %RF at 10-PV and 30-PV aquifer sizes.....	75
Figure 6.17 Simulated water influx rate and gas rate versus %RF at 70-PV and 100-PV aquifer sizes.....	75
Figure 6.18 Simulated relative permeability to water profile at 50% RF in 100 PV aquifer size.....	76
Figure 6.19 Simulated relative permeability to water profile at 70% RF in 100-PV aquifer size.....	76
Figure 6.20 Difference between simulated field pressure and shut-in bottom hole pressure versus %RF at 1-PV and 10-PV aquifer sizes in 50 mD and 500 mD reservoirs	77
Figure 6.21 Difference between simulated field pressure and shut-in bottom hole pressure versus %RF at 30-PV, 70-PV and 100-PV aquifer sizes in 50 mD and 500 mD reservoirs.....	78
Figure 6.22 Simulated cumulative water influx versus %RF for all aquifer sizes in 50 mD and 500 mD reservoirs	79

Figure 6.23 Simulated field pressure versus %RF for all aquifer sizes in 50 mD and 500 mD reservoirs	79
Figure 6.24 Simulated water production rate versus %RF at 1-PV and 10-PV aquifer size in 50 mD and 500 mD reservoirs.....	80
Figure 6.25 Simulated water production rate versus %RF at 30-PV, 70-PV and 100-PV aquifer size in 50 mD and 500 mD reservoirs.....	80
Figure 6.26 Simulated water saturation profile in the 500 mD reservoir at water breakthrough or 72% RF in 10-PV aquifer size.....	81
Figure 6.27 Simulated water saturation profile in the 50 mD reservoir at 72% RF in 10-PV aquifer size.....	81
Figure 6.28 Simulated water saturation profile in the 500 mD reservoir at abandonment condition in 1-PV aquifer size.....	82
Figure 6.29 Simulated gas rate versus %RF for all aquifer sizes in 50 mD and 500 mD reservoirs	82
Figure 6.30 Recovery factor for all aquifer sizes in 50 mD and 500 mD reservoirs	83
Figure 6.31 Simulated reservoir pressure in the 500 mD reservoir at abandonment condition in 1-PV aquifer size.....	83
Figure 6.32 Simulated reservoir pressure in the 50 mD reservoir at abandonment condition in 1-PV aquifer size.....	84
Figure 6.33 Simulated water saturation profile in the 500 mD reservoir at abandonment condition in 10-PV aquifer size.....	84
Figure 6.34 Simulated water saturation profile in the 50 mD reservoir at abandonment condition in 10-PV aquifer size.....	85
Figure 6.35 Simulated field pressure and flowing bottom hole pressure versus %RF at 1-PV, 30-PV and 100-PV aquifer size in 50 mD and 500 mD reservoirs.....	86

Figure 6.36 Simulated water influx rate and gas rate versus %RF at 1-PV aquifer size in 50 mD and 500 mD reservoirs	87
Figure 6.37 Simulated water influx rate and gas rate versus %RF at 10-PV aquifer size in 50 mD and 500 mD reservoirs	87
Figure 6.38 Simulated water influx rate and gas rate versus %RF at 30-PV aquifer size in 50 mD and 500 mD reservoirs	88
Figure 6.39 Simulated water influx rate and gas rate versus %RF at 70-PV aquifer size in 50 mD and 500 mD reservoirs	88
Figure 6.40 Simulated water influx rate and gas rate versus %RF at 100-PV aquifer size in 50 mD and 500 mD reservoirs	89
Figure 6.41 Simulated and calculated W_e at 1-PV aquifer size, case 1-4.....	91
Figure 6.42 Error of calculated W_e at 1-PV aquifer size, case 1-4.....	91
Figure 6.43 Simulated and calculated W_e at 10-PV aquifer size, case 5-8	92
Figure 6.44 Error of calculated W_e at 10-PV aquifer size, case 5-8.....	92
Figure 6.45 Simulated and calculated W_e at 30-PV aquifer size, case 9-12	93
Figure 6.46 Error of calculated W_e at 30-PV aquifer size, case 9-12	93
Figure 6.47 Simulated and calculated W_e at 70-PV aquifer size, case 13-16.....	94
Figure 6.48 Error of calculated W_e at 70-PV aquifer size, case 13-16	94
Figure 6.49 Simulated and calculated W_e at 100-PV aquifer size, case 17-20.....	95
Figure 6.50 Error of calculated W_e at 100-PV aquifer size, case 17-20.....	95
Figure 6.51 Error percentage of van Everdingen & Hurst calculated W_e in 50 mD reservoir by using field pressure	97
Figure 6.52 p/z versus G_p without aquifer support for 50 mD reservoir, case 1-3.....	100
Figure 6.53 p/z versus G_p at 1-PV aquifer size for 50 mD reservoir, case 4-6	100
Figure 6.54 p/z versus G_p at 10-PV aquifer size for 50 mD reservoir, case 7-9	101

Figure 6.55 p/z versus G_p at 30-PV aquifer size for 50 mD reservoir, case 10-12.....	101
Figure 6.56 p/z versus G_p at 70-PV aquifer size for 50 mD reservoir, case 13-15.....	102
Figure 6.57 p/z versus G_p at 100-PV aquifer size for 50 mD reservoir, case 16-18.....	102
Figure 6.58 Error of estimated OGIP for 50 mD water-drive dry-gas reservoir by p/z versus G_p plot	103
Figure 6.59 p/z versus G_p without aquifer support for 500 mD reservoir, case 19-21	106
Figure 6.60 p/z versus G_p at 1-PV aquifer size for 500 mD reservoir, case 22-24.....	107
Figure 6.61 p/z versus G_p at 10-PV aquifer size for 500 mD reservoir, case 25-27.....	107
Figure 6.62 p/z versus G_p at 30-PV aquifer size for 500 mD reservoir, case 28-30.....	108
Figure 6.63 p/z versus G_p at 70-PV aquifer size for 500 mD reservoir, case 31-33.....	108
Figure 6.64 p/z versus G_p at 100-PV aquifer size for 500 mD reservoir, case 34-36 ...	109
Figure 6.65 Error of estimated OGIP for 500 mD water-drive dry-gas reservoir by p/z versus G_p plot	110
Figure 6.66 $(G_p B_g + W_p B_w) / (B_g - B_{gi})$ versus $W_e / (B_g - B_{gi})$ at 1-PV aquifer size and 6-hour shut-in duration for 50 mD reservoir, case 1-4	116
Figure 6.67 $(G_p B_g + W_p B_w) / (B_g - B_{gi})$ versus $W_e / (B_g - B_{gi})$ at 1-PV aquifer size and 1-day shut-in duration for 50 mD reservoir, case 5-8	117
Figure 6.68 $(G_p B_g + W_p B_w) / (B_g - B_{gi})$ versus $W_e / (B_g - B_{gi})$ at 1-PV aquifer size and 7-day shut-in duration for 50 mD reservoir, case 9-12	118
Figure 6.69 $(G_p B_g + W_p B_w) / (B_g - B_{gi})$ versus $W_e / (B_g - B_{gi})$ at 10-PV aquifer size and 6-hour shut-in duration for 50 mD reservoir, case 13-16	121
Figure 6.70 $(G_p B_g + W_p B_w) / (B_g - B_{gi})$ versus $W_e / (B_g - B_{gi})$ at 10-PV aquifer size and 1-day shut-in duration for 50 mD reservoir, case 17-20	122
Figure 6.71 $(G_p B_g + W_p B_w) / (B_g - B_{gi})$ versus $W_e / (B_g - B_{gi})$ at 10-PV aquifer size and 7-day shut-in duration for 50 mD reservoir, case 21-24	123

Figure 6.72 $(G_p B_g + W_p B_w)/(B_g - B_{gi})$ versus $W_e/(B_g - B_{gi})$ at 30-PV aquifer size and 6-hour shut-in duration for 50 mD reservoir, case 25-28	126
Figure 6.73 $(G_p B_g + W_p B_w)/(B_g - B_{gi})$ versus $W_e/(B_g - B_{gi})$ at 30-PV aquifer size and 1-day shut-in duration for 50 mD reservoir, case 29-32	127
Figure 6.74 $(G_p B_g + W_p B_w)/(B_g - B_{gi})$ versus $W_e/(B_g - B_{gi})$ at 30-PV aquifer size and 7-day shut-in duration for 50 mD reservoir, case 33-36	128
Figure 6.75 $(G_p B_g + W_p B_w)/(B_g - B_{gi})$ versus $W_e/(B_g - B_{gi})$ at 70-PV aquifer size and 6-hour shut-in duration for 50 mD reservoir, case 37-40	131
Figure 6.76 $(G_p B_g + W_p B_w)/(B_g - B_{gi})$ versus $W_e/(B_g - B_{gi})$ at 70-PV aquifer size and 1-day shut-in duration for 50 mD reservoir, case 41-44	132
Figure 6.77 $(G_p B_g + W_p B_w)/(B_g - B_{gi})$ versus $W_e/(B_g - B_{gi})$ at 70-PV aquifer size and 7-day shut-in duration for 50 mD reservoir, case 45-48	133
Figure 6.78 $(G_p B_g + W_p B_w)/(B_g - B_{gi})$ versus $W_e/(B_g - B_{gi})$ from van Everdingen & Hurst water influx model at 70-PV aquifer size and 1-day shut-in duration for 50 mD reservoir without the error from x-axis	135
Figure 6.79 $(G_p B_g + W_p B_w)/(B_g - B_{gi})$ versus $W_e/(B_g - B_{gi})$ from van Everdingen & Hurst water influx model at 70-PV aquifer size and 1-day shut-in duration for 50 mD reservoir without the error from y-axis	135
Figure 6.80 $(G_p B_g + W_p B_w)/(B_g - B_{gi})$ versus $W_e/(B_g - B_{gi})$ at 100-PV aquifer size and 6-hour shut-in duration for 50 mD reservoir, case 49-52	137
Figure 6.81 $(G_p B_g + W_p B_w)/(B_g - B_{gi})$ versus $W_e/(B_g - B_{gi})$ at 100-PV aquifer size and 1-day shut-in duration for 50 mD reservoir, case 53-56	138
Figure 6.82 $(G_p B_g + W_p B_w)/(B_g - B_{gi})$ versus $W_e/(B_g - B_{gi})$ at 100-PV aquifer size and 7-day shut-in duration for 50 mD reservoir, case 57-60	139
Figure 6.83 Error of estimated OGIP for 50 mD water-drive dry-gas reservoir by $(G_p B_g + W_p B_w)/(B_g - B_{gi})$ versus $W_e/(B_g - B_{gi})$ plot.....	141

Figure 6.84 $(G_p B_g + W_p B_w) / (B_g - B_{gi})$ versus $W_e / (B_g - B_{gi})$ at 1-PV aquifer size for 500 mD reservoir, case 1-3	151
Figure 6.85 $(G_p B_g + W_p B_w) / (B_g - B_{gi})$ versus $W_e / (B_g - B_{gi})$ at 10-PV aquifer size for 500 mD reservoir, case 4-6	153
Figure 6.86 $(G_p B_g + W_p B_w) / (B_g - B_{gi})$ versus $W_e / (B_g - B_{gi})$ at 30-PV aquifer size for 500 mD reservoir, case 7-9	155
Figure 6.87 $(G_p B_g + W_p B_w) / (B_g - B_{gi})$ versus $W_e / (B_g - B_{gi})$ at 70-PV aquifer size for 500 mD reservoir, case 10-12	156
Figure 6.88 $(G_p B_g + W_p B_w) / (B_g - B_{gi})$ versus $W_e / (B_g - B_{gi})$ at 100-PV aquifer size for 500 mD reservoir, case 13-15	158
Figure 6.89 Error of estimated OGIP for 500 mD water-drive dry-gas reservoir by $(G_p B_g + W_p B_w) / (B_g - B_{gi})$ versus $W_e / (B_g - B_{gi})$ plot using van Everdingen & Hurst water influx model	160
Figure 6.90 Error of van Everdingen & Hurst calculated W_e for 500 mD reservoir	162
Figure 6.91 p/z versus G_p without aquifer support and 6-hour shut-in duration for 50 mD reservoir, case 1-3	167
Figure 6.92 p/z versus G_p without aquifer support and 1-day shut-in duration for 50 mD reservoir, case 4-6	167
Figure 6.93 p/z versus G_p without aquifer support and 7-day shut-in duration for 50 mD reservoir, case 7-9	168
Figure 6.94 p/z versus G_p at 1-PV aquifer size and 6-hour shut-in duration for 50 mD reservoir, case 10-12	168
Figure 6.95 p/z versus G_p at 1-PV aquifer size and 1-day shut-in duration for 50 mD reservoir, case 13-15	169
Figure 6.96 p/z versus G_p at 1-PV aquifer size and 7-day shut-in duration for 50 mD reservoir, case 16-18	169

Figure 6.97 p/z versus G_p at 10-PV aquifer size and 6-hour shut-in duration for 50 mD reservoir, case 19-21	170
Figure 6.98 p/z versus G_p at 10-PV aquifer size and 1-day shut-in duration for 50 mD reservoir, case 22-24	170
Figure 6.99 p/z versus G_p at 10-PV aquifer size and 7-day shut-in duration for 50 mD reservoir, case 25-27	171
Figure 6.100 p/z versus G_p at 30-PV aquifer size and 6-hour shut-in duration for 50 mD reservoir, case 28-30.....	171
Figure 6.101 p/z versus G_p at 30-PV aquifer size and 1-day shut-in duration for 50 mD reservoir, case 31-33.....	172
Figure 6.102 p/z versus G_p at 30-PV aquifer size and 7-day shut-in duration for 50 mD reservoir, case 34-36.....	172
Figure 6.103 p/z versus G_p at 70-PV aquifer size and 6-hour shut-in duration for 50 mD reservoir, case 37-39.....	173
Figure 6.104 p/z versus G_p at 70-PV aquifer size and 1-day shut-in duration for 50 mD reservoir, case 40-42.....	173
Figure 6.105 p/z versus G_p at 70-PV aquifer size and 7-day shut-in duration for 50 mD reservoir, case 43-45.....	174
Figure 6.106 p/z versus G_p at 100-PV aquifer size and 6-hour shut-in duration for 50 mD reservoir, case 46-48.....	174
Figure 6.107 p/z versus G_p at 100-PV aquifer size and 1-day shut-in duration for 50 mD reservoir, case 49-51.....	175
Figure 6.108 p/z versus G_p at 100-PV aquifer size and 7-day shut-in duration for 50 mD reservoir, case 52-54.....	175
Figure 6.109 Error of estimated OGIP for 50 mD water-drive dry-gas reservoir by p/z versus G_p plot for various amounts of historical data.....	176

Figure 6.110 p/z versus G_p without aquifer support and 6-hour shut-in duration for 500 mD reservoir, case 1-3.....	181
Figure 6.111 p/z versus G_p without aquifer support and 1-day shut-in duration for 500 mD reservoir, case 4-6.....	181
Figure 6.112 p/z versus G_p without aquifer support and 7-days shut-in duration for 500 mD reservoir, case 7-9.....	182
Figure 6.113 p/z versus G_p at 1-PV aquifer size and 6-hour shut-in duration for 500 mD reservoir, case 10-12.....	182
Figure 6.114 p/z versus G_p at 1-PV aquifer size and 1-day shut-in duration for 500 mD reservoir, case 13-15.....	183
Figure 6.115 p/z versus G_p at 1-PV aquifer size and 7-day shut-in duration for 500 mD reservoir, case 16-18.....	183
Figure 6.116 p/z versus G_p at 10-PV aquifer size and 6-hour shut-in duration for 500 mD reservoir, case 19-21.....	184
Figure 6.117 p/z versus G_p at 10-PV aquifer size and 1-day shut-in duration for 500 mD reservoir, case 22-24.....	184
Figure 6.118 p/z versus G_p at 10-PV aquifer size and 7-day shut-in duration for 500 mD reservoir, case 25-27.....	185
Figure 6.119 p/z versus G_p at 30-PV aquifer size and 6-hour shut-in duration for 500 mD reservoir, case 28-30.....	185
Figure 6.120 p/z versus G_p at 30-PV aquifer size and 1-day shut-in duration for 500 mD reservoir, case 31-33.....	186
Figure 6.121 p/z versus G_p at 30-PV aquifer size and 7-day shut-in duration for 500 mD reservoir, case 34-36.....	186
Figure 6.122 p/z versus G_p at 70-PV aquifer size and 6-hour shut-in duration for 500 mD reservoir, case 37-39.....	187

Figure 6.123 p/z versus G_p at 70-PV aquifer size and 1-day shut-in duration for 500 mD reservoir, case 40-42.....	187
Figure 6.124 p/z versus G_p at 70-PV aquifer size and 7-day shut-in duration for 500 mD reservoir, case 43-45.....	188
Figure 6.125 p/z versus G_p at 100-PV aquifer size and 6-hour shut-in duration for 500 mD reservoir, case 46-48.....	188
Figure 6.126 p/z versus G_p at 100-PV aquifer size and 1-day shut-in duration for 500 mD reservoir, case 49-51.....	189
Figure 6.127 p/z versus G_p at 100-PV aquifer size and 7-day shut-in duration for 500 mD reservoir, case 52-54.....	189
Figure 6.128 Error of estimated OGIP for 500 mD water-drive dry-gas reservoir by p/z versus G_p plot for various amounts of historical data.....	190
Figure 6.129 $(G_p B_g + W_p B_w)/(B_g - B_{gi})$ versus $W_e/(B_g - B_{gi})$ at 1-PV aquifer size and 6-hour shut-in duration for 50 mD reservoir, case 1-3.....	195
Figure 6.130 $(G_p B_g + W_p B_w)/(B_g - B_{gi})$ versus $W_e/(B_g - B_{gi})$ at 1-PV aquifer size and 1-day shut-in duration for 50 mD reservoir, case 4-6.....	196
Figure 6.131 $(G_p B_g + W_p B_w)/(B_g - B_{gi})$ versus $W_e/(B_g - B_{gi})$ at 1-PV aquifer size and 7-day shut-in duration for 50 mD reservoir, case 7-9.....	197
Figure 6.132 $(G_p B_g + W_p B_w)/(B_g - B_{gi})$ versus $W_e/(B_g - B_{gi})$ at 10-PV aquifer size and 6-hour shut-in duration for 50 mD reservoir, case 10-12	199
Figure 6.133 $(G_p B_g + W_p B_w)/(B_g - B_{gi})$ versus $W_e/(B_g - B_{gi})$ at 10-PV aquifer size and 1-day shut-in duration for 50 mD reservoir, case 13-15	200
Figure 6.134 $(G_p B_g + W_p B_w)/(B_g - B_{gi})$ versus $W_e/(B_g - B_{gi})$ at 10-PV aquifer size and 7-day shut-in duration for 50 mD reservoir, case 16-18	201
Figure 6.135 $(G_p B_g + W_p B_w)/(B_g - B_{gi})$ versus $W_e/(B_g - B_{gi})$ at 30-PV aquifer size and 6-hour shut-in duration for 50 mD reservoir, case 19-21	203

Figure 6.136 $(G_p B_g + W_p B_w)/(B_g - B_{gi})$ versus $W_e/(B_g - B_{gi})$ at 30-PV aquifer size and 1-day shut-in duration for 50 mD reservoir, case 22-24	204
Figure 6.137 $(G_p B_g + W_p B_w)/(B_g - B_{gi})$ versus $W_e/(B_g - B_{gi})$ at 30-PV aquifer size and 7-day shut-in duration for 50 mD reservoir, case 25-27	205
Figure 6.138 $(G_p B_g + W_p B_w)/(B_g - B_{gi})$ versus $W_e/(B_g - B_{gi})$ at 70-PV aquifer size and 6-hour shut-in duration for 50 mD reservoir, case 28-30	207
Figure 6.139 $(G_p B_g + W_p B_w)/(B_g - B_{gi})$ versus $W_e/(B_g - B_{gi})$ at 70-PV aquifer size and 1-day shut-in duration for 50 mD reservoir, case 31-33	208
Figure 6.140 $(G_p B_g + W_p B_w)/(B_g - B_{gi})$ versus $W_e/(B_g - B_{gi})$ at 70-PV aquifer size and 7-day shut-in duration for 50 mD reservoir, case 34-36	209
Figure 6.141 $(G_p B_g + W_p B_w)/(B_g - B_{gi})$ versus $W_e/(B_g - B_{gi})$ at 100-PV aquifer size and 6-hour shut-in duration for 50 mD reservoir, case 37-39.....	211
Figure 6.142 $(G_p B_g + W_p B_w)/(B_g - B_{gi})$ versus $W_e/(B_g - B_{gi})$ at 100-PV aquifer size and 1-day shut-in duration for 50 mD reservoir, case 40-42	212
Figure 6.143 $(G_p B_g + W_p B_w)/(B_g - B_{gi})$ versus $W_e/(B_g - B_{gi})$ at 100-PV aquifer size and 7-day shut-in duration for 50 mD reservoir, case 43-45	213
Figure 6.144 Error of estimated OGIP for 50 mD water-drive dry-gas reservoir by $(G_p B_g + W_p B_w)/(B_g - B_{gi})$ versus $W_e/(B_g - B_{gi})$ plot for various amounts of historical data.....	215
Figure 6.145 $(G_p B_g + W_p B_w)/(B_g - B_{gi})$ versus $W_e/(B_g - B_{gi})$ at 1-PV aquifer size and 6-hour shut-in duration for 500 mD reservoir, case 1-3.....	221
Figure 6.146 $(G_p B_g + W_p B_w)/(B_g - B_{gi})$ versus $W_e/(B_g - B_{gi})$ at 1-PV aquifer size and 1-day shut-in duration for 500 mD reservoir, case 4-6.....	222
Figure 6.147 $(G_p B_g + W_p B_w)/(B_g - B_{gi})$ versus $W_e/(B_g - B_{gi})$ at 1-PV aquifer size and 7-day shut-in duration for 500 mD reservoir, case 7-9.....	223
Figure 6.148 $(G_p B_g + W_p B_w)/(B_g - B_{gi})$ versus $W_e/(B_g - B_{gi})$ at 10-PV aquifer size and 6-hour shut-in duration for 500 mD reservoir, case 10-12	225

Figure 6.149 $(G_p B_g + W_p B_w) / (B_g - B_{gi})$ versus $W_e / (B_g - B_{gi})$ at 10-PV aquifer size and 1-day shut-in duration for 500 mD reservoir, case 13-15	226
Figure 6.150 $(G_p B_g + W_p B_w) / (B_g - B_{gi})$ versus $W_e / (B_g - B_{gi})$ at 10-PV aquifer size and 7-day shut-in duration for 500 mD reservoir, case 16-18	227
Figure 6.151 $(G_p B_g + W_p B_w) / (B_g - B_{gi})$ versus $W_e / (B_g - B_{gi})$ at 30-PV aquifer size and 6-hour shut-in duration for 500 mD reservoir, case 19-21	229
Figure 6.152 $(G_p B_g + W_p B_w) / (B_g - B_{gi})$ versus $W_e / (B_g - B_{gi})$ at 30-PV aquifer size and 1-day shut-in duration for 500 mD reservoir, case 22-24	230
Figure 6.153 $(G_p B_g + W_p B_w) / (B_g - B_{gi})$ versus $W_e / (B_g - B_{gi})$ at 30-PV aquifer size and 7-day shut-in duration for 500 mD reservoir, case 25-27	231
Figure 6.154 $(G_p B_g + W_p B_w) / (B_g - B_{gi})$ versus $W_e / (B_g - B_{gi})$ at 70-PV aquifer size and 6-hour shut-in duration for 500 mD reservoir, case 28-30	233
Figure 6.155 $(G_p B_g + W_p B_w) / (B_g - B_{gi})$ versus $W_e / (B_g - B_{gi})$ at 70-PV aquifer size and 1-day shut-in duration for 500 mD reservoir, case 31-33	234
Figure 6.156 $(G_p B_g + W_p B_w) / (B_g - B_{gi})$ versus $W_e / (B_g - B_{gi})$ at 70-PV aquifer size and 7-day shut-in duration for 500 mD reservoir, case 34-36	235
Figure 6.157 $(G_p B_g + W_p B_w) / (B_g - B_{gi})$ versus $W_e / (B_g - B_{gi})$ at 100-PV aquifer size and 6-hour shut-in duration for 500 mD reservoir, case 37-39	237
Figure 6.158 $(G_p B_g + W_p B_w) / (B_g - B_{gi})$ versus $W_e / (B_g - B_{gi})$ at 100-PV aquifer size and 1-day shut-in duration for 500 mD reservoir, case 40-42	238
Figure 6.159 $(G_p B_g + W_p B_w) / (B_g - B_{gi})$ versus $W_e / (B_g - B_{gi})$ at 100-PV aquifer size and 7-day shut-in duration for 500 mD reservoir, case 43-45	239
Figure 6.160 Error of estimated OGIP for 500 mD water-drive dry-gas reservoir by $(G_p B_g + W_p B_w) / (B_g - B_{gi})$ versus $W_e / (B_g - B_{gi})$ plot for various amounts of historical data	241
Figure 6.161 Left: R-squared value and error in estimated OGIP	248
Figure 6.162 Left: R-squared value and error in estimated OGIP	249

Figure 6.163 Left: R-squared value and error in estimated OGIP	251
Figure 6.164 Left: R-squared value and error in estimated OGIP	253
Figure 6.165 R-squared value and error in estimated OGIP at 100-PV aquifer size for 50 mD, case 17-20	254
Figure 6.166 Error percentage of estimated OGIP in 50 mD water-drive dry-gas reservoir by $(G_p B_g + W_p B_w) / (B_g - B_{gi})$ versus $W_e / (B_g - B_{gi})$ plot with unknown aquifer size.....	255
Figure 6.167 Estimated aquifer size in 50 mD water-drive dry-gas reservoir by $(G_p B_g + W_p B_w) / (B_g - B_{gi})$ versus $W_e / (B_g - B_{gi})$ plot with unknown aquifer size.	255
Figure 6.168 Left: R-squared value and error in estimated OGIP	260
Figure 6.169 Left: R-square value and error in estimated OGIP	260
Figure 6.170 Left: R-square value and error in estimated OGIP	261
Figure 6.171 Left: R-square value and error in estimated OGIP	261
Figure 6.172 Left: R-square value and error in estimated OGIP	261
Figure 6.173 Estimated aquifer size and error percentage in 500 mD water-drive dry-gas reservoir by $(G_p B_g + W_p B_w) / (B_g - B_{gi})$ versus $W_e / (B_g - B_{gi})$ plot and van Everdingen & Hurst water influx model with unknown aquifer size.....	262
Figure 6.174 Error percentage of estimated OGIP in 500 mD water-drive dry-gas reservoir by $(G_p B_g + W_p B_w) / (B_g - B_{gi})$ versus $W_e / (B_g - B_{gi})$ plot and van Everdingen & Hurst water influx model with unknown aquifer size.....	263

List of Abbreviations

cp	Centipoise
deg	Degree
°F	Degree Fahrenheit
FBHP	Flowing bottom hole pressure, (psia)
FPR	Field pressure, (psia)
ft	Feet
ft ²	Square feet
FTHP	Flowing tubing head pressure
in	Inch
mD	Millidarcy
MMscf	Million standard cubic foot
MMscfd	Million standard cubic foot per day
Mscf	Thousand standard cubic foot
OGIP	Original gas in place
psia	Pound per square inch absolute
PV	Pore volume
PVT	Pressure-Volume-Temperature
rb	Reservoir barrel
rb/Mscf	Reservoir barrel per thousand standard cubic foot
RF	Recovery factor
SBHP	Shut in bottom hole pressure, (psia)

Nomenclatures

\emptyset	Porosity
μ	Fluid viscosity
B_g	Gas formation volume factor
B_{gi}	Gas formation volume factor at initial reservoir pressure
B_w	Water formation volume factor
c_f	Formation compressibility
c_w	Water compressibility
\bar{c}	Total compressibility
G	Original gas in place
G_p	Cumulative gas production
h	Reservoir thickness
J	Productivity index
k	Absolute permeability
k_{rw}	Relative permeability to water
L	Reservoir length
p	Reservoir pressure
\bar{p}_a	Average aquifer pressure
p_i	Initial reservoir pressure
p_D	Dimensionless pressure
p_D'	Dimensionless derivative pressure
p_{wf}	Bottom hole flowing pressure
q	Fluid flow rate

q_D	Dimensionless flow rate
q_w	Water influx rate
r	Reservoir radius
r_{eD}	Dimensionless radius
r_e	Outer aquifer radius
r_o	Outer reservoir radius
r_w	Well bore radius
S_w	Water saturation
S_{wi}	Initial water saturation
t	Time
t_D	Dimensionless time
w	Reservoir width
W	Total volume of water
W_D	Dimensionless cumulative water influx
W_e	Cumulative water influx
W_{ei}	Initial amount of encroachable water
W_p	Cumulative water production
z	Gas compressibility factor
z_i	Gas compressibility factor at initial reservoir pressure

CHAPTER 1

INTRODUCTION

1.1 Background

Original gas in place (OGIP) is the most important piece of information for reservoir management plan and economic decision since it indicates the amount of gas initially in the reservoir. One of the most commonly used methods to determine OGIP is material balance equation. Since the main drive mechanism in gas reservoirs is either depletion-drive or water-drive, two forms of material balance equation, one for depletion-drive and the other for water-drive, are used.

Material balance equation is based on the principle of the conservation of mass. With a tank model concept that does not take reservoir geometry and flow in porous media into account, under the assumption of homogeneous pore volume, constant temperature, uniform pressure, and uniform hydrocarbon saturation distribution, OGIP can be estimated by considering the fluid expansion behavior.

Material balance equation for water-drive gas reservoir is more complicate and requires more information than the one for depletion-drive gas reservoir. The additional information required for water-drive material balance equation is water influx. Unfortunately, the water influx cannot be measured directly like other information such as pressure and cumulative production. The water influx is calculated by applying a water influx model to the production data and the aquifer properties.

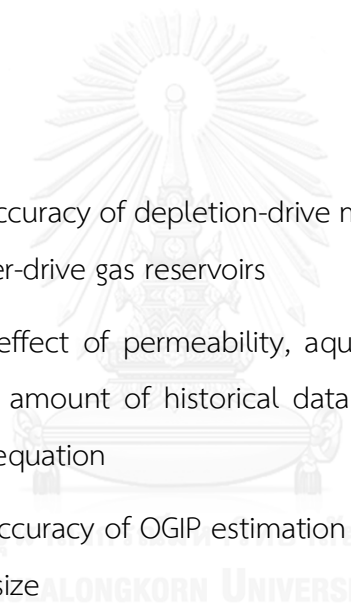
Water influx model selection is a challenge since each model has different assumptions and mathematical approach, suitable for different reservoir-aquifer systems. Aquifer size is another challenge because it is usually an unknown parameter.

In the Gulf of Thailand, gas reservoirs with water-drive mechanism are common. During depletion, the pressure at the reservoir-aquifer boundary drops, leading to water encroachment. Often, reservoir engineers mistakenly use the depletion-drive material balance equation to analyze data obtained from a water-drive reservoir since the

aquifer response is not clearly seen. This mistake leads to erroneous estimation of the OGIP.

In this study, we first aim to investigate the error obtained from using the depletion-drive material balance equation to determine OGIP in water-drive gas reservoirs. The second objective is to investigate the effect of parameters on the accuracy of OGIP estimation when the water-drive material balance equation is applied. The third objective is to investigate the feasibility of OGIP estimation if the aquifer size is unknown.

1.2 Objectives

- 
- a) To evaluate the accuracy of depletion-drive material balance equation in OGIP estimation in water-drive gas reservoirs
 - b) To evaluate the effect of permeability, aquifer size, shut-in duration, water influx model and amount of historical data on the accuracy of water-drive material balance equation
 - c) To evaluate the accuracy of OGIP estimation in water-drive gas reservoirs with unknown aquifer size

1.3 Outline of Thesis

This thesis consists of seven chapters as follows:

Chapter 1, Introduction, provides the background of OGIP estimation in water drive gas reservoirs and the objectives of this thesis.

Chapter 2, Literature Review, introduces previous studies that are related to water-drive gas reservoir behavior, water influx calculation and OGIP estimation in water-drive gas reservoirs.

Chapter 3, Theory and Concept, presents the detailed concept and calculation steps of material balance equations and water influx models.

Chapter 4, Thesis Methodology, presents the detailed method and the values of parameters to be studied in each section.

Chapter 5, Reservoir Simulation Model, provides the details of the reservoir simulation model construction.

Chapter 6, Results and Discussions, presents the results from the simulation and the discussions on the effect of each parameter.

Chapter 7, Conclusions and Recommendations, provides the conclusions and recommendations of this thesis.



CHAPTER 2

LITERATURE REVIEW

2.1 Material Balance Equation in Water-drive Gas Reservoir

Elahmady and Wattenbarger [1] observed some field production data that the p/z versus G_p plots in some water-drive gas reservoirs yielded a straight line like depletion-drive gas reservoirs, especially at the early time. This phenomenon can cause the misinterpretation in reservoir drive mechanism and significant overestimation in OGIP. They also simulated some synthetic water-drive gas reservoirs to show that the combination of the unsteady state nature of the aquifers and certain rate schedules can yield a straight line in p/z versus G_p plot.

2.2 Water Influx Models

van Everdingen and Hurst [2] applied the Laplace transformation to solve the diffusivity equation of the flow of water from an aquifer to a reservoir in an unsteady state condition. Two sets of solutions are developed, the first one is the constant terminal pressure case and the second one is the constant terminal rate case. In the constant terminal pressure case, the terminal boundary pressure is assumed to be zero at time zero onward, the cumulative amount of fluid flowing across the boundary can be calculated as a function of time. In the constant terminal rate case, a unit rate of fluid is assumed to flow across the boundary from time zero onward. The cumulative pressure drop can be calculated as a function of time. The solutions of constant terminal pressure case are used for water influx calculation. This calculation technique provides accurate results but superposition calculation is required.

Fetkovich [3] proposed a method to calculate the water influx by utilizing the pseudosteady-state aquifer productivity index and the material balance equation on

the aquifer. This method is simple and requires no superposition calculation since the water influx problem is separated into a rate equation and a material balance equation. The concept of flow from an aquifer into a reservoir is the same as the flow from a reservoir into a wellbore. Therefore, this method cannot be applied for an infinite aquifer and a very large finite aquifer because the initial transient flow period is long.

Carter and Tracy [4] developed a method for water influx calculation that requires no superposition calculation and is more simple than the method of van Everdingen and Hurst. This method applies the assumption of constant water influx rate in finite time periods. The accuracy of this method is close to the method of van Everdingen and Hurst.

2.3 Polynomial Approach to van Everdingen-Hurst Dimensionless Variables

Accurate values of p_D , p_D' and q_D for either the finite or infinite radial aquifer were obtainable using Klins et al. [5] polynomial approximations, which could produce solutions up to 15 times faster than traditional table lookup. The method require no interpolation because r_D and t_D implicit in the calculations. Six sets of polynomial were proposed. Using the polynomials to calculate values of p_D for finite and infinite aquifers yielded less than 0.03 and 0.02% average absolute errors when compared to values calculated by the numerically correct solutions. Similarly, the results from calculating finite and infinite q_D estimates differed from their numerically correct counterparts by less than 0.10 and 0.05%, respectively, in terms of average absolute errors.

2.4 Material Balance Equation in Water-drive Gas Reservoir with Unknown Aquifer Properties

A graphical method for estimating OGIP in finite water-drive gas reservoirs was proposed by Abdul-Majeed [6]. His method does not require information on aquifer

and rock properties. Analyzing van Everdingen and Hurst model, Abdul-Majeed found that when the value of the ratio between aquifer radius to reservoir radius (r_e/r_o) was less than six, the dimensionless water influx hardly altered when there was an increase in dimensionless time. The reservoir reached the steady state flow condition in a very short time. At such state, the dimensionless water influx become independent of time and was related only to r_e/r_o . From the observation, the material balance equation was rearranged into a linear form, with slope equals to the reciprocal of OGIP ($1/G$). The method can find both the size of aquifer from axis intercept and the time to reach pseudo steady state flow conditions. Usable only for water-drive gas reservoirs with r_e/r_o less than six, the method was verified by a good result from an actual case.

A technique for finding both the OGIP and aquifer performance was proposed by Vega and Wattenbarger [7]. Their approach requires no prior knowledge of aquifer properties and geometry. Aquifer influence functions (AIF) and the normalized absolute error function (A_N) were utilized. To verify the technique, synthetic data were used. Many OGIP values were assumed and then used to calculate A_N , which was minimized by optimizing AIF. The minimum A_N corresponded to the actual or optimum OGIP. The values of A_N could be very low and almost identical for different assumed OGIP values in the low region. A minimum value could almost always be identified. There was a risk for data set that led to non-unique solutions, but such risk was small.

Chen et al. [8] developed a technique that material balance for a gas reservoir and van Everdingen & Hurst water influx model were solved simultaneously to estimate OGIP and aquifer properties. They applied this technique to a water-drive gas reservoir in Port Arthur field in Texas, U.S.A. A plot between G_o and $W_e E/(1-E/E_i)$ was generated. If the correct R_{eD} was used for water influx calculation, the plot would be a straight line. If the other properties such as porosity, permeability, thickness and water encroachment angle were correct, the slope of the straight line should be equal to 1. Since many aquifer properties were unknown, trial and error was required. The simplex search method was applied to establish an automatic parameter adjusting method. The estimated OGIP of the water-drive gas reservoir was close to a unique solution of 60.6 BCF even many different combinations of aquifer properties were

obtained. In order to verify the estimated OGIP, a numerical simulator was used to match the production history. The estimated OGIP from reservoir simulation was 56.2 BCF which was close to 60.6 BCF.

A new method for determining OGIP from depletion performance data in water-drive gas reservoirs without aquifer geometry or properties required was presented by Gajdica et al. [9] Their method was applied to 32 gas reservoirs and provided better results than the steady-state and unsteady-state methods. The inputs of this method are monthly gas production and shut-in bottomhole pressure (SBHP). Aquifer influx is determined by material balance equation. Linear programming (LP) is used to match the aquifer behavior. Various OGIP assumptions are tried until the optimal value is found. The method assumes the uniform pressure throughout the reservoir and equal to the pressure at the original gas-water contact (GWC). The aquifer influence function is defined as the response of reservoir pressure at the GWC to a unit rate of water influx. The reservoir pressure can be represented by SBHP, and the water influx rate can be determined by a material balance equation based on the withdrawal rates of the reservoir. Then, aquifer influence function can be calculated by applying linear programming technique. The optimum aquifer influence function yields the minimum of the sum of the difference between observed and calculated pressures. For the months without measured SBHP, the reservoir pressure is estimated by linear interpolation on p/z plot. For each assumed OGIP, aquifer influx is calculated. Then, aquifer influence function is calculated by linear programming technique. These steps are repeated for various assumed OGIP until the OGIP that yields the minimum error is found.

Bhuiyan et al. [10] presented a new approach to determine original hydrocarbon in place (OHIP), aquifer constant and water influx from pressure and production history without requirement of pre-selection of water influx models. This approach rearranges the material balance equation in order to calculate an aquifer constant from OHIP, reservoir pressure, time, cumulative production, etc. The correct OHIP is the one that yield the same value of aquifer constant for a given period of time. First of all, an OHIP value needs to be assumed. Then, the aquifer constant and

water influx for each time will be calculated. Least square technique is applied to the calculated aquifer constant values and the corresponding time period to find a correlation coefficient. When the correct OHIP is found, the corresponding correlation coefficient value will be the highest value and approach to unity. This proposed technique was successfully verified with more than 40 reservoirs.



CHAPTER 3

THEORY AND CONCEPT

The theory and calculation of material balance equations for dry-gas reservoirs and the selected water influx models are represented in this chapter. This chapter includes the concept of reservoir simulation also.

3.1 Material Balance Equations

Material balance is an effective technique for estimating OGIP. Material balance equation upholds the principle of mass conservation. Although this technique can only be applied after production, it estimates only the gas volumes that are in pressure communication, which are the amount likely to be partially recovered by the producing wells. Material balance can provide a clear understanding of the predominant reservoir drive mechanism if adequate production and pressure histories are available. For a volumetric dry-gas reservoir that has gas expansion as its primary reservoir drive mechanism, a plot of p/z vs. G_p will be a straight line. Deviations from this straight line are signs of other internal or external energy sources.

3.1.1 Depletion-Drive Dry-Gas Reservoirs

Since volumetric reservoirs are completely enclosed, they receive no external energy from aquifer or other sources. The dominant drive mechanism is gas expansion as the reservoir pressure declines (rock and connate water expansions are considered to be negligible). Because gases can be as much as 100 or even 1,000 times more compressible than liquids, gas expansion is a very efficient drive mechanism. Recovery factor can be up to 90% of OGIP.

Reservoir PV is assumed to be constant over the producing life of the reservoir. Using the single tank model, material balance equation is shown in Eq 3.1.

$$GB_{gi} = (G - G_p)B_g \quad \text{--- (3.1)}$$

where

G	= original gas in place
G_p	= cumulative gas production
B_{gi}	= gas formation volume factor at initial reservoir pressure
B_g	= gas formation volume factor after gas production
GB_{gi}	= reservoir PV occupied by gas at initial reservoir pressure
$(G - G_p)B_g$	= reservoir PV occupied by gas after gas production

Eq. 3.1 can be rearranged as

$$G_p = G \left(1 - \frac{B_{gi}}{B_g} \right) \quad \text{--- (3.2)}$$

If we substitute B_{gi}/B_g with $(z_i p)/(z p_i)$, into Eq. 3.2, we obtain an equation in terms of surface gas production and reservoir pressure:

$$G_p = G \left(1 - \frac{z_i p}{z p_i} \right) \quad \text{--- (3.3)}$$

where

p_i	= initial reservoir pressure
p	= reservoir pressure after gas production
z_i	= gas compressibility factor at initial reservoir pressure
z	= gas compressibility factor after gas production

We can rewrite Eq. 3.3 as

$$\frac{p}{z} = \frac{p_i}{z_i} \left(1 - \frac{G_p}{G} \right) = \frac{p_i}{z_i} - \frac{p_i}{z_i G} G_p \quad \text{--- (3.4)}$$

A plot of p/z vs. G_p will be a straight line for volumetric gas reservoir as depicted in Figure 3.1. OGIP is the x-intercept.

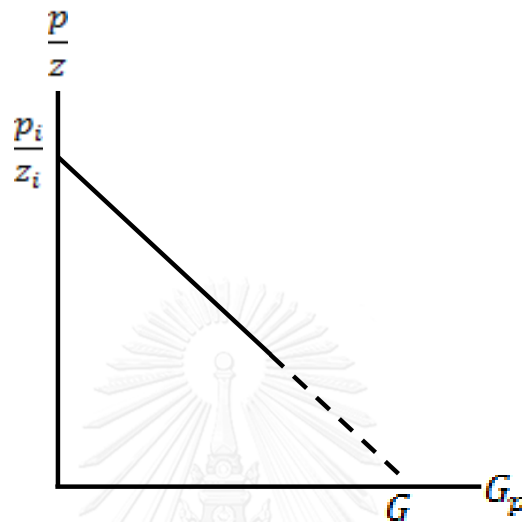


Figure 3.1 Plot of p/z vs. G_p

3.1.2 Water-Drive Dry-Gas Reservoirs

If there is water influx into the reservoir, the reservoir PV occupied by the gas at initial conditions is reduced by an amount equal to the volume of encroaching water. Material balance calculations must therefore take into account such reduction. Eq. 3.5 shows the new material balance equation.

$$GB_{gi} = (G - G_p)B_g + \Delta V_p \quad \text{--- (3.5)}$$

where

GB_{gi} and $(G - G_p)B_g$ are the same as Eq. 3.1

ΔV_p = change in reservoir PV occupied by gas at later conditions due to encroaching water

The change in gas pore volume is affected by both water influx and produced water:

$$\Delta V_p = W_e - W_p B_w \quad \text{--- (3.6)}$$

where

W_e = cumulative water influx

W_p = cumulative water production

B_w = water formation volume factor

Combining Eq. 3.5 and 3.6 results in

$$GB_{gi} = (G - G_p)B_g + W_e - W_p B_w \quad \text{--- (3.7)}$$

which can be rearranged to yield

$$\frac{G_p B_g + W_p B_w}{(B_g - B_{gi})} = G + \frac{W_e}{(B_g - B_{gi})} \quad \text{--- (3.8)}$$

From Eq. 8, if the major reservoir drive mechanism is water influx, $[(G_p B_g) + (W_p B_w)] / (B_g - B_{gi})$ vs. $W_e / (B_g - B_{gi})$ will be plotted as a straight line with a slope equal to one and an intercept equal to G as illustrated in Figure 3.2. A water influx model affects the functional form of W_e . Any water influx model, such as steady state, unsteady state, or pseudosteady state, can be used.

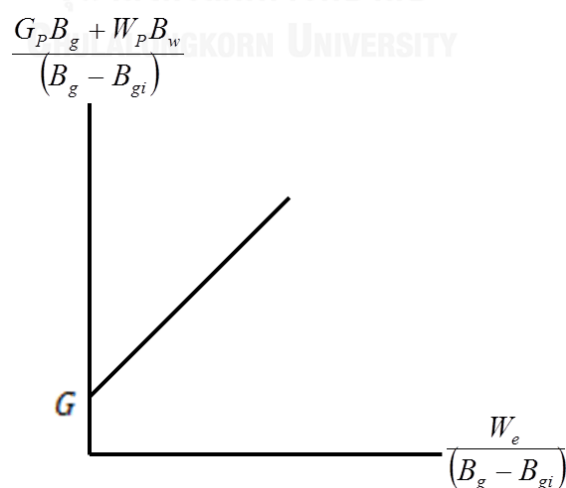


Figure 3.2 Plot of $[(G_p B_g) + (W_p B_w)] / (B_g - B_{gi})$ vs. $W_e / (B_g - B_{gi})$

3.2 Cole Plot [11]

Depletion-drive and water-drive gas reservoirs can be distinguished using Cole plot. From the material balance equation for gas reservoirs in Eq. 3.8, Cole [11] proposed plotting the term $G_p B_g / (B_g - B_{gi})$ on the y-axis and the corresponding cumulative gas production on the x-axis.

In depletion-drive gas reservoirs, the term $(W_e - W_p B_w) / (B_g - B_{gi})$ becomes zero and the plot is horizontal line with the y-intercept equal to OGIP. If the reservoir is water-drive, the same term does not go to zero and the plot will have some slope and will be above the depletion drive line.

For water-drive reservoir, Cole proposed that value of OGIP can be obtained from extrapolating back the plot to the y-intercept. But this method is not suitable for estimating OGIP because the correct line slope is very hard to find. Nevertheless, the technique is still useful for distinguishing between depletion drive and water-drive reservoirs.

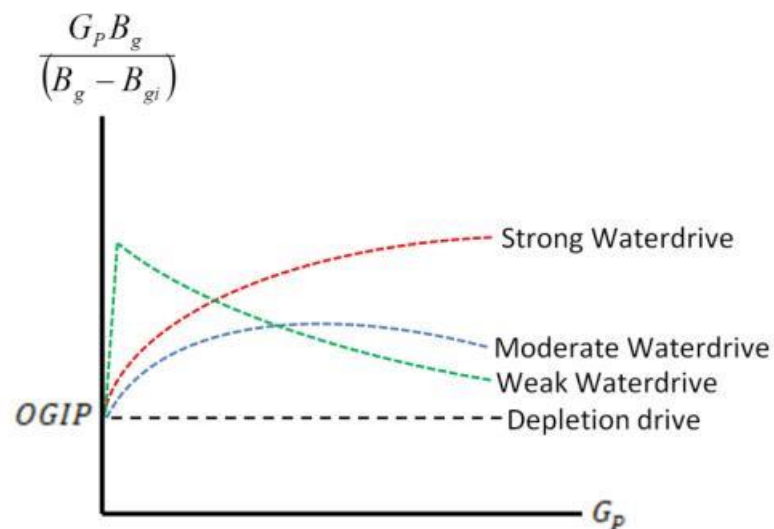


Figure 3.3 Cole plots in water-drive and depletion-drive reservoirs (after Dake [12])

Figure 3.3 shows different types of water-drive curves and depletion-drive curve. Under a weak water-drive, term $G_p B_g / (B_g - B_{gi})$ decreases with time unlike that of a strong or

moderate water-drive. Before its slope becomes negative, the weak water-drive plot has a short period of positive slope. Points in this early stage of reservoir life are easily scattered if there are errors in pressure measurement. Therefore, it is difficult to use such plot to establish OGIP.

3.3 Water Influx Models

The concept and detailed calculation of the selected water influx models for this thesis are shown in this section.

3.2.1 Simple Aquifer Model

Eq. 3.9 shows a simple aquifer model for an aquifer with similar size as the reservoir itself. Since the aquifer is considered to be relatively small, it is assumed that a pressure drop in the reservoir is immediately transmitted throughout the entire reservoir-aquifer system. The amount of water influx, W_e , can be calculated as:

$$W_e = \bar{c}W\Delta p \quad \text{--- (3.9)}$$

where

\bar{c} = total aquifer compressibility ($c_w + c_f$)

W = total volume of water in the aquifer

Δp = pressure drop at the original reservoir-aquifer boundary

3.2.2 van Everdingen & Hurst Model [2]

The flow from an aquifer into a cylindrical reservoir can be represented by the flow equation for oil into a wellbore, with the only difference in the term of radial scale. When an oil well starts producing at a constant rate, q , and before the reservoir boundary effects are felt, the pressure response at the wellbore can be described under transient flow condition. As time increases, the flow may change to late transient flow and semi steady state flow condition. The general equation for calculating the wellbore pressure at any flow condition is

$$p_D(t_D) = 2\pi_{DA} + \frac{1}{2} \ln \frac{4t_D}{\gamma} - \frac{1}{2} p_{D(MBH)}(t_{DA}) \quad \text{--- (3.10)}$$

where

$$p_D(t_D) = \frac{2\pi kh}{q\mu} (p_i - p_{wf}) \quad \text{--- (3.11)}$$

which is the dimensionless pressure function for the constant terminal rate case. It determines the pressure drop at r_w caused by a rate change from zero to q at the inner boundary at time $t = 0$.

Oppositely, influx is calculated as a function of a given pressure drop at the inner boundary of the system. Hurst and van Everdingen [2] applied the Laplace transformation to solve the radial diffusivity equation for the aquifer-reservoir system. Applying dimensionless variables the equation can be written as

$$\frac{1}{r_D} \frac{\partial}{\partial r_D} \left(r_D \frac{\partial p_D}{\partial r_D} \right) = \frac{\partial p_D}{\partial t_D} \quad \text{--- (3.12)}$$

where

$$r_D = \frac{r}{r_o} \quad \text{--- (3.13)}$$

and

$$t_D = \frac{kt}{\phi\mu cr_o^2} \quad \text{--- (3.14)}$$

where

\emptyset = aquifer porosity

r_o is the outer radius of the reservoir and all the other parameters in Eq. 3.13 and 3.14 refer to aquifer properties.

Hurst and van Everdingen [2] derived constant terminal pressure solutions for Eq. 3.12 in terms of the dimensionless influx rate defined by:

$$q_D(t_D) = \frac{q\mu}{2\pi kh\Delta p} \quad \text{--- (3.15)}$$

where $q_D(t_D)$ is the dimensionless influx rate evaluated at $r_D = 1$ and describes the change in rate from zero to q due to a pressure drop Δp applied at the outer reservoir boundary r_o at time $t = 0$. Integrating Eq. 3.15 with respect to time results in Eq. 3.16.

$$\frac{\mu}{2\pi kh\Delta p} \int_0^t q dt = \int_0^{t_D} q_D(t_D) \frac{dt}{dt_D} dt_D \quad \text{--- (3.16)}$$

which gives

$$\frac{W_e \mu}{2\pi kh\Delta p} = W_D(t_D) \frac{\phi \mu \bar{c} r_o^2}{k} \quad \text{--- (3.17)}$$

and therefore

$$W_e = 2\pi \phi \bar{h} \bar{c} r_o^2 \Delta p W_D(t_D) \quad \text{--- (3.18)}$$

where

W_e = cumulative water influx due to a pressure drop Δp at r_o at $t = 0$

$W_D(t_D)$ = dimensionless cumulative water influx function giving the dimensionless influx per unit pressure drop imposed at the reservoir-aquifer boundary at $t = 0$

Eq. 3.18 is often expressed as

$$W_e = U \Delta p W_D(t_D) \quad \text{--- (3.19)}$$

where U is the aquifer constant for radial geometry

$$U = 2\pi f \bar{\phi} h c r_o^2 \quad \text{--- (3.20)}$$

and

$$f = \frac{(\text{encroachment angle})^\circ}{360^\circ} \quad \text{--- (3.21)}$$

For radial aquifers, W_D is regularly presented in tabular form or as a set of polynomial expressions as a function of t_D for a range of ratios of the aquifer to reservoir radius $r_{eD} = r_e/r_o$.

Different aquifer geometries require different calculations of the dimensionless time and aquifer constant.

3.2.2.1 Radial Aquifer Geometry

For radial reservoir-aquifer system as shown in Figure 3.4, the dimensionless time and aquifer constant can be calculated from Eq. 3.22 and Eq. 3.23, respectively.

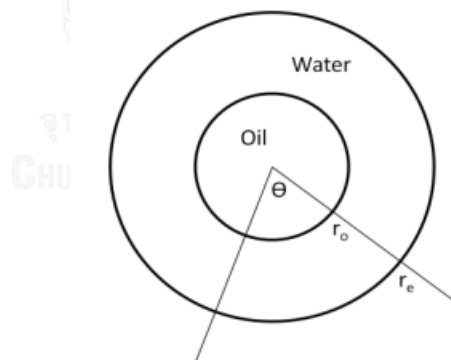


Figure 3.4 Radial aquifer geometry

$$t_D = \frac{kt}{\bar{\phi} \mu c r_o^2} \quad \text{--- (3.22)}$$

$$U = 2\pi f \bar{\phi} h c r_o^2 \quad \text{--- (3.23)}$$

3.2.2.2 Linear Aquifer Geometry

The dimensionless time and aquifer constant of linear reservoir-aquifer system, Figure 3.5, can be calculated from Eq. 3.24 and Eq. 3.25, respectively.

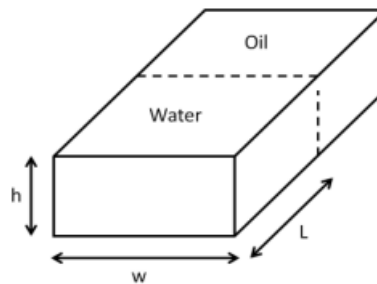


Figure 3.5 Linear aquifer geometry

$$t_D = \frac{kt}{\phi\mu cL^2} \quad \text{--- (3.24)}$$

$$U = wLh\phi c \quad \text{--- (3.25)}$$

Depending on whether the aquifer is bounded or infinite, characteristics of the plots of W_D versus t_D can vary.

3.2.2.3 Bounded Aquifer

There is a value of t_D for which the dimensionless water influx reaches a constant maximum value, regardless of the geometry. As shown in Eq. 3.26 and 3.27, the value depends on the geometry.

$$\text{Radial:} \quad W_D(\max) = \frac{1}{2} (r_{eD}^2 - 1) \quad \text{--- (3.26)}$$

$$\text{Linear:} \quad W_D(\max) = 1 \quad \text{--- (3.27)}$$

Once the plateau level of W_D has been achieved, the minimum value of t_D at this point is large enough for the instantaneous pressure drop Δp to be felt throughout the aquifer.

3.2.2.4 Infinite Aquifer

For this case, because the water influx is governed by transient flow conditions, W_D does not reach its maximum value. For radial aquifer, values of W_D can be obtained from the graphs for $r_{eD} = \alpha$. For an infinite linear aquifer, however, the plot of W_D is not available. Instead, the cumulative water influx can be obtained directly using Eq. 3.28.

$$W_e = 2hw \sqrt{\frac{\phi k \bar{c} t}{\pi \mu}} \Delta p \quad \text{--- (3.28)}$$

When doing the history matching of observed reservoir pressure, the theory needs to be extended to calculate the cumulative water influx that corresponds to a continuous pressure drop at the reservoir-aquifer boundary. It is a common practice to split the continuous decline into a series of discrete pressure steps. The water influx can then be calculated from the pressure drop between each step, Δp , using Eq. 3.19. Superposition of the separate influxes, with respect to time, yields the cumulative water influx.

Figure 3.6 shows the recommended method for approximating the continuous pressure decline into a series of pressure steps.

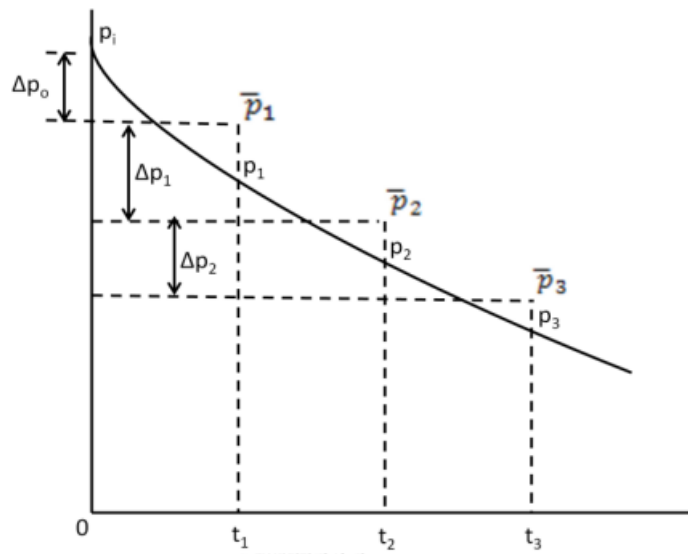


Figure 3.6 Series of discrete pressure steps

Assuming that the observed reservoir pressures are equal to the pressures at the original hydrocarbon-water contact, let their pressure values be $p_i, p_1, p_2, p_3, \dots$ etc., at times $0, t_1, t_2, t_3, \dots$ etc. The following equation calculates the average pressure levels during the time intervals.

$$\begin{aligned} \bar{p}_1 &= \frac{p_i + p_1}{2} \\ \bar{p}_2 &= \frac{p_1 + p_2}{2} \\ \bar{p}_j &= \frac{p_{j-1} + p_j}{2} \end{aligned} \quad \text{--- (3.29)}$$

The pressure drops at times $0, t_1, t_2, \dots$ etc. are

$$\begin{aligned} \Delta p_0 &= p_i - \bar{p}_1 = p_i - \frac{p_i + p_1}{2} = \frac{p_i - p_1}{2} \\ \Delta p_1 &= \bar{p}_1 - \bar{p}_2 = \frac{p_i + p_1}{2} - \frac{p_1 + p_2}{2} = \frac{p_i - p_2}{2} \\ \Delta p_2 &= \bar{p}_2 - \bar{p}_3 = \frac{p_1 + p_2}{2} - \frac{p_2 + p_3}{2} = \frac{p_1 - p_3}{2} \\ \Delta p_j &= \bar{p}_j - \bar{p}_{j+1} = \frac{p_{j-1} + p_j}{2} - \frac{p_j + p_{j+1}}{2} = \frac{p_{j-1} - p_{j+1}}{2} \end{aligned} \quad \text{--- (3.30)}$$

Superposition is required to calculate the value of W_e at some arbitrary time T , which corresponds to the end of the n^{th} time step.

$$W_e(T) = U[\Delta p_0 W_D(T_D) + \Delta p_1 W_D(T_D - t_{D1}) + \Delta p_2 W_D(T_D - t_{D2}) + \dots + \Delta p_{n-1} W_D(T_D - t_{Dn-1})] \quad \text{--- (3.31)}$$

where Δp_j is the pressure drop at time t_j , given by Eq. 3.30, and $W_D(T_D - t_{Dj})$ is the dimensionless cumulative water influx, for the dimensionless time $T_D - t_{Dj}$ during which the effect of the pressure drop is felt. Summing the terms in the above equation yields

$$W_e(T) = U \sum_{j=0}^{n-1} \Delta p_j W_D(T_D - t_{Dj}) \quad \text{--- (3.32)}$$

For an infinite, linear aquifer, the cumulative water influx at time T due to a step-like pressure decline at the aquifer-reservoir boundary can be calculated using Eq. 3.28 as

$$W_e(T) = 2hw \sqrt{\frac{\phi k c}{\pi \mu}} \sum_{j=0}^{n-1} \Delta p_j \sqrt{T - t_j} \quad \text{--- (3.33)}$$

3.2.3 Fetkovich Model [3]

In this approach, the flow of aquifer water into a reservoir is modeled in exactly the same way as the flow of oil from a reservoir into a well. An inflow equation is:

$$q_w = \frac{dW_e}{dt} = J(\bar{p}_a - p) \quad \text{--- (3.34)}$$

where

- q_w = water influx rate
- J = aquifer productivity index
- p = reservoir pressure, i.e. pressure at the gas water contact
- \bar{p}_a = average aquifer pressure

Eq. 3.34 is evaluated using the simple aquifer model

$$W_e = \bar{c}W_i(p_i - \bar{p}_a) \quad \text{--- (3.35)}$$

where p_i is the initial pressure in the aquifer and reservoir. Eq. 3.35 can be rearranged as

$$\bar{p}_a = p_i \left(1 - \frac{W_e}{\bar{c}W_i p_i} \right) = p_i \left(1 - \frac{W_e}{W_{ei}} \right) \quad \text{--- (3.36)}$$

where $W_{ei} = \bar{c}W_i p_i$ is the initial amount of encroachable water. It also represents the maximum possible expansion of the aquifer. Differentiating Eq. 3.36 with respect to time yields

$$\frac{dW_e}{dt} = -\frac{W_{ei}}{p_i} \frac{d\bar{p}_a}{dt} \quad \text{--- (3.37)}$$

Substituting Eq. 3.37 into Eq. 3.34, we then have

$$\frac{d\bar{p}_a}{\bar{p}_a - p} = -\frac{Jp_i}{W_{ei}} dt \quad \text{--- (3.38)}$$

Integrating Eq. 3.38 by assuming the boundary pressure p stays constant over the period of interest, for the initial condition at $t = 0$ ($W_e = 0$, $\bar{p}_a = p_i$), with a pressure drop $\Delta p = p_i - p$ at the reservoir boundary, results in

$$\ln(\bar{p}_a - p) = -\frac{Jp_i t}{W_{ei}} + C \quad \text{--- (3.39)}$$

where $C = \ln(p_i - p)$, and therefore

$$\bar{p}_a - p = (p_i - p)e^{-Jp_i t / W_{ei}} \quad \text{--- (3.40)}$$

Applying this equation to Eq. 32 gives

$$\frac{dW_e}{dt} = J(p_i - p)e^{-Jp_i t / W_{ei}} \quad \text{--- (3.41)}$$

The following equation is constructed from integrating Eq. 3.41 for the stated initial conditions.

$$W_e = \frac{W_{ei}}{p_i} (p_i - p) \left(1 - e^{-Jp_i t / W_{ei}} \right) \quad \text{--- (3.42)}$$

As t tends to infinity, then Eq. 3.42 becomes

$$W_e = \frac{W_{ei}}{p_i} (p_i - p) = \bar{c} W_i (p_i - p) \quad \text{--- (3.43)}$$

which is the maximum amount of water influx that could occur after the pressure drop $p_i - p$ has been transmitted throughout the aquifer.

In actual use, the boundary pressure varies continuously according to time. Eq. 3.42, which was derived for a constant inner boundary pressure, is therefore not applicable. It seems necessary to apply the superposition theorem. However, Fetkovich showed that Eq. 3.42 can be expressed such that superposition is no longer required. For the influx during the first time step Δt_1 , Eq. 3.42 can be rewritten as

$$\Delta W_{e1} = \frac{W_{ei}}{p_i} (p_i - \bar{p}_1) \left(1 - e^{-J p_i \Delta t_1 / W_{ei}} \right) \quad \text{--- (3.44)}$$

where \bar{p}_1 is the average reservoir boundary pressure during the first time interval.

For the second interval,

$$\Delta W_{e2} = \frac{W_{ei}}{p_i} (\bar{p}_{a1} - \bar{p}_2) \left(1 - e^{-J p_i \Delta t_2 / W_{ei}} \right) \quad \text{--- (3.45)}$$

where \bar{p}_{a1} is the average aquifer pressure at the end of the first time interval and can be calculated by Eq. 3.36

$$\bar{p}_{a1} = p_i \left(1 - \frac{\Delta W_{e1}}{W_{ei}} \right) \quad \text{--- (3.46)}$$

The general equation for the n^{th} time period is

$$\Delta W_{en} = \frac{W_{ei}}{p_i} (\bar{p}_{an-1} - \bar{p}_n) \left(1 - e^{-J p_i \Delta t_n / W_{ei}} \right) \quad \text{--- (3.47)}$$

where

$$\bar{p}_{an-1} = p_i \left(1 - \frac{\sum_{j=1}^{n-1} \Delta W_{ej}}{W_{ei}} \right) \quad \text{--- (3.48)}$$

The values of \overline{p}_n , the average reservoir boundary pressure, are calculated, as

$$\overline{p}_n = \frac{P_{n-1} + P_n}{2} \quad \text{--- (3.49)}$$

Using Eq. 3.47 and 3.48 stepwise, Fetkovitch [3] showed that for various aquifer geometries of finite aquifers, the calculated water influx closely matched the results obtained using the unsteady state influx theory of Hurst and van Everdingen.

Values of aquifer productivity index J for each geometry and flow conditions are available in Table 3.1. It is assumed that the pressure at the external boundary of the aquifer is constant at its initial value p_i so it becomes unnecessary to keep updating the average pressure in the aquifer.

Table 3.1 Productivity index for each flow condition and aquifer geometry [3]

Flow Condition	Radial Aquifers Geometry	Linear Aquifers Geometry
Semi Steady State	$\frac{2\pi fkh}{\mu \left(\ln \frac{r_e}{r_o} - \frac{3}{4} \right)}$	$3 \frac{khw}{\mu L}$
Steady State	$\frac{2\pi fkh}{\mu \ln \frac{r_e}{r_o}}$	$\frac{khw}{\mu L}$

Referring to Eq. 3.41,

$$q_w = \frac{dW_e}{dt} = J(p_i - p) e^{-Jp_i t / W_{ei}} \quad \text{--- (3.41)}$$

in steady state case, W_{ei} is infinite and therefore

$$q_w = \frac{dW_e}{dt} = J(p_i - p) \quad \text{--- (3.50)}$$

The cumulative water influx after integration is

$$W_e = J \int_0^t (p_i - p) dt \quad \text{--- (3.51)}$$

J expressions presented in table 1 were derived under the assumption that $(r_w/r_e)^2$ was negligible. For small radial aquifers, this assumption is not always applicable. However, Fetkovitch model was shown to be applicable to the same degree as Hurst and van Everdingen model, even for values of r_{eD} as small as three.

For very large or infinite aquifers, transient flow conditions dictate the initial flow of water into the reservoir. During the transient flow period, it is impossible to derive a simple expression for J . Hence, Fetkovitch model becomes unusable.

3.2.4 Carter and Tracy Model [4]

van Everdingen and Hurst [2] developed the method for water influx calculation from the exact solutions to the radial diffusivity equation. Their method requires very complex calculations due to its need of superposition. Carter and Tracy [4] therefore proposed a direct calculation technique that does not require superposition.

The water influx process can be approximated using a series of constant rate influx intervals. Therefore, the cumulative water influx during the j^{th} interval can be written as

$$W_e(t_{Dj}) = \sum_{n=0}^{j-1} q_{Dn} (t_{Dn+1} - t_{Dn}) \quad \text{--- (3.52)}$$

Eq. 3.52 can be rewritten as

$$W_e(t_{Dj}) = \sum_{n=0}^{i-1} q_{Dn} (t_{Dn+1} - t_{Dn}) + \sum_{n=i}^{j-1} q_{Dn} (t_{Dn+1} - t_{Dn}) \quad \text{--- (3.53)}$$

or

$$W_e(t_{Dj}) = W_e(t_{Di}) + \sum_{n=i}^{j-1} q_{Dn} (t_{Dn+1} - t_{Dn}) \quad \text{--- (3.54)}$$

The cumulative water up to the j^{th} interval can be written as a function of variable pressure, using the convolution integral, as shown below:

$$W_e(t_{Dj}) = U \int_0^{t_{Dj}} \Delta p(\lambda) \frac{d}{d\lambda} [Q_{pD}(t - \lambda)] d\lambda \quad \text{--- (3.55)}$$

After combining Eq. 3.54 and 3.55 and performing Laplace transformation, the cumulative water influx is described below

$$W_{en} = W_{en-1} + (t_{Dn} - t_{Dn-1}) \left[\frac{U \Delta p_n - W_{en-1} P'_D(t_{Dn})}{P_D(t_{Dn}) - t_{Dn-1} P'_D(t_{Dn})} \right] \quad \text{--- (3.56)}$$

where U and t_D are the same variables as in the van Everdingen-Hurst model and

$$\Delta p_n = p_{a,i} - p_n$$

3.3 Numerical Simulation Concept

Reservoir simulators, dedicated computer programs, are used to simulate fluid flow in a reservoir. The programs perform mathematical calculation addressing the fluid flow within and between specified reservoir regions. With simulators, various production scenarios can be generated and their corresponding reservoir performances can be studied.

A simulator visualizes the reservoir as grids. Each grid block represents a volume in the reservoir that contains representative rock and fluids. The rock parameters are porosity, permeability, fluid saturations, relative permeability relationship, capillary pressure and compressibility. The fluid parameters are compressibility, solution gas/oil ratio, formation volume factor, density and viscosity.

The values of permeability, layer thickness, porosity, fluid content, elevation and pressure are needed in order to solve the fluid flow equation at each block face. The well data is then extrapolated into the inter-well reservoir volume.

CHAPTER 4

THESIS METHODOLOGY

The detailed methodology of this thesis is described in this chapter. The first step is the construction of the reservoir simulation model as described in Section 4.1. The second step is the selection of the analytical aquifer method in ECLIPSE 100 as shown in Section 4.2. After the reservoir simulation model with the selected analytical aquifer method is constructed, the production profile is generated by ECLIPSE 100. The generated production profile is used in W_e and OGIP estimation as described in Section 4.3 to 4.7.

4.1 Reservoir Simulation Model Construction

Step 1: Construct a hypothetical gas reservoir with a radial aquifer in a commercial reservoir simulator ECLIPSE 100. The selected reservoir and fluid properties are based on the generic values of dry-gas reservoirs.

Step 2: Assign a single well to produce gas from the reservoir. The well is opened for production for 30 consecutive days and then shut in for SBHP measurement alternatively until the abandonment. The measured shut-in SBHP is used to represent the reservoir pressure.

4.2 ECLIPSE 100 Analytical Aquifer Method Comparison

Step 1: Apply Fetkovich analytical aquifer and Carter & Tracy analytical aquifer as the radial aquifer in ECLIPSE 100.

Step 2: Compare the simulated W_e , SBHP, G_p and W_p from Fetkovich analytical aquifer and Carter & Tracy analytical aquifer.

The selected parameter to be studied is listed below:

- Aquifer size: 1 PV, 10 PV, 30 PV, 70 PV and 100 PV

4.3 Water Influx Model Comparison

Step 1: Calculate W_e from the simulated production profile by applying simple aquifer model, Fetkovich, van Everdingen & Hurst and Carter & Tracy water influx model.

Step 2: Compare the calculated W_e from Step 1 with the simulated W_e .

The selected parameter to be studied is listed below:

- Aquifer size: 1 PV, 10 PV, 30 PV, 70 PV and 100 PV

4.4 OGIP Estimation Using a Plot of p/z versus G_p for 50 mD and 500 mD Water-drive Dry-gas Reservoir

Step 1: Plot p/z versus G_p from the simulated production profile.

Step 2: Fit the p/z versus G_p plot with a straight line, the estimated OGIP is the x-intercept.

The selected parameters to be studied are listed below:

- Aquifer size: 0 PV, 1 PV, 10 PV, 30 PV, 70 PV and 100 PV
- Shut-in duration: 6 hours, 1 day and 7 days
- Amount of historical data: 25% RF, 50% RF and abandonment condition

The reasons for selecting these parameters are listed below:

- The aquifer size represents the level of pressure support from the aquifer.
- The shut-in duration affects the accuracy of SBHP on representing the actual reservoir pressure.
- The amount of historical data represents the availability of data used in material balance.

4.5 OGIP Estimation Using a Plot of $(G_p B_g + W_p B_w) / (B_g - B_{gi})$ versus $W_e / (B_g - B_{gi})$ for 50 mD Water-drive Dry-gas Reservoir

Step 1: Calculate W_e from the simulated production profiles by applying one of the water influx models

Step 2: Plot $(G_p B_g + W_p B_w) / (B_g - B_{gi})$ versus $W_e / (B_g - B_{gi})$ from the simulated production profiles and the calculated W_e from Step 1.

Step 3: Select the late time period before liquid loading of the plot and fit with a unit-slope straight line, the estimated OGIP is the y-intercept.

The selected parameters to be studied are listed below:

- Aquifer size: 1 PV, 10 PV, 30 PV, 70 PV and 100 PV
- Shut-in duration: 6 hours, 1 day and 7 days
- Water influx model: Simple aquifer model, Fetkovich model, van Everdingen & Hurst model and Carter & Tracy model
- Amount of historical data: 25% RF, 50% RF and abandonment condition (this parameter is applied only to the cases of van Everdingen & Hurst model)

4.6 OGIP Estimation Using a Plot of $(G_p B_g + W_p B_w)/(B_g - B_{gi})$ versus $W_e/(B_g - B_{gi})$ for 500 mD Water-drive Dry-gas Reservoir

Step 1: Calculate W_e from the simulated production profiles by applying van Everdingen & Hurst water influx model.

Step 2: Plot $(G_p B_g + W_p B_w)/(B_g - B_{gi})$ versus $W_e/(B_g - B_{gi})$ from the simulated production profiles and the calculated W_e from Step 1.

Step 3: Select the late time period before liquid loading of the plot and fit with a unit-slope straight line, estimated OGIP is the y-intercept.

The selected parameters to be studied are listed below:

- Aquifer size: 1 PV, 10 PV, 30 PV, 70 PV and 100 PV
- Shut-in duration: 6 hours, 1 day and 7 days
- Amount of historical data: 25% RF, 50% RF and abandonment condition

4.7 OGIP Estimation from Unknown Aquifer Size for 50 mD and 500 mD Water-drive Dry-gas Reservoir

Step 1: Assume a value of aquifer size and calculate W_e from the simulated production profiles by applying one of the water influx models

Step 2: Plot $(G_p B_g + W_p B_w)/(B_g - B_{gi})$ versus $W_e/(B_g - B_{gi})$ from the simulated production profiles and the calculated W_e from Step 1.

Step 3: Select the late time period before liquid loading of the plot and fit with a unit-slope straight line, the estimated OGIP of this assumed aquifer size is the y-intercept.

Step 4: Calculate R-squared value of the fitted unit-slope straight line.

Step 5: Change the assumed aquifer size and repeat step 1 to 4, the final estimated OGIP is corresponding to the assumed aquifer size that yield the maximum R-squared value.

The selected parameters to be studied are listed below:

- Aquifer size: 1 PV, 10 PV, 30 PV, 70 PV and 100 PV
- Water influx model: Simple aquifer model, Fetkovich model, van Everdingen & Hurst model and Carter & Tracy model (Only van Everdingen & Hurst water influx model is applied for 500 mD cases)



CHAPTER 5

RESERVOIR SIMULATION MODEL

In order to generate production data for a water-drive dry-gas reservoir, a hypothetical reservoir model with an aquifer was constructed in a commercial reservoir simulator ECLIPSE 100. The grid geometry and sizes along with other reservoir properties are shown in this chapter.

5.1 Reservoir Properties

Table 5.1 shows the reservoir properties to be used in the reservoir model for production data generating. Since the flow of fluid in a reservoir is typically radial, radial flow geometry was selected. The reservoir area is 2,544,690 ft² or 58 acres which is the normal size of gas reservoirs in the Gulf of Thailand. The horizontal permeability is based on well testing data and the ratio of vertical to horizontal permeability 0.1 is applied. The remaining reservoir properties are based on the mean statistical values of dry-gas reservoirs. The detail of ECLIPSE 100 input is shown in Appendix A.

Table 5.1 Reservoir properties

Parameters	Value
Grid geometry	Radial
Grid number	30 x 30 x 10
Grid size	30 ft x 12 deg x 5 ft
Reservoir area	2,544,690 ft ²
Reservoir thickness	50 ft

Table 5.1 Reservoir properties (continued)

Parameters	Value
Reservoir top depth	6000 ft
Initial reservoir pressure	3500 psia
Reservoir temperature	200 °F
Porosity	0.2
Initial water saturation	0.4
Original gas in place	3211 MMscf
Horizontal permeability	50 mD
Vertical permeability	5 mD

A radial water-drive gas reservoir model with a single well was constructed as shown in Figure 5.1. The red area represents the gas reservoir and the blue area represents the aquifer.

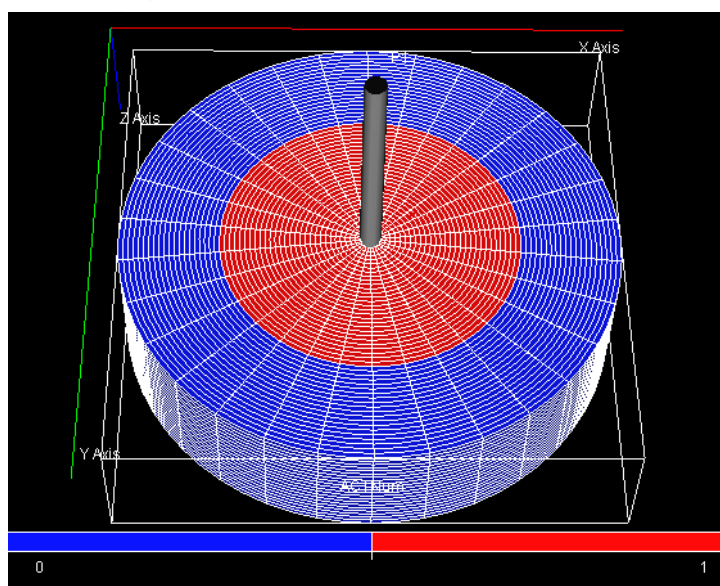


Figure 5.1 Radial water-drive gas reservoir model

5.2 PVT Properties

The selected gas specific gravity is 0.7. The gas PVT data in Table 5.2 were based on the correlations in ECLIPSE 100 reservoir simulator. The water and rock properties are shown in Table 5.3.

Table 5.2 Dry-gas PVT properties

Pressure (psia)	FVF (rb/Mscf)	Viscosity (cp)
600	5.24135	0.01382
768.42	4.03452	0.01407
936.84	3.26483	0.01436
1105.26	2.73275	0.01468
1273.68	2.34431	0.01503
1442.11	2.04941	0.01542
1610.53	1.81892	0.01584
1778.95	1.63469	0.01628
1947.37	1.48484	0.01676
2115.79	1.36123	0.01726
2284.21	1.25807	0.01778
2452.63	1.17115	0.01833
2621.05	1.09727	0.01889
2789.47	1.03401	0.01946
2957.89	0.97947	0.02004

Table 5.2 Dry-gas PVT properties (continued)

Pressure (psia)	FVF (rb/Mscf)	Viscosity (cp)
3114.16	0.93533	0.02059
3294.74	0.8908	0.02122
3500	0.84715	0.02194
3631.58	0.82243	0.0224
3800	0.79396	0.02298

Table 5.3 Water and rock properties at reference pressure 3500 psia

Parameters	Value
Water formation volume factor	1.020998 rb/stb
Water compressibility	$3.06298 \times 10^{-6} \text{ psi}^{-1}$
Water viscosity	0.3018746 cp
Rock compressibility	$1.529896 \times 10^{-6} \text{ psi}^{-1}$

5.3 Well Characteristics and Production Limitations

Well characteristics, operating conditions and abandonment condition are shown in Table 5.4. The selected minimum tubing head pressure is 400 psia based on the platform pipeline pressure in the Gulf of Thailand. The selected abandonment gas rate is 0.2 MMscfd based on the measurement range of the general gas flow meter in test separator.

Table 5.4 Well characteristics, operating conditions and abandonment condition

Parameters	Value
Wellbore diameter	6.5 in
Skin	0.4
Tubing inside diameter	2.441 in
Tubing roughness	0.0006 in
Tubing head pressure	400 psia
Maximum gas rate	2 MMscfd
Abandonment gas rate	0.2 MMscfd

5.4 SCAL

The relative permeability to gas and water are shown in Figure 5.2 and Figure 5.3, respectively. The residual gas saturation is 0.2. The connate water saturation is 0.4. Capillary pressure is neglected.

SGFN (Gas Saturation Functions)

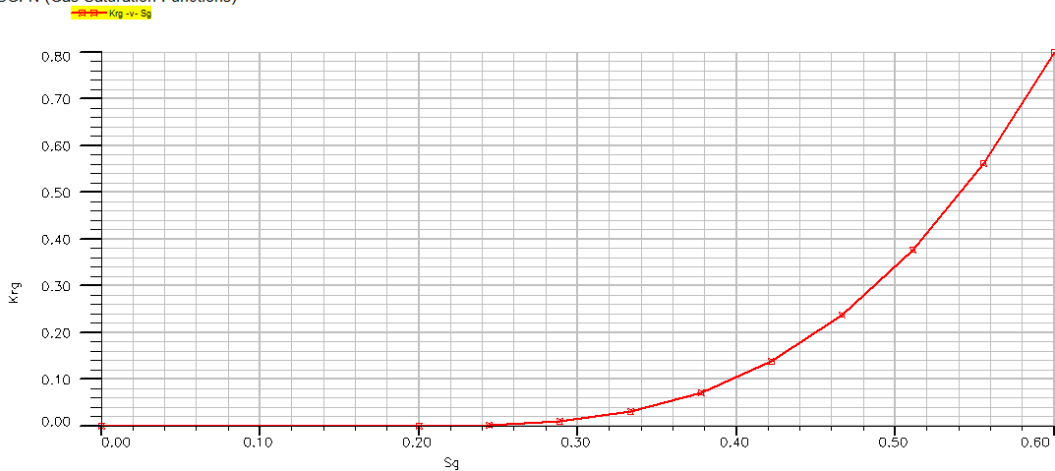


Figure 5.2 The relative permeability to gas

SWFN (Water Saturation Functions)

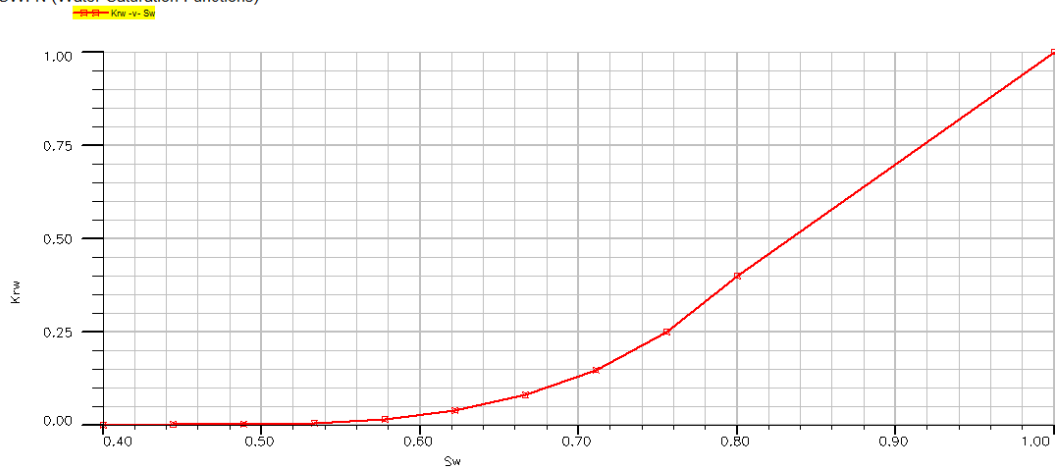


Figure 5.3 The relative permeability to water

5.5 VFP

Vertical lift performance was generated from PROSPER. The gas flow in 2.441” tubing for various water-gas ratios and tubing head pressures as shown in Table 5.5 from top of the reservoir depth to surface was simulated. The detail of PROSPER input is shown in Appendix B.

Table 5.5 Parameters used in VFP table calculation

Tubing head pressure (psia)	Water gas ratio (stb/MMscf)
399.7	0
745.8	111.11
1091.9	222.22
1438	333.33
1784.1	444.44
2130.3	555.56
2476.4	666.67

Table 5.5 Parameters used in VFP table calculation (continued)

Tubing head pressure (psia)	Water gas ratio (stb/MMscf)
2822.5	777.78
3168.6	888.89
3514.7	1000



CHAPTER 6

RESULTS AND DISCUSSIONS

The results and discussions are described in this chapter. The comparison of analytical aquifer methods in ECLIPSE 100 is shown in Section 6.1. The effects of aquifer size and permeability on the reservoir behavior are discussed in Section 6.2 and Section 6.3. Section 6.4 represents the comparison of water influx models. Section 6.5 to Section 6.8 show the results and discussions about the effects of aquifer size, permeability, shut-in duration, water influx model and amount of historical data on OGIP estimation. The results of OGIP estimation from unknown aquifer size are discussed in Section 6.9.

6.1 ECLIPSE 100 Analytical Aquifer Method Comparison

There are 2 analytical aquifer methods in ECLIPSE 100 which are Fetkovich and Carter & Tracy analytical aquifer methods. The objective of this section is to compare the simulation result from these 2 analytical aquifer methods.

Table 6.1 shows the parameters to study the effect of analytical aquifer methods in ECLIPSE 100 on simulation result. The reservoir permeability and shut-in duration for SBHP measurement for all these cases are 50 mD and 1 day, respectively.

Table 6.1 Parameters to be studied on the effect of analytical aquifer methods

Case	Aquifer size (PV)	Analytical aquifer method
1	1	Fetkovich
2		Carter & Tracy
3	10	Fetkovich
4		Carter & Tracy

Table 6.1 Parameters to be studied on the effect of analytical aquifer methods
(continued)

Case	Aquifer size (PV)	Analytical aquifer method
5	30	Fetkovich
6		Carter & Tracy
7	70	Fetkovich
8		Carter & Tracy
9	100	Fetkovich
10		Carter & Tracy

Figure 6.1 to Figure 6.5 illustrate that Fetkovich and Carter & Tracy analytical aquifer methods in ECLIPSE 100 give very similar values of W_e , SBHP, G_p and W_p for all aquifer sizes. Fetkovich analytical aquifer method in ECLIPSE 100 was selected for this thesis due to more convenient data input process.

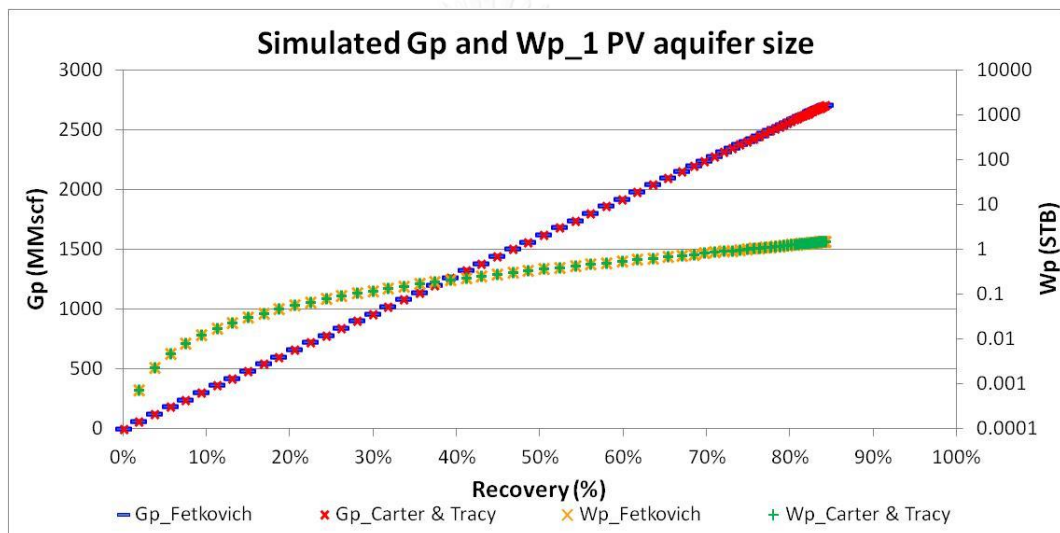
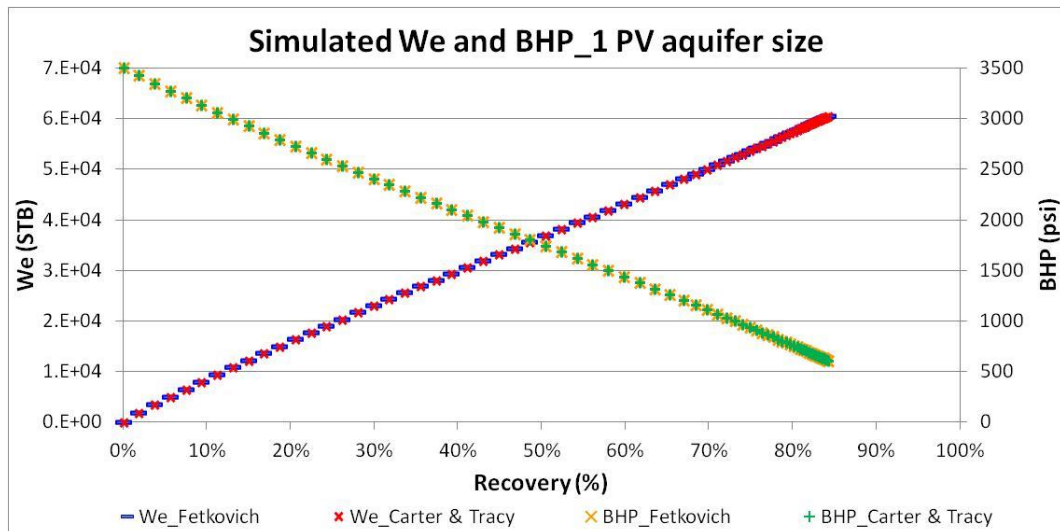


Figure 6.1 Simulated W_e , $SBHP$, G_p and W_p versus %RF at 1-PV aquifer size, case 1-2

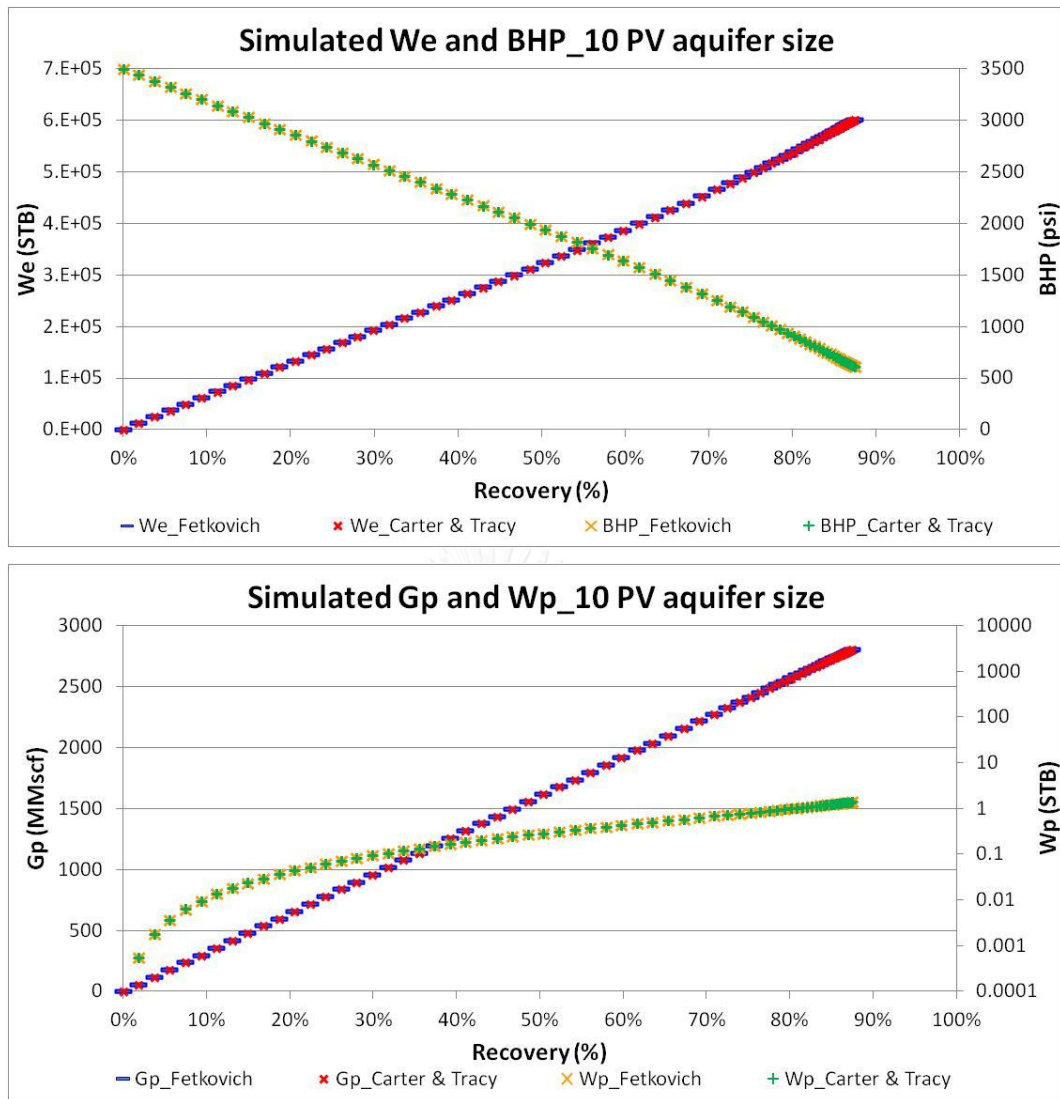


Figure 6.2 Simulated W_e , $SBHP$, G_p and W_p versus %RF at 10-PV aquifer size, case 3-4

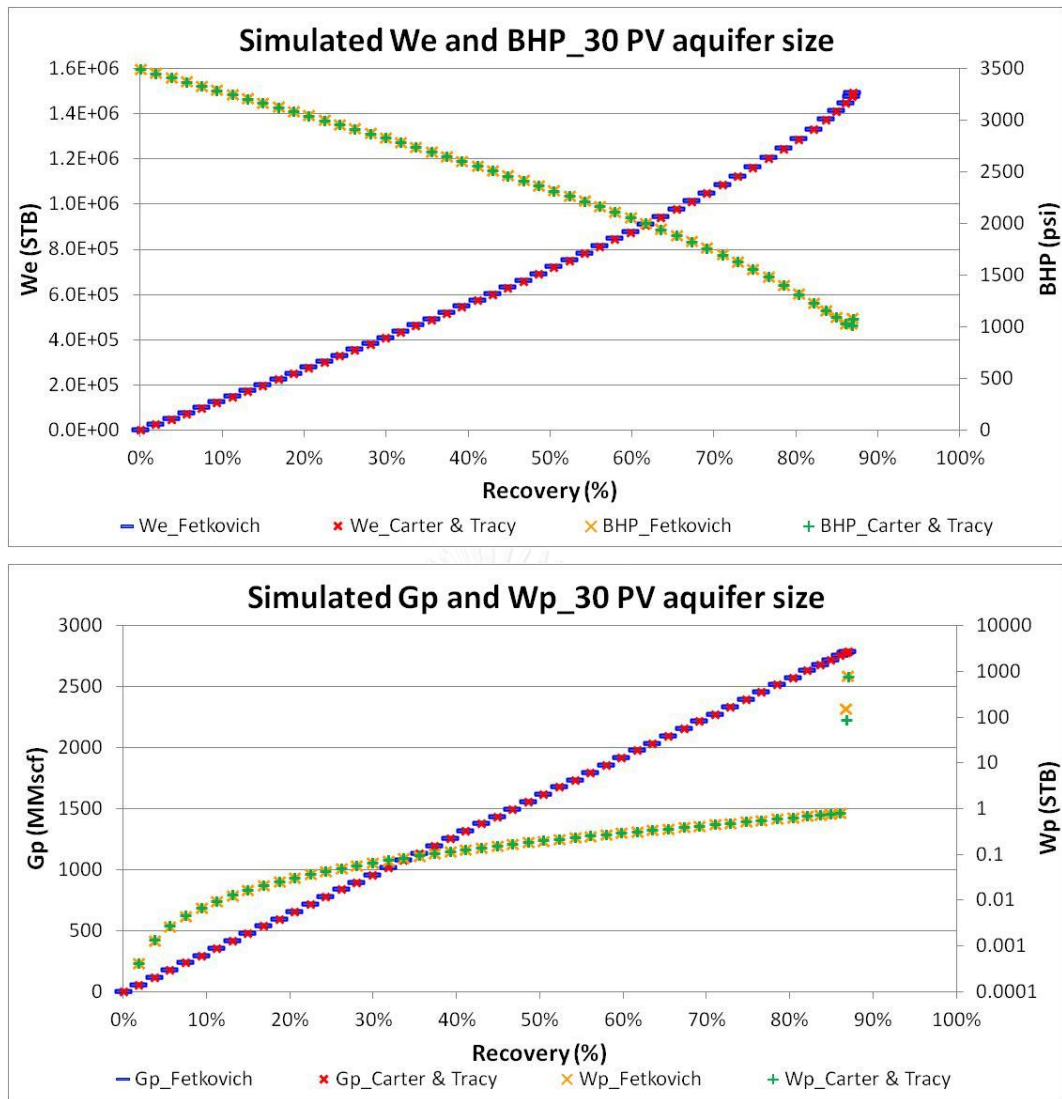


Figure 6.3 Simulated W_e , $SBHP$, G_p and W_p versus %RF at 30-PV aquifer size, case 5-6

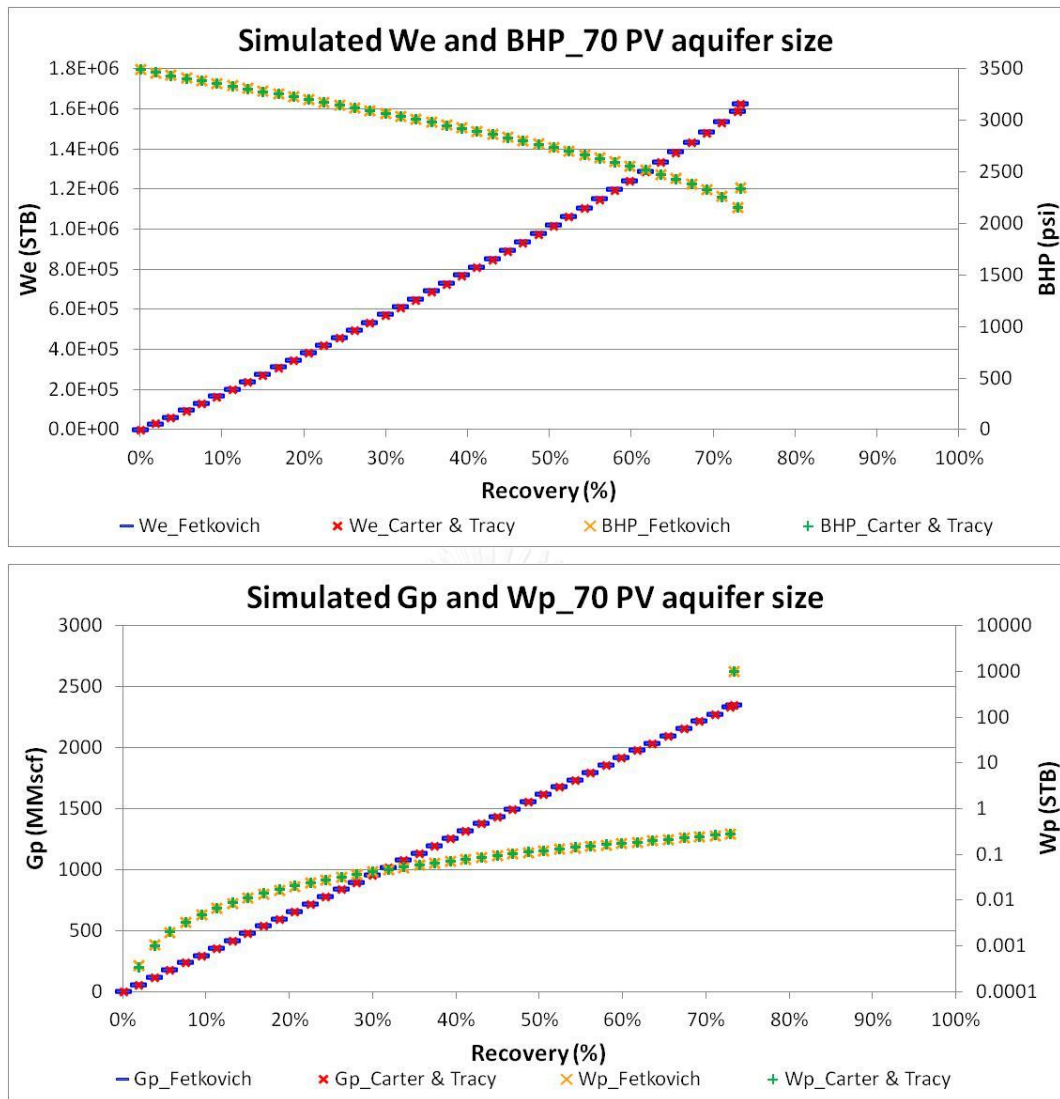


Figure 6.4 Simulated W_e , $SBHP$, G_p and W_p versus %RF at 70-PV aquifer size, case 7-8

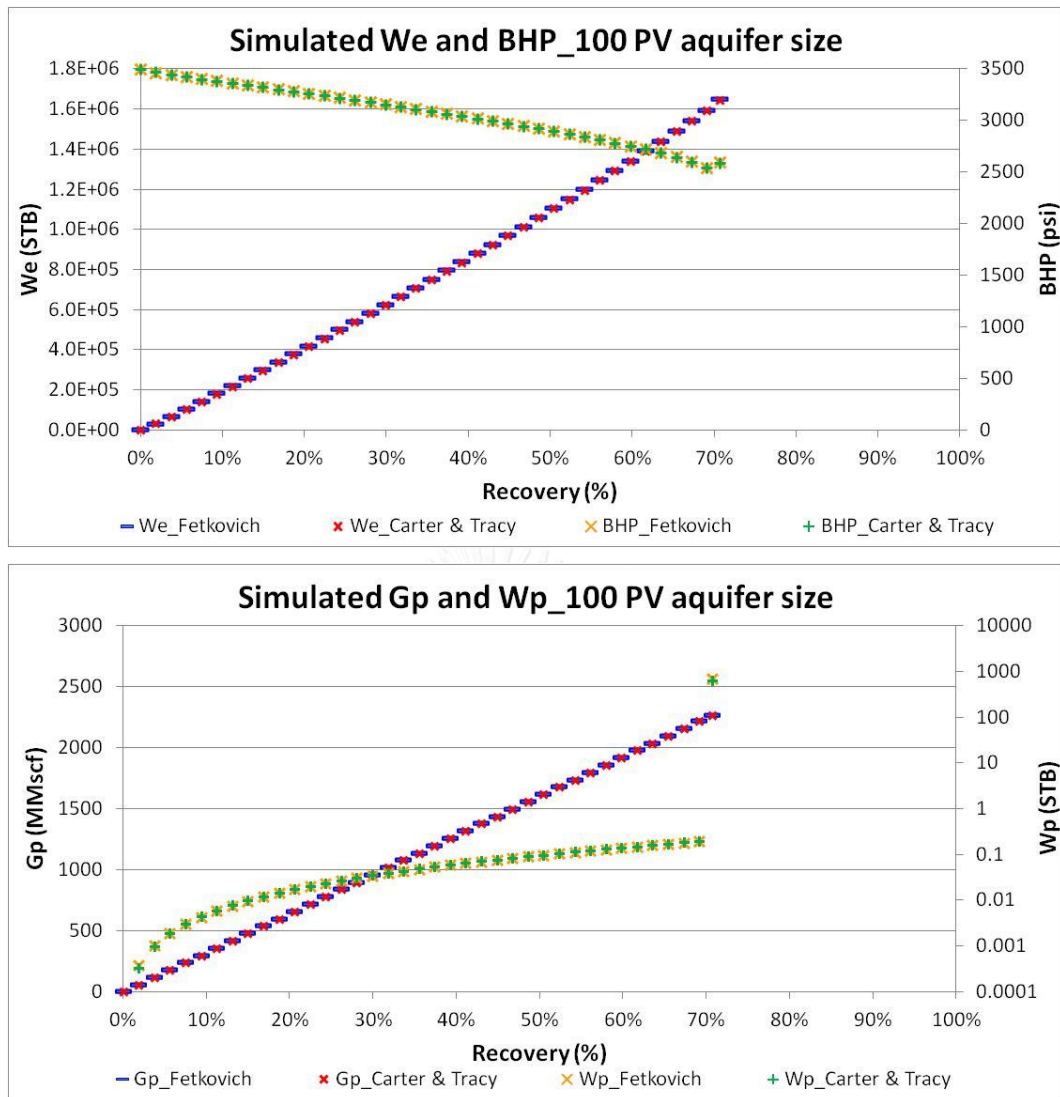


Figure 6.5 Simulated W_e , $SBHP$, G_p and W_p versus %RF at 100-PV aquifer size, case 9-

6.2 Effect of Aquifer Size

The objective of this section is to study the effect of aquifer size on the reservoir behavior. The reservoir permeability, shut-in duration for SBHP measurement and aquifer sizes in this section are the same as those in Section 6.1.

6.2.1 Reservoir Pressure

The reservoir pressure remains higher in the larger aquifer size case compared to the smaller aquifer size case at the same %RF as shown in Figure 6.6 because the larger the aquifer size, the higher the pressure support from the aquifer to the reservoir in term of the higher amount of W_e as shown in Figure 6.7.

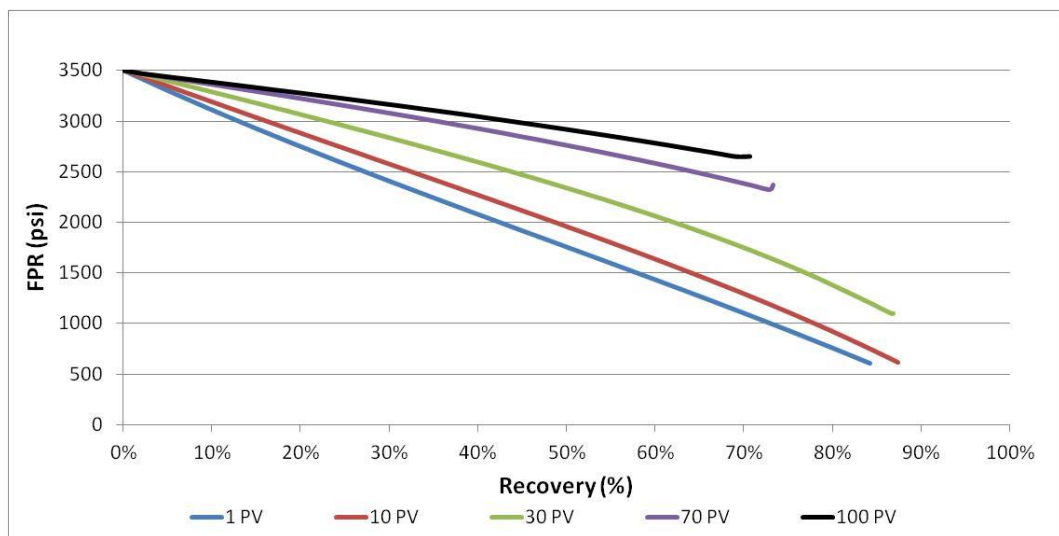


Figure 6.6 Simulated field pressure versus %RF for all aquifer sizes

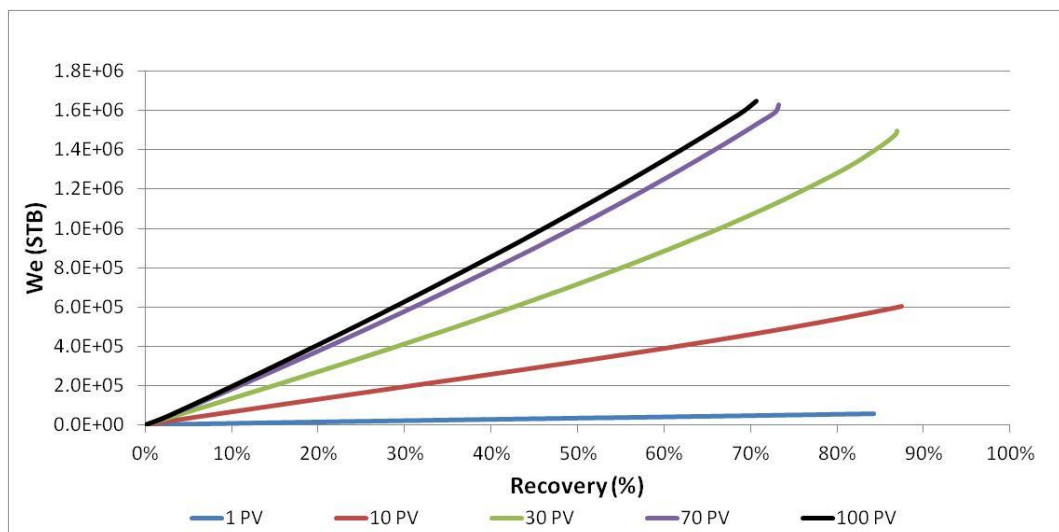


Figure 6.7 Simulated cumulative water influx versus %RF for all aquifer sizes

In all aquifer size, the reservoir pressure decrease when the %RF increases. At late time before the abandonment, the reservoir pressure in 70-PV and 100-PV aquifer size cases increase again because the withdrawal fluid rate, gas and water production, is less than water influx rate.

6.2.2 Water Production Rate

Water production rate at early time is low as shown in Figure 6.8 because it is from connate water expansion. Water production rate in 30-PV, 70-PV and 100-PV aquifer size suddenly increase at late time and make the well reach the abandonment condition due to liquid loading in the wellbore. The rapid increasing of water production is because of the water breakthrough as shown in Figure 6.9 for the example of 100-PV aquifer size. The initial water saturation in the reservoir is 0.4. When the water breaks through, the water saturation near wellbore, especially at the lower part of the reservoir, is higher than 0.4.

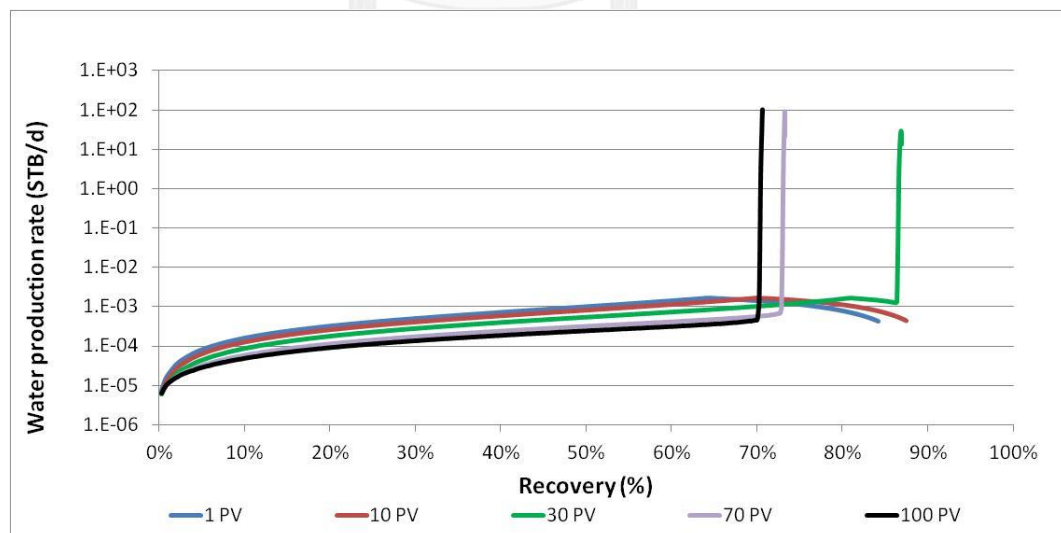


Figure 6.8 Simulated water production rate versus %RF for all aquifer sizes

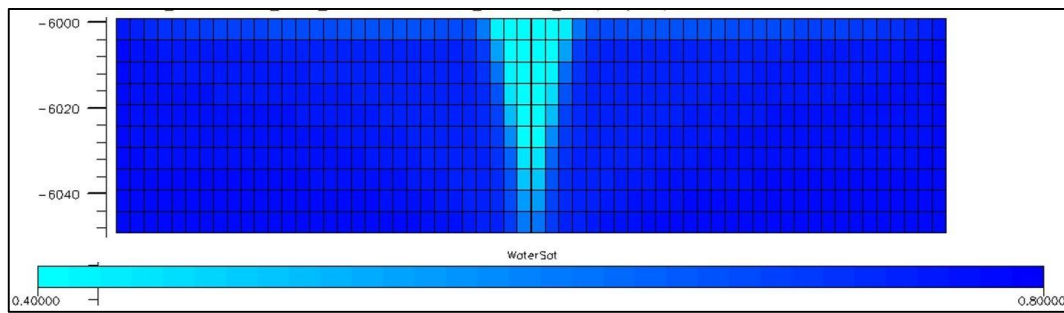


Figure 6.9 Simulated water saturation profile in the reservoir at water breakthrough in 100-PV case

In Figure 6.10, water saturation near wellbore at the abandonment condition in 1-PV aquifer size is still around the initial water saturation, meaning that there is no water breakthrough in this case.

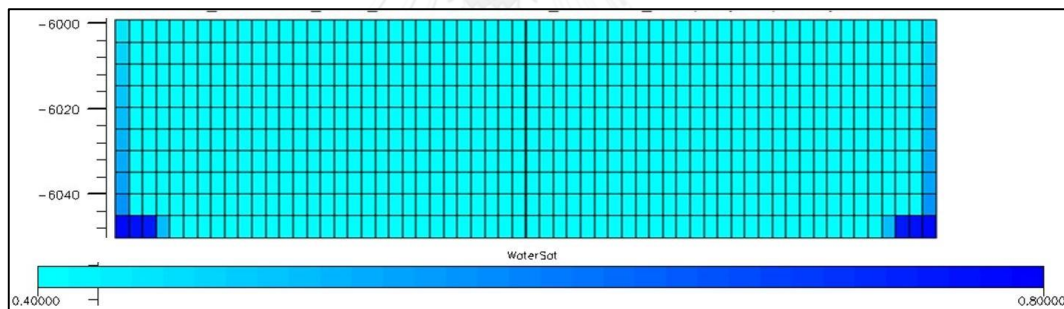


Figure 6.10 Simulated water saturation profile in the reservoir at the abandonment condition in 1-PV case

6.2.3 Gas Rate

In the 1-PV and 10-PV aquifer cases, the wells reach the abandonment due to reservoir pressure depletion. The plots of simulated gas rate vs. %RF of these cases in Figure 6.11 start with plateau gas rate of 2 MMscfd until 64% and 71% RF and start to decline continuously to the abandonment gas rate of 0.2 MMscfd.

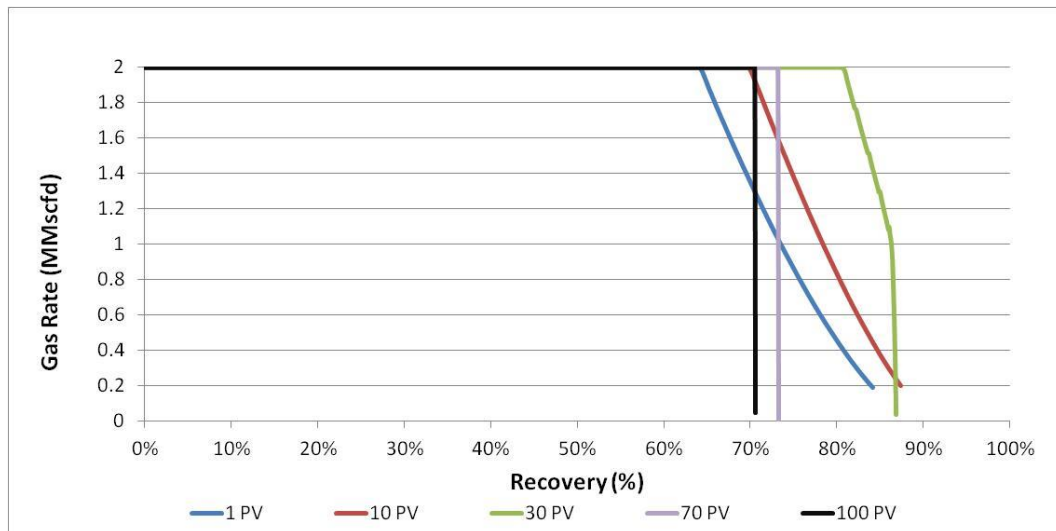


Figure 6.11 Simulated gas rate versus %RF for all aquifer sizes

After the plateau period, gas rate of the 30-PV aquifer case in Figure 6.11 declines continuously to be around 1 MMscfd before suddenly drops below 0.2 MMscfd. The gas rate decline period is due to the reservoir pressure depletion but the sudden drop of gas rate is due to liquid loading from water breakthrough.

In the 70-PV and 100-PV aquifer cases, there is no gas rate decline period from reservoir pressure depletion. When water breaks through, gas rate suddenly drops to the abandonment condition due to liquid loading in the wellbore. Since water breakthrough in 100-PV aquifer happens earlier than the one in 70-PV aquifer, then the well reaches abandonment condition earlier.

From Figure 6.11, the longest plateau period of gas rate is in 30-PV aquifer size because of more pressure support than 1-PV and 10-PV aquifer size and the water breakthrough in 30-PV aquifer size is not too early like 70-PV and 100-PV aquifer cases.

6.2.4 Gas Recovery Factor

Since reservoir-aquifer systems are radial and reservoir properties are homogeneous, the displacement process of water influx is a piston-like displacement

without early water breakthrough. This causes high gas recovery factor in the range of 70%-88% for all aquifer sizes as shown in Figure 6.12.

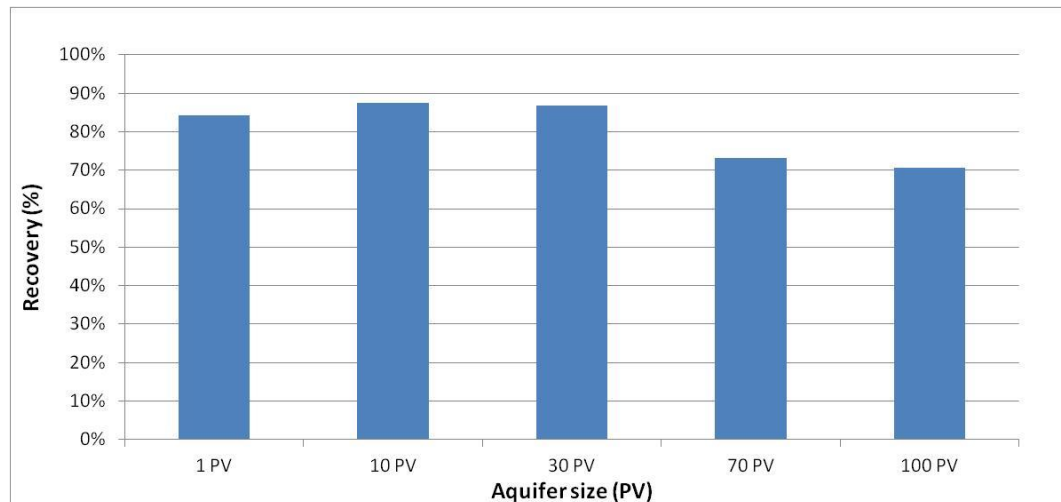


Figure 6.12 Gas recovery factor for all aquifer sizes

For small aquifer sizes (1 PV and 10 PV), recovery factor increases when the aquifer size increases due to more pressure support from the larger aquifer. For the moderate to large aquifer sizes (30 PV, 70 PV and 100 PV), recovery factor decreases when the aquifer size increases because of earlier liquid loading in the wellbore.

6.2.5 Drawdown Pressure

The difference between reservoir pressure and FBHP or drawdown pressure as shown in Figure 6.13 in all aquifer size increase with %RF during the gas rate plateau period because of the increasing of water production as shown in Figure 6.8 and water saturation near the wellbore.

The end of the gas rate plateau period is when the slope of the FBHP suddenly changes (64% and 81% depletion in 1-PV and 30-PV aquifer size, respectively). For the 100-PV aquifer size, the end of the gas rate plateau period is very close to the

abandonment condition at 71% depletion due to sudden liquid loading in the wellbore.

During the decline period, pressure drawdown decreases with %RF due to decrease in gas rate as shown in Figure 6.11.

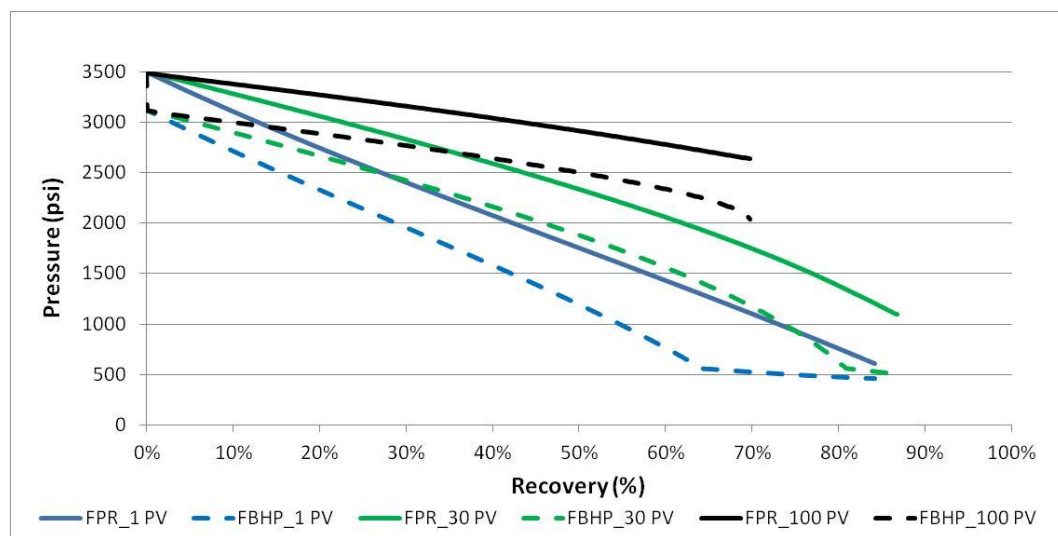


Figure 6.13 Simulated field pressure and flowing bottom hole pressure versus %RF at 1-PV, 30-PV and 100-PV aquifer sizes

6.2.6 Pressure Loss in Tubing

The difference between FBHP and FTHP or pressure loss in the tubing as shown in Figure 6.14 in all aquifer size decrease with %RF during the production plateau period. The reason is the decreasing of FBHP and FTHP from reservoir pressure depletion cause less hydrostatic gas column in the tubing. Pressure loss in the tubing is the summation of the hydrostatic loss, the accelerating loss and the friction loss. During the production plateau period, the friction loss increases with %RF because the actual volume of gas at lower pressure is higher but the decreasing of the hydrostatic is more significant.

The decreasing of pressure loss in the tubing with %RF in large aquifer cases is smaller than the one in small aquifer cases because the reservoir pressure is better maintained by the aquifer.

During the decline period, pressure loss in the tubing decreases with %RF because of the less hydrostatic gradient due to lower pressure and the less friction loss due to the decreasing of gas rate.

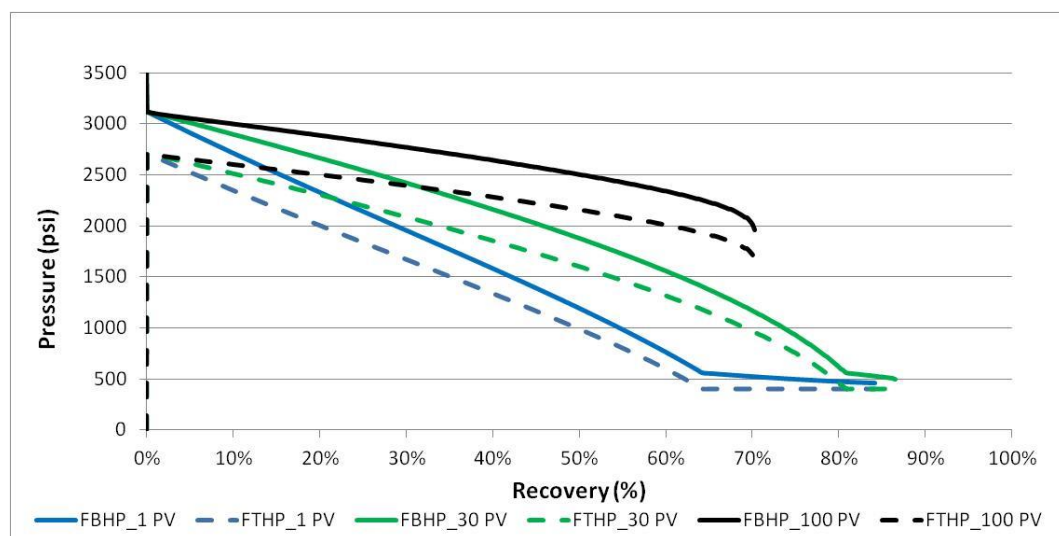


Figure 6.14 Simulated flowing bottom hole pressure and flowing tubing head pressure versus %RF at 1-PV, 30-PV and 100-PV aquifer sizes

6.2.7 Water Influx Rate

Figure 6.15 to Figure 6.17 show that the water influx rate in all aquifer size suddenly drop at the end of the gas rate plateau period because of the total fluid withdrawal of gas and water, from the reservoir decreases.

The water influx rate in all aquifer size fluctuates because the well is open for production for 30 days and then shut in for SBHP measurement for 1 day until abandonment.

Water influx rate in 1-PV aquifer size as shown in Figure 6.15 decreases with %RF because the aquifer is too small to provide high amount of water influx to the reservoir.

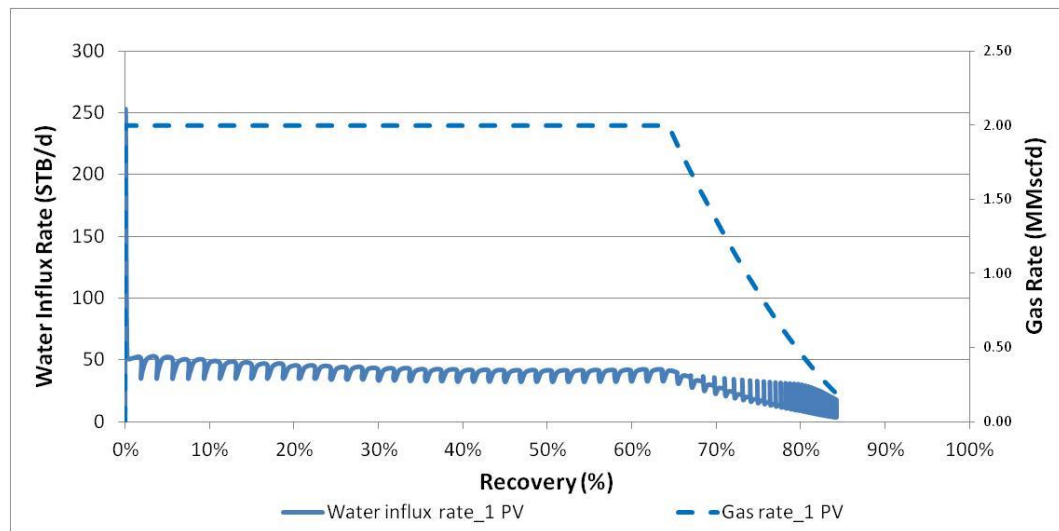


Figure 6.15 Simulated water influx rate and gas rate versus %RF at 1-PV aquifer size

From Figure 6.16 and Figure 6.17, water influx rate in 30-PV, 70-PV and 100-PV aquifer cases increases with %RF. The aquifer size in these cases is large enough to supply high amount of water influx to the reservoir. When water influx invades into the reservoir, k_{rw} of the invaded zone becomes higher as shown in Figure 6.18 and Figure 6.19 and water can move easier. The higher the depletion level, the more the water influx and the larger the invaded zone.

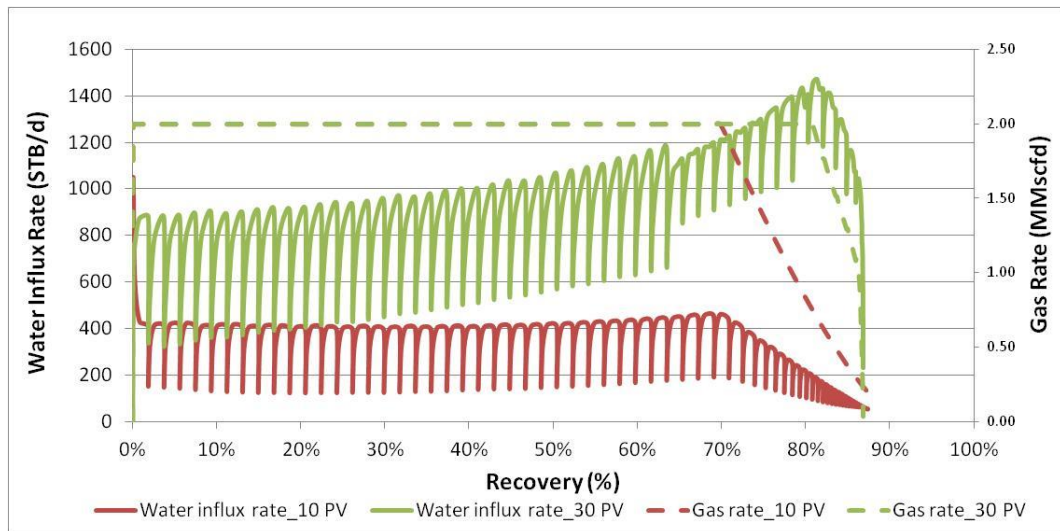


Figure 6.16 Simulated water influx rate and gas rate versus %RF at 10-PV and 30-PV aquifer sizes

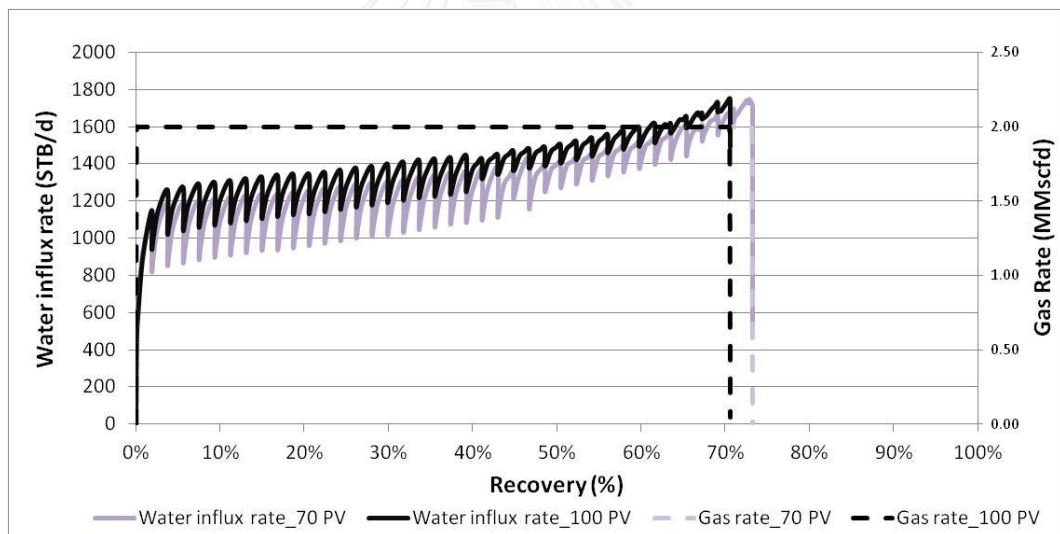


Figure 6.17 Simulated water influx rate and gas rate versus %RF at 70-PV and 100-PV aquifer sizes

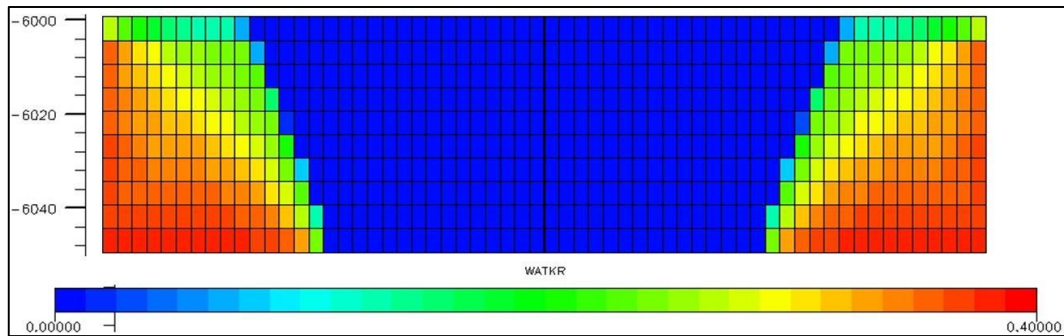


Figure 6.18 Simulated relative permeability to water profile at 50% RF in 100 PV aquifer size

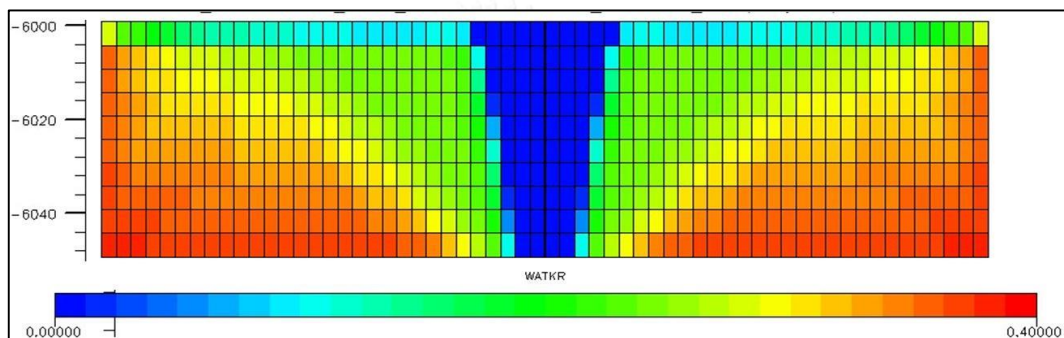


Figure 6.19 Simulated relative permeability to water profile at 70% RF in 100-PV aquifer size

6.3 Effect of Permeability

The objective of this section is to study the effect of permeability by comparing the behavior of 50 mD and 500 mD reservoirs. The shut-in duration for SBHP measurement and aquifer sizes in this section are the same as those in Section 6.1.

6.3.1 SBHP Build up Rate

The differences between SBHP and reservoir pressure for 50 mD reservoir are higher than those for 500 mD reservoir for all aquifer sizes as shown in Figure 6.20 and

Figure 6.21. The reason is the SBHP in high permeability reservoir can build up to approach the reservoir pressure faster than the one in low permeability reservoir.

In the cases of 1-PV and 10-PV aquifer with 50 mD reservoir, SBHP build up rate slightly decreases from the beginning and increases again in late time period. In the cases of 1-PV and 10-PV aquifer with 500 mD reservoir, SBHP build up rate increases when %RF increases.

In the 30-PV, 70-PV and 100-PV aquifer sizes, SBHP build up rate decreases when %RF increases in both 50 mD and 500 mD reservoirs.

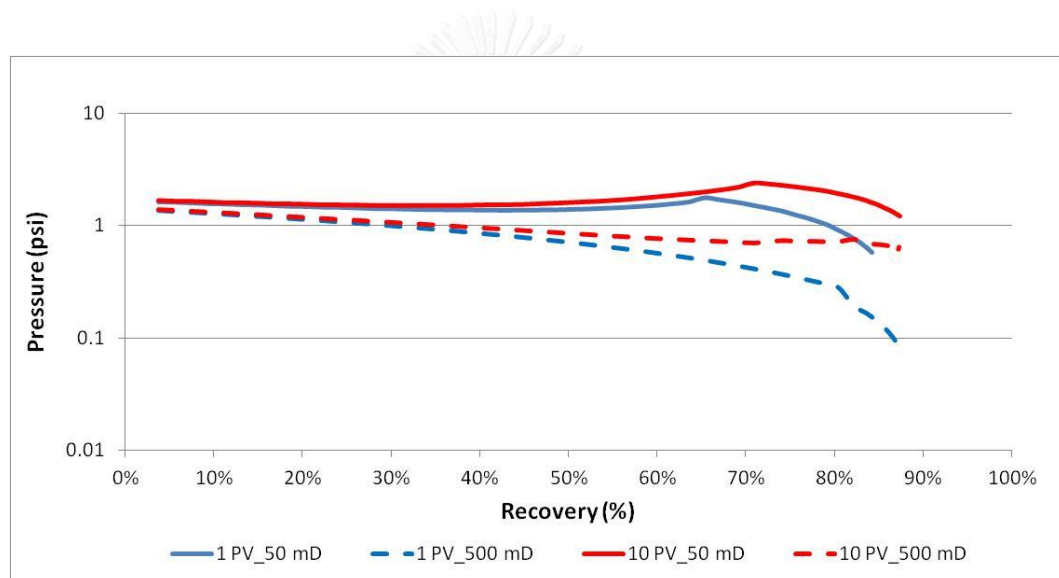


Figure 6.20 Difference between simulated field pressure and shut-in bottom hole pressure versus %RF at 1-PV and 10-PV aquifer sizes in 50 mD and 500 mD reservoirs

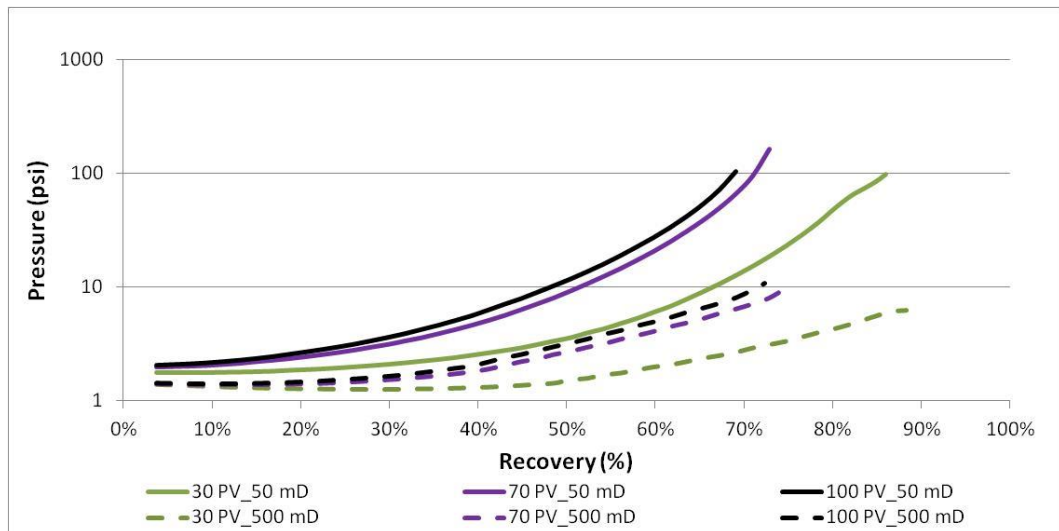


Figure 6.21 Difference between simulated field pressure and shut-in bottom hole pressure versus %RF at 30-PV, 70-PV and 100-PV aquifer sizes in 50 mD and 500 mD reservoirs

6.3.2 Reservoir Pressure

Figure 6.22 shows that at the same aquifer size and %RF, W_e in 500 mD reservoir is higher than the one in 50 mD reservoir and the difference increases with aquifer size and %RF. The higher W_e in 500 mD reservoir causes better maintained reservoir pressure in 500 mD reservoir than 50 mD reservoir as shown in Figure 6.23.

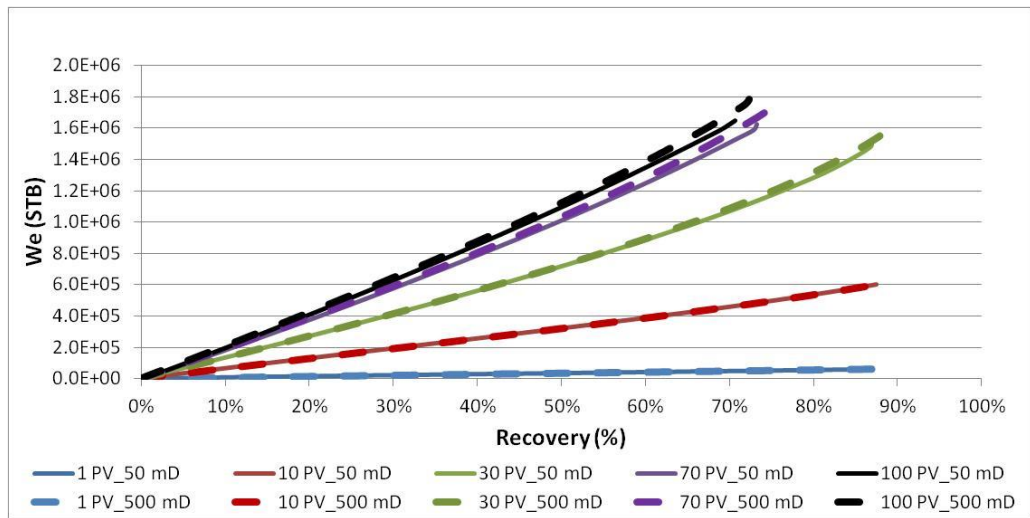


Figure 6.22 Simulated cumulative water influx versus %RF for all aquifer sizes in 50 mD and 500 mD reservoirs

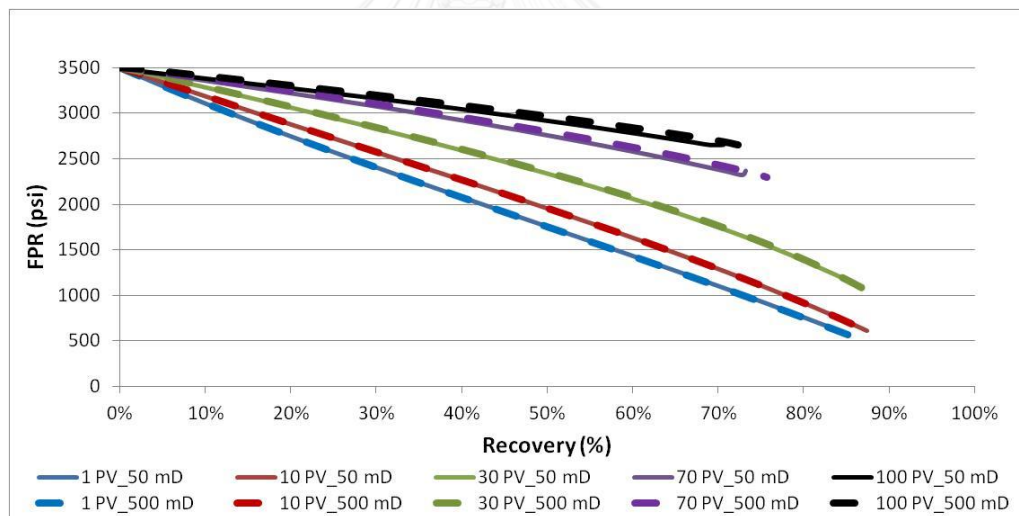


Figure 6.23 Simulated field pressure versus %RF for all aquifer sizes in 50 mD and 500 mD reservoirs

6.3.3 Water Production Rate

Figure 6.24 and Figure 6.25 show that the sudden increase in water production rate or water breakthrough for 500 mD reservoir occurs faster than that for 50 mD reservoir.

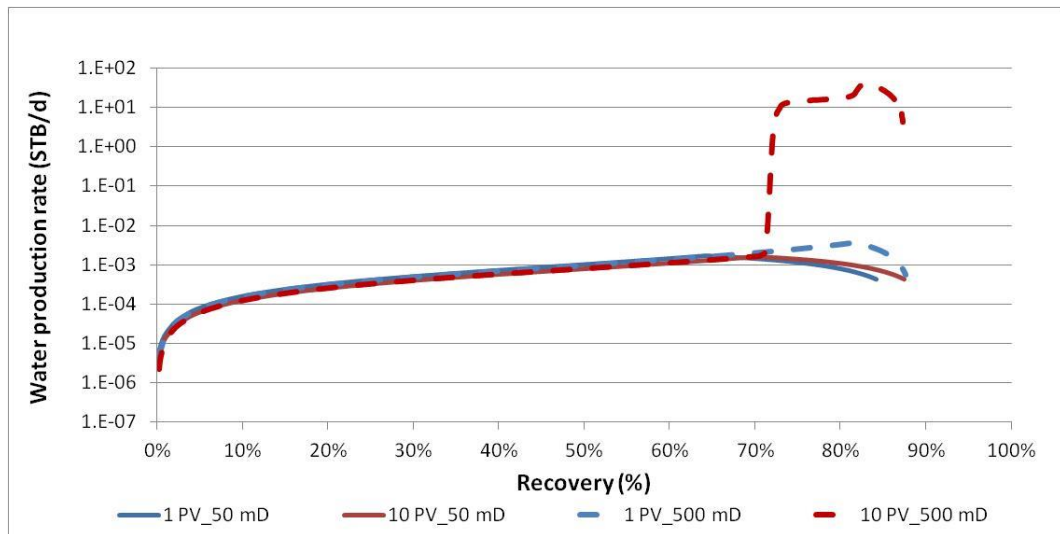


Figure 6.24 Simulated water production rate versus %RF at 1-PV and 10-PV aquifer size in 50 mD and 500 mD reservoirs

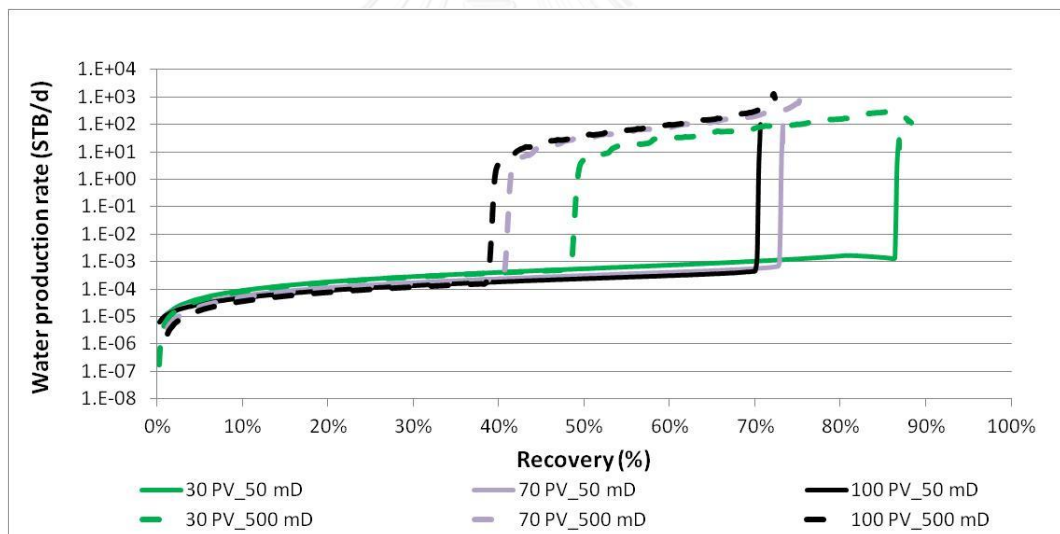


Figure 6.25 Simulated water production rate versus %RF at 30-PV, 70-PV and 100-PV aquifer size in 50 mD and 500 mD reservoirs

The 10-PV aquifer size is used as the example to show water saturation profile at water breakthrough in 500 mD reservoir as shown in Figure 6.26. Water saturation near the wellbore at the lower part of the reservoir is higher than initial water

saturation. At the same %RF of 72%, water saturation near the wellbore of 50 mD reservoir is still around initial water saturation as shown in Figure 6.27.

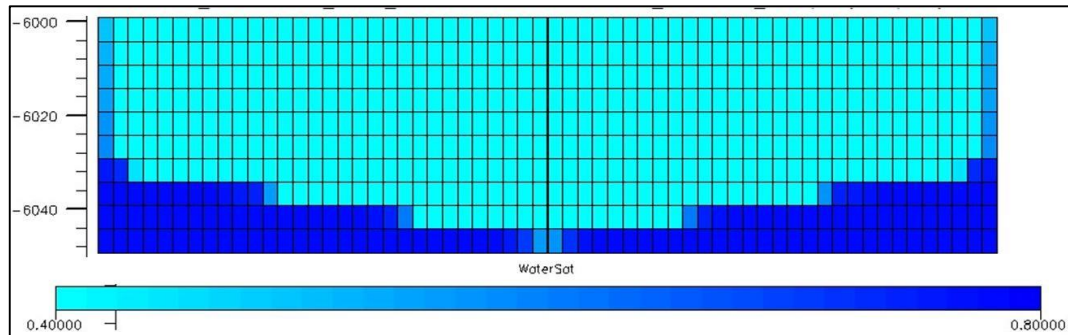


Figure 6.26 Simulated water saturation profile in the 500 mD reservoir at water breakthrough or 72% RF in 10-PV aquifer size

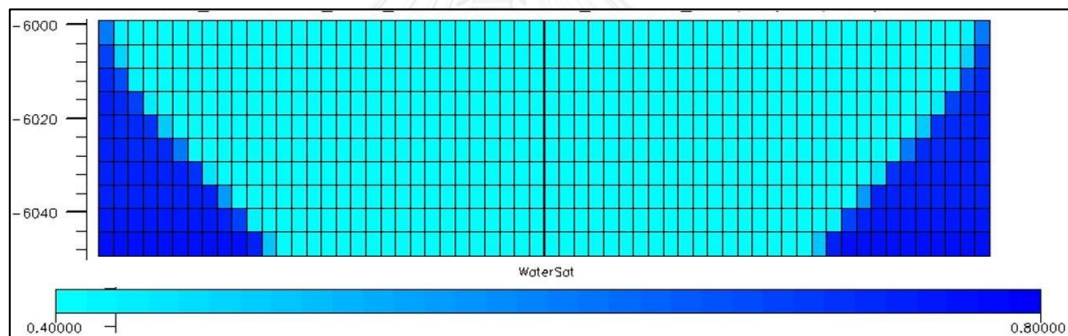


Figure 6.27 Simulated water saturation profile in the 50 mD reservoir at 72% RF in 10-PV aquifer size

The 1-PV aquifer size is the only case in 500 mD reservoir that has no water breakthrough. Figure 6.28 shows water saturation profile of this case at abandonment. Water saturation near the wellbore is still around initial water saturation.

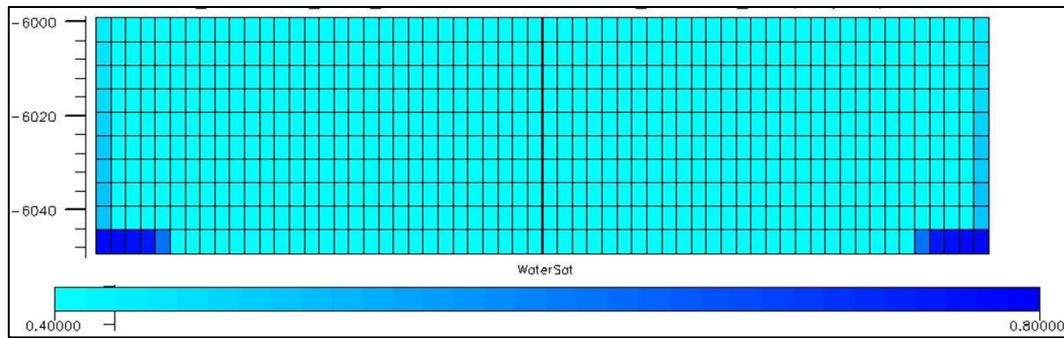


Figure 6.28 Simulated water saturation profile in the 500 mD reservoir at abandonment condition in 1-PV aquifer size

6.3.4 Gas Rate and Recovery Factor

Figure 6.29 and Figure 6.30 show comparison of gas rate profile and recovery factor between 50 mD and 500 mD reservoirs at the same aquifer size.

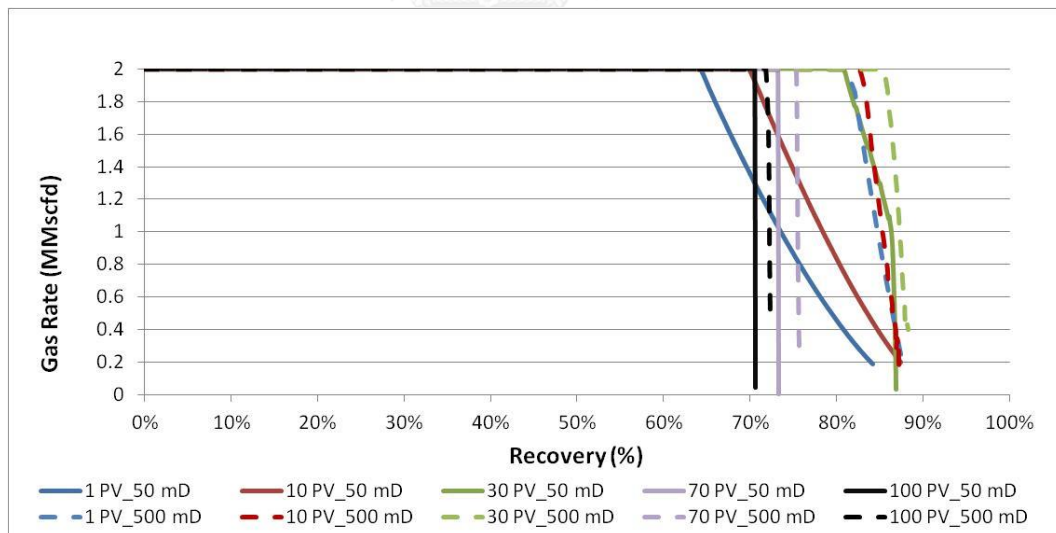


Figure 6.29 Simulated gas rate versus %RF for all aquifer sizes in 50 mD and 500 mD reservoirs

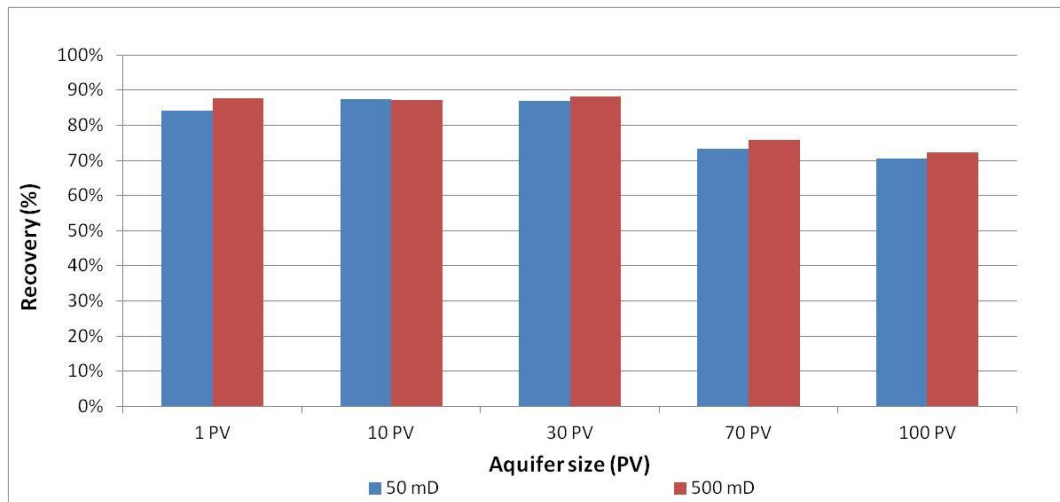


Figure 6.30 Recovery factor for all aquifer sizes in 50 mD and 500 mD reservoirs

In 1-PV aquifer size, the plateau period for 500 mD reservoir is longer than that for 50 mD reservoir and the recovery factor is also higher for 500 mD reservoir. The main reason of these behaviors is because of less drawdown pressure in 500 mD reservoir as shown in Figure 6.35 since the difference of W_e or pressure support from aquifer in 50 mD and 500 mD reservoirs is very small as shown in Section 6.3.2. The reservoir pressure at the abandonment for 500 mD reservoir is lower than that for 50 mD reservoir as shown in Figure 6.31 and Figure 6.32.

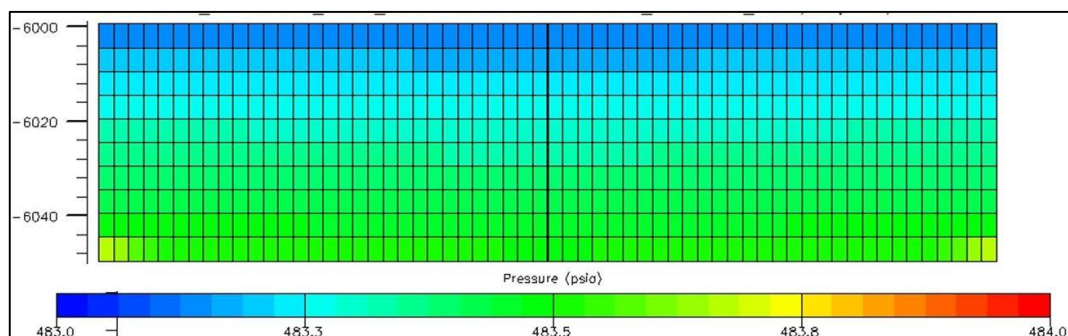


Figure 6.31 Simulated reservoir pressure in the 500 mD reservoir at abandonment condition in 1-PV aquifer size

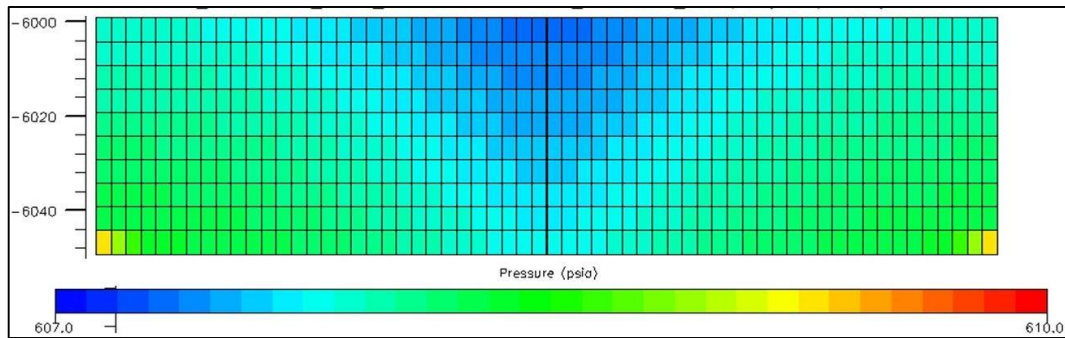


Figure 6.32 Simulated reservoir pressure in the 50 mD reservoir at abandonment condition in 1-PV aquifer size

In 10-PV aquifer size, the gas rate plateau period for 500 mD reservoir is longer than that for 50 mD reservoir because of less drawdown pressure, similar to the behavior of 1-PV aquifer size. However, the recovery factor in 500 mD reservoir is equal to 50 mD reservoir, 87%. The reason is liquid loading happens in 500 mD reservoir but not in 50 mD reservoir as shown in Figure 6.24, Figure 6.33 and Figure 6.34. The effects of less drawdown pressure and liquid loading in 500 mD reservoir cancel out.

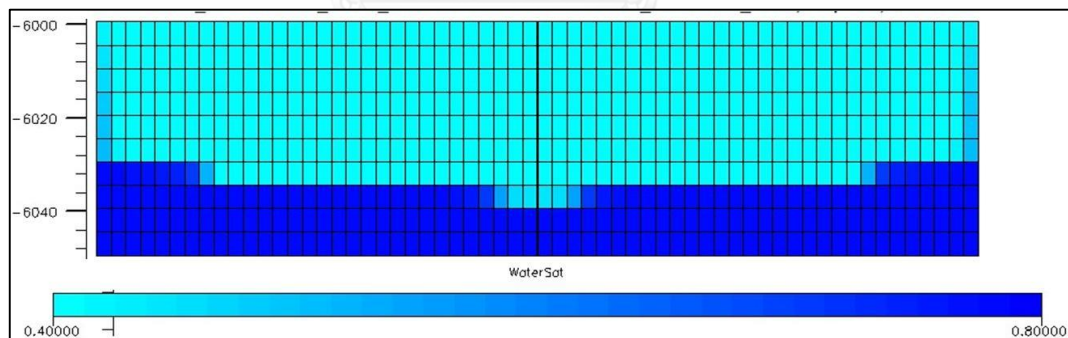


Figure 6.33 Simulated water saturation profile in the 500 mD reservoir at abandonment condition in 10-PV aquifer size

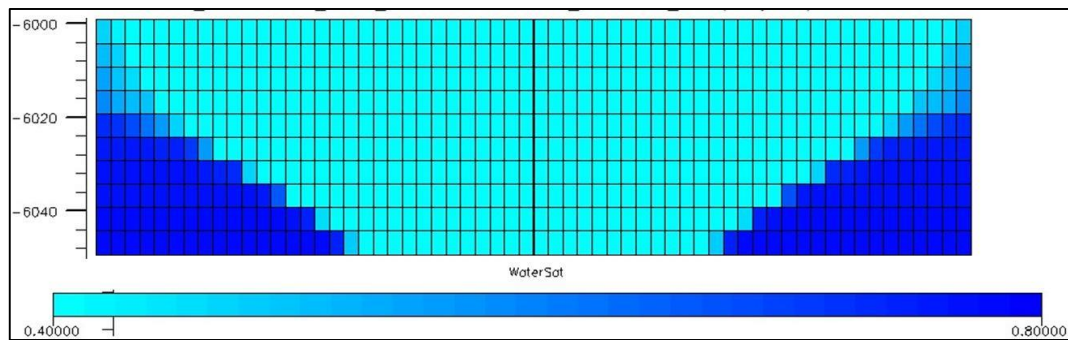


Figure 6.34 Simulated water saturation profile in the 50 mD reservoir at abandonment condition in 10-PV aquifer size

In 30-PV, 70-PV and 100-PV aquifer sizes, the well reach the abandonment condition due to liquid loading. The longer gas rate plateau period and the higher recovery factor in 500 mD reservoir are mainly from less drawdown pressure as shown in Figure 6.35 and also higher pressure support from aquifer as shown in Section 6.3.2.

6.3.5 Drawdown Pressure

Drawdown pressure in 500 mD reservoir is lower than that in 50 mD reservoir in all aquifer sizes as shown in Figure 6.35 since drawdown pressure is inversely proportional to permeability.

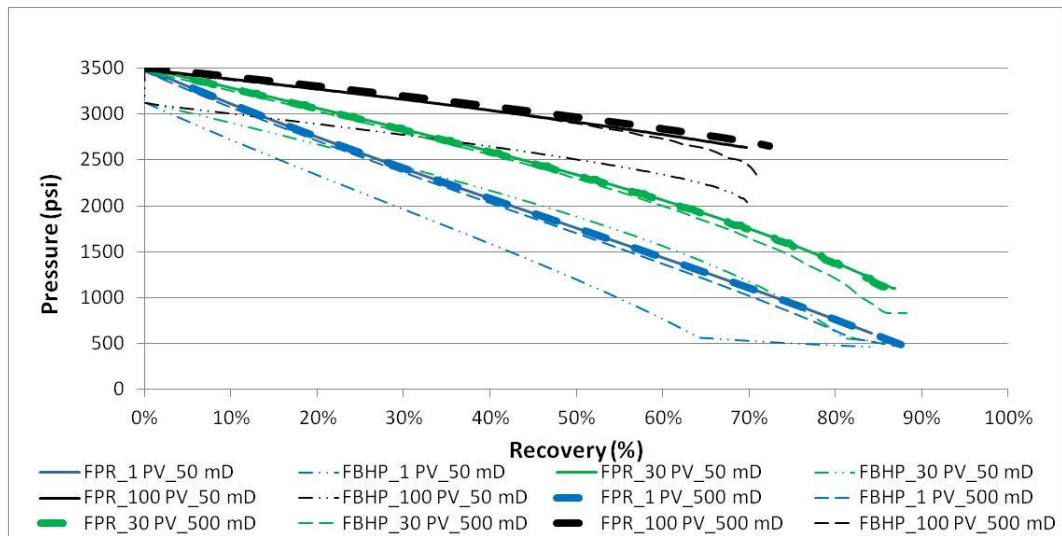


Figure 6.35 Simulated field pressure and flowing bottom hole pressure versus %RF at 1-PV, 30-PV and 100-PV aquifer size in 50 mD and 500 mD reservoirs

6.3.6 Water Influx Rate

In 1-PV and 10-PV aquifer sizes, water influx rates in 50 mD and 500 mD reservoirs during the gas rate plateau period are not significantly different. The difference between 50 mD and 500 mD reservoir is the longer gas rate plateau period in 500 mD reservoir as mentioned in Section 6.3.4, which makes the water influx rate in 500 mD reservoir higher than that in 50 mD reservoir after the decline period of 50 mD reservoir as shown in Figure 6.36 and Figure 6.37.

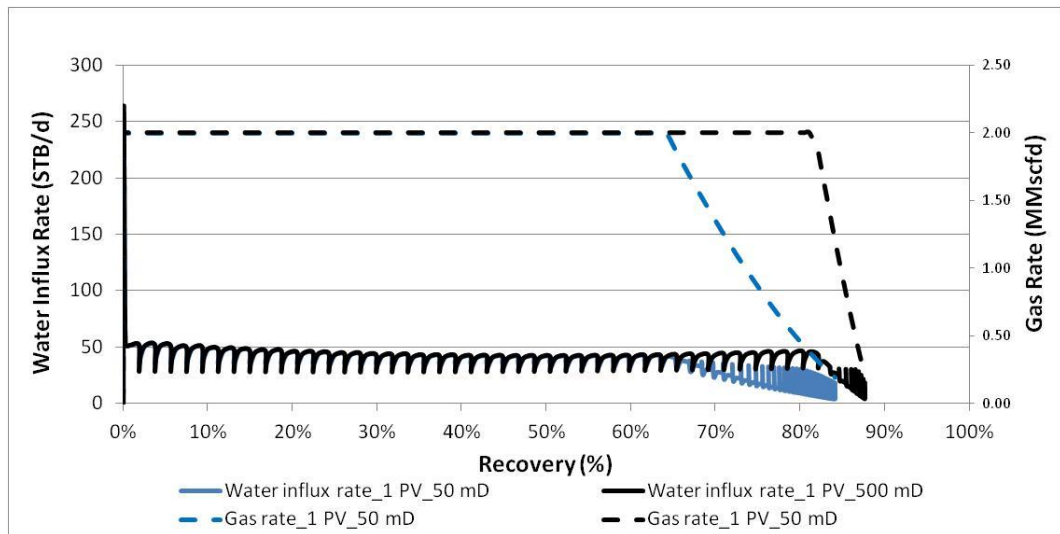


Figure 6.36 Simulated water influx rate and gas rate versus %RF at 1-PV aquifer size in 50 mD and 500 mD reservoirs

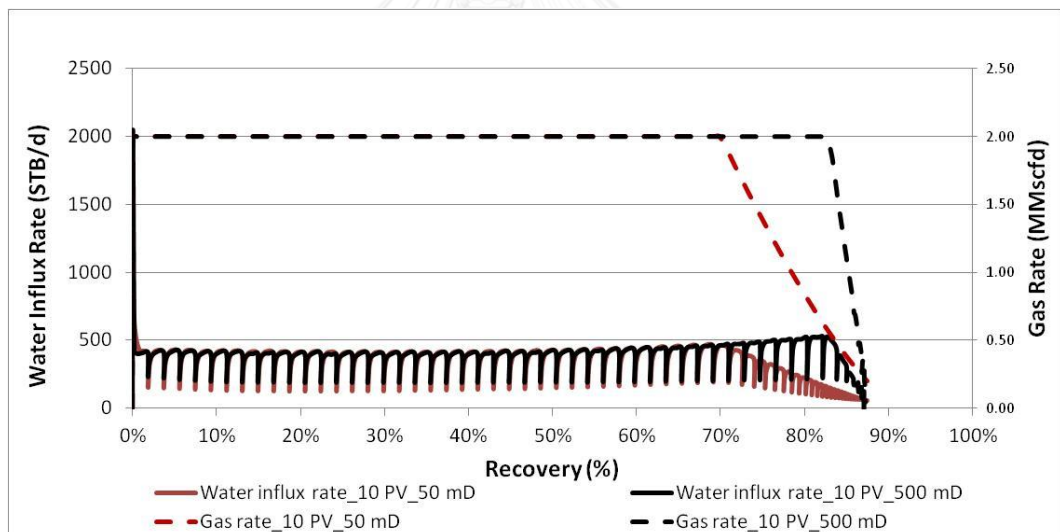


Figure 6.37 Simulated water influx rate and gas rate versus %RF at 10-PV aquifer size in 50 mD and 500 mD reservoirs

In 30-PV, 70-PV and 100-PV aquifer sizes, water influx rate in 500 mD reservoir become significantly higher than that in 50 mD reservoir in the late time of the plateau period as shown in Figure 6.38 to Figure 6.40. The difference in water influx rate is due to better permeability and higher fluid withdrawal rate from 500 mD reservoir, higher

water production rate from 500 mD reservoir as shown in Figure 6.25. The difference increases with aquifer size and %RF.

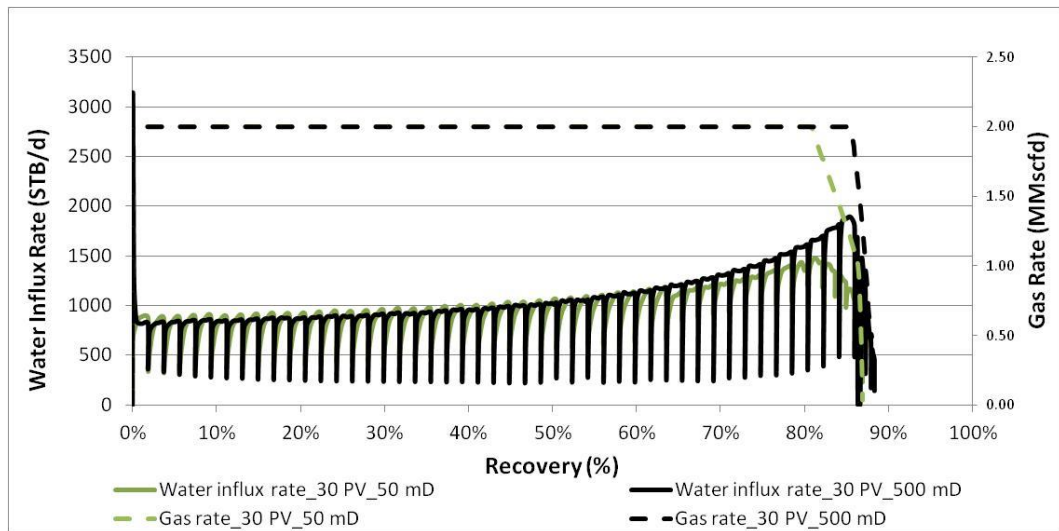


Figure 6.38 Simulated water influx rate and gas rate versus %RF at 30-PV aquifer size in 50 mD and 500 mD reservoirs

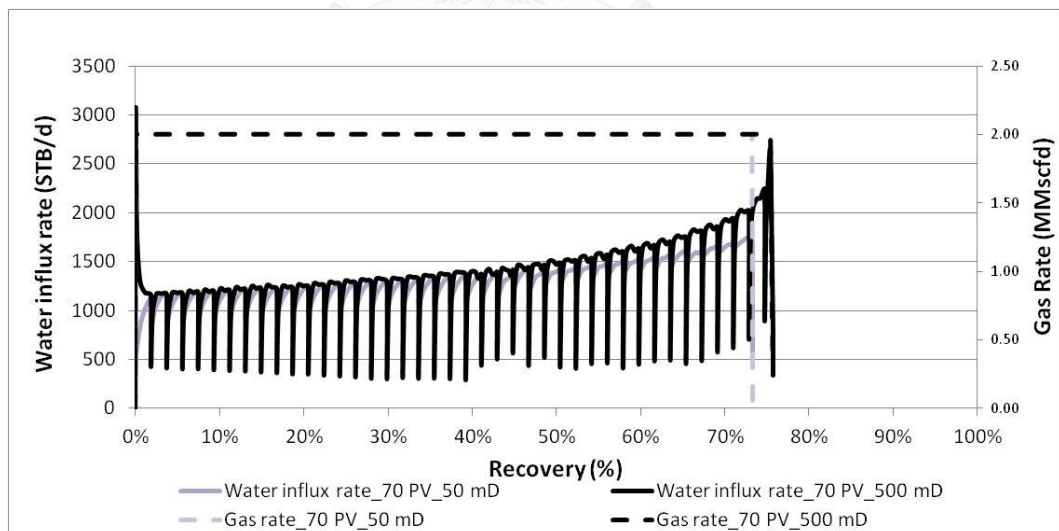


Figure 6.39 Simulated water influx rate and gas rate versus %RF at 70-PV aquifer size in 50 mD and 500 mD reservoirs

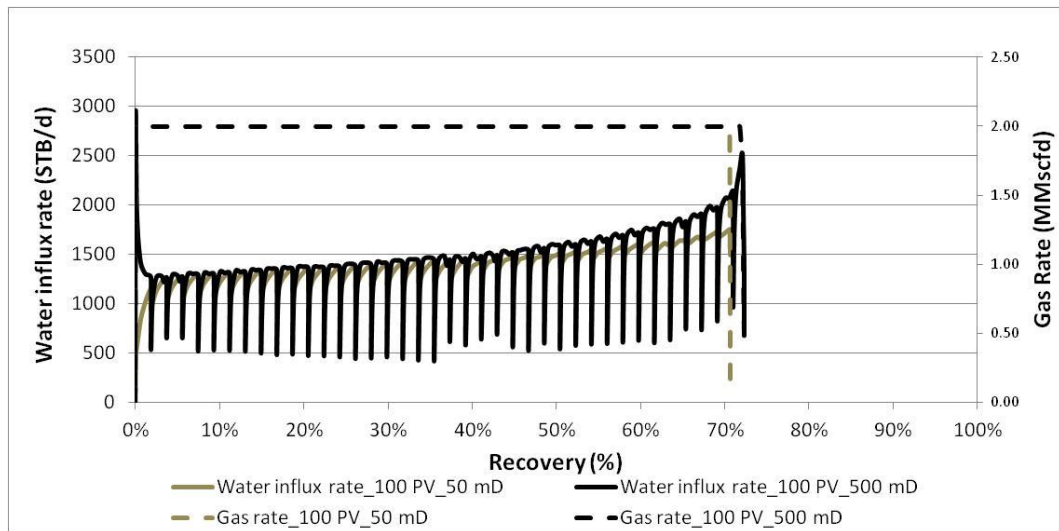


Figure 6.40 Simulated water influx rate and gas rate versus %RF at 100-PV aquifer size in 50 mD and 500 mD reservoirs

6.4 Water Influx Model Comparison

ECLIPSE 100 can generate W_e value of any reservoir-aquifer model, the value of W_e from ECLIPSE 100 in this thesis is defined as “simulated W_e ”.

In reality, the value of W_e cannot be measured directly like the other parameters such as SBHP or G_p . A water influx model is needed to be applied to production data and aquifer properties in order to calculate W_e . The value of W_e from the calculation in this thesis is defined as “calculated W_e ”.

Each water influx model has different assumptions and numerical approaches. Different water influx models can give different values of W_e .

The objective of this section is to compare the accuracy of the calculated W_e from different water influx models with the value of simulated W_e .

Table 6.2 shows the parameters to be studied in this section. The reservoir permeability and shut-in duration for SBHP measurement for all these cases are 50 mD and 1 day, respectively.

Table 6.2 Parameters to be studied on the accuracy of calculated W_e from different water influx models

Case	Aquifer size (PV)	Water influx model
1	1	Simple aquifer model
2		Fetkovich
3		van Everdingen & Hurst
4		Carter & Tracy
5	10	Simple aquifer model
6		Fetkovich
7		van Everdingen & Hurst
8		Carter & Tracy
9	30	Simple aquifer model
10		Fetkovich
11		van Everdingen & Hurst
12		Carter & Tracy
13	70	Simple aquifer model
14		Fetkovich
15		van Everdingen & Hurst
16		Carter & Tracy
17	100	Simple aquifer model
18		Fetkovich
19		van Everdingen & Hurst
20		Carter & Tracy

In 1-PV and 10-PV aquifer cases, simple aquifer model and Carter & Tracy water influx model are more accurate than Fetkovich and van Everdingen & Hurst water influx model as shown in Figure 6.41 to Figure 6.44.

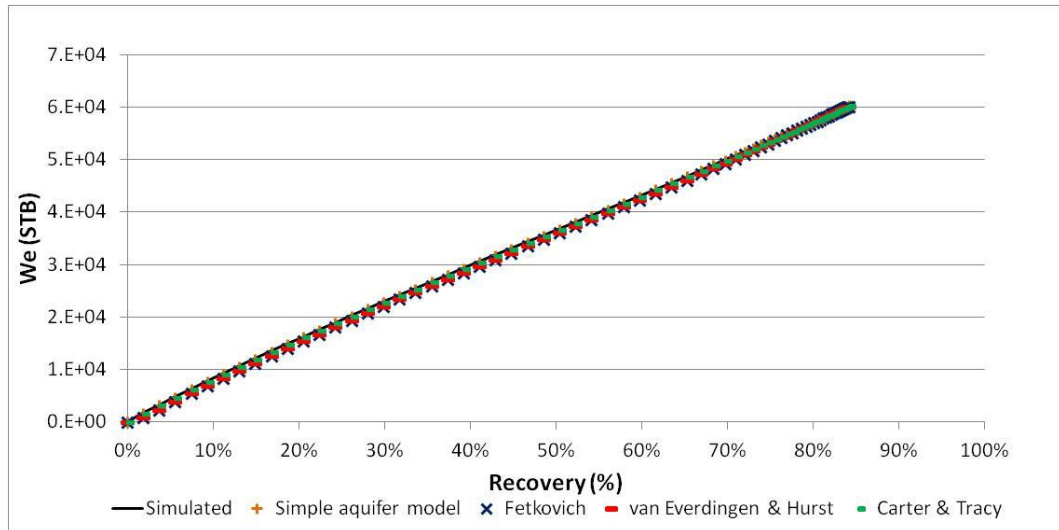


Figure 6.41 Simulated and calculated W_e at 1-PV aquifer size, case 1-4

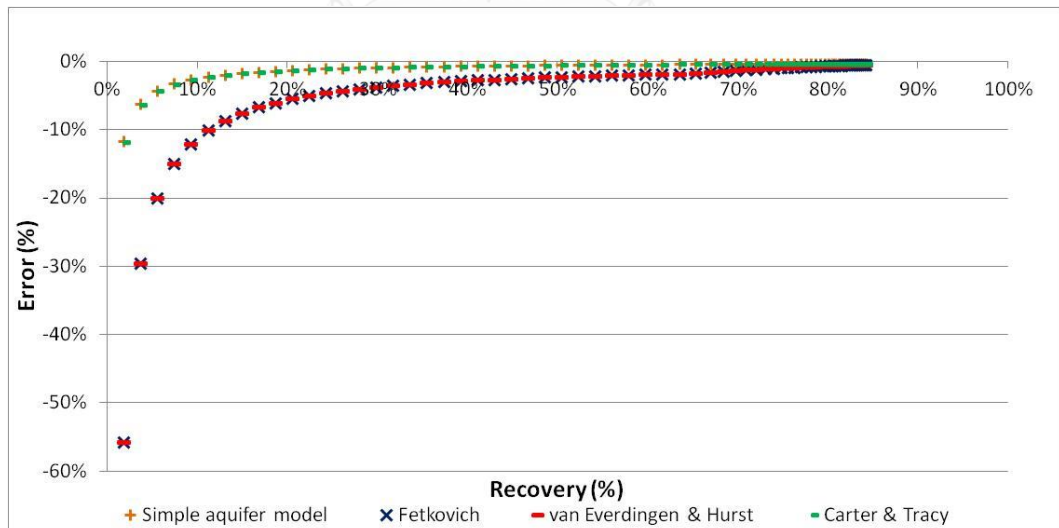


Figure 6.42 Error of calculated W_e at 1-PV aquifer size, case 1-4

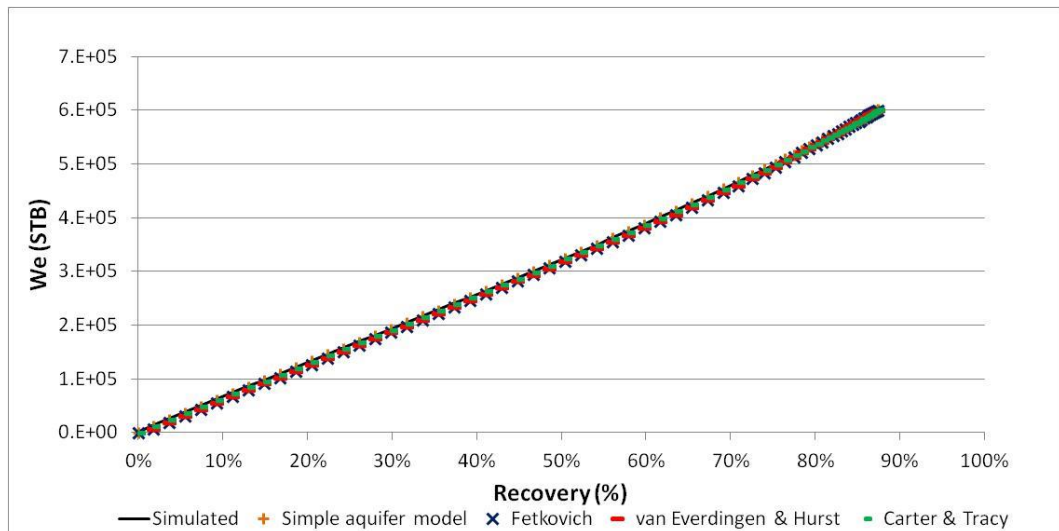


Figure 6.43 Simulated and calculated W_e at 10-PV aquifer size, case 5-8

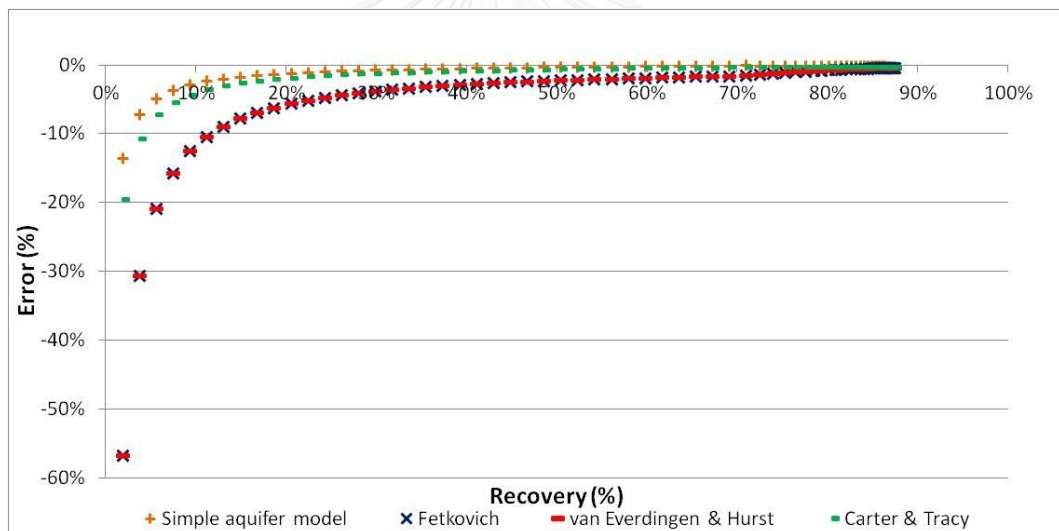


Figure 6.44 Error of calculated W_e at 10-PV aquifer size, case 5-8

Carter & Tracy water influx model give similar W_e value to simple aquifer model in 1-PV and 10-PV aquifer cases. As aquifer size becomes larger, Figure 6.45 to Figure 6.50, Carter & Tracy water influx model tends to give similar W_e value to Fetkovich and van Everdingen & Hurst water influx models.

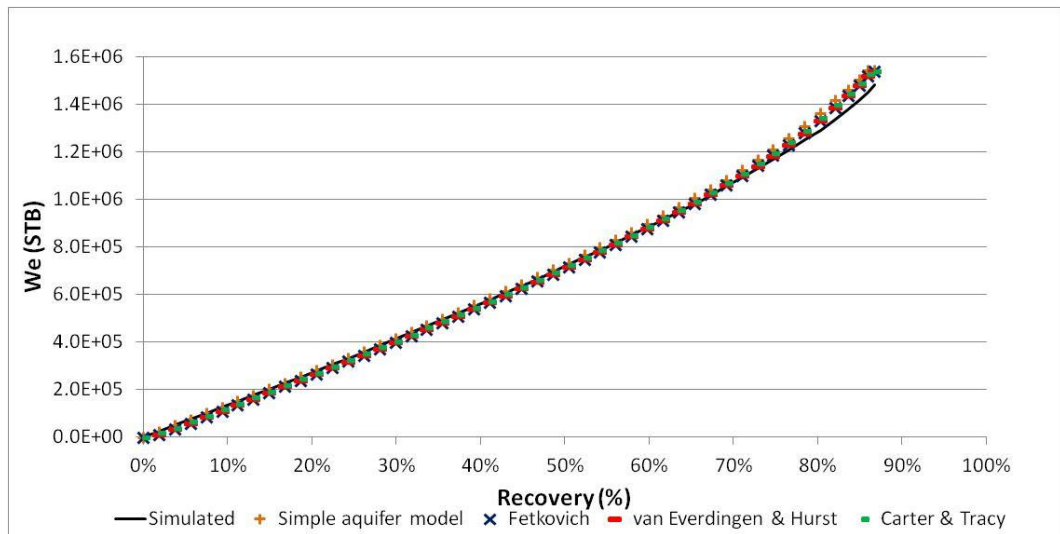


Figure 6.45 Simulated and calculated W_e at 30-PV aquifer size, case 9-12

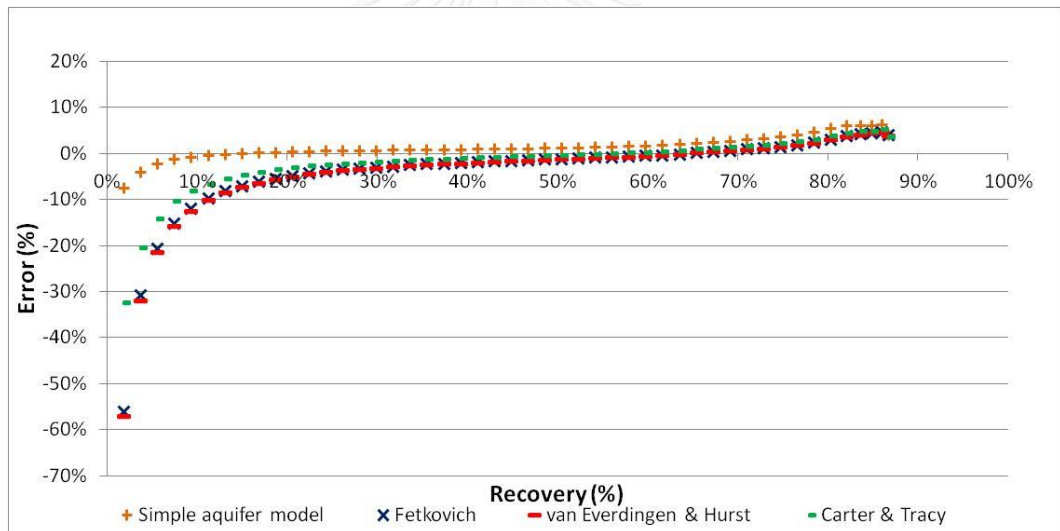


Figure 6.46 Error of calculated W_e at 30-PV aquifer size, case 9-12

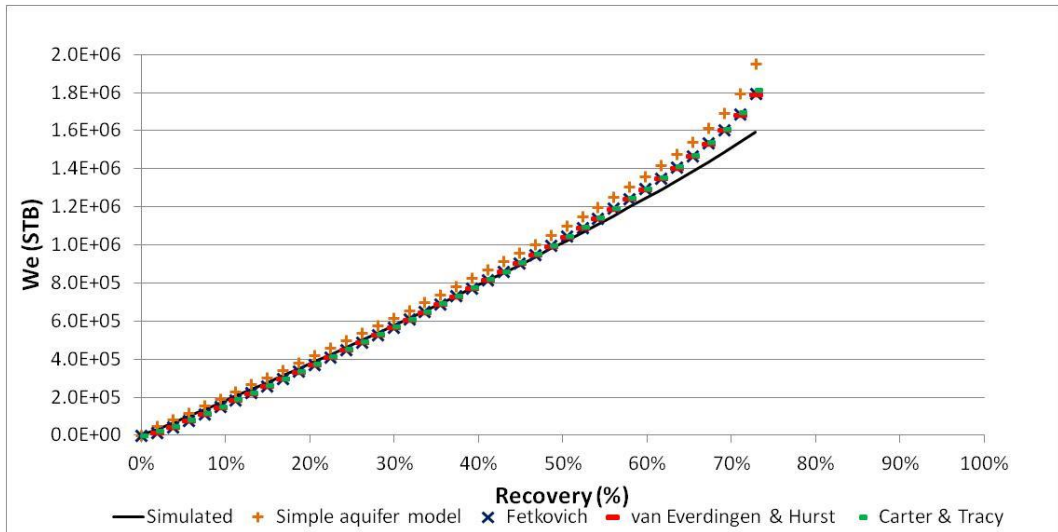


Figure 6.47 Simulated and calculated W_e at 70-PV aquifer size, case 13-16

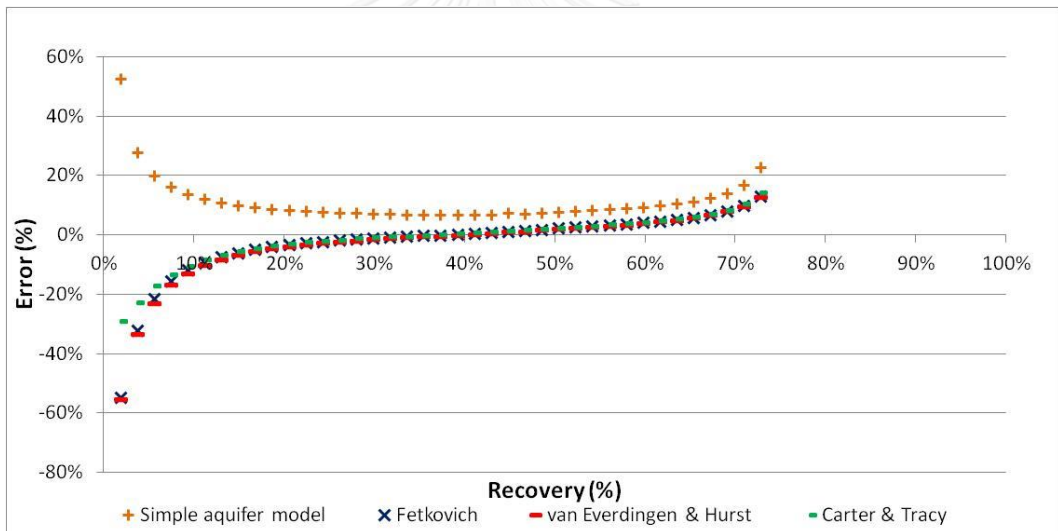


Figure 6.48 Error of calculated W_e at 70-PV aquifer size, case 13-16

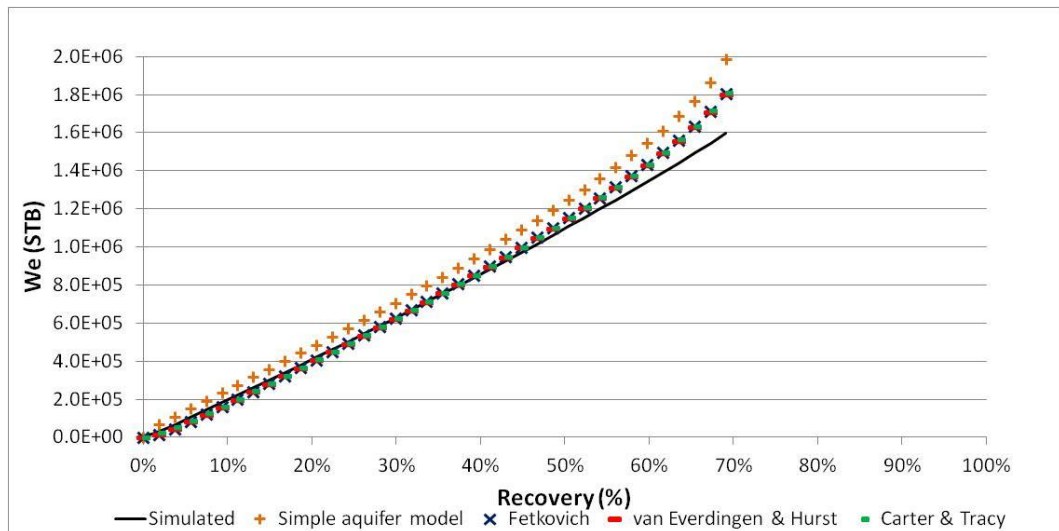


Figure 6.49 Simulated and calculated W_e at 100-PV aquifer size, case 17-20

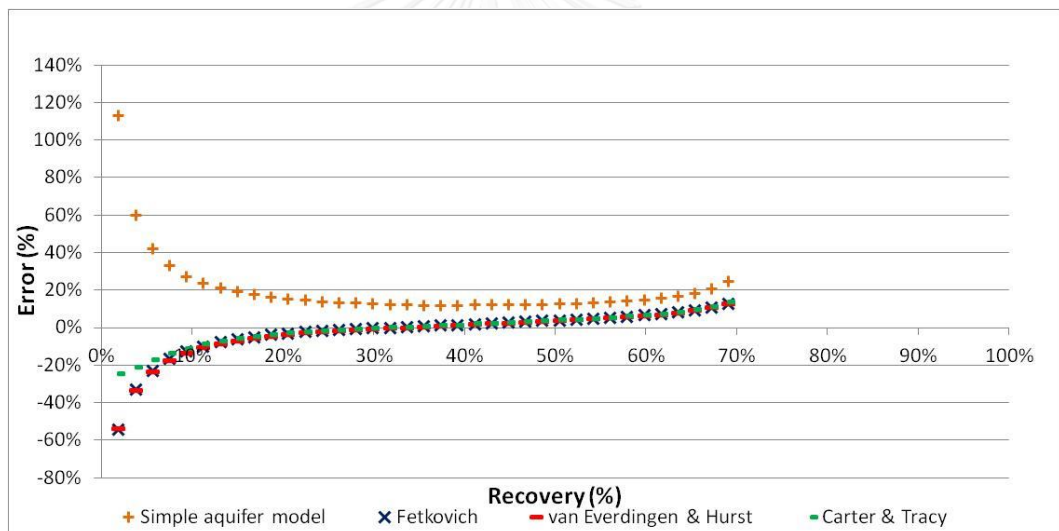


Figure 6.50 Error of calculated W_e at 100-PV aquifer size, case 17-20

Figure 6.47 to Figure 6.50 indicate that Fetkovich, van Everdingen & Hurst and Carter & Tracy water influx models are more accurate than simple aquifer model for 70-PV and 100-PV aquifer sizes. The reason is simple aquifer model is applicable to only small aquifers because it assumes that a pressure drop in the reservoir is immediately transmitted throughout the whole reservoir-aquifer system. This assumption is not valid in large aquifers; therefore, simple aquifer model gives too much W_e value. In small to moderate aquifer sizes (1 PV, 10 PV and 30 PV), simple

aquifer model still give the maximum W_e value compared to the other water influx models due to this assumption as shown in Figure 6.41 to Figure 6.46.

Figure 6.45 to Figure 6.50 indicate that in 30-PV, 70-PV and 100-PV aquifer sizes, Fetkovich, van Everdingen & Hurst and Carter & Tracy water influx model give higher value of W_e than the simulated W_e in the late time period. There are 2 reasons behind this behavior. The first one is because the SBHP in 50 mD reservoir cannot build up high enough to represent the actual reservoir pressure and the difference becomes larger when %RF increases as shown in Section 6.3.1. The second reason is because the water influx models do not consider the movement of gas-water contact.

Figure 6.51 represents the error of calculated W_e from van Everdingen & Hurst water influx model by applying field pressure instead of SBHP in 50 mD reservoir for 30-PV, 70-PV and 100-PV aquifer sizes. The error of calculated W_e in these aquifer sizes are still positive in the late time period but the magnitude of the errors are significantly lower than the one from SBHP as shown in Figure 6.46, Figure 6.48 and Figure 6.50 because the effect of non-representative SBHP is eliminated. The remaining positive error is from the effect of the movement of gas-water contact.

In all aquifer size, Fetkovich and van Everdingen & Hurst water influx model give very similar W_e value same as Fetkovich's experiment result [3].

In summary, Carter & Tracy water influx model is the most accurate model in all cases.

At the early time, the calculated W_e from all water influx models are lower than the simulated W_e in all aquifer sizes, except simple aquifer model in 70-PV and 100-PV aquifer sizes. This error is from numerical error since the calculation in ECLIPSE 100 is fully implicit but the calculated W_e from all water influx model are from explicit calculation. At 70-PV and 100-PV aquifer sizes, the calculated W_e from simple aquifer model are higher than the simulated W_e because the effect of overestimation of W_e in large aquifer from simple aquifer model is higher than the effect from numerical error.

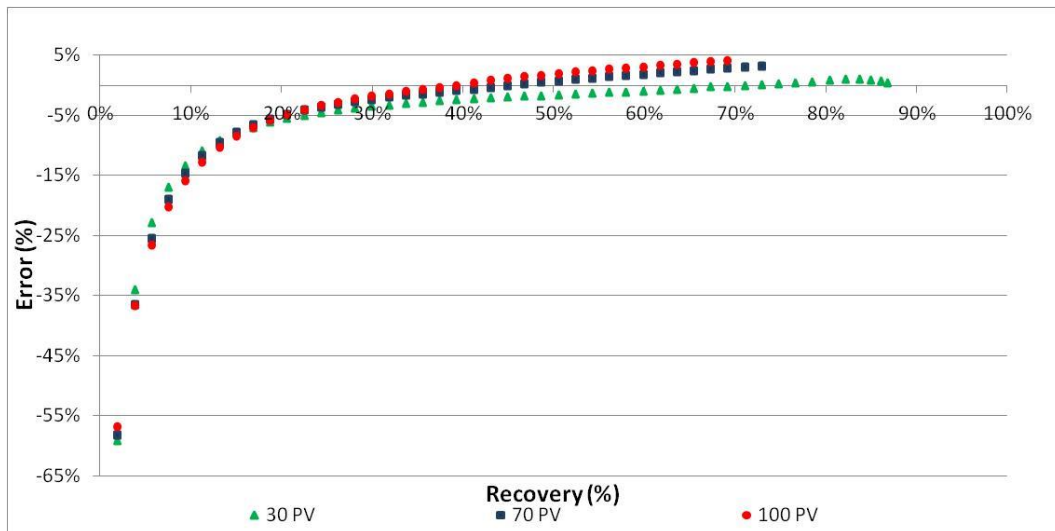


Figure 6.51 Error percentage of van Everdingen & Hurst calculated W_e in 50 mD reservoir by using field pressure

6.5 OGIP Estimation Using p/z versus G_p Plot for 50 mD and 500 mD Water-drive Dry-gas Reservoir

The OGIP value of water-drive dry-gas reservoir can be estimated by the y-intercept of $(G_p B_g + W_p B_w)/(B_g - B_{gi})$ versus $W_e/(B_g - B_{gi})$ plot while the OGIP value of volumetric dry-gas reservoir can be estimated by the x-intercept of the p/z versus G_p plot.

In reality, the reservoir drive mechanism is sometimes not clearly identified. This may lead to using inappropriate Material balance method for OGIP estimation.

The objective of this section is to verify the feasibility of OGIP estimation in water-drive dry-gas reservoir by applying p/z versus G_p plot. Table 6.3 shows the parameters to be studied in this section. These parameters are selected because they have impacts on the reservoir behavior. The aquifer size represents the level of pressure support from the aquifer to the reservoir as shown in Section 6.2.1. The shut-in duration affects the accuracy of SBHP on representing the actual reservoir pressure. Apart from shut-in duration, the accuracy of SBHP is affected by permeability also.

Table 6.3 Parameters to be studied on the feasibility of OGIP estimation in water-drive dry-gas reservoir by applying p/z versus G_p plot.

Case	Permeability (mD)	Aquifer size (PV)	Shut-in duration
1	50	0	6 hours
2			1 day
3			7 days
4		1	6 hours
5			1 day
6			7 days
7		10	6 hours
8			1 day
9			7 days
10		30	6 hours
11			1 day
12			7 days
13		70	6 hours
14			1 day
15			7 days
16		100	6 hours
17			1 day
18			7 days
19	500	0	6 hours
20			1 day

Table 6.3 Parameters to be studied on the feasibility of OGIP estimation in water-drive dry-gas reservoir by applying p/z versus G_p plot. (continued)

Case	Permeability (mD)	Aquifer size (PV)	Shut-in duration
21	500	0	7 days
22		1	6 hours
23			1 day
24			7 days
25			10
26		1 day	
27		7 days	
28		30	6 hours
29			1 day
30			7 days
31		70	6 hours
32			1 day
33			7 days
34		100	6 hours
35			1 day
36			7 days

Figure 6.52 displays p/z versus G_p plots for the case without aquifer while Figure 6.53 to Figure 6.57 are the p/z versus G_p plots with the estimated OGIP value for 50 mD water-drive dry-gas reservoir having different aquifer sizes and shut-in durations for SBHP measurement.

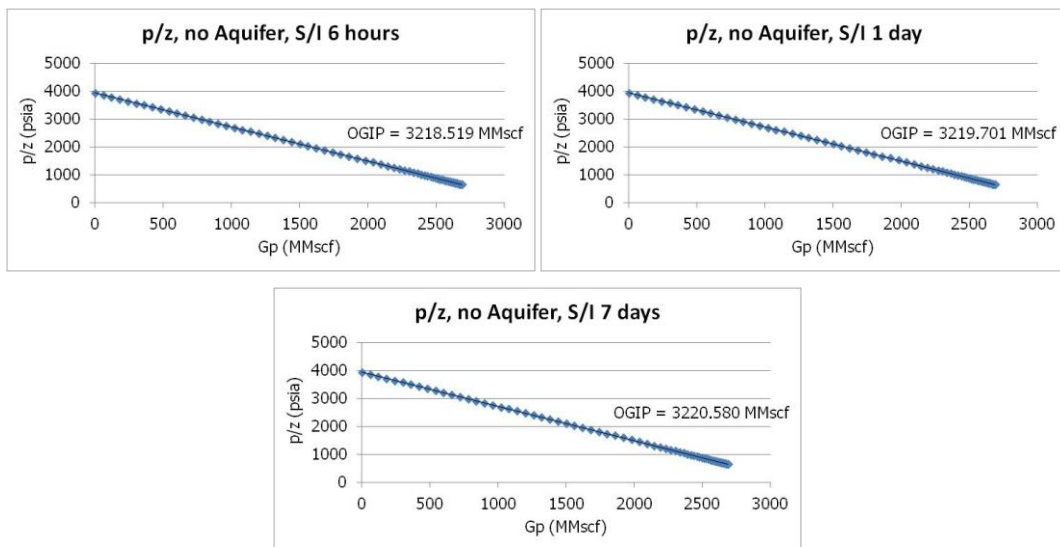


Figure 6.52 p/z versus G_p without aquifer support for 50 mD reservoir, case 1-3

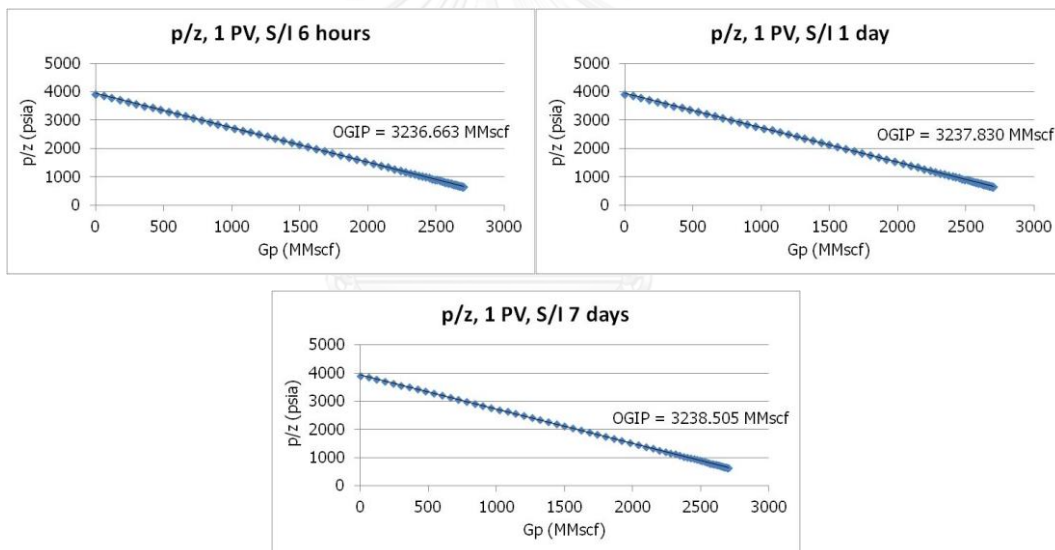


Figure 6.53 p/z versus G_p at 1-PV aquifer size for 50 mD reservoir, case 4-6

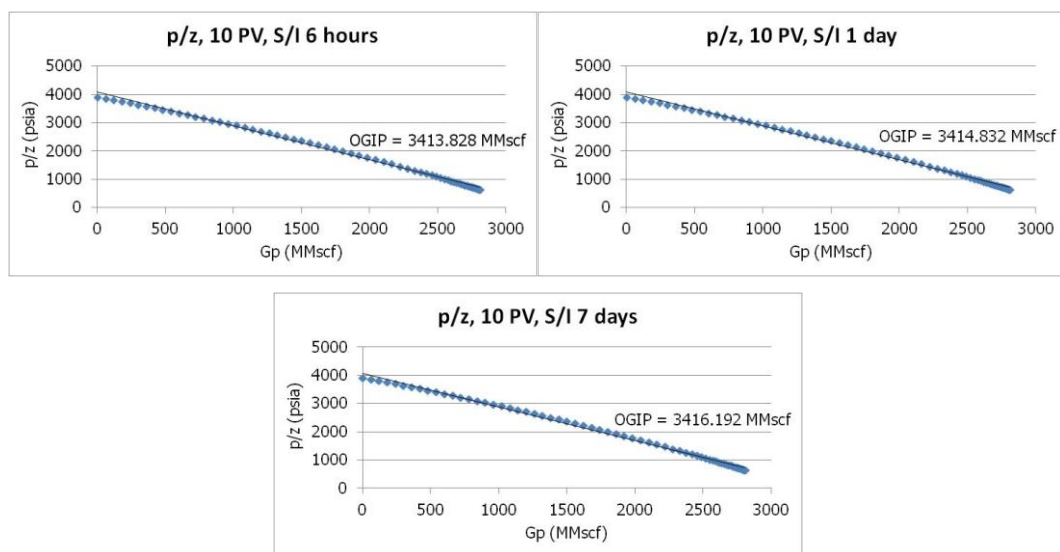


Figure 6.54 p/z versus G_p at 10-PV aquifer size for 50 mD reservoir, case 7-9

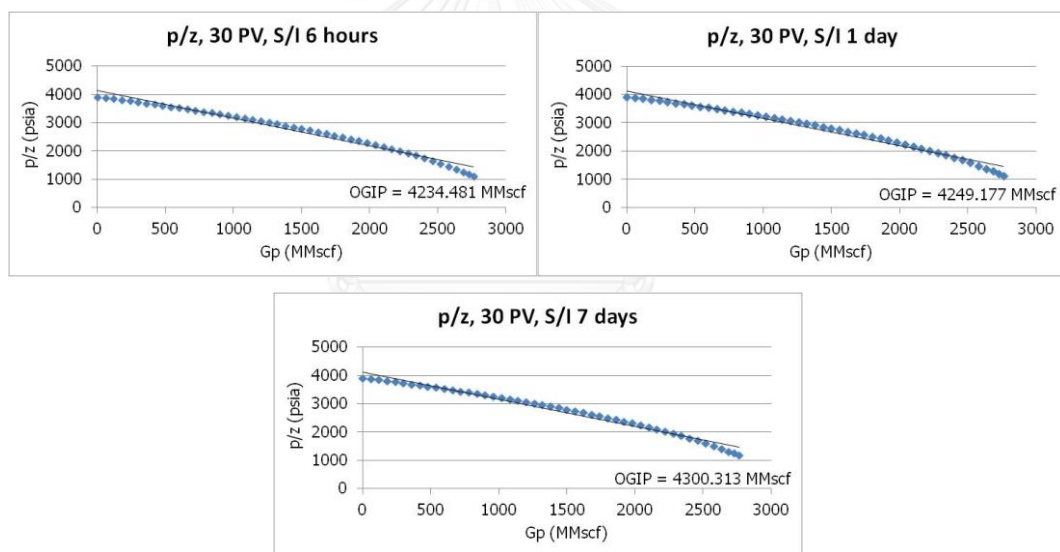


Figure 6.55 p/z versus G_p at 30-PV aquifer size for 50 mD reservoir, case 10-12

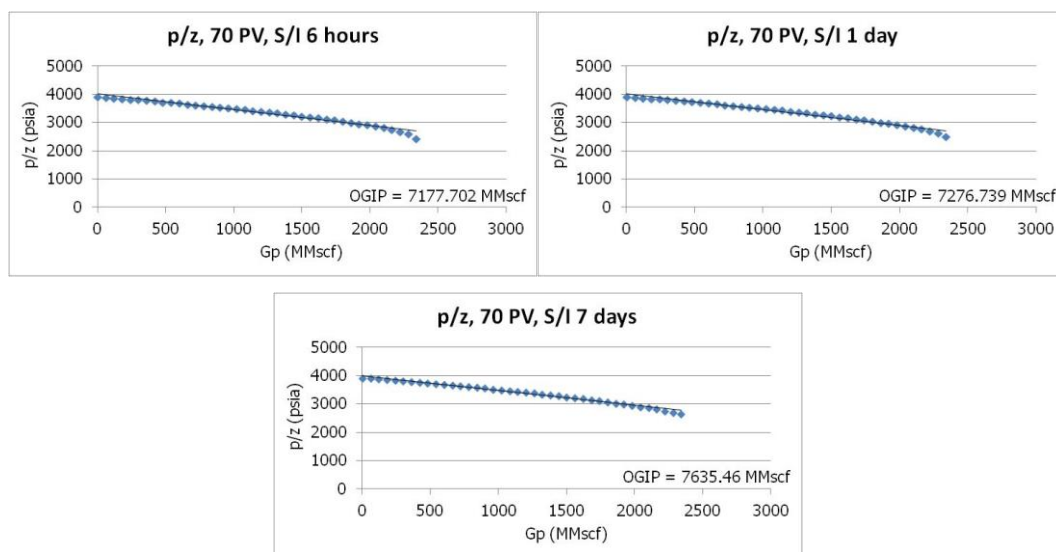


Figure 6.56 p/z versus G_p at 70-PV aquifer size for 50 mD reservoir, case 13-15

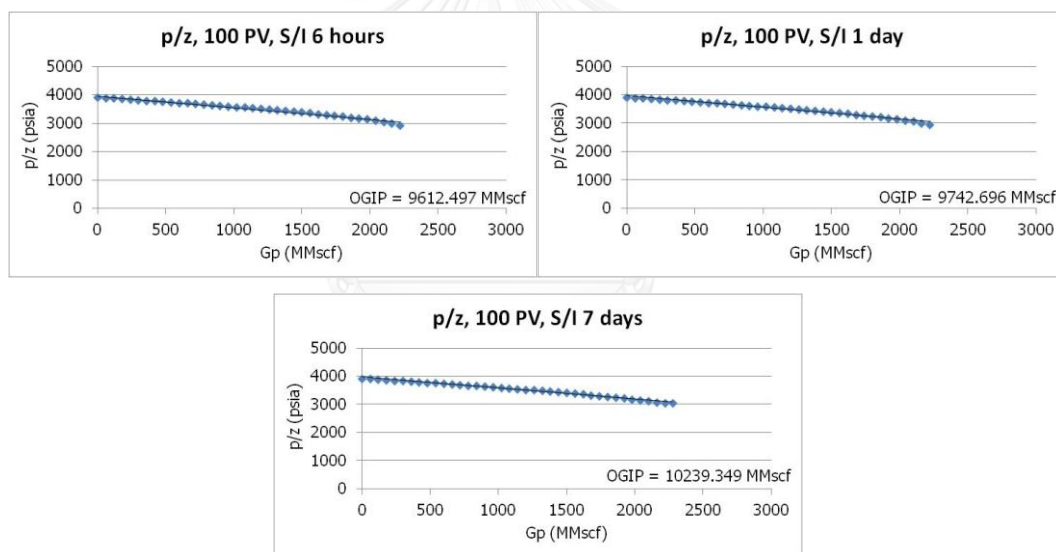


Figure 6.57 p/z versus G_p at 100-PV aquifer size for 50 mD reservoir, case 16-18

The p/z versus G_p plots for 10-PV, 30-PV, 70-PV and 100-PV aquifer sizes in Figure 6.54 to Figure 6.57 are not exactly straight line. They show a convex trend, and the R-squared values of these cases in Table 6.4 are not exactly one.

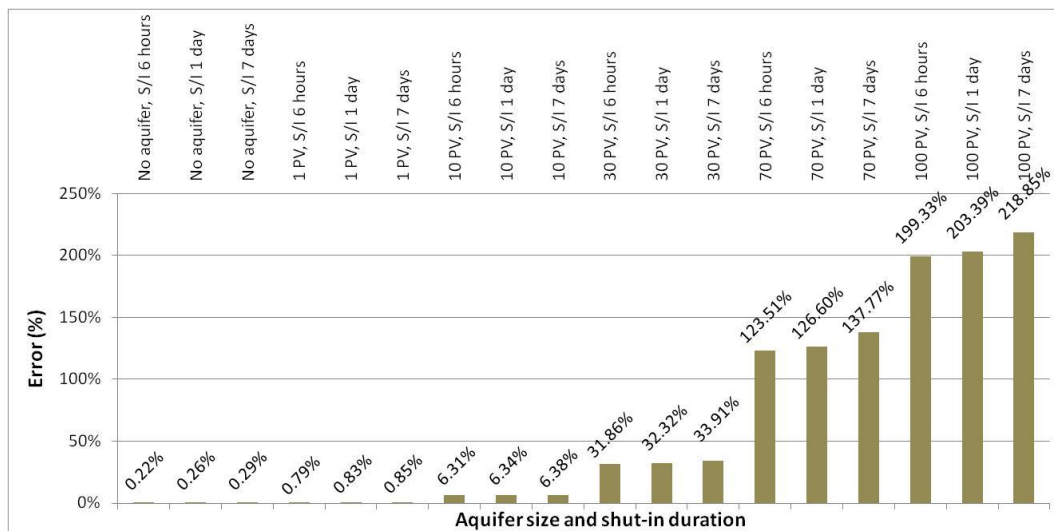


Figure 6.58 Error of estimated OGIP for 50 mD water-drive dry-gas reservoir by p/z versus G_p plot

Table 6.4 Result of OGIP estimation for 50 mD water-drive dry-gas reservoir by p/z versus G_p plot

Case	Aquifer size (PV)	Shut-in duration	Estimated OGIP (MMscf)	Error (%)	R-squared
1	0	6 hours	3218.519	0.22%	1.000
2		1 day	3219.701	0.26%	1.000
3		7 days	3220.580	0.29%	1.000
4	1	6 hours	3236.663	0.79%	1.000
5		1 day	3237.830	0.83%	1.000
6		7 days	3238.505	0.85%	1.000
7	10	6 hours	3413.828	6.31%	0.997
8		1 day	3414.832	6.34%	0.997
9		7 days	3416.192	6.38%	0.997

Table 6.4 Result of OGIP estimation for 50 mD water-drive dry-gas reservoir by p/z versus G_p plot

Case	Aquifer size (PV)	Shut-in duration	Estimated OGIP (MMscf)	Error (%)	R-squared
10	30	6 hours	4234.481	31.86%	0.976
11		1 day	4249.177	32.32%	0.977
12		7 days	4300.313	33.91%	0.980
13	70	6 hours	7177.702	123.51%	0.970
14		1 day	7276.739	126.60%	0.975
15		7 days	7635.460	137.77%	0.986
16	100	6 hours	9612.497	199.33%	0.980
17		1 day	9742.696	203.39%	0.983
18		7 days	10239.350	218.85%	0.990

Table 6.5 Accuracy of OGIP estimation for 50 mD water-drive dry-gas reservoir by p/z versus G_p plot

Aquifer size (PV)	Shut-in duration	Accuracy
0 and 1	6 hours, 1 day and 7 days	Accurate
10		Acceptable
30, 70 and 100		Not acceptable

Accurate: error<5%, Acceptable: error<10%, Not acceptable: error>=10%

There are two reasons behind this non-straight line behavior. The first reason is from the nature of water-drive dry-gas reservoir. With water support, p/z versus G_p plot will deviate from straight line since the slope of the plot changes with time as proved by Material balance equation in water-drive dry-gas reservoir as follows:

$$GB_{gi} = (G - G_p)B_g + W_e - W_p B_w \quad \text{--- (6.1)}$$

$$G_p B_g = G(B_g - B_{gi}) + (W_e - W_p B_w) \quad \text{--- (6.2)}$$

$$G_p = G \left(1 - \frac{B_{gi}}{B_g} \right) + \frac{(W_e - W_p B_w)}{B_g} \quad \text{--- (6.3)}$$

$$\frac{G_p}{G} = \left(1 - \frac{z_i p}{z p_i} \right) + \frac{z_i p (W_e - W_p B_w)}{z p_i G B_{gi}} \quad \text{--- (6.4)}$$

$$\frac{z_i p}{z p_i} \left(1 - \frac{(W_e - W_p B_w)}{G B_{gi}} \right) = 1 - \frac{G_p}{G} \quad \text{--- (6.5)}$$

$$\frac{p}{z} \left(1 - \frac{(W_e - W_p B_w)}{G B_{gi}} \right) = \frac{p_i}{z_i} \left(1 - \frac{G_p}{G} \right) \quad \text{--- (6.6)}$$

$$\frac{p}{z} = \frac{\frac{p_i}{z_i} \left(1 - \frac{G_p}{G} \right)}{\left(1 - \frac{(W_e - W_p B_w)}{G B_{gi}} \right)} \quad \text{--- (6.7)}$$

The second reason is because the differences between SBHP and the actual reservoir pressure increase as time increases in moderate to large aquifer size cases as mentioned in Section 6.3.1, Figure 6.21. This can be demonstrated by the R-squared values of the moderate to large aquifer sizes, 30 PV, 70 PV and 100 PV. The longer shut-in duration, the plot is more likely to be a straight line.

Figure 6.58 indicates that the estimated OGIP values from p/z versus G_p plot are always higher than the actual one, positive error percentage. The overestimation

is because the p/z versus G_p plot does not take into account the effect of pressure support by the water influx from the aquifer to the reservoir. The magnitude of the error of the estimated OGIP increases when the aquifer size increases due to more water influx and pressure support from the larger aquifer. The errors in no aquifer support cases are still positive but the magnitudes are very small since these errors are from numerical error only, not the effect of pressure support from the aquifer.

A longer shut-in duration for the same aquifer size gives a larger estimated OGIP value due to more time for SBHP to approach the actual reservoir pressure. The R-squared values for 30-PV, 70-PV and 100-PV aquifer sizes increase with shut-in duration because the convex trend in these cases decreases when the shut-in duration increases.

Figure 6.59 displays p/z versus G_p plots for the case without aquifer while Figure 6.60 to Figure 6.64 are the p/z versus G_p plots with the estimated OGIP value for 500 mD water-drive dry-gas reservoir having different aquifer sizes and shut-in durations for SBHP measurement.

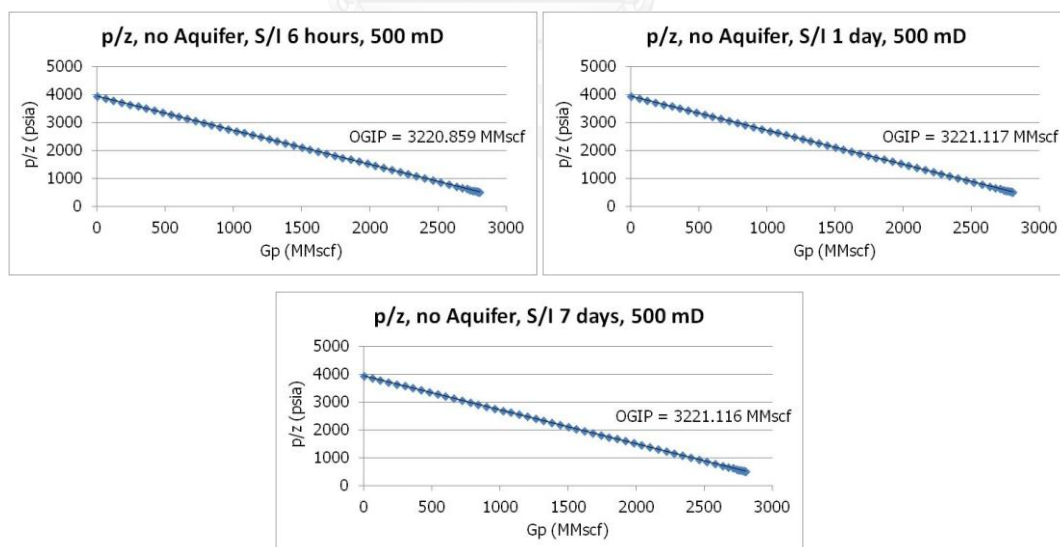


Figure 6.59 p/z versus G_p without aquifer support for 500 mD reservoir, case 19-21

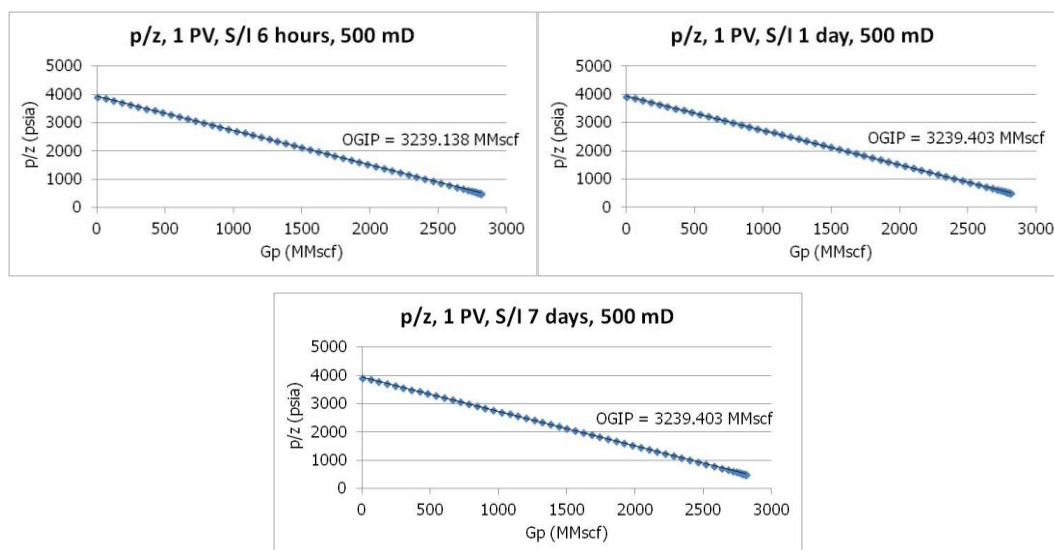


Figure 6.60 p/z versus G_p at 1-PV aquifer size for 500 mD reservoir, case 22-24

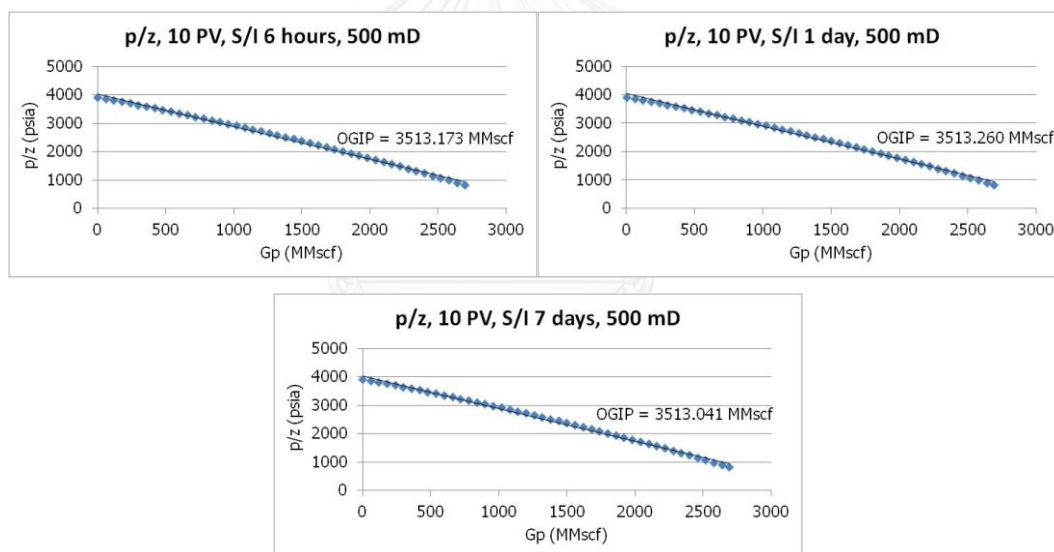


Figure 6.61 p/z versus G_p at 10-PV aquifer size for 500 mD reservoir, case 25-27

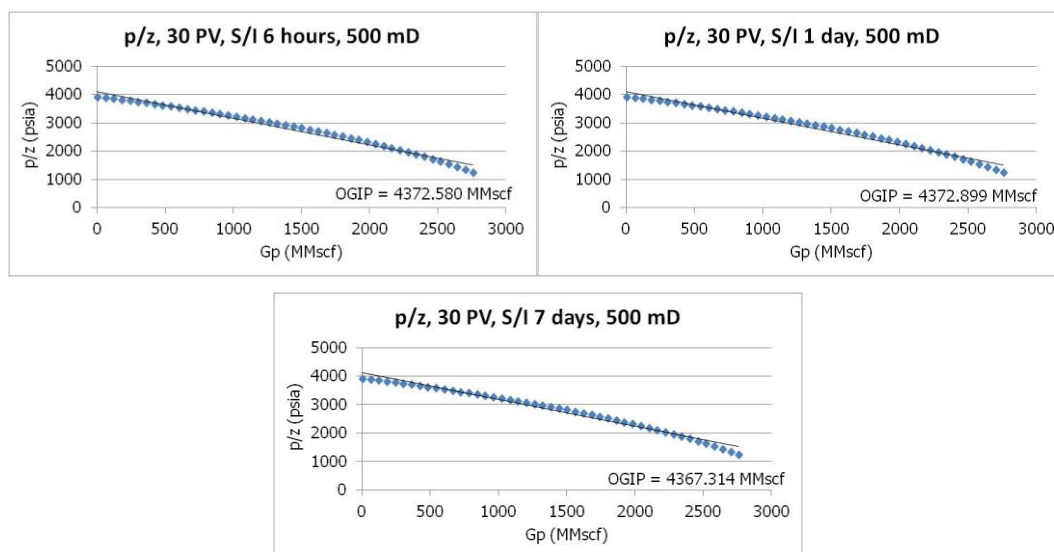


Figure 6.62 p/z versus G_p at 30-PV aquifer size for 500 mD reservoir, case 28-30

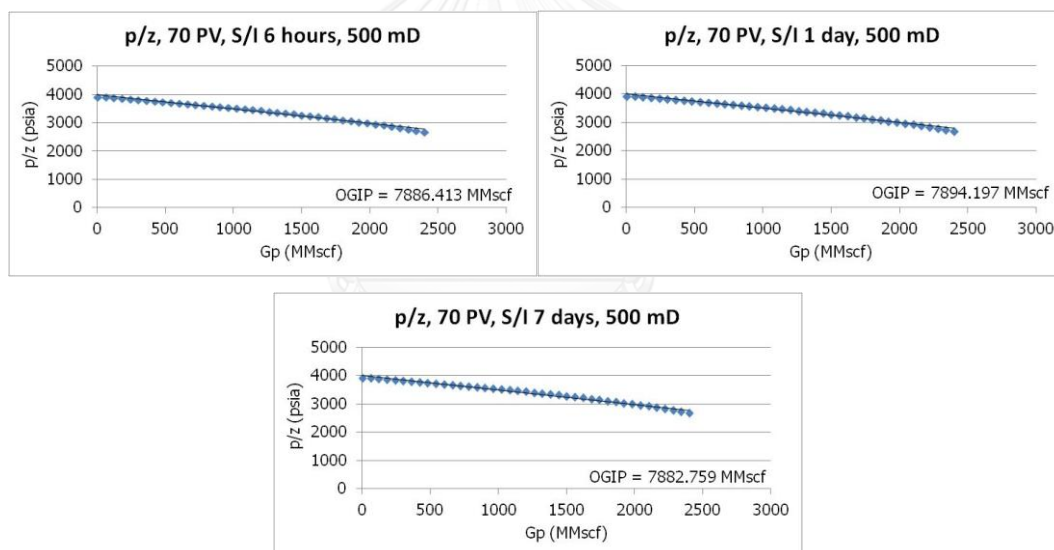


Figure 6.63 p/z versus G_p at 70-PV aquifer size for 500 mD reservoir, case 31-33

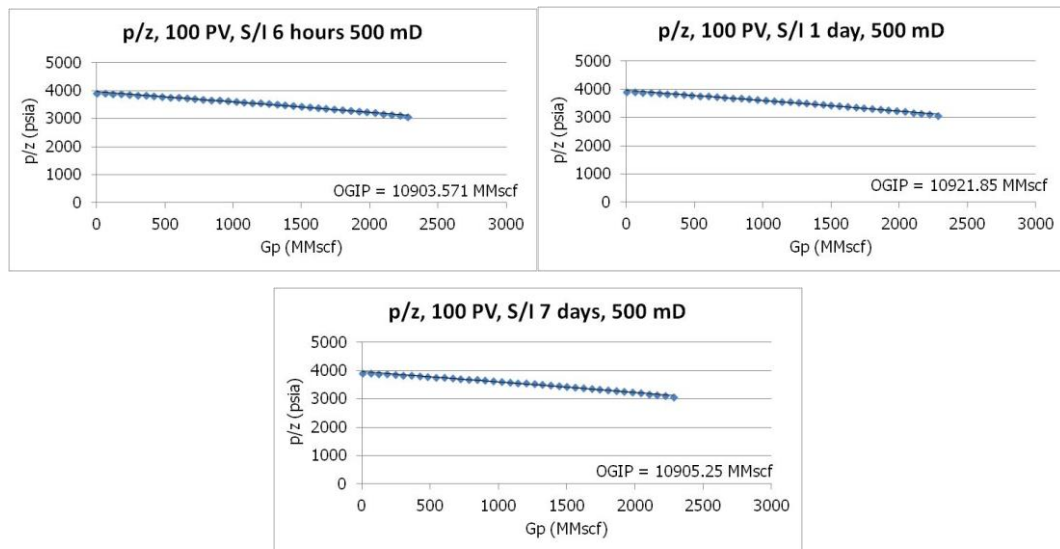


Figure 6.64 p/z versus G_p at 100-PV aquifer size for 500 mD reservoir, case 34-36

The convex trend in p/z versus G_p plots in 10-PV, 30-PV, 70-PV and 100-PV aquifer size cases in Figure 6.61 to Figure 6.64 are not as obvious as in 50 mD reservoir cases. This is demonstrated by the higher R-squared values in 500 mD reservoir cases as shown in Table 6.6. This is because the differences between SBHP and the actual reservoir pressure in 500 mD reservoir are smaller than the ones in 50 mD reservoir as mentioned in Section 6.3.1, Figure 6.21.

Figure 6.65 shows a similar trend as Figure 6.58 that the estimated OGIP values from this method are higher than the actual value and the magnitude of error increases with aquifer size.

The shut-in duration for 500 mD reservoir does not affect the value of the estimated OGIP as for 50 mD reservoir because SBHP can build up to approach the actual reservoir pressure faster in 500 mD reservoir as mentioned in Section 6.3.1.

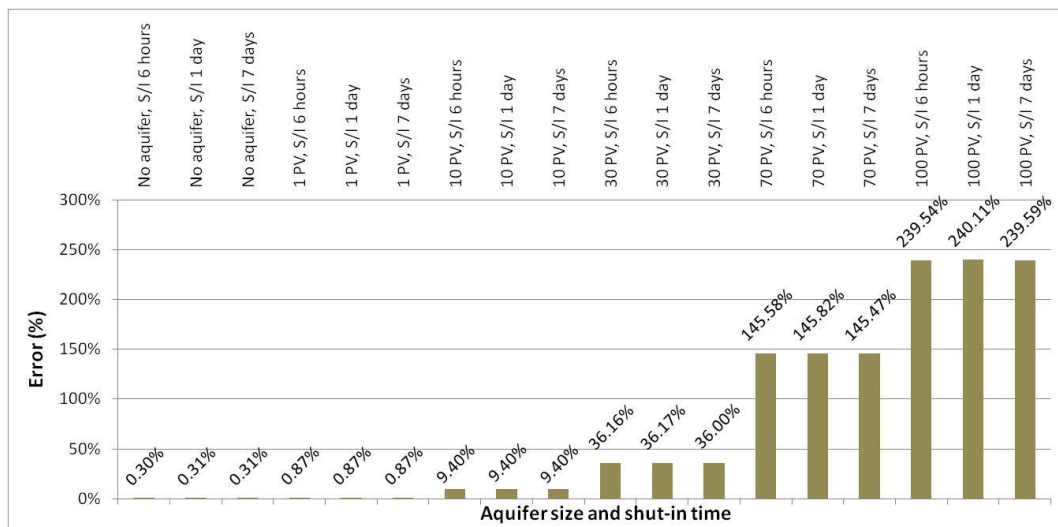


Figure 6.65 Error of estimated OGIP for 500 mD water-drive dry-gas reservoir by p/z versus G_p plot

For the same aquifer size and shut-in duration, the values of the estimated OGIP in 500 mD reservoir are higher than those for 50 mD reservoir because of the faster SBHP build up rate and the higher amount of water influx in 500 mD reservoir.

Table 6.6 Result of OGIP estimation for 500 mD water-drive dry-gas reservoir by p/z versus G_p plot

Case	Aquifer size (PV)	Shut-in duration	Estimated OGIP (MMscf)	Error (%)	R-squared
19	0	6 hours	3220.859	0.30%	1.000
20		1 day	3221.117	0.31%	1.000
21		7 days	3221.116	0.31%	1.000
22	1	6 hours	3239.138	0.87%	1.000
23		1 day	3239.403	0.87%	1.000
24		7 days	3239.403	0.87%	1.000

Table 6.6 Result of OGIP estimation for 500 mD water-drive dry-gas reservoir by p/z versus G_p plot (continued)

Case	Aquifer size (PV)	Shut-in duration	Estimated OGIP (MMscf)	Error (%)	R-squared
25	10	6 hours	3513.173	9.40%	0.996
26		1 day	3513.260	9.40%	0.996
27		7 days	3513.041	9.40%	0.996
28	30	6 hours	4372.580	36.16%	0.981
29		1 day	4372.899	36.17%	0.981
30		7 days	4367.314	36.00%	0.981
31	70	6 hours	7886.413	145.58%	0.988
32		1 day	7894.197	145.82%	0.988
33		7 days	7882.759	145.47%	0.988
34	100	6 hours	10903.570	239.54%	0.992
35		1 day	10921.850	240.11%	0.992
36		7 days	10905.25.0	239.59%	0.992

Table 6.7 Accuracy of OGIP estimation for 500 mD water-drive dry-gas reservoir by p/z versus G_p plot

Aquifer size (PV)	Shut-in duration	Accuracy
0 and 1	6 hours, 1 day and 7 days	Accurate
10		Acceptable
30, 70 and 100		Not acceptable

Accurate: error<5%, Acceptable: error<10%, Not acceptable: error>=10%

6.6 OGIP Estimation Using $(G_p B_g + W_p B_w)/(B_g - B_{gi})$ versus $W_e/(B_g - B_{gi})$ Plot for 50 mD Water-drive Dry-gas Reservoir

In water-drive dry-gas reservoir, the value of OGIP can be estimated by the y-intercept of the $(G_p B_g + W_p B_w)/(B_g - B_{gi})$ versus $W_e/(B_g - B_{gi})$ plot. All of the parameters in this equation are from the simulated production data directly except W_e . The value of W_e in this equation is a calculated W_e from a selected water influx model.

The objective of this section is to investigate the effect of aquifer size, shut-in duration and water influx model on the accuracy of OGIP estimation by applying $(G_p B_g + W_p B_w)/(B_g - B_{gi})$ versus $W_e/(B_g - B_{gi})$ plot. Table 6.8 shows the parameters to be studied in this section.

Table 6.8 Parameters to be studied on the accuracy of OGIP estimation for 50 mD water-drive dry-gas reservoir by applying $(G_p B_g + W_p B_w)/(B_g - B_{gi})$ versus $W_e/(B_g - B_{gi})$ plot

Case	Aquifer size (PV)	Shut-in duration	Water influx model
1	1	6 hours	Simple aquifer model
2			Fetkovich
3			van Everdingen & Hurst
4			Carter & Tracy
5		1 day	Simple aquifer model
6			Fetkovich
7			van Everdingen & Hurst
8			Carter & Tracy
9		7 days	Simple aquifer model

Table 6.8 Parameters to be studied on the accuracy of OGIP estimation for 50 mD water-drive dry-gas reservoir by applying $(G_p B_g + W_p B_w)/(B_g - B_{gi})$ versus $W_e/(B_g - B_{gi})$ plot
(continued)

Case	Aquifer size (PV)	Shut-in duration	Water influx model
10	1	7 days	Fetkovich
11			van Everdingen & Hurst
12			Carter & Tracy
13	10	6 hours	Simple aquifer model
14			Fetkovich
15			van Everdingen & Hurst
16			Carter & Tracy
17		1 day	Simple aquifer model
18			Fetkovich
19			van Everdingen & Hurst
20			Carter & Tracy
21		7 days	Simple aquifer model
22			Fetkovich
23			van Everdingen & Hurst
24			Carter & Tracy
25	30	6 hours	Simple aquifer model
26			Fetkovich
27			van Everdingen & Hurst
28			Carter & Tracy

Table 6.8 Parameters to be studied on the accuracy of OGIP estimation for 50 mD water-drive dry-gas reservoir by applying $(G_p B_g + W_p B_w)/(B_g - B_{gi})$ versus $W_e/(B_g - B_{gi})$ plot
(continued)

Case	Aquifer size (PV)	Shut-in duration	Water influx model
29	30	1 day	Simple aquifer model
30			Fetkovich
31			van Everdingen & Hurst
32			Carter & Tracy
33		7 days	Simple aquifer model
34			Fetkovich
35			van Everdingen & Hurst
36			Carter & Tracy
37	70	6 hours	Simple aquifer model
38			Fetkovich
39			van Everdingen & Hurst
40			Carter & Tracy
41		1 day	Simple aquifer model
42			Fetkovich
43			van Everdingen & Hurst
44			Carter & Tracy
45		7 days	Simple aquifer model
46			Fetkovich
47			van Everdingen & Hurst

Table 6.8 Parameters to be studied on the accuracy of OGIP estimation for 50 mD water-drive dry-gas reservoir by applying $(G_p B_g + W_p B_w)/(B_g - B_{gi})$ versus $W_e/(B_g - B_{gi})$ plot
(continued)

Case	Aquifer size (PV)	Shut-in duration	Water influx model
48	70	7 days	Carter & Tracy
49	100	6 hours	Simple aquifer model
50			Fetkovich
51			van Everdingen & Hurst
52			Carter & Tracy
53		1 day	Simple aquifer model
54			Fetkovich
55			van Everdingen & Hurst
56			Carter & Tracy
57		7 days	Simple aquifer model
58			Fetkovich
59			van Everdingen & Hurst
60			Carter & Tracy

The term $(G_p B_g + W_p B_w)/(B_g - B_{gi})$ or y-axis value represents the effect of withdrawal fluid, gas and water, from the reservoir, and the term $W_e/(B_g - B_{gi})$ or x-axis value represents the effect of water influx into the reservoir. At steady state or pseudo-steady state in water-drive dry-gas reservoir, the slope of $(G_p B_g + W_p B_w)/(B_g - B_{gi})$ versus $W_e/(B_g - B_{gi})$ plot will be one because of the constant reservoir PV assumption.

Figure 6.66 to Figure 6.77 and Figure 6.80 to Figure 6.82 are $(G_p B_g + W_p B_w)/(B_g - B_{gi})$ versus $W_e/(B_g - B_{gi})$ plots for 50 mD water-drive dry-gas reservoir having different aquifer sizes and shut-in durations, using four different water influx models.

For 1-PV aquifer size, as shown in Figure 6.66 to Figure 6.68, the aquifer size is too small to see obvious aquifer support behavior. The slopes of $(G_p B_g + W_p B_w)/(B_g - B_{gi})$ versus $W_e/(B_g - B_{gi})$ plots are never equal to one for the whole reservoir life.

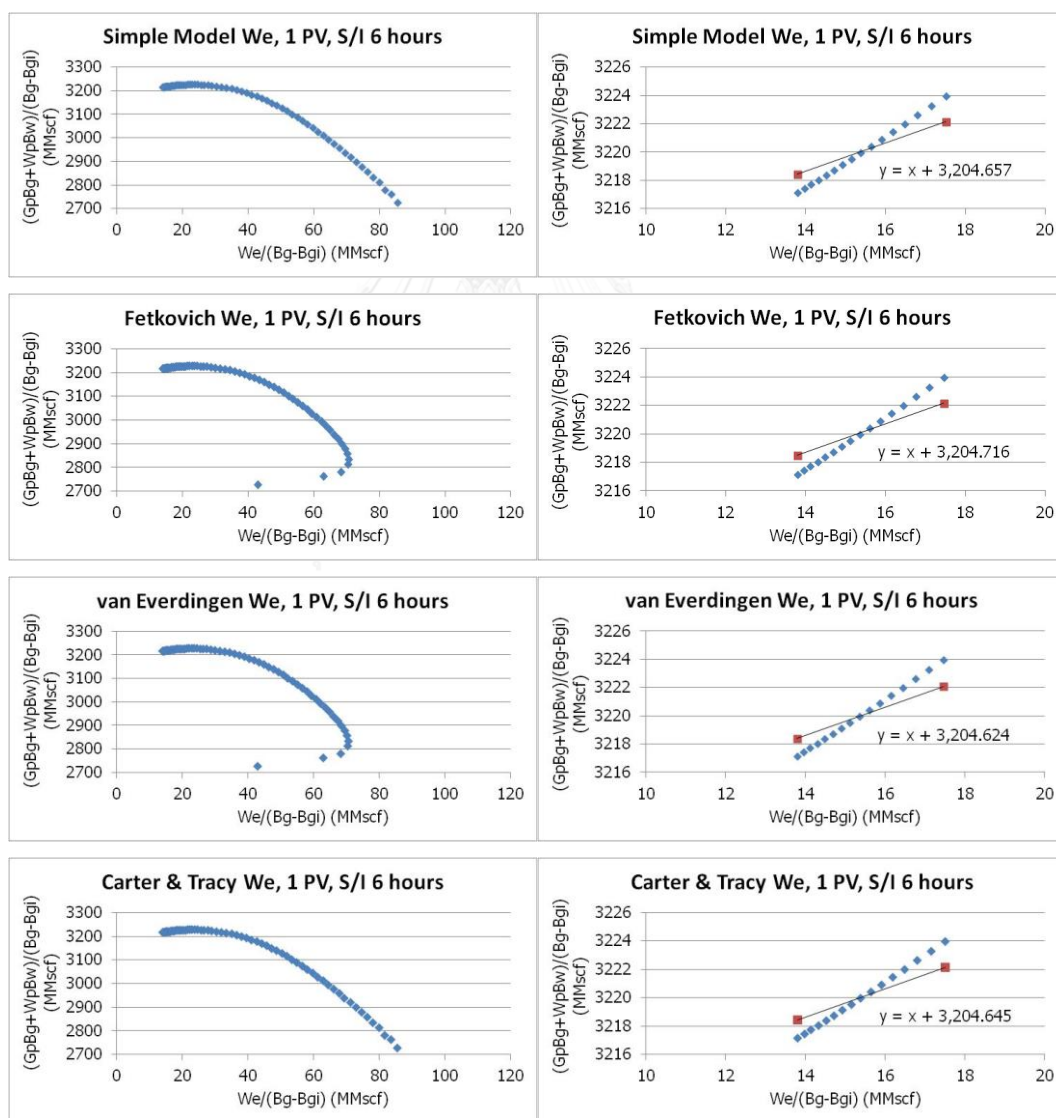


Figure 6.66 $(G_p B_g + W_p B_w)/(B_g - B_{gi})$ versus $W_e/(B_g - B_{gi})$ at 1-PV aquifer size and 6-hour shut-in duration for 50 mD reservoir, case 1-4

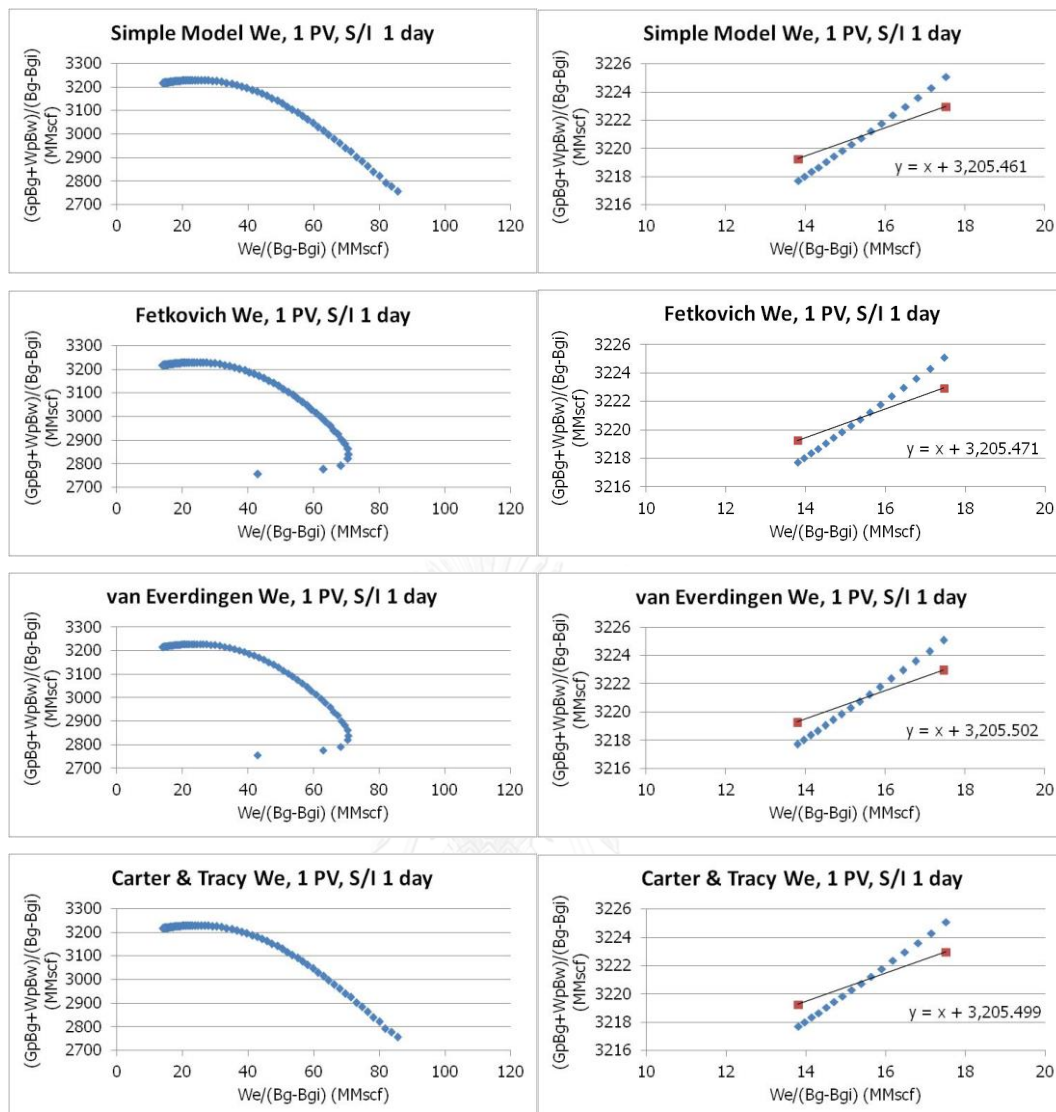


Figure 6.67 $(G_p B_g + W_p B_w) / (B_g - B_{gi})$ versus $W_e / (B_g - B_{gi})$ at 1-PV aquifer size and 1-day shut-in duration for 50 mD reservoir, case 5-8

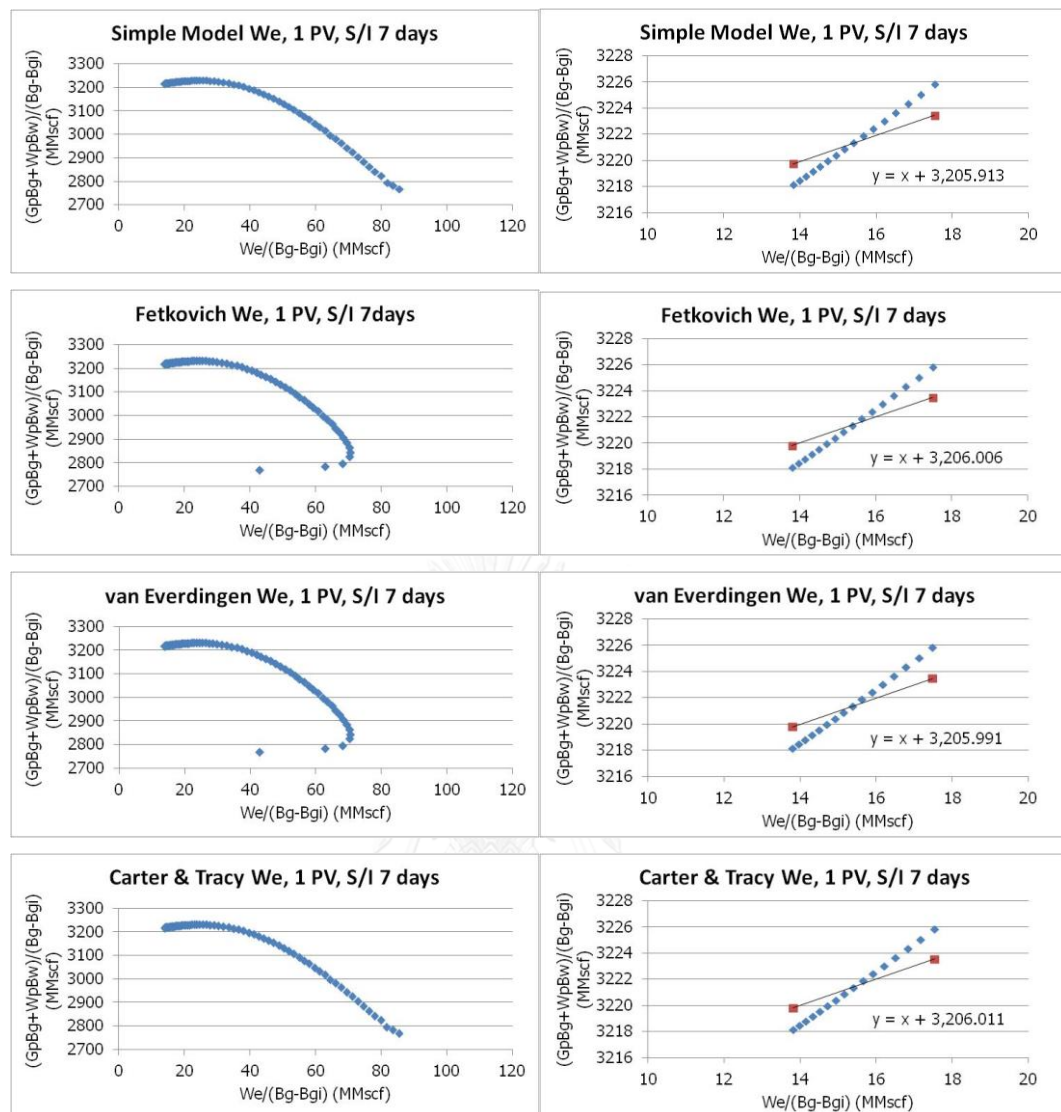


Figure 6.68 $(G_p B_g + W_p B_w)/(B_g - B_{gi})$ versus $W_e/(B_g - B_{gi})$ at 1-PV aquifer size and 7-day shut-in duration for 50 mD reservoir, case 9-12

The shapes of the plots using simple aquifer model and Carter & Tracy water influx model are similar but different from those using van Everdingen & Hurst and Fetkovich water influx model. In van Everdingen & Hurst and Fetkovich water influx model cases, the slopes are positive at very early times before turning negative at the value of $W_e/(B_g - B_{gi})$ around 70 MMscf or 10% RF. Figure 6.42 indicates that the values of calculated W_e from van Everdingen & Hurst and Fetkovich water influx model are very similar and smaller than the values from simple aquifer model and Carter & Tracy

water influx model, especially in the early times. When %RF is lower than 10%, the calculated W_e from van Everdingen & Hurst and Fetkovich water influx models are significantly lower than the simulated W_e but the magnitude of the error decreases very quick to be around 12% error at 10% RF. This means that the increasing rate of the values of calculated W_e or the numerator of the term $W_e/(B_g-B_{gi})$ in van Everdingen & Hurst and Fetkovich water influx model cases are very high when %RF is lower than 10%. Then, the slopes of $(G_p B_g + W_p B_w)/(B_g - B_{gi})$ versus $W_e/(B_g - B_{gi})$ plot during this period are positive.

The late trend of $(G_p B_g + W_p B_w)/(B_g - B_{gi})$ versus $W_e/(B_g - B_{gi})$ plots were fitted with a unit slope straight line for OGIP estimation. The estimated OGIP values for 1-PV aquifer size are around 3204 to 3206 MMscf or -0.21% to -0.17% error depending on water influx model being used as shown in Table 6.9. The R-squared values of these fitting are in the range of 0.73 to 0.79, which does not represent a good fitting.

Table 6.9 Result of OGIP estimation at 1-PV aquifer size for 50 mD water-drive dry-gas reservoir by $(G_p B_g + W_p B_w)/(B_g - B_{gi})$ versus $W_e/(B_g - B_{gi})$ plot

Shut-in duration	Water influx model	Estimated OGIP (MMscf)	Error (%)	R-squared
6 hours	Simple aquifer model	3,204.657	-0.21%	0.791
	Fetkovich	3,204.716	-0.21%	0.786
	van Everdingen & Hurst	3,204.624	-0.21%	0.786
	Carter & Tracy	3,204.645	-0.21%	0.791
1 day	Simple aquifer model	3,205.461	-0.18%	0.754
	Fetkovich	3,205.471	-0.18%	0.749
	van Everdingen & Hurst	3,205.502	-0.18%	0.749
	Carter & Tracy	3,205.499	-0.18%	0.754
7 days	Simple aquifer model	3,205.913	-0.17%	0.732

Table 6.9 Result of OGIP estimation at 1-PV aquifer size for 50 mD water-drive dry-gas reservoir by $(G_p B_g + W_p B_w)/(B_g - B_{gi})$ versus $W_e/(B_g - B_{gi})$ plot (continued)

Shut-in duration	Water influx model	Estimated OGIP (MMscf)	Error (%)	R-squared
7 days	Fetkovich	3,206.006	-0.17%	0.729
	van Everdingen & Hurst	3,205.991	-0.17%	0.729
	Carter & Tracy	3,206.011	-0.17%	0.734

The actual slopes of the latest trend of $(G_p B_g + W_p B_w)/(B_g - B_{gi})$ versus $W_e/(B_g - B_{gi})$ plots of all shut-in durations and water influx models are in the range of 1.85 to 2. If the latest trends are fitted with a straight line without fixing the slope to be one, the R-squared values will be around 1 and the estimated OGIPs will be around 3189 to 3191 MMscf or -0.69 to -0.63% error.

Since the errors of the estimated OGIPs from p/z versus G_p plot are around 0.79% to 0.85% as shown in Table 6.4, then OGIP estimates for 1-PV aquifer size by $(G_p B_g + W_p B_w)/(B_g - B_{gi})$ versus $W_e/(B_g - B_{gi})$ and p/z versus G_p plot are not significantly different and considered to be accurate.

Furthermore, water influx model does not affect the accuracy of OGIP estimation because the aquifer size is very small (only 1 PV). The pressure support from W_e is low. Then, the difference in the calculated W_e between model does not affect much. From Figure 6.42, the calculated W_e from all water influx models at the late time are also similar and close to the simulated W_e .

From Table 6.9, the longer shut-in duration, the more accurate value of the estimated OGIP because the SBHP can build up to be closer to the actual reservoir pressure.

In 10-PV aquifer size, as shown in Figure 6.69 to Figure 6.71, $(G_p B_g + W_p B_w)/(B_g - B_{gi})$ versus $W_e/(B_g - B_{gi})$ plots start to form positive unit slope at the value of $W_e/(B_g - B_{gi})$ around 260 to 285 MMscf or around 73% RF.

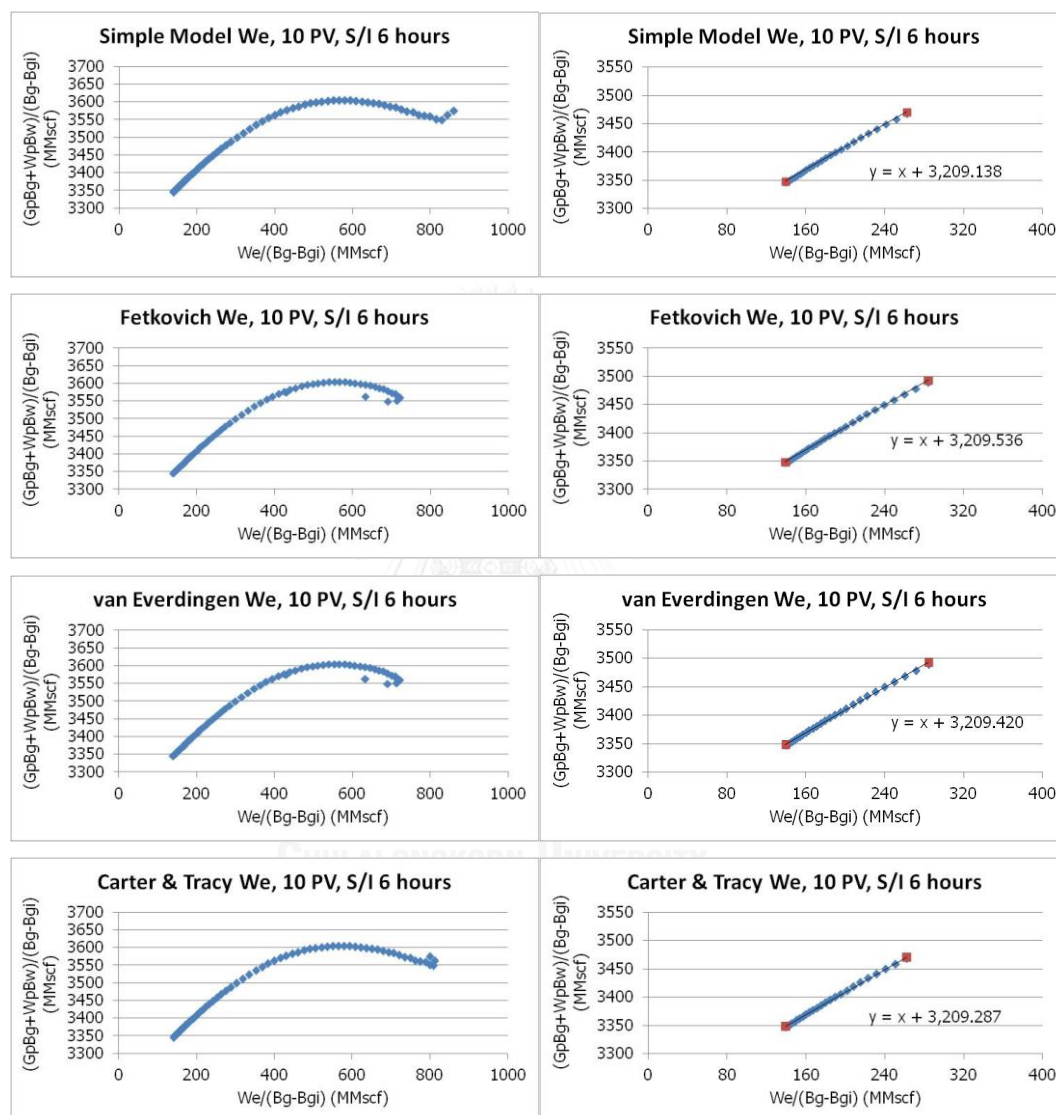


Figure 6.69 $(G_p B_g + W_p B_w)/(B_g - B_{gi})$ versus $W_e/(B_g - B_{gi})$ at 10-PV aquifer size and 6-hour shut-in duration for 50 mD reservoir, case 13-16

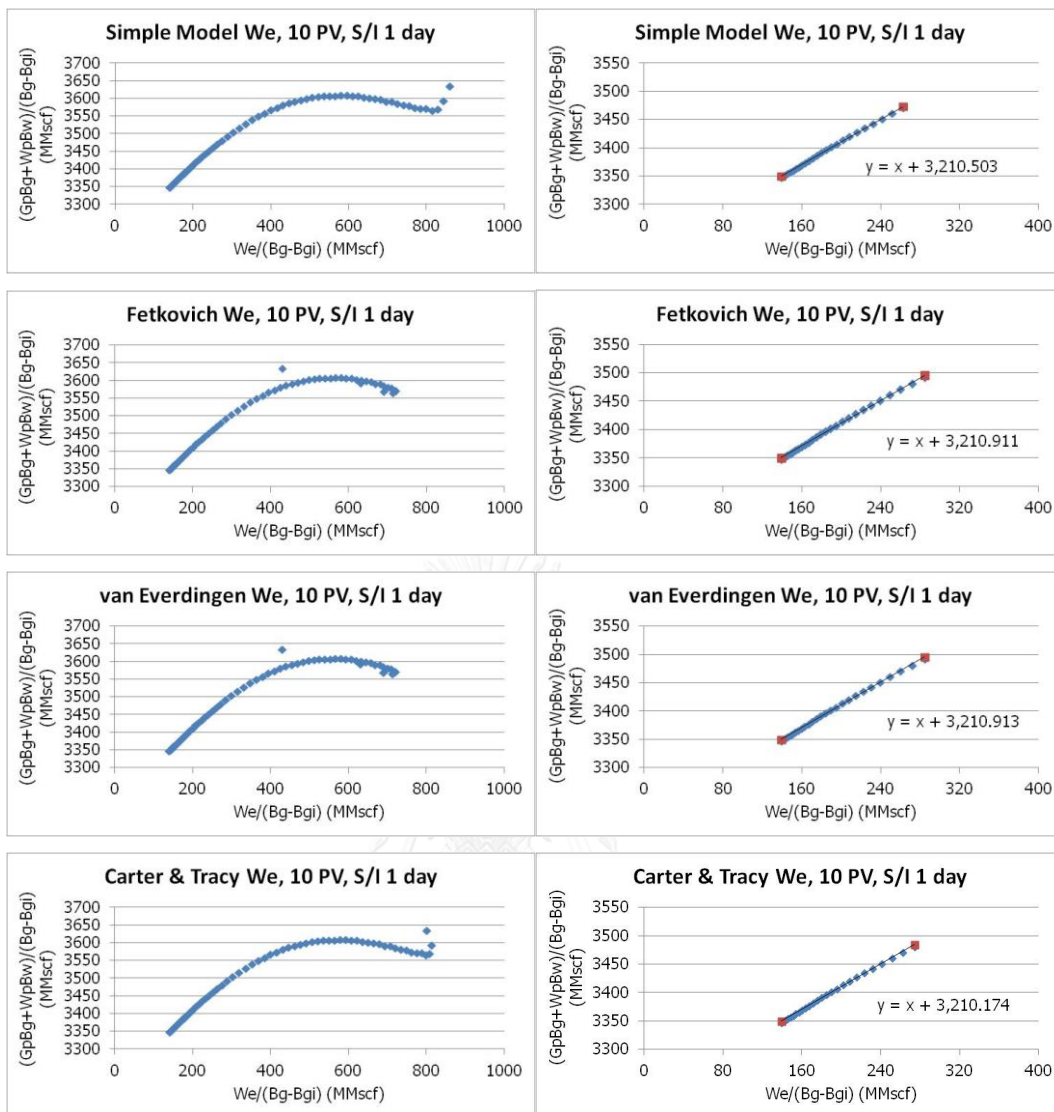


Figure 6.70 $(G_p B_g + W_p B_w) / (B_g - B_{gi})$ versus $W_e / (B_g - B_{gi})$ at 10-PV aquifer size and 1-day shut-in duration for 50 mD reservoir, case 17-20

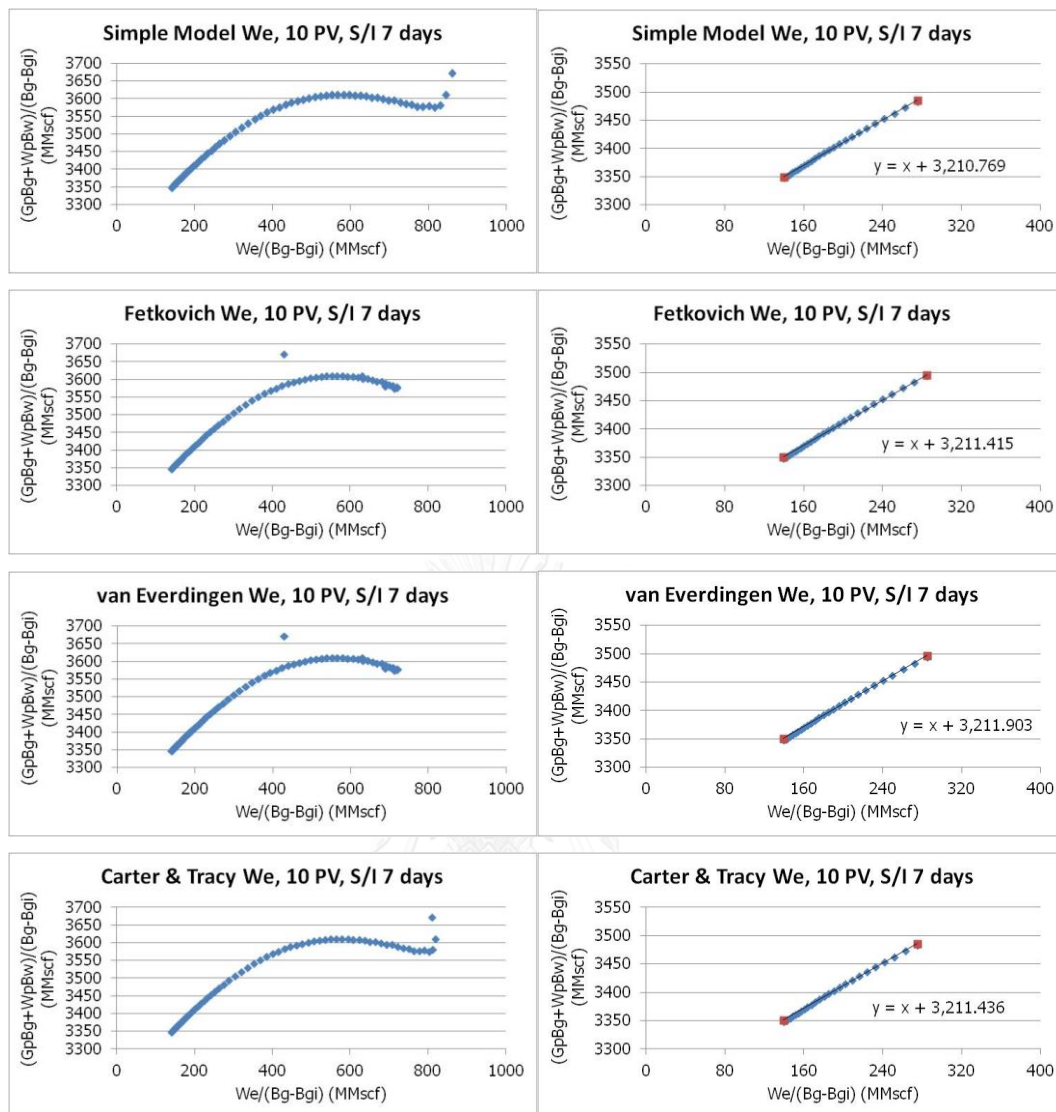


Figure 6.71 $(G_p B_g + W_p B_w)/(B_g - B_{gi})$ versus $W_e/(B_g - B_{gi})$ at 10-PV aquifer size and 7-day shut-in duration for 50 mD reservoir, case 21-24

The slopes of $(G_p B_g + W_p B_w)/(B_g - B_{gi})$ versus $W_e/(B_g - B_{gi})$ plots are negative at early times, like 1-PV aquifer size. The steepness becomes smaller as time increases until the slope turns positive, and the steepness becomes higher until the slope equals to 1 and keeps constant.

The shapes of $(G_p B_g + W_p B_w)/(B_g - B_{gi})$ versus $W_e/(B_g - B_{gi})$ plots for van Everdingen & Hurst and Fetkovich water influx models are very similar for all shut-in durations

because the calculated W_e from these two water influx models are almost the same as shown in Figure 6.44.

The shapes of the $(G_p B_g + W_p B_w)/(B_g - B_{gi})$ versus $W_e/(B_g - B_{gi})$ plots for all water influx models are similar except the very early period which are different from model to model. The reason of this difference is from the different value of calculated W_e at the very early time as shown in Figure 6.44. The calculated W_e from van Everdingen & Hurst and Fetkovich water influx models are significantly lower than the simulated W_e , and the magnitude of the error decreases fast during the period before 10% RF. Then, the value of $W_e/(B_g - B_{gi})$ becomes higher as time increases. This explanation is applied to the shape of $(G_p B_g + W_p B_w)/(B_g - B_{gi})$ versus $W_e/(B_g - B_{gi})$ plot from Carter & Tracy water influx model at very early times as well.

A unit slope straight line was used to fit to the latest trend of $(G_p B_g + W_p B_w)/(B_g - B_{gi})$ versus $W_e/(B_g - B_{gi})$ plots. R-squared values of these fitting are in the range of 0.998 to 0.999 as shown in Table 6.10. The estimated OGIPs in all shut-in duration are around 3209 to 3212 MMscf or -0.07% to 0.02% error which is considered to be very accurate.

Table 6.10 Result of OGIP estimation at 10-PV aquifer size for 50 mD water-drive dry-gas reservoir by $(G_p B_g + W_p B_w)/(B_g - B_{gi})$ versus $W_e/(B_g - B_{gi})$ plot

Shut-in duration	Water influx model	Estimated OGIP (MMscf)	Error (%)	R-squared
6 hours	Simple aquifer model	3,209.138	-0.07%	0.999
	Fetkovich	3,209.536	-0.06%	0.998
	van Everdingen & Hurst	3,209.420	-0.06%	0.998
	Carter & Tracy	3,209.287	-0.06%	0.999
1 day	Simple aquifer model	3,210.503	-0.03%	0.999
	Fetkovich	3,210.911	-0.01%	0.998
	van Everdingen & Hurst	3,210.913	-0.01%	0.998

Table 6.10 Result of OGIP estimation at 10-PV aquifer size for 50 mD water-drive dry-gas reservoir by $(G_p B_g + W_p B_w)/(B_g - B_{gi})$ versus $W_e/(B_g - B_{gi})$ plot (continued)

Shut-in duration	Water influx model	Estimated OGIP (MMscf)	Error (%)	R-squared
1 day	Carter & Tracy	3,210.174	-0.04%	0.999
7 days	Simple aquifer model	3,210.769	-0.02%	0.998
	Fetkovich	3,211.415	0.00%	0.998
	van Everdingen & Hurst	3,211.903	0.02%	0.998
	Carter & Tracy	3,211.436	0.00%	0.998

As depicted in Table 6.10, water influx model does not affect the accuracy of the estimated OGIP. This is because the aquifer size is small. The effect of W_e is not significant. In addition, the calculated W_e from all water influx models at late times are similar and close to the simulated W_e as shown in Figure 6.44.

A longer shut-in duration yields higher and more accurate value of estimated OGIP due to more representative SBHP as shown in Figure 6.83.

For 30-PV aquifer size, the aquifer support behavior or the positive slopes of $(G_p B_g + W_p B_w)/(B_g - B_{gi})$ versus $W_e/(B_g - B_{gi})$ plots can be seen since the beginning as shown in Figure 6.72 to Figure 6.74.

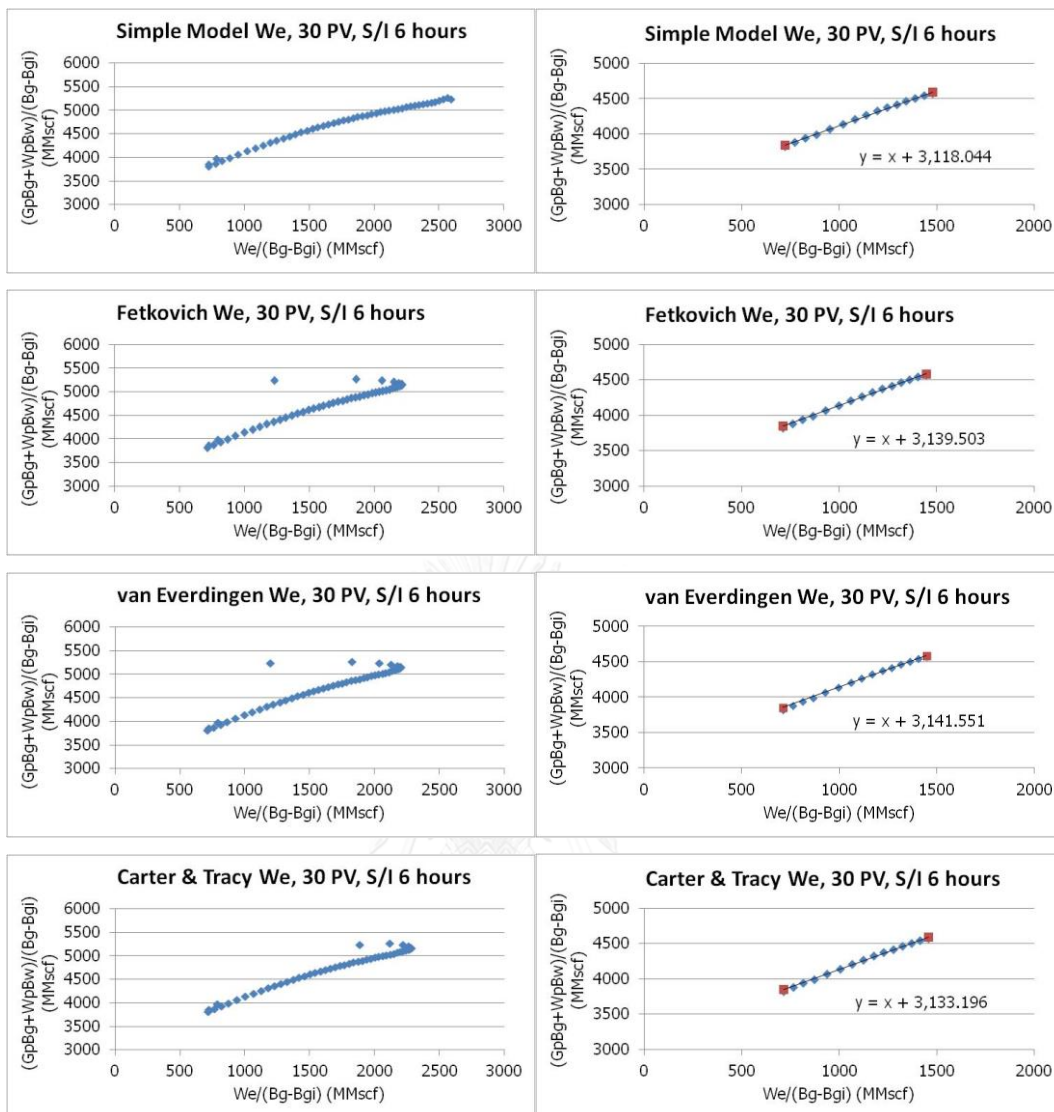


Figure 6.72 $(G_p B_g + W_p B_w) / (B_g - B_{gi})$ versus $W_e / (B_g - B_{gi})$ at 30-PV aquifer size and 6-hour shut-in duration for 50 mD reservoir, case 25-28

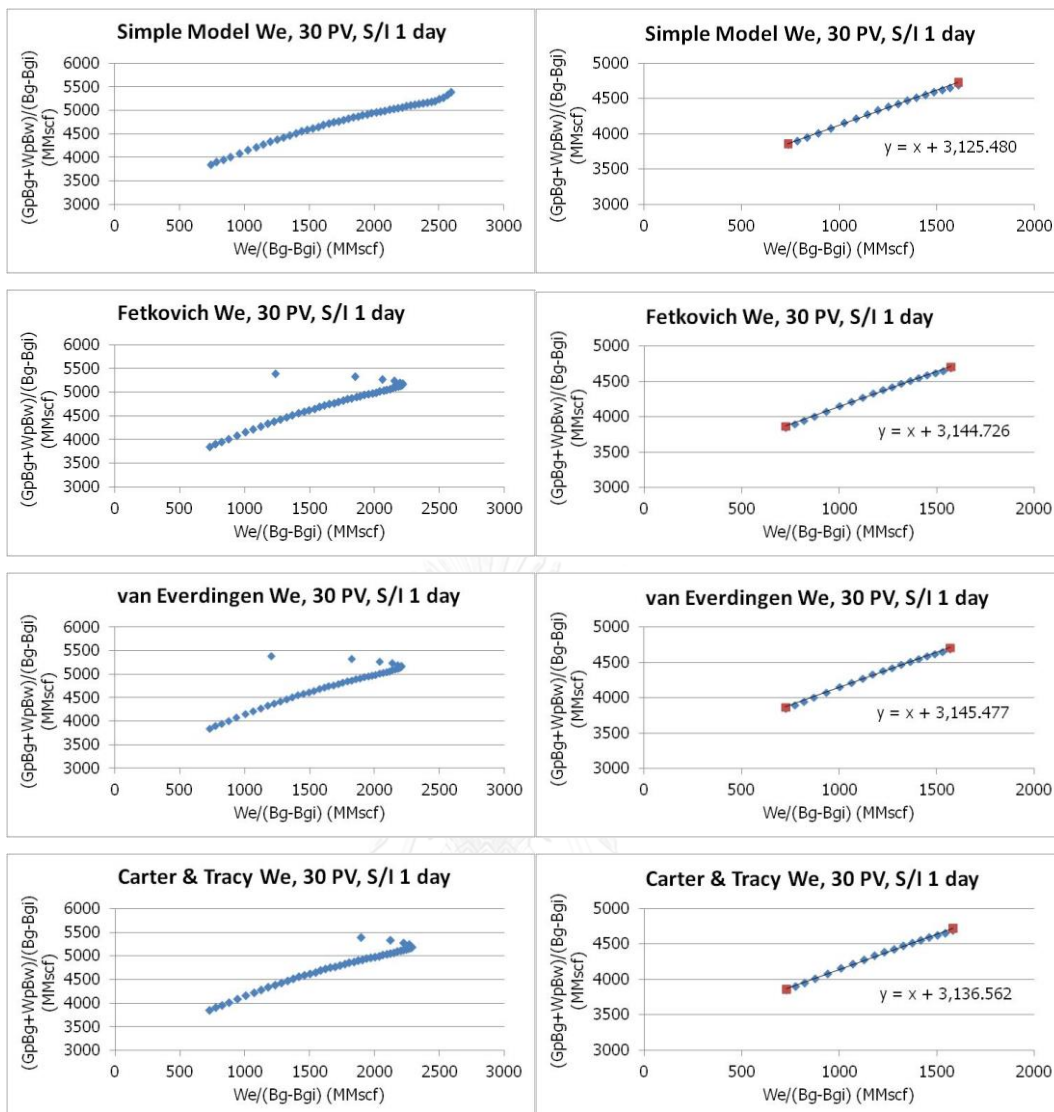


Figure 6.73 $(G_p B_g + W_p B_w) / (B_g - B_{gi})$ versus $W_e / (B_g - B_{gi})$ at 30-PV aquifer size and 1-day shut-in duration for 50 mD reservoir, case 29-32

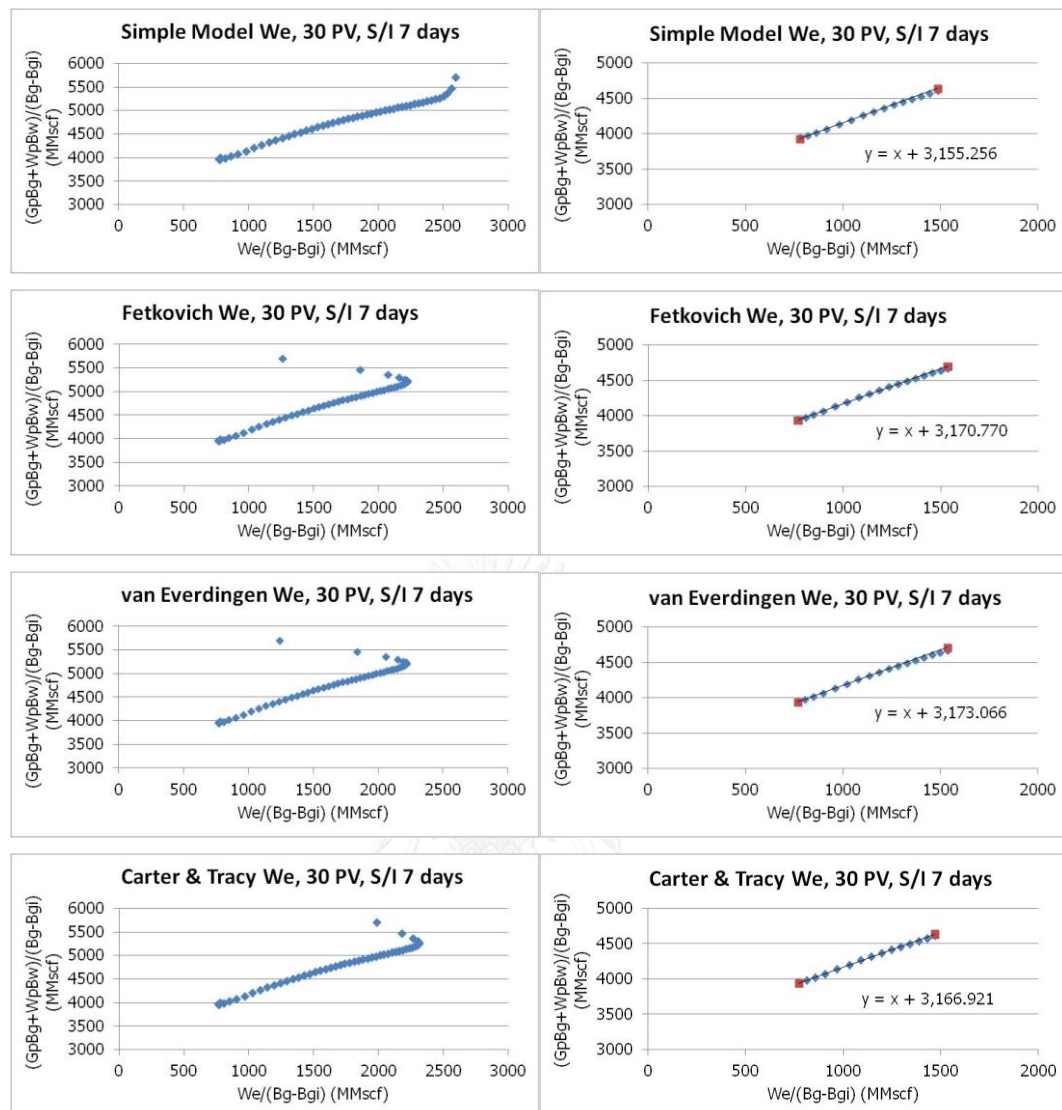


Figure 6.74 $(G_p B_g + W_p B_w)/(B_g - B_{gi})$ versus $W_e/(B_g - B_{gi})$ at 30-PV aquifer size and 7-day shut-in duration for 50 mD reservoir, case 33-36

The shapes of $(G_p B_g + W_p B_w)/(B_g - B_{gi})$ versus $W_e/(B_g - B_{gi})$ plots for all water influx models are similar except the early time period that the plots for simple aquifer model deviates from the others. Figure 6.46 shows that van Everdingen & Hurst, Fetkovich and Carter & Tracy water influx models give similar values of calculated W_e which are lower than the values from simple aquifer model. The reason for different shapes of $(G_p B_g + W_p B_w)/(B_g - B_{gi})$ versus $W_e/(B_g - B_{gi})$ plots at early times is the same as that mentioned in 1-PV and 10-PV aquifer size cases, which is the different value of calculated W_e .

The late trends of $(G_p B_g + W_p B_w)/(B_g - B_{gi})$ versus $W_e/(B_g - B_{gi})$ plots were fitted with a unit slope straight line for OGIP estimation. The R-squared values, as shown in Table 6.11, are in the range of 0.996 to 0.998 which represent good fitting. The values of estimated OGIP are in the range of 3118 to 3173 MMscf or -2.9% to -1.2% error.

Table 6.11 Result of OGIP estimation at 30-PV aquifer size for 50 mD water-drive dry-gas reservoir by $(G_p B_g + W_p B_w)/(B_g - B_{gi})$ versus $W_e/(B_g - B_{gi})$ plot

Shut-in duration	Water influx model	Estimated OGIP (MMscf)	Error (%)	R-squared
6 hours	Simple aquifer model	3,118.04	-2.90%	0.998
	Fetkovich	3,139.50	-2.24%	0.997
	van Everdingen & Hurst	3,141.55	-2.17%	0.997
	Carter & Tracy	3,133.20	-2.43%	0.998
1 day	Simple aquifer model	3,125.48	-2.67%	0.996
	Fetkovich	3,144.73	-2.07%	0.998
	van Everdingen & Hurst	3,145.48	-2.05%	0.998
	Carter & Tracy	3,136.56	-2.33%	0.997
7 days	Simple aquifer model	3,155.26	-1.75%	0.997
	Fetkovich	3,170.77	-1.26%	0.997
	van Everdingen & Hurst	3,173.07	-1.19%	0.997
	Carter & Tracy	3,166.92	-1.38%	0.998

The effect of water influx model on the accuracy of OGIP estimation is observed from Figure 6.83. The estimated OGIP from van Everdingen & Hurst and Fetkovich water influx model are similar and higher than the ones from Carter & Tracy and simple

aquifer model for all shut-in durations. This behavior is aligned with the result of calculated W_e in Figure 6.46 that the calculated W_e from van Everdingen & Hurst and Fetkovich are lower than those from Carter & Tracy and simple aquifer model. Since the estimated OGIPs in these aquifer size cases are underestimated, the error of estimated OGIPs from van Everdingen & Hurst and Fetkovich water influx model are lower than those from Carter & Tracy and simple aquifer model.

The effect of shut-in duration on the accuracy of OGIP estimation is the same as in the other aquifer size cases, i.e., 1-PV and 10-PV, the longer shut-in duration, the more accurate the estimated OGIP.

In 70-PV aquifer size cases, the shapes of $(G_p B_g + W_p B_w) / (B_g - B_{gi})$ versus $W_e / (B_g - B_{gi})$ plots for van Everdingen & Hurst, Fetkovich and Carter & Tracy water influx models are similar and different from those for simple aquifer model in all shut-in durations as shown in Figure 6.75 to Figure 6.77. They begin with positive slope, and the steepness becomes smaller as time increases until the plots turn into the new trend with another positive slope which is the main positive slope trend, at around 24% RF. The plots of $(G_p B_g + W_p B_w) / (B_g - B_{gi})$ versus $W_e / (B_g - B_{gi})$ from simple aquifer model begins with negative slope, and the steepness become smaller until the slope becomes positive. The main positive slope trend happens around 11% to 21% RF, depending on shut-in duration. The early trends of $(G_p B_g + W_p B_w) / (B_g - B_{gi})$ versus $W_e / (B_g - B_{gi})$ plots for simple aquifer model are different from those for van Everdingen & Hurst, Fetkovich and Carter & Tracy water influx models due to the difference in calculate W_e from simple aquifer model from the others as shown in Figure 6.48.

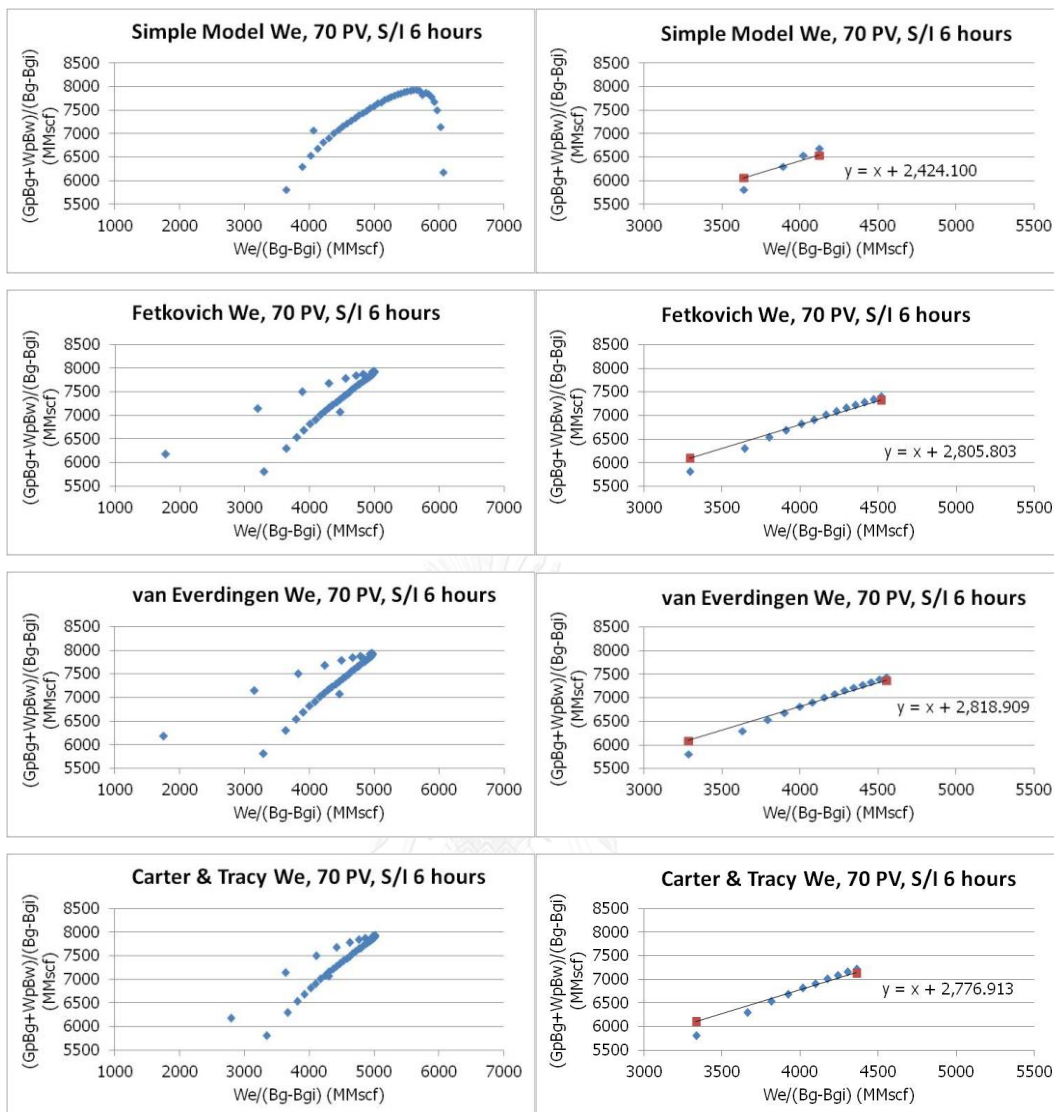


Figure 6.75 $(G_p B_g + W_p B_w) / (B_g - B_{gi})$ versus $W_e / (B_g - B_{gi})$ at 70-PV aquifer size and 6-hour shut-in duration for 50 mD reservoir, case 37-40

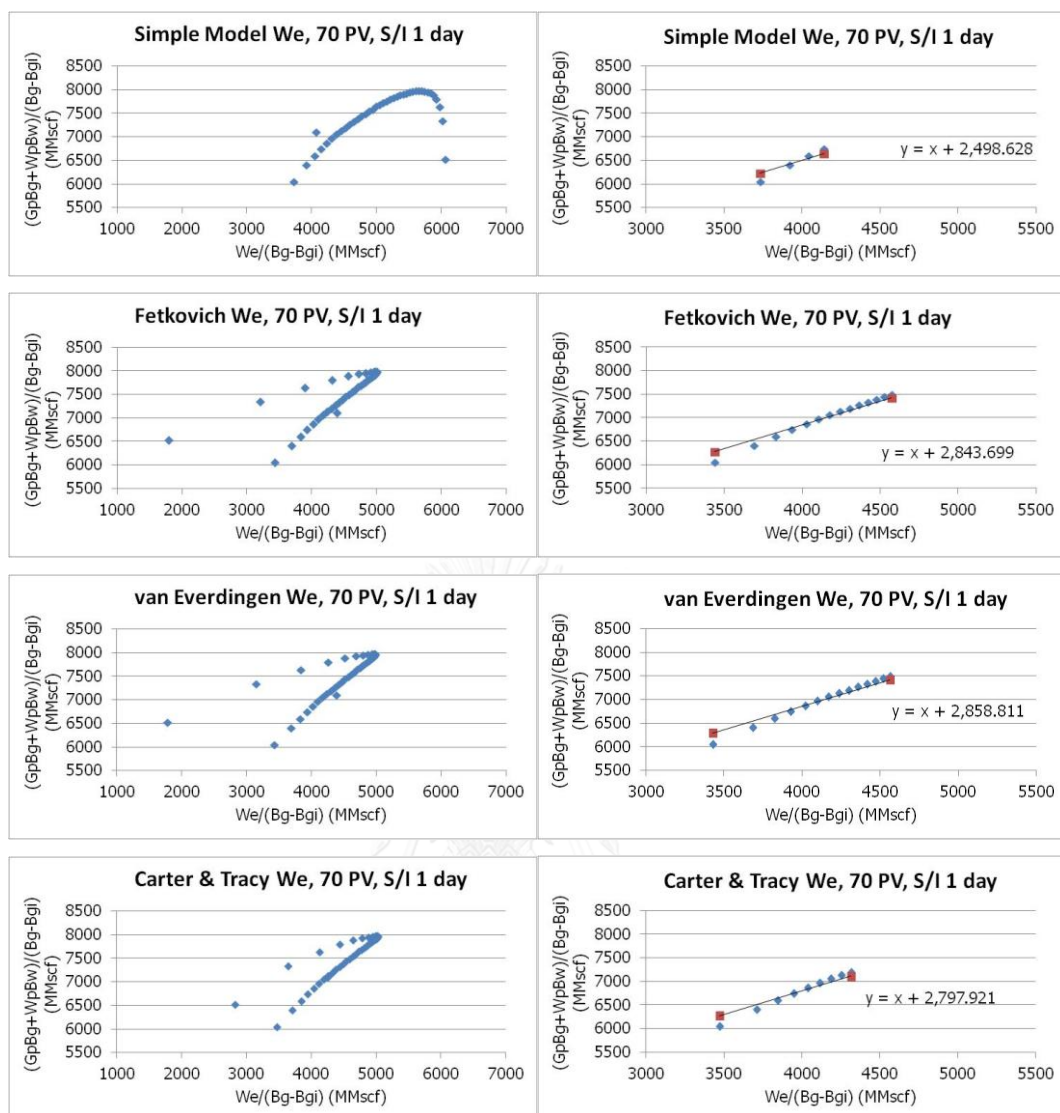


Figure 6.76 $(G_p B_g + W_p B_w) / (B_g - B_{gi})$ versus $W_e / (B_g - B_{gi})$ at 70-PV aquifer size and 1-day shut-in duration for 50 mD reservoir, case 41-44

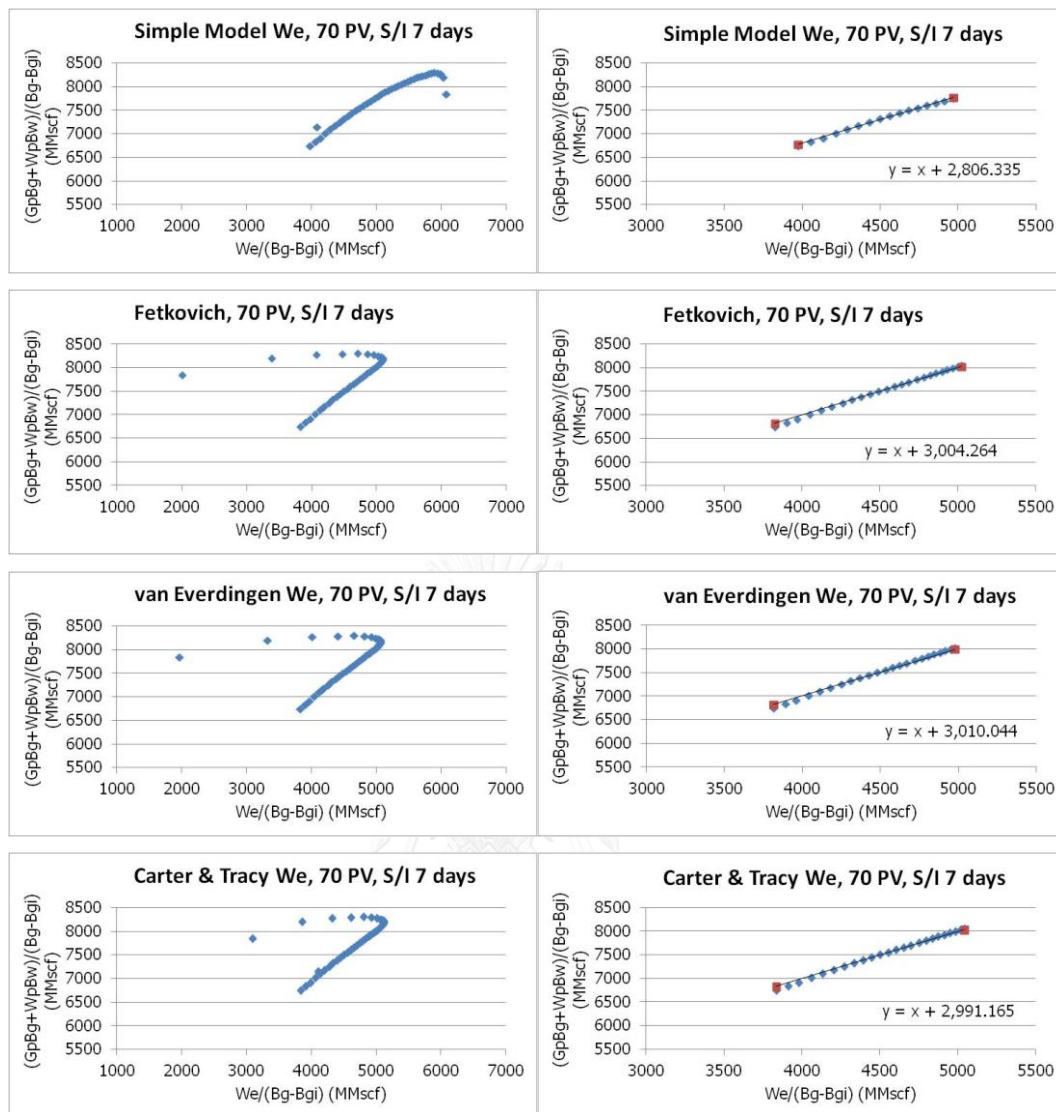


Figure 6.77 $(G_p B_g + W_p B_w) / (B_g - B_{gi})$ versus $W_e / (B_g - B_{gi})$ at 70-PV aquifer size and 7-day shut-in duration for 50 mD reservoir, case 45-48

The latest trends of $(G_p B_g + W_p B_w) / (B_g - B_{gi})$ versus $W_e / (B_g - B_{gi})$ plots are quite fit with a unit slope straight line for OGIP estimation but the R-squared values at 6-hour and 1-day shut-in duration cases are not close enough to one as tabulated in Table 6.12. There are two reasons that make the slope of $(G_p B_g + W_p B_w) / (B_g - B_{gi})$ versus $W_e / (B_g - B_{gi})$ plots in the late times not exactly equal to one as shown in Figure 6.75 and Figure 6.76. The first reason is the error in $W_e / (B_g - B_{gi})$ or x-axis value, and the second reason is the error in $(G_p B_g + W_p B_w) / (B_g - B_{gi})$ or y-axis value. These two errors are from the

difference between the SBHP and the actual reservoir pressure as mentioned in Section 6.3.1. The effects of these errors are demonstrated in Figure 6.78 and Figure 6.79.

Table 6.12 Result of OGIP estimation at 70-PV aquifer size for 50 mD water-drive dry-gas reservoir by $(G_p B_g + W_p B_w)/(B_g - B_{gi})$ versus $W_e/(B_g - B_{gi})$ plot

Shut-in duration	Water influx model	Estimated OGIP (MMscf)	Error (%)	R-squared
6 hours	Simple aquifer model	2,424.10	-24.51%	0.799
	Fetkovich	2,805.80	-12.63%	0.947
	van Everdingen & Hurst	2,818.91	-12.22%	0.95
	Carter & Tracy	2,776.91	-13.53%	0.923
1 day	Simple aquifer model	2,498.63	-22.19%	0.823
	Fetkovich	2,843.70	-11.45%	0.955
	van Everdingen & Hurst	2,858.81	-10.98%	0.955
	Carter & Tracy	2,797.92	-12.87%	0.927
7 days	Simple aquifer model	2,806.34	-12.61%	0.996
	Fetkovich	3,004.26	-6.45%	0.993
	van Everdingen & Hurst	3,010.04	-6.27%	0.992
	Carter & Tracy	2,991.17	-6.86%	0.994

From Figure 6.78, if the value of $W_e/(B_g - B_{gi})$ or x-axis value are calculated based on the actual reservoir pressure, $(G_p B_g + W_p B_w)/(B_g - B_{gi})$ versus $W_e/(B_g - B_{gi})$ plot at the late time will have slope more than one. That means the error from y-axis makes the slope of $(G_p B_g + W_p B_w)/(B_g - B_{gi})$ versus $W_e/(B_g - B_{gi})$ plot to be higher than one.

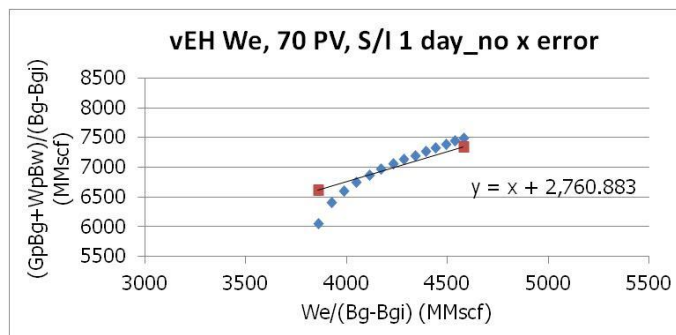


Figure 6.78 $(G_p B_g + W_p B_w)/(B_g - B_{gi})$ versus $W_e/(B_g - B_{gi})$ from van Everdingen & Hurst water influx model at 70-PV aquifer size and 1-day shut-in duration for 50 mD reservoir without the error from x-axis

From Figure 6.79, if the value of $(G_p B_g + W_p B_w)/(B_g - B_{gi})$ or y-axis value are calculated based on the actual reservoir pressure, $(G_p B_g + W_p B_w)/(B_g - B_{gi})$ versus $W_e/(B_g - B_{gi})$ plot at the late time will have slope less than one. That means the error from x-axis makes the slope of $(G_p B_g + W_p B_w)/(B_g - B_{gi})$ versus $W_e/(B_g - B_{gi})$ plot to be less than one. From Figure 6.75 and Figure 6.76, the slope of $(G_p B_g + W_p B_w)/(B_g - B_{gi})$ versus $W_e/(B_g - B_{gi})$ plots are more than one. This means the error from y-axis has more impact than the error from x-axis.

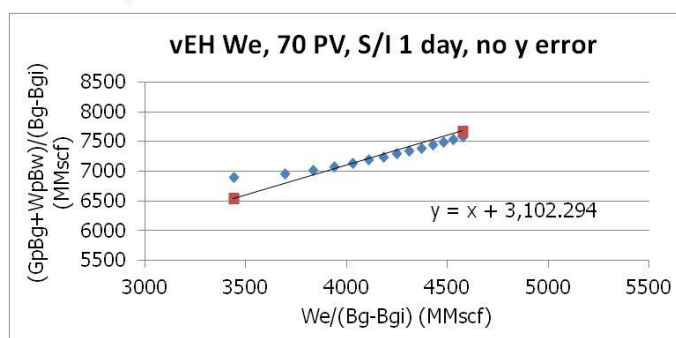


Figure 6.79 $(G_p B_g + W_p B_w)/(B_g - B_{gi})$ versus $W_e/(B_g - B_{gi})$ from van Everdingen & Hurst water influx model at 70-PV aquifer size and 1-day shut-in duration for 50 mD reservoir without the error from y-axis

The latest trends from simple aquifer model at 6-hour and 1-day shut-in durations are significantly shorter than those from the remaining water influx models because simple aquifer model yields higher value but lower increasing rate of the calculated W_e than the other water influx models at the late time as shown in Figure 6.48. This causes more increasing rate of the steepness of $(G_p B_g + W_p B_w)/(B_g - B_{gi})$ versus $W_e/(B_g - B_{gi})$ plots from simple aquifer model. At 7-day shut-in duration, the latest trends from simple aquifer model are significantly longer than the ones from 6-hour and 1-day shut-in duration because of lower increasing rate of the steepness of $(G_p B_g + W_p B_w)/(B_g - B_{gi})$ versus $W_e/(B_g - B_{gi})$ plots at the late time. The reason of this behavior is because longer shut-in duration gives higher SBHP, which is more realistic. This leads to more accurate value of calculated W_e .

The simple aquifer model yields the lower value of estimated OGIP than other water influx models in all shut-in durations because of its higher value of calculated W_e .

A longer shut-in duration gives higher and more accurate values of estimated OGIP and higher values of R-square in all water influx models as shown in Table 6.12.

The difference between the estimated OGIP from simple aquifer model and other water influx models become smaller when the shut-in duration becomes longer because the calculated W_e from simple aquifer model is more sensitive to the reservoir pressure, which is represented by SBHP, than other water influx models due to the assumption of immediately transmitted pressure drop throughout the entire reservoir-aquifer system.

For 100-PV aquifer size, the shapes of $(G_p B_g + W_p B_w)/(B_g - B_{gi})$ versus $W_e/(B_g - B_{gi})$ plots for all water influx models, as shown in Figure 6.80 to Figure 6.82, are similar to the shapes of the plots for 70-PV aquifer size because of the same reason. The simple aquifer model still provides significantly higher value of calculated W_e than other water influx models, especially in the larger aquifer size cases.

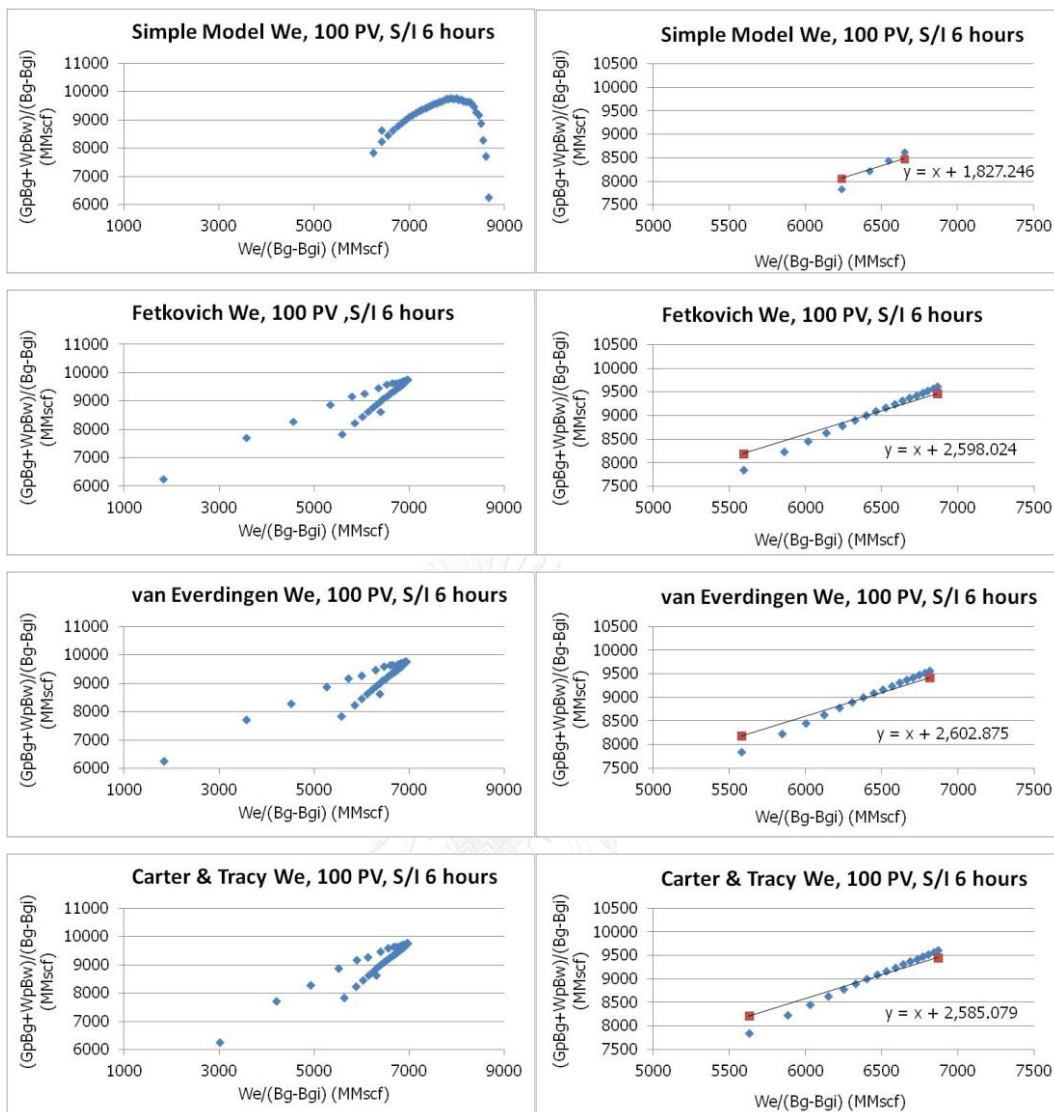


Figure 6.80 $(G_p B_g + W_p B_w) / (B_g - B_{gi})$ versus $W_e / (B_g - B_{gi})$ at 100-PV aquifer size and 6-hour shut-in duration for 50 mD reservoir, case 49-52

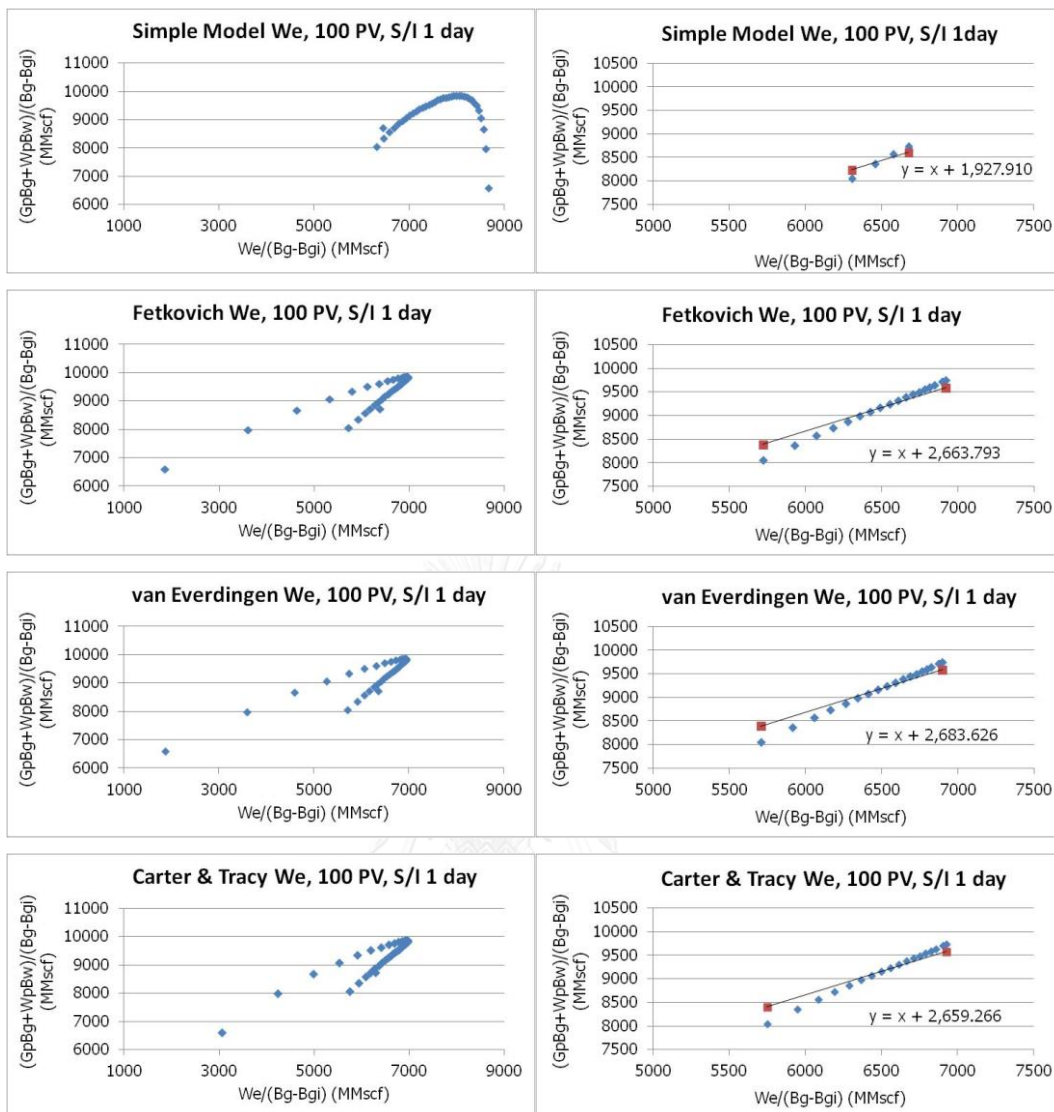


Figure 6.81 $(G_p B_g + W_p B_w) / (B_g - B_{gi})$ versus $W_e / (B_g - B_{gi})$ at 100-PV aquifer size and 1-day shut-in duration for 50 mD reservoir, case 53-56

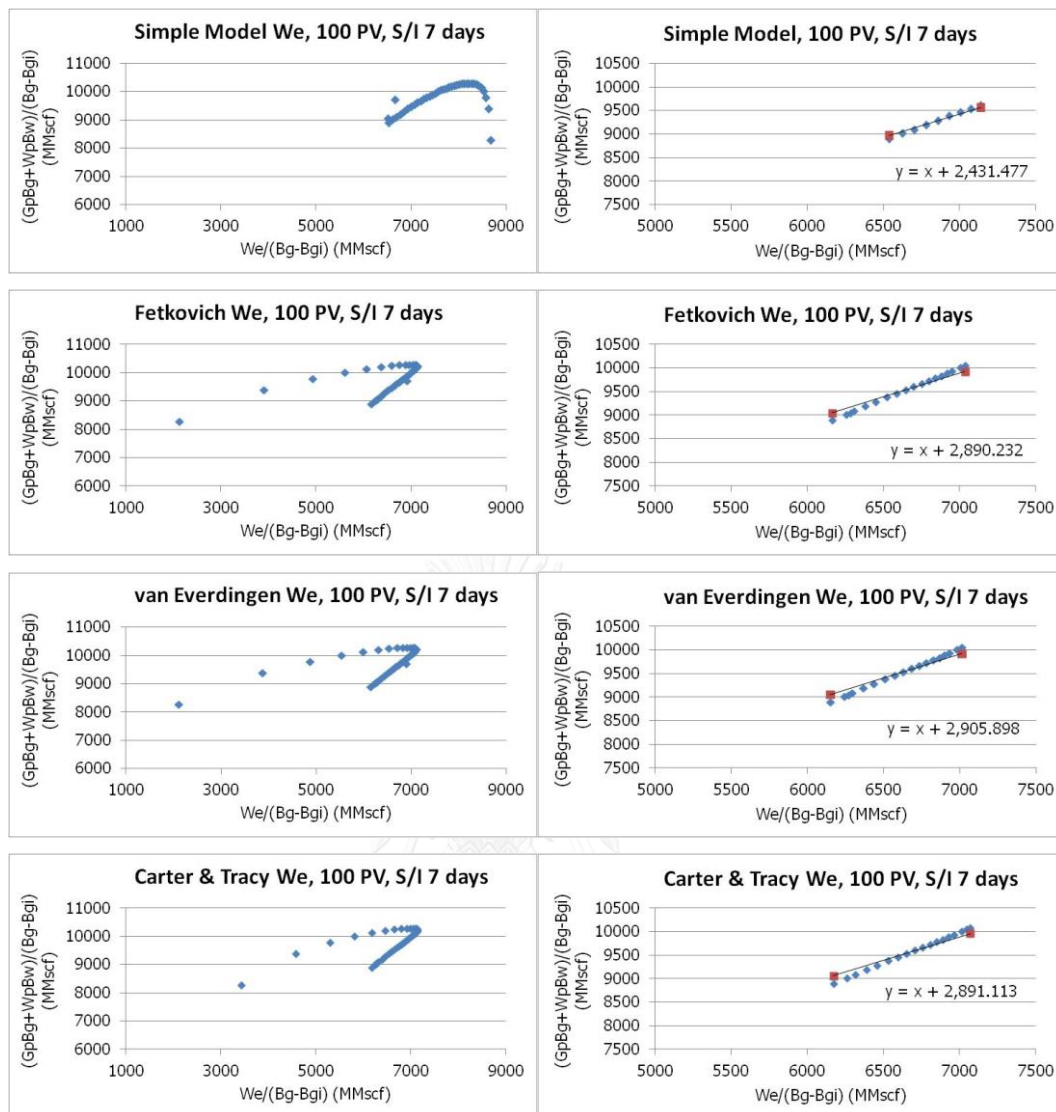


Figure 6.82 $(G_p B_g + W_p B_w) / (B_g - B_{gi})$ versus $W_e / (B_g - B_{gi})$ at 100-PV aquifer size and 7-day shut-in duration for 50 mD reservoir, case 57-60

The late trends of $(G_p B_g + W_p B_w) / (B_g - B_{gi})$ versus $W_e / (B_g - B_{gi})$ plots to be applied for OGIP estimation from simple aquifer model are still shorter than the ones from other water influx models due to the same reason as in 70-PV aquifer size cases.

The estimated OGIP from simple aquifer model are significantly lower than the ones from other water influx models. These differences are more than those in 70-PV aquifer size cases because larger aquifer size can lead to more overestimation in calculated W_e from simple aquifer model. The error percentages of estimated OGIP

from simple aquifer model are in the range between -43% to -24%, depending on the shut-in duration as shown in Table 6.13. Other water influx models give the error percentages of calculated OGIP in the range between -20% to -10%, depending on the shut-in duration.

Table 6.13 Result of OGIP estimation at 100-PV aquifer size for 50 mD water-drive dry-gas reservoir by $(G_p B_g + W_p B_w)/(B_g - B_{gi})$ versus $W_e/(B_g - B_{gi})$ plot

Shut-in duration	Water influx model	Estimated OGIP (MMscf)	Error (%)	R-squared
6 hours	Simple aquifer model	1,827.25	-43.10%	0.766
	Fetkovich	2,598.02	-19.10%	0.924
	van Everdingen & Hurst	2,602.88	-18.95%	0.92
	Carter & Tracy	2,585.08	-19.50%	0.915
1 day	Simple aquifer model	1,927.91	-39.97%	0.79
	Fetkovich	2,663.79	-17.05%	0.922
	van Everdingen & Hurst	2,683.63	-16.43%	0.919
	Carter & Tracy	2,659.27	-17.19%	0.915
7 days	Simple aquifer model	2,431.48	-24.28%	0.975
	Fetkovich	2,890.23	-10.00%	0.943
	van Everdingen & Hurst	2,905.90	-9.51%	0.94
	Carter & Tracy	2,891.11	-9.97%	0.945

The $(G_p B_g + W_p B_w)/(B_g - B_{gi})$ versus $W_e/(B_g - B_{gi})$ plots for 100-PV aquifer size deviate from a unit slope straight line more than those in 70-PV aquifer size cases because of

larger difference between SBHP and actual reservoir pressure as mentioned in Section 6.3.1.

The values of estimated OGIP from longer shut-in durations are higher and more accurate for all water influx models as shown in Table 6.13. The R-squared values also increase with shut-in duration.

As the shut-in duration becomes longer, the difference between the estimated OGIPs from simple aquifer model and other water influx models become smaller. This behavior can be explained by the same explanation in 70-PV aquifer size cases.

As shown in Figure 6.83 and Table 6.14, a longer shut-in duration gives more accurate estimated OGIPs and R-squared values as the SBHP builds up to better represent the actual reservoir pressure.

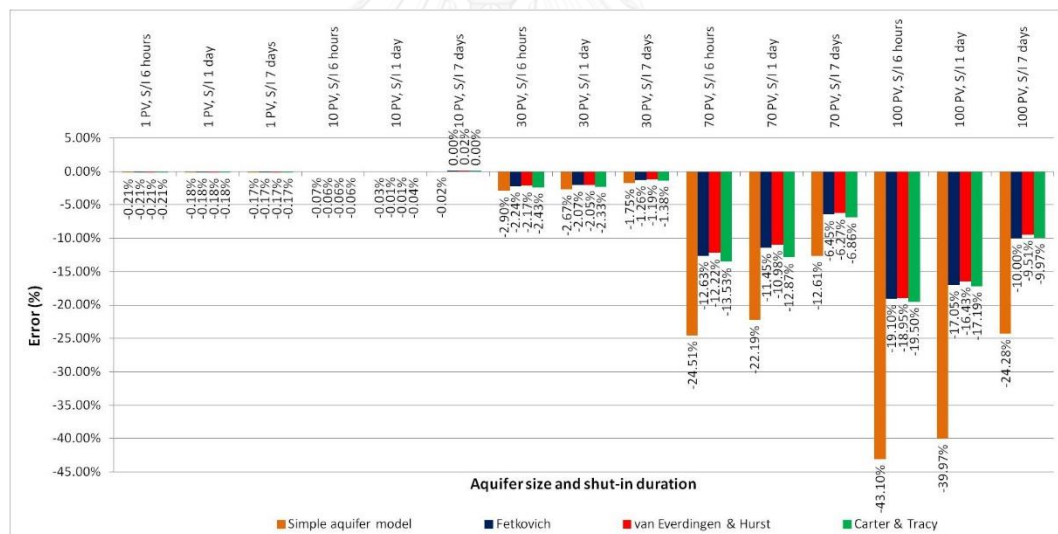


Figure 6.83 Error of estimated OGIP for 50 mD water-drive dry-gas reservoir by $(G_p B_g + W_p B_w) / (B_g - B_{gi})$ versus $W_e / (B_g - B_{gi})$ plot

In term of aquifer size, the estimated OGIP values for 1-PV and 10-PV aquifer size are very accurate. The errors are less than -0.22%. The error of estimated OGIPs becomes larger when the aquifer size is larger than 10 PV since the calculated values of W_e from all water influx models tend to be higher than the simulated W_e values in

the late time period. This difference is more significant in the cases of larger aquifer sizes as shown in Figure 6.46 to Figure 6.50. The reasons that calculated W_e values are higher than the simulated W_e are because the SBHP cannot build up enough to represent the actual reservoir pressure and these water influx models do not consider the movement of water contact, as mentioned in Section 6.4.

The errors of estimated OGIPs are similar for all water influx models in small to moderate aquifer sizes (1 PV, 10 PV and 30 PV). In contrast, for large aquifer size cases (70 PV and 100 PV), the errors of estimated OGIPs from Fetkovich, van Everdingen & Hurst and Carter & Tracy water influx models are similar and significantly lower than the errors from the simple aquifer model. This is because the simple aquifer model is applicable to only small aquifers because of its assumption that pressure drop in the reservoir is immediately transmitted throughout the whole reservoir-aquifer system. This assumption is not valid for large aquifers. Therefore, the simple aquifer model gives too high W_e values and leads to too small OGIP estimates.

Table 6.14 Result of OGIP estimation for 50 mD water-drive dry-gas reservoir by $(G_p B_g + W_p B_w) / (B_g - B_{gi})$ versus $W_e / (B_g - B_{gi})$ plot

Case	Aquifer size (PV)	Shut-in duration	Water influx model	Estimated OGIP (MMscf)	Error (%)	R-squared
1	1	6 hours	Simple aquifer model	3,204.66	-0.21%	0.791
2			Fetkovich	3,204.72	-0.21%	0.786
3			van Everdingen & Hurst	3,204.62	-0.21%	0.786
4			Carter & Tracy	3,204.65	-0.21%	0.791

Table 6.14 Result of OGIP estimation for 50 mD water-drive dry-gas reservoir by $(G_p B_g + W_p B_w) / (B_g - B_{gi})$ versus $W_e / (B_g - B_{gi})$ plot (continued)

Case	Aquifer size (PV)	Shut-in duration	Water influx model	Estimated OGIP (MMscf)	Error (%)	R-squared	
5	1	1 day	Simple aquifer model	3,205.46	-0.18%	0.754	
6			Fetkovich	3,205.47	-0.18%	0.749	
7			van Everdingen & Hurst	3,205.50	-0.18%	0.749	
8			Carter & Tracy	3,205.50	-0.18%	0.754	
9		7 days	Simple aquifer model	3,205.91	-0.17%	0.732	
10			Fetkovich	3,206.01	-0.17%	0.729	
11			van Everdingen & Hurst	3,205.99	-0.17%	0.729	
12			Carter & Tracy	3,206.01	-0.17%	0.734	
13		10	6 hours	Simple aquifer model	3,209.14	-0.07%	0.999
14				Fetkovich	3,209.54	-0.06%	0.998
15				van Everdingen & Hurst	3,209.42	-0.06%	0.998
16				Carter & Tracy	3,209.29	-0.06%	0.999

Table 6.14 Result of OGIP estimation for 50 mD water-drive dry-gas reservoir by $(G_p B_g + W_p B_w) / (B_g - B_{gi})$ versus $W_e / (B_g - B_{gi})$ plot (continued)

Case	Aquifer size (PV)	Shut-in duration	Water influx model	Estimated OGIP (MMscf)	Error (%)	R-squared
17	10	1 day	Simple aquifer model	3,210.50	-0.03%	0.999
18			Fetkovich	3,210.91	-0.01%	0.998
19			van Everdingen & Hurst	3,210.91	-0.01%	0.998
20			Carter & Tracy	3,210.17	-0.04%	0.999
21		7 days	Simple aquifer model	3,210.77	-0.02%	0.998
22			Fetkovich	3,211.42	0.00%	0.998
23			van Everdingen & Hurst	3,211.90	0.02%	0.998
24			Carter & Tracy	3,211.44	0.00%	0.998
25	30	6 hours	Simple aquifer model	3,118.04	-2.90%	0.998
26			Fetkovich	3,139.50	-2.24%	0.997
27			van Everdingen & Hurst	3,141.55	-2.17%	0.997
28			Carter & Tracy	3,133.20	-2.43%	0.998

Table 6.14 Result of OGIP estimation for 50 mD water-drive dry-gas reservoir by
 $(G_p B_g + W_p B_w) / (B_g - B_{gi})$ versus $W_e / (B_g - B_{gi})$ plot (continued)

Case	Aquifer size (PV)	Shut-in duration	Water influx model	Estimated OGIP (MMscf)	Error (%)	R-squared
29	30	1 day	Simple aquifer model	3,125.48	-2.67%	0.996
30			Fetkovich	3,144.73	-2.07%	0.998
31			van Everdingen & Hurst	3,145.48	-2.05%	0.998
32			Carter & Tracy	3,136.56	-2.33%	0.997
33		7 days	Simple aquifer model	3,155.26	-1.75%	0.997
34			Fetkovich	3,170.77	-1.26%	0.997
35			van Everdingen & Hurst	3,173.07	-1.19%	0.997
36			Carter & Tracy	3,166.92	-1.38%	0.998
37	70	6 hours	Simple aquifer model	2,424.10	-24.51%	0.799
38			Fetkovich	2,805.80	-12.63%	0.947
39			van Everdingen & Hurst	2,818.91	-12.22%	0.95
40			Carter & Tracy	2,776.91	-13.53%	0.923

Table 6.14 Result of OGIP estimation for 50 mD water-drive dry-gas reservoir by $(G_p B_g + W_p B_w)/(B_g - B_{gi})$ versus $W_e/(B_g - B_{gi})$ plot (continued)

Case	Aquifer size (PV)	Shut-in duration	Water influx model	Estimated OGIP (MMscf)	Error (%)	R-squared
41	70	1 day	Simple aquifer model	2,498.63	-22.19%	0.823
42			Fetkovich	2,843.70	-11.45%	0.955
43			van Everdingen & Hurst	2,858.81	-10.98%	0.955
44			Carter & Tracy	2,797.92	-12.87%	0.927
45		7 days	Simple aquifer model	2,806.34	-12.61%	0.996
46			Fetkovich	3,004.26	-6.45%	0.993
47			van Everdingen & Hurst	3,010.04	-6.27%	0.992
48			Carter & Tracy	2,991.17	-6.86%	0.994
49	100	6 hours	Simple aquifer model	1,827.25	-43.10%	0.766
50			Fetkovich	2,598.02	-19.10%	0.924
51			van Everdingen & Hurst	2,602.88	-18.95%	0.92
52			Carter & Tracy	2,585.08	-19.50%	0.915

Table 6.14 Result of OGIP estimation for 50 mD water-drive dry-gas reservoir by $(G_p B_g + W_p B_w) / (B_g - B_{gi})$ versus $W_e / (B_g - B_{gi})$ plot (continued)

Case	Aquifer size (PV)	Shut-in duration	Water influx model	Estimated OGIP (MMscf)	Error (%)	R-squared
53	100	1 day	Simple aquifer model	1,927.91	-39.97%	0.79
54			Fetkovich	2,663.79	-17.05%	0.922
55			van Everdingen & Hurst	2,683.63	-16.43%	0.919
56			Carter & Tracy	2,659.27	-17.19%	0.915
57		7 days	Simple aquifer model	2,431.48	-24.28%	0.975
58			Fetkovich	2,890.23	-10.00%	0.943
59			van Everdingen & Hurst	2,905.90	-9.51%	0.94
60			Carter & Tracy	2,891.11	-9.97%	0.945

Table 6.15 Accuracy of OGIP estimation for 50 mD water-drive dry-gas reservoir by
 $(G_p B_g + W_p B_w) / (B_g - B_{gi})$ versus $W_e / (B_g - B_{gi})$ plot

Aquifer size (PV)	Shut-in duration	Water influx model	Accuracy
1, 10 and 30	6 hours, 1 day and 7 days	Simple aquifer model , Fetkovich	Accurate
70	6 hours and 1 day	, van Everdingen & Hurst and Carter & Tracy	Not acceptable
	7 days	Simple aquifer model	Not acceptable
		Fetkovich, van Everdingen & Hurst and Carter & Tracy	Acceptable
100	6 hours and 1 day	Simple aquifer model , Fetkovich , van Everdingen & Hurst and Carter & Tracy	Not acceptable
	7 days	Simple aquifer model	Not acceptable
		Fetkovich, van Everdingen & Hurst and Carter & Tracy	Acceptable

Accurate: error < 5%, Acceptable: error < 10%, Not acceptable: error ≥ 10%

6.7 OGIP Estimation Using $(G_p B_g + W_p B_w)/(B_g - B_{gi})$ versus $W_e/(B_g - B_{gi})$ Plot for 500 mD Water-drive Dry-gas Reservoir

The objective of this section is to study the effect of aquifer size and shut-in duration on the accuracy of OGIP estimation in 500 mD water-drive dry-gas reservoir by applying $(G_p B_g + W_p B_w)/(B_g - B_{gi})$ versus $W_e/(B_g - B_{gi})$ plot. Table 6.16 shows the parameters to be studied in this section.

Only van Everdingen & Hurst water influx model is applied in this section because it yields the most accurate value of estimated OGIP for all aquifer sizes and shut-in durations as shown in Section 6.6.

Table 6.16 Parameters to be studied on the accuracy of OGIP estimation for 500 mD water-drive dry-gas reservoir by applying $(G_p B_g + W_p B_w)/(B_g - B_{gi})$ versus $W_e/(B_g - B_{gi})$ plot

Case	Aquifer size (PV)	Shut-in duration
1	1	6 hours
2		1 day
3		7 days
4	10	6 hours
5		1 day
6		7 days
7	30	6 hours
8		1 day
9		7 days
10	70	6 hours
11		1 day

Table 6.16 Parameters to be studied on the accuracy of OGIP estimation for 500 mD water-drive dry-gas reservoir by applying $(G_p B_g + W_p B_w)/(B_g - B_{gi})$ versus $W_e/(B_g - B_{gi})$ plot (continued)

Case	Aquifer size (PV)	Shut-in duration
12	70	7 days
13	100	6 hours
14		1 day
15		7 days

The plots of $(G_p B_g + W_p B_w)/(B_g - B_{gi})$ versus $W_e/(B_g - B_{gi})$ in 500 mD water-drive dry-gas reservoir for different aquifer sizes and shut-in durations are shown in Figure 6.84 to Figure 6.88.

For 1-PV aquifer size, the shapes of $(G_p B_g + W_p B_w)/(B_g - B_{gi})$ versus $W_e/(B_g - B_{gi})$ plots, Figure 6.84, are similar to those for van Everdingen & Hurst water influx model in 1-PV aquifer size, 50 mD reservoir cases, as shown in Figure 6.66 to Figure 6.68. The aquifer support behavior is hardly visible due to the small aquifer size.

The estimated OGIP values from fitting the latest trends of $(G_p B_g + W_p B_w)/(B_g - B_{gi})$ versus $W_e/(B_g - B_{gi})$ plots with a unit slope straight line are around 3204 MMscf or -0.24% error as depicted in Table 6.17. The R-squared values are in the range of 0.72 to 0.75, which does not represent good fitting.

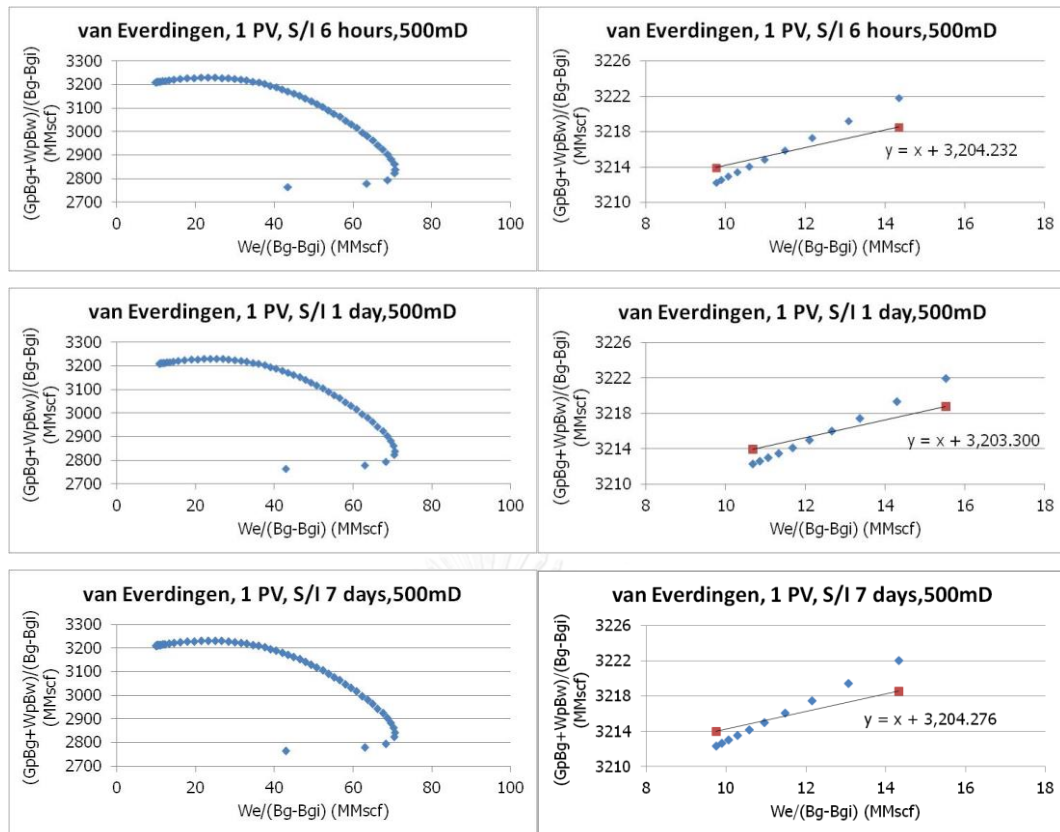


Figure 6.84 $(G_p B_g + W_p B_w)/(B_g - B_{gi})$ versus $W_e/(B_g - B_{gi})$ at 1-PV aquifer size for 500 mD reservoir, case 1-3

Table 6.17 Result of OGIP estimation at 1-PV aquifer size for 500 mD water-drive dry-gas reservoir by $(G_p B_g + W_p B_w)/(B_g - B_{gi})$ versus $W_e/(B_g - B_{gi})$ plot

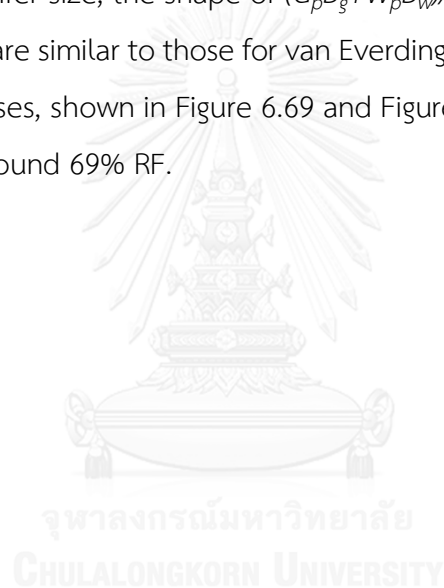
Shut-in duration	Estimated OGIP (MMscf)	Error (%)	R-squared
6 hours	3,204.23	-0.22%	0.730
1 day	3,203.30	-0.25%	0.749
7 days	3,204.28	-0.22%	0.721

The late trends of $(G_p B_g + W_p B_w)/(B_g - B_{gi})$ versus $W_e/(B_g - B_{gi})$ plots of all shut-in duration have the actual slope around 2. If the latest trends are fitted with a straight line without fixing the slope to be 1, the estimated OGIP will be around 3191 to 3192 MMscf or -0.63 to -0.60% error and the R-squared values will be around 1.

The estimated OGIP from $(G_p B_g + W_p B_w) / (B_g - B_{gi})$ versus $W_e / (B_g - B_{gi})$ plots in 500 mD reservoir are similar to those in 50 mD reservoir as illustrated in Figure 6.66 to Figure 6.68.

Results in Table 6.17 indicate that the shut-in duration does not affect the accuracy of the estimated OGIP in 500 mD reservoir as it does in 50 mD reservoir because the SBHP can build up to represent the actual reservoir pressure faster in 500 mD reservoir as mentioned in Section 6.3.1.

For 10-PV aquifer size, the shape of $(G_p B_g + W_p B_w) / (B_g - B_{gi})$ versus $W_e / (B_g - B_{gi})$ plots shown in Figure 6.85 are similar to those for van Everdingen & Hurst water influx model in 50 mD reservoir cases, shown in Figure 6.69 and Figure 6.71. The plots start to have positive unit slope around 69% RF.



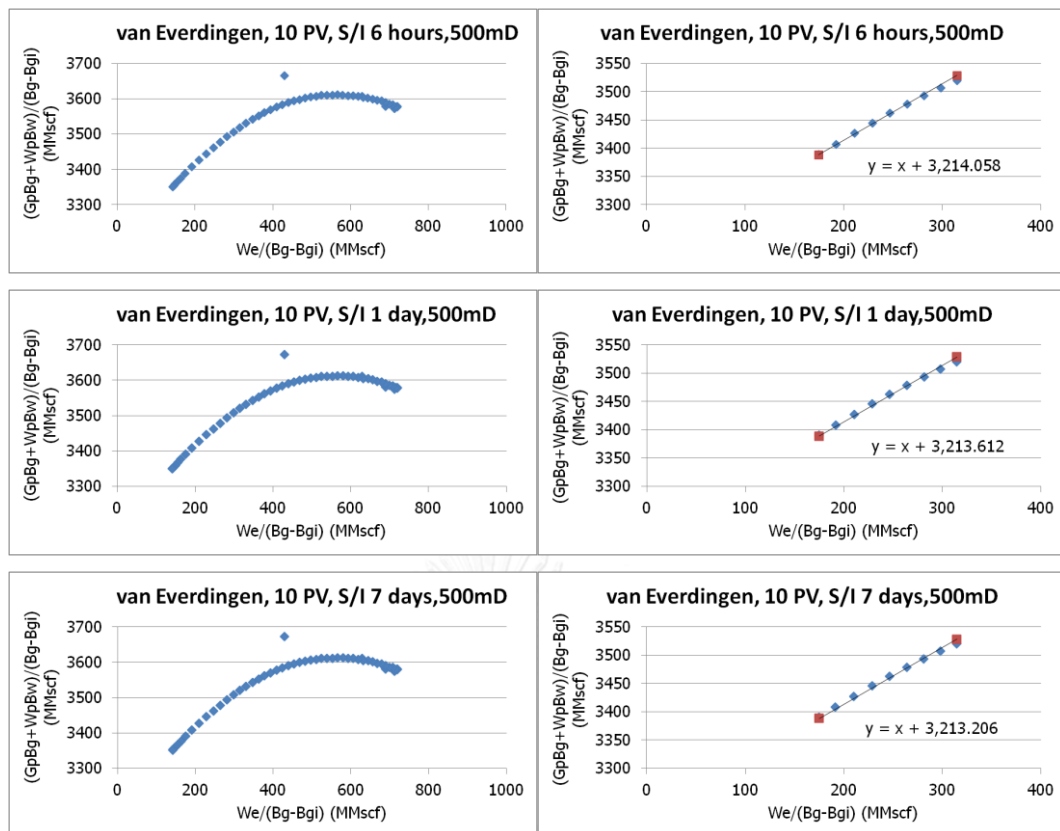


Figure 6.85 $(G_p B_g + W_p B_w)/(B_g - B_{gi})$ versus $W_e/(B_g - B_{gi})$ at 10-PV aquifer size for 500 mD reservoir, case 4-6

The late trends before liquid loading of the $(G_p B_g + W_p B_w)/(B_g - B_{gi})$ versus $W_e/(B_g - B_{gi})$ plots were fitted with a unit slope straight line for OGIP estimation as shown in Figure 6.85. The R-squared values are in the range between 0.991 to 0.992 as shown in Table 6.18. The values of estimated OGIP are in the range between 3213 to 3214 MMscf or 0.06% to 0.09% error which are close to the values in 50 mD reservoir.

The shut-in duration does not have any impact on the estimated OGIP.

Table 6.18 Result of OGIP estimation at 10-PV aquifer size for 500 mD water-drive dry-gas reservoir by $(G_p B_g + W_p B_w)/(B_g - B_{gi})$ versus $W_e/(B_g - B_{gi})$ plot

Shut-in duration	Estimated OGIP (MMscf)	Error (%)	R-squared
6 hours	3,214.06	0.09%	0.991

Table 6.18 Result of OGIP estimation at 10-PV aquifer size for 500 mD water-drive dry-gas reservoir by $(G_p B_g + W_p B_w)/(B_g - B_{gi})$ versus $W_e/(B_g - B_{gi})$ plot

Shut-in duration	Estimated OGIP (MMscf)	Error (%)	R-squared
1 day	3,213.61	0.07%	0.992
7 days	3,213.21	0.06%	0.992

For 30-PV aquifer size, the shapes of $(G_p B_g + W_p B_w)/(B_g - B_{gi})$ versus $W_e/(B_g - B_{gi})$ plots as shown in Figure 6.86 are similar to those for van Everdingen & Hurst water influx model in 50 mD reservoir cases. The positive slope of $(G_p B_g + W_p B_w)/(B_g - B_{gi})$ versus $W_e/(B_g - B_{gi})$ plots or aquifer support behavior are observed since the early time period or 15% RF.

The late trend of $(G_p B_g + W_p B_w)/(B_g - B_{gi})$ versus $W_e/(B_g - B_{gi})$ plots before liquid loading are fitted with a unit slope straight line as shown in Figure 6.86. The values of estimated OGIP are in the range between 3175 to 3178 MMscf or -1.12% to -1.04% error as shown in Table 6.19. The R-squared values are around 0.967, indicating the good fitting.

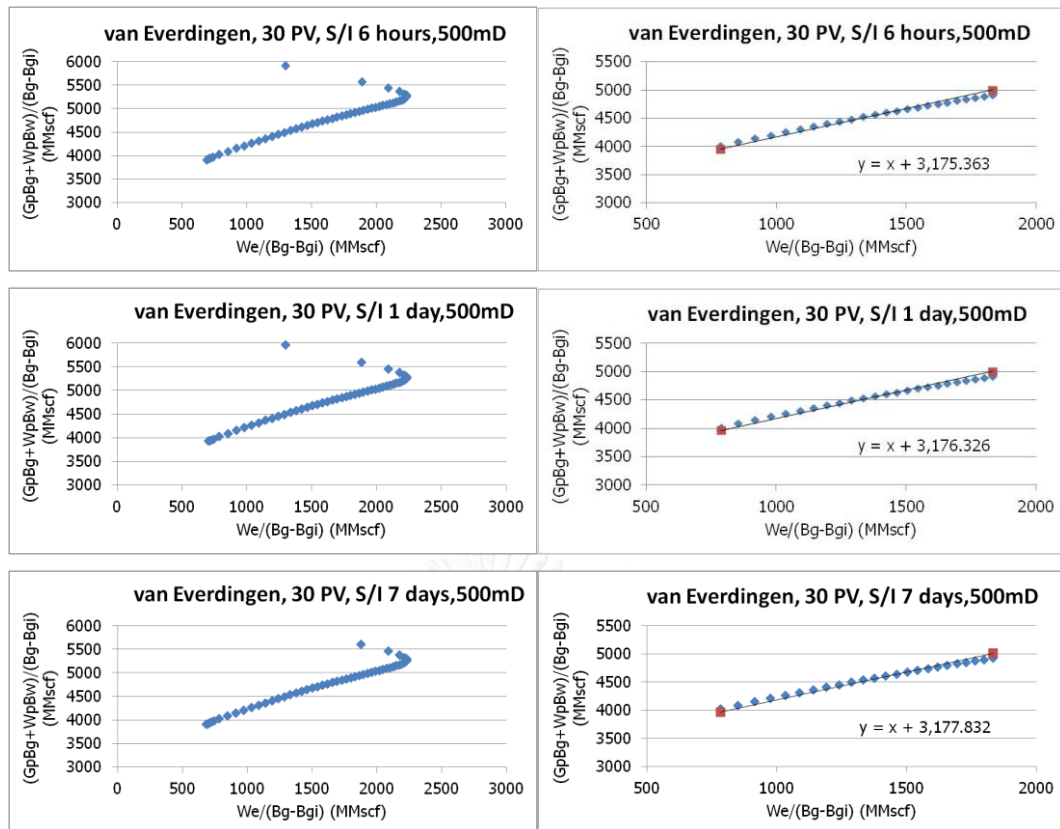


Figure 6.86 $(G_p B_g + W_p B_w)/(B_g - B_{gi})$ versus $W_e/(B_g - B_{gi})$ at 30-PV aquifer size for 500 mD reservoir, case 7-9

Table 6.19 Result of OGIP estimation at 30-PV aquifer size for 500 mD water-drive dry-gas reservoir by $(G_p B_g + W_p B_w)/(B_g - B_{gi})$ versus $W_e/(B_g - B_{gi})$ plot

Shut-in duration	Estimated OGIP (MMscf)	Error (%)	R-squared
6 hours	3,175.36	-1.12%	0.967
1 day	3,176.33	-1.09%	0.967
7 days	3,177.83	-1.04%	0.968

The estimated OGIPs in 30-PV aquifer size in 500 mD reservoir are slightly more accurate, around 1%, than those in 50 mD reservoir as shown in Figure 6.83 because the SBHP in 500 mD reservoir can build up to represent the actual reservoir pressure better than the SBHP in 50 mD reservoir and the calculated W_e in 50 mD reservoir is

more accurate than the ones in 500 mD reservoir as shown in Figure 6.46 and Figure 6.90.

From Table 6.19, there is no obvious relationship between the shut-in duration and the accuracy of OGIP estimation in 30-PV aquifer size since the error of OGIP estimation in all shut-in duration are quite similar.

For 70-PV aquifer size, the shapes of $(G_p B_g + W_p B_w)/(B_g - B_{gi})$ versus $W_e/(B_g - B_{gi})$ plots as shown in Figure 6.87 are similar to those in 30-PV aquifer size cases in Figure 6.86. The positive slopes of $(G_p B_g + W_p B_w)/(B_g - B_{gi})$ versus $W_e/(B_g - B_{gi})$ plots or aquifer support behavior start at 19% RF.

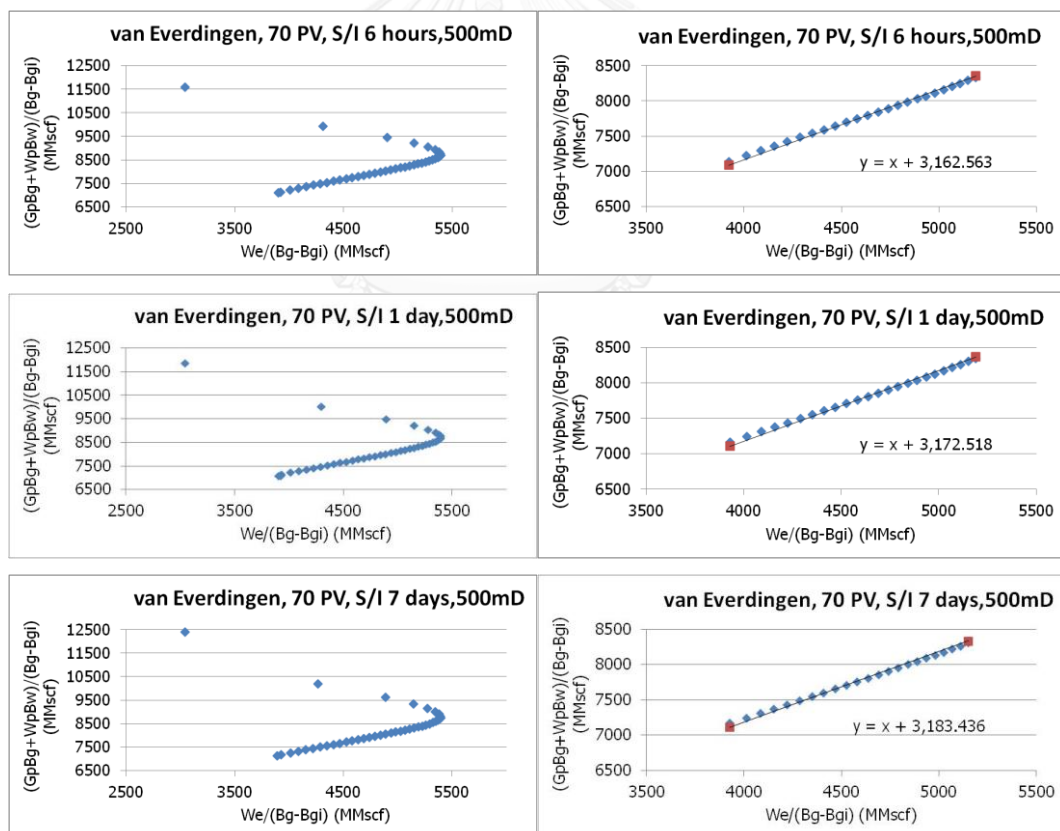


Figure 6.87 $(G_p B_g + W_p B_w)/(B_g - B_{gi})$ versus $W_e/(B_g - B_{gi})$ at 70-PV aquifer size for 500 mD reservoir, case 10-12

The late trend of $(G_p B_g + W_p B_w)/(B_g - B_{gi})$ versus $W_e/(B_g - B_{gi})$ plots before liquid loading were fitted with a unit slope straight line as shown in Figure 6.87. The R-squared values are 0.993, indicating the good fitting. The values of estimated OGIP are in the range between 3162 to 3183 MMscf or -1.52% to -0.87% error as shown in Table 6.20.

Table 6.20 Result of OGIP estimation at 70-PV aquifer size for 500 mD water-drive dry-gas reservoir by $(G_p B_g + W_p B_w)/(B_g - B_{gi})$ versus $W_e/(B_g - B_{gi})$ plot

Shut-in duration	Estimated OGIP (MMscf)	Error (%)	R-squared
6 hours	3,162.56	-1.52%	0.993
1 day	3,172.52	-1.21%	0.993
7 days	3,183.44	-0.87%	0.993

The errors of estimated OGIP in 70-PV aquifer size cases in 500 mD reservoir are in the range of -12.22% to -6.27% as shown in Figure 6.83 which are significantly higher than the error in 500 mD reservoir. The reason of the less accurate OGIP estimation in 500 mD reservoir is the overestimated W_e as mentioned in Section 6.4, Figure 6.48.

Table 6.20 indicates that the shut-in duration also has impact on the OGIP estimation. The longer the shut-in duration, the higher the value of estimated OGIP. The impact of shut-in duration in 500 mD reservoir is not significant as in 50 mD.

For 100-PV aquifer size, the shapes of $(G_p B_g + W_p B_w)/(B_g - B_{gi})$ versus $W_e/(B_g - B_{gi})$ plots as shown in Figure 6.88 are similar to the ones in 30-PV and 70-PV aquifer size cases in Figure 6.86 and Figure 6.87. The positive slopes of $(G_p B_g + W_p B_w)/(B_g - B_{gi})$ versus $W_e/(B_g - B_{gi})$ plots or aquifer support behavior start at 20% RF.

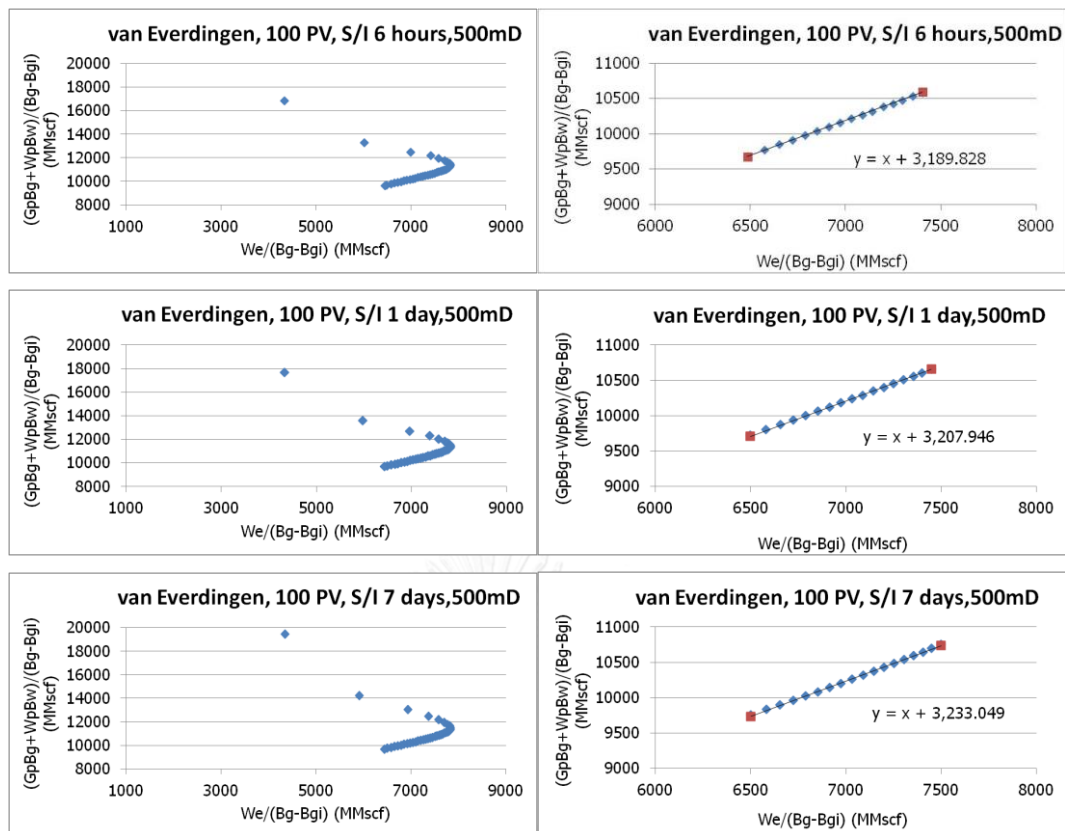


Figure 6.88 $(G_p B_g + W_p B_w)/(B_g - B_{gi})$ versus $W_e/(B_g - B_{gi})$ at 100-PV aquifer size for 500 mD reservoir, case 13-15

The late trend of $(G_p B_g + W_p B_w)/(B_g - B_{gi})$ versus $W_e/(B_g - B_{gi})$ plots before liquid loading were fitted with a unit slope straight line as shown in Figure 6.88. The R-squared values are 0.999 which represent the good fitting. The values of estimated OGIP are in the range between 3199 to 3233 MMscf or -0.67% to 0.68% error as shown in Table 6.21.

Table 6.21 Result of OGIP estimation at 100-PV aquifer size for 500 mD water-drive dry-gas reservoir by $(G_p B_g + W_p B_w)/(B_g - B_{gi})$ versus $W_e/(B_g - B_{gi})$ plot

Shut-in duration	Estimated OGIP (MMscf)	Error (%)	R-squared
6 hours	3,189.83	-0.67%	0.999

Table 6.21 Result of OGIP estimation at 100-PV aquifer size for 500 mD water-drive dry-gas reservoir by $(G_p B_g + W_p B_w)/(B_g - B_{gi})$ versus $W_e/(B_g - B_{gi})$ plot (continued)

Shut-in duration	Estimated OGIP (MMscf)	Error (%)	R-squared
1 day	3,207.95	-0.10%	0.999
7 days	3,233.05	0.68%	0.999

The OGIP estimation in 500 mD reservoir is significantly more accurate than those in 50 mD reservoir. The error of estimated OGIP in 100-PV aquifer size cases in 50 mD reservoir are in the range between -18.95% to -9.51% as shown in Figure 6.83. The reason of different accuracy levels in OGIP estimation is the overestimated W_e in 50 mD, Figure 6.50, because SBHP cannot build up to be close enough to the actual reservoir pressure.

The shut-in duration also affects the accuracy of OGIP estimation as shown in Table 6.21. The longer shut-in duration yields the higher value of estimated OGIP. The level of shut-in duration impact is significantly lower than the one in 50 mD reservoir.

Figure 6.89 and Table 6.22 represent the result of OGIP estimation by $(G_p B_g + W_p B_w)/(B_g - B_{gi})$ versus $W_e/(B_g - B_{gi})$ plot and van Everdingen & Hurst water influx model in 500 mD reservoir.

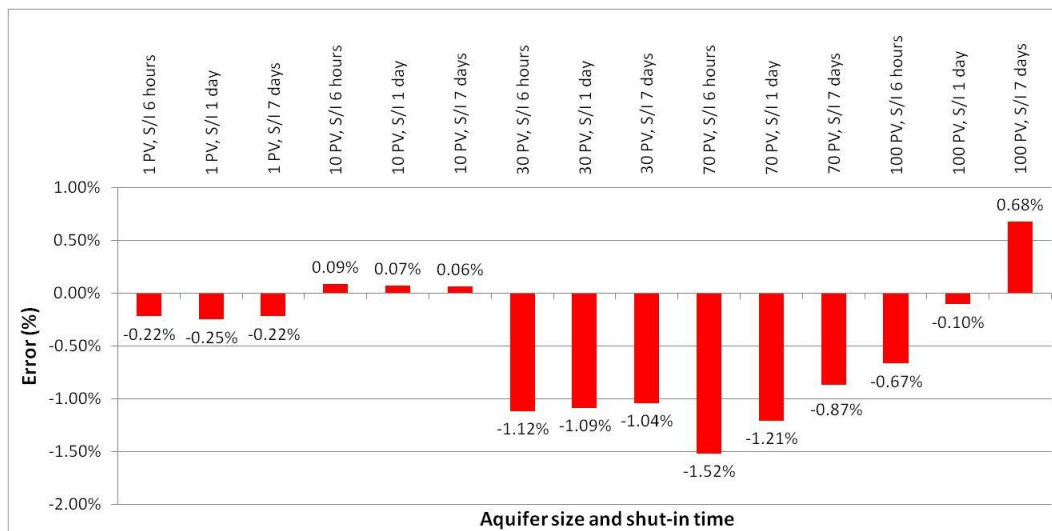


Figure 6.89 Error of estimated OGIP for 500 mD water-drive dry-gas reservoir by $(G_p B_g + W_p B_w)/(B_g - B_{gi})$ versus $W_e/(B_g - B_{gi})$ plot using van Everdingen & Hurst water influx model

Table 6.22 Result of OGIP estimation for 500 mD water-drive dry-gas reservoir by $(G_p B_g + W_p B_w)/(B_g - B_{gi})$ versus $W_e/(B_g - B_{gi})$ plot

Case	Aquifer size (PV)	Shut-in duration	Estimated OGIP (MMscf)	Error (%)	R-squared
1	1	6 hours	3,204.23	-0.22%	0.730
2		1 day	3,203.30	-0.25%	0.749
3		7 days	3,204.28	-0.22%	0.721
4	10	6 hours	3,214.06	0.09%	0.991
5		1 day	3,213.61	0.07%	0.992
6		7 days	3,213.21	0.06%	0.992
7	30	6 hours	3,175.36	-1.12%	0.967
8		1 day	3,176.33	-1.09%	0.967

Table 6.22 Result of OGIP estimation for 500 mD water-drive dry-gas reservoir by $(G_p B_g + W_p B_w)/(B_g - B_{gi})$ versus $W_e/(B_g - B_{gi})$ plot (continued)

Case	Aquifer size (PV)	Shut-in duration	Estimated OGIP (MMscf)	Error (%)	R-squared
9	30	7 days	3,177.83	-1.04%	0.968
10	70	6 hours	3,162.56	-1.52%	0.993
11		1 day	3,172.52	-1.21%	0.993
12		7 days	3,183.44	-0.87%	0.993
13	100	6 hours	3,189.83	-0.67%	0.999
14		1 day	3,207.95	-0.10%	0.999
15		7 days	3,233.05	0.68%	0.999

Table 6.23 Accuracy of OGIP estimation for 500 mD water-drive dry-gas reservoir by $(G_p B_g + W_p B_w)/(B_g - B_{gi})$ versus $W_e/(B_g - B_{gi})$ plot

Aquifer size (PV)	Shut-in duration	Accuracy
1, 10, 30, 70 and 100	6 hours, 1 day and 7 days	Accurate

Accurate: error < 5%, Acceptable: error < 10%, Not acceptable: error ≥ 10%

For small aquifer sizes (1 PV and 10 PV), the error percentages of the estimated OGIP are very low. The magnitudes are less than 0.3%. In moderate to large aquifer sizes (30 PV, 70 PV and 100 PV), the errors increase to be in the range between -1.52% to 0.68%. There is no clear relationship between aquifer size and the error of estimated OGIP.

The accuracy of OGIP estimation in 500 mD reservoir is higher than 50 mD reservoir for all aquifer sizes, and the difference in accuracy level between 500 mD

and 50 mD reservoirs becomes higher in a larger aquifer because the difference between the SBHP build up rate in 50 mD and 500 mD increases with aquifer size as mentioned in Section 6.3.1.

In 500 mD reservoir, the error of the calculated W_e does not vary with the aquifer size as it does in 50 mD reservoir as depicted in Figure 6.90. Then, the errors of the estimated OGIP in small and large aquifer size cases are less than 2.5%, which are not significantly different.

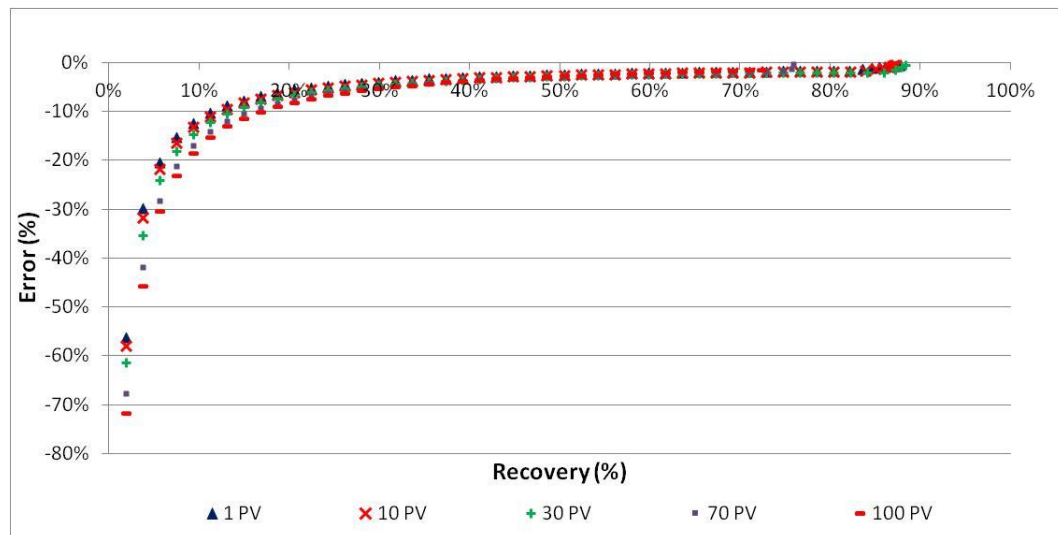


Figure 6.90 Error of van Everdingen & Hurst calculated W_e for 500 mD reservoir

For small to moderate aquifer sizes (1 PV, 10 PV and 30 PV), shut-in duration has no impact on the accuracy of OGIP estimation. In contrast, shut-in duration has effect on the estimated OGIP in large aquifer size cases (70 PV and 100 PV) because the SBHP build up rate in 500 mD reservoir also decreases when aquifer size increases as shown in Figure 6.20 and Figure 6.21. The increasing of the difference between SBHP and the actual reservoir pressure causes more error in both y-axis and x-axis values of $(G_p B_g + W_p B_w) / (B_g - B_{gi})$ versus $W_e / (B_g - B_{gi})$ plot. The error in x-axis value will be more significant in the larger aquifer size because of the higher impact from W_e or aquifer support behavior.

6.8 Effect of the Amount of Historical Data

The effect of the amount of historical data on the feasibility and accuracy of OGIP estimation in water-drive dry-gas reservoir by p/z versus G_p and $(G_p B_g + W_p B_w)/(B_g - B_{gi})$ versus $W_e/(B_g - B_{gi})$ plot is studied in this section. The reason for studying the effect of this parameter is because the sooner the OGIP can be estimated the better the reservoir management plan can be initiated.

Table 6.24 shows the parameters to be studied in this section. van Everdingen & Hurst water influx model is selected for calculation of W_e in $(G_p B_g + W_p B_w)/(B_g - B_{gi})$ versus $W_e/(B_g - B_{gi})$ plot in this section because it gives the most accurate value of estimated OGIP as mentioned in Section 6.6.

Table 6.24 Parameters to be studied on the effect of the amount of historical data on the feasibility and accuracy of OGIP estimation

Case	Aquifer size (PV)	Shut-in duration	Amount of historical data
1	0	6 hours	From initial condition to 25% RF
2			From initial condition to 50% RF
3			From initial condition to abandonment
4		1 day	From initial condition to 25% RF
5			From initial condition to 50% RF
6			From initial condition to abandonment
7		7 days	From initial condition to 25% RF
8			From initial condition to 50% RF
9			From initial condition to abandonment

Table 6.24 Parameters to be studied on the effect of the amount of historical data on the feasibility and accuracy of OGIP estimation (continued)

Case	Aquifer size (PV)	Shut-in duration	Amount of historical data
10	1	6 hours	From initial condition to 25% RF
11			From initial condition to 50% RF
12			From initial condition to abandonment
13		1 day	From initial condition to 25% RF
14			From initial condition to 50% RF
15			From initial condition to abandonment
16		7 days	From initial condition to 25% RF
17			From initial condition to 50% RF
18			From initial condition to abandonment
19	10	6 hours	From initial condition to 25% RF
20			From initial condition to 50% RF
21			From initial condition to abandonment
22		1 day	From initial condition to 25% RF
23			From initial condition to 50% RF
24			From initial condition to abandonment
25		7 days	From initial condition to 25% RF
26			From initial condition to 50% RF
27			From initial condition to abandonment

Table 6.24 Parameters to be studied on the effect of the amount of historical data on the feasibility and accuracy of OGIP estimation (continued)

Case	Aquifer size (PV)	Shut-in duration	Amount of historical data	
28	30	6 hours	From initial condition to 25% RF	
29			From initial condition to 50% RF	
30			From initial condition to abandonment	
31		1 day	From initial condition to 25% RF	
32			From initial condition to 50% RF	
33			From initial condition to abandonment	
34		7 days	From initial condition to 25% RF	
35			From initial condition to 50% RF	
36			From initial condition to abandonment	
37		70	6 hours	From initial condition to 25% RF
38				From initial condition to 50% RF
39				From initial condition to abandonment
40	1 day		From initial condition to 25% RF	
41			From initial condition to 50% RF	
42			From initial condition to abandonment	
43	7 days		From initial condition to 25% RF	
44			From initial condition to 50% RF	
45			From initial condition to abandonment	

Table 6.24 Parameters to be studied on the effect of the amount of historical data on the feasibility and accuracy of OGIP estimation (continued)

Case	Aquifer size (PV)	Shut-in duration	Amount of historical data
46	100	6 hours	From initial condition to 25% RF
47			From initial condition to 50% RF
48			From initial condition to abandonment
49		1 day	From initial condition to 25% RF
50			From initial condition to 50% RF
51			From initial condition to abandonment
52		7 days	From initial condition to 25% RF
53			From initial condition to 50% RF
54			From initial condition to abandonment

6.8.1 p/z versus G_p for 50 mD Water-drive Dry-gas Reservoir

Figure 6.91 to Figure 6.93 Figure 6.59 display p/z versus G_p plots for the case without aquifer while Figure 6.94 to Figure 6.108 represent the p/z versus G_p plots with the estimated OGIP value in 50 mD water-drive dry-gas reservoir at different aquifer sizes, shut-in durations and amounts of historical data. The larger amount of historical data, the plots are more deviated from straight line.

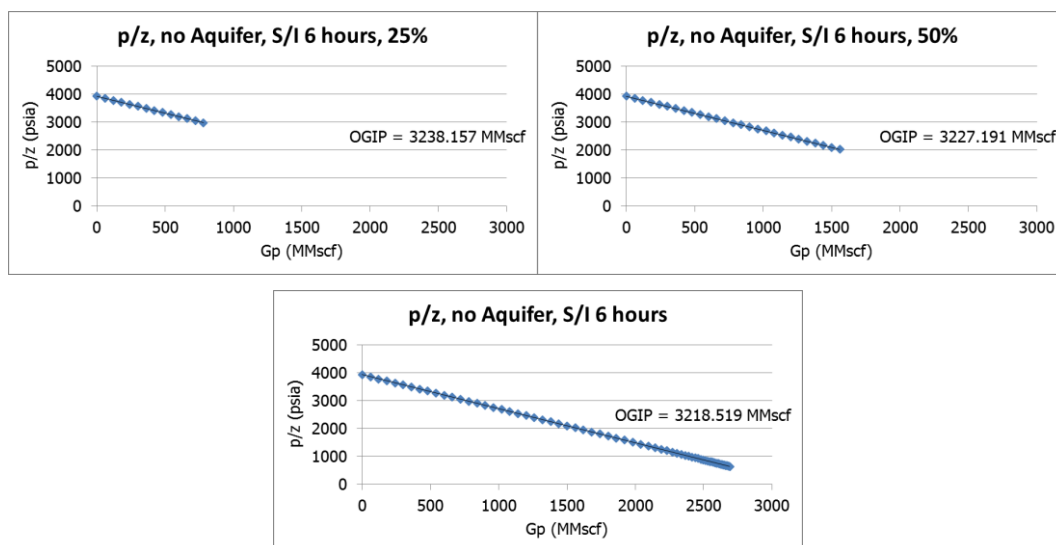


Figure 6.91 p/z versus G_p without aquifer support and 6-hour shut-in duration for 50 mD reservoir, case 1-3

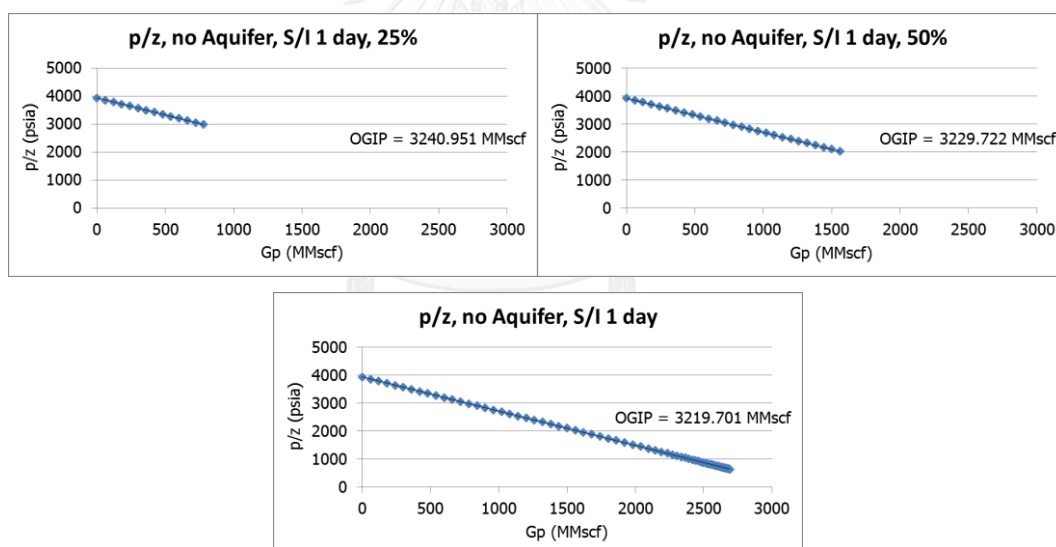


Figure 6.92 p/z versus G_p without aquifer support and 1-day shut-in duration for 50 mD reservoir, case 4-6

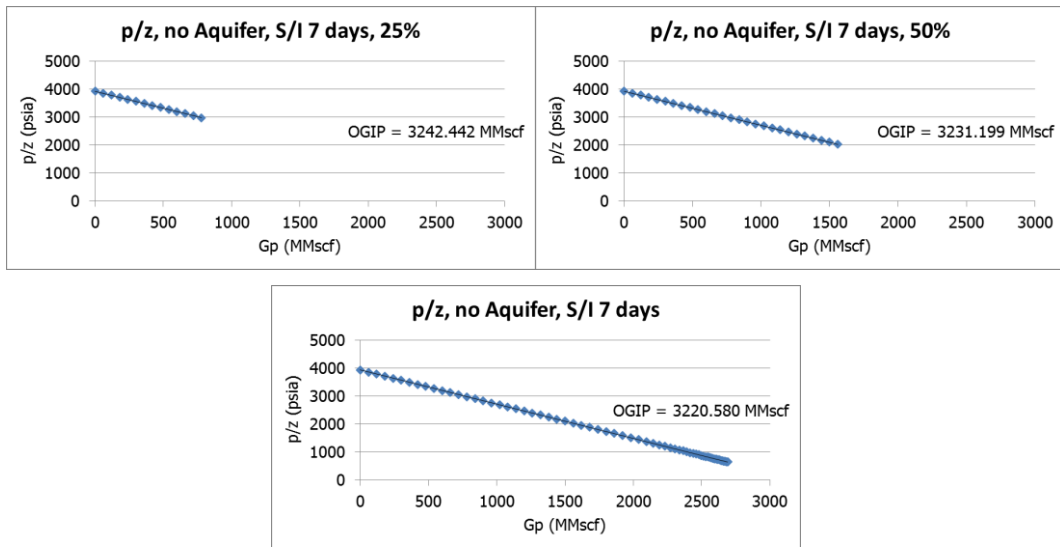


Figure 6.93 p/z versus G_p without aquifer support and 7-day shut-in duration for 50 mD reservoir, case 7-9

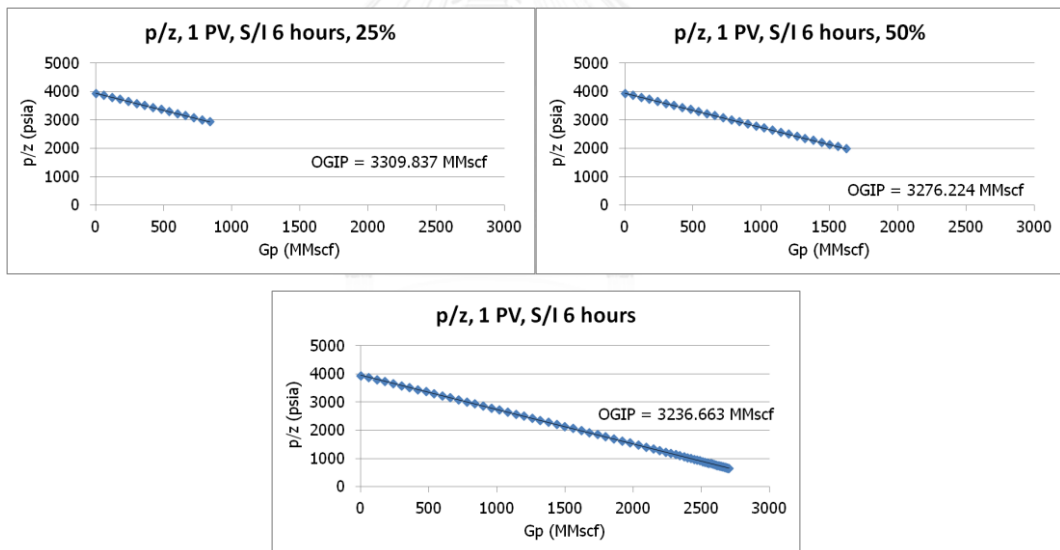


Figure 6.94 p/z versus G_p at 1-PV aquifer size and 6-hour shut-in duration for 50 mD reservoir, case 10-12

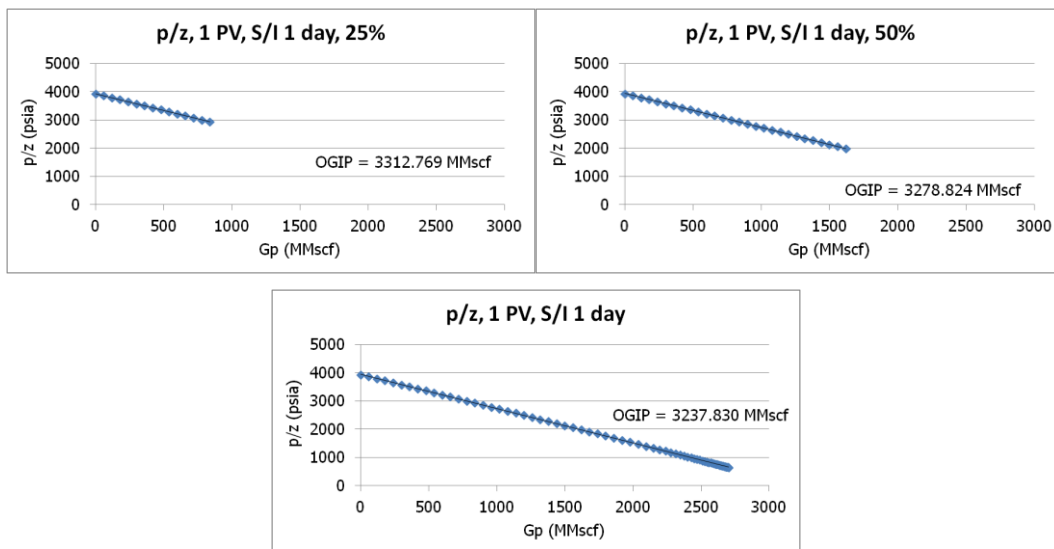


Figure 6.95 p/z versus G_p at 1-PV aquifer size and 1-day shut-in duration for 50 mD reservoir, case 13-15

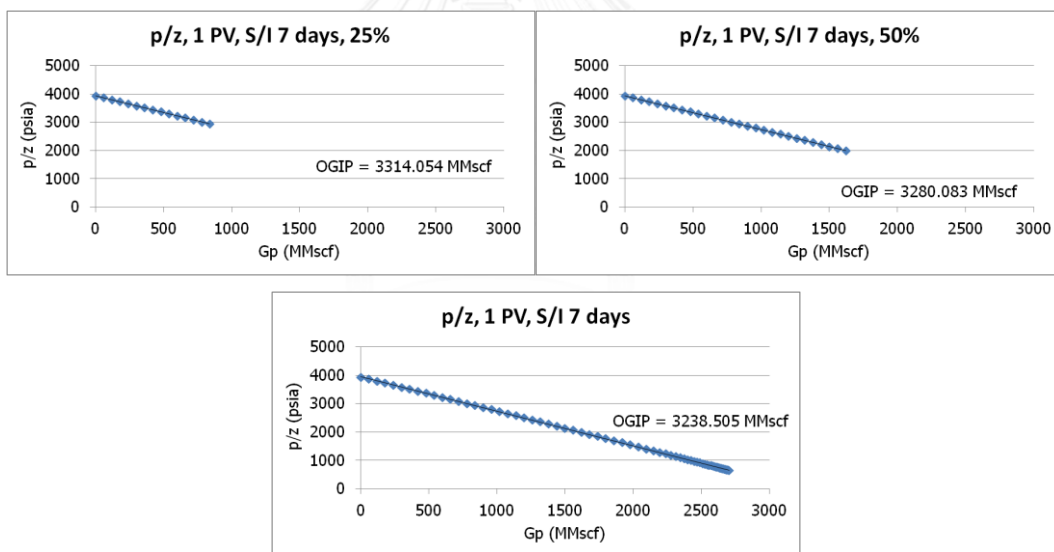


Figure 6.96 p/z versus G_p at 1-PV aquifer size and 7-day shut-in duration for 50 mD reservoir, case 16-18

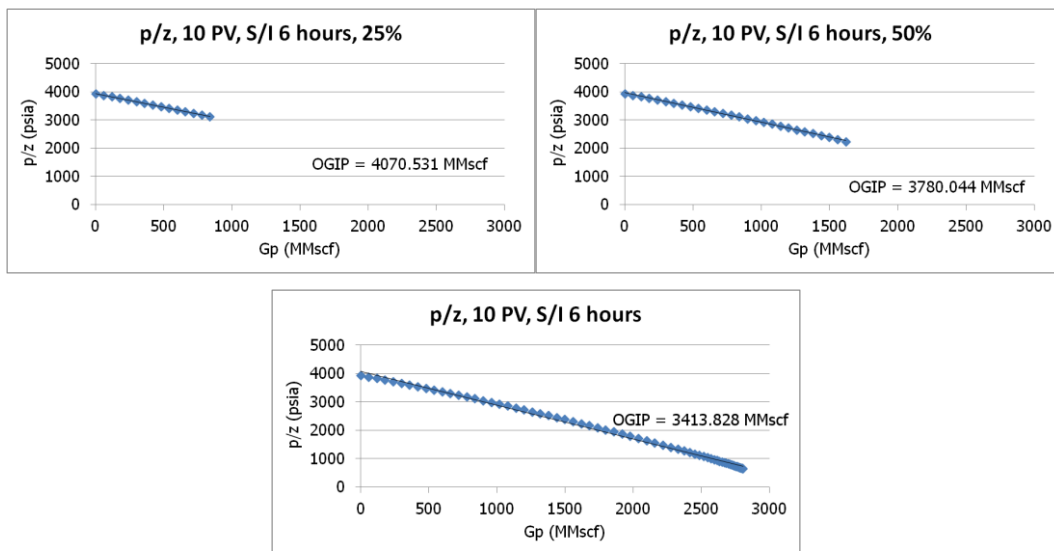


Figure 6.97 p/z versus G_p at 10-PV aquifer size and 6-hour shut-in duration for 50 mD reservoir, case 19-21

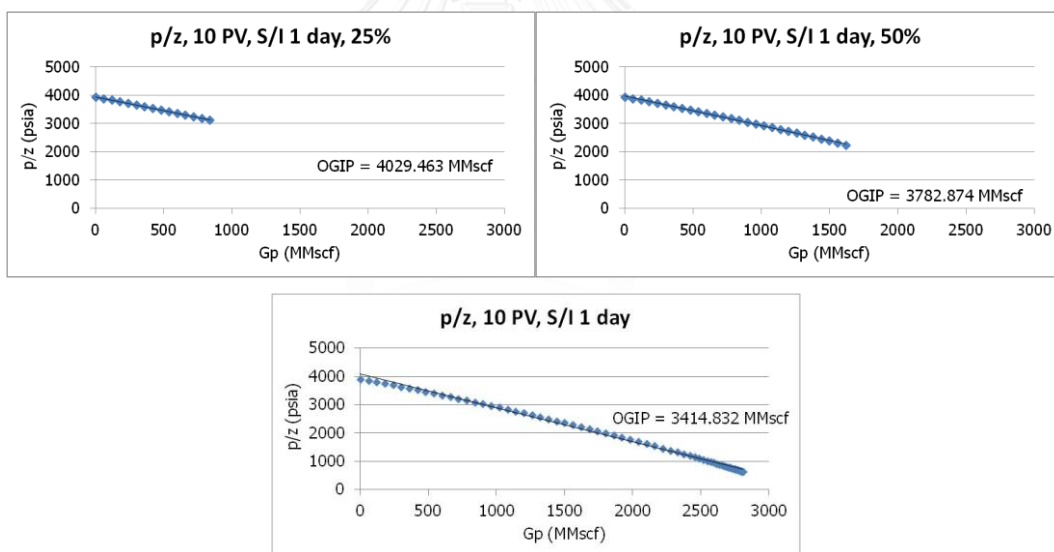


Figure 6.98 p/z versus G_p at 10-PV aquifer size and 1-day shut-in duration for 50 mD reservoir, case 22-24

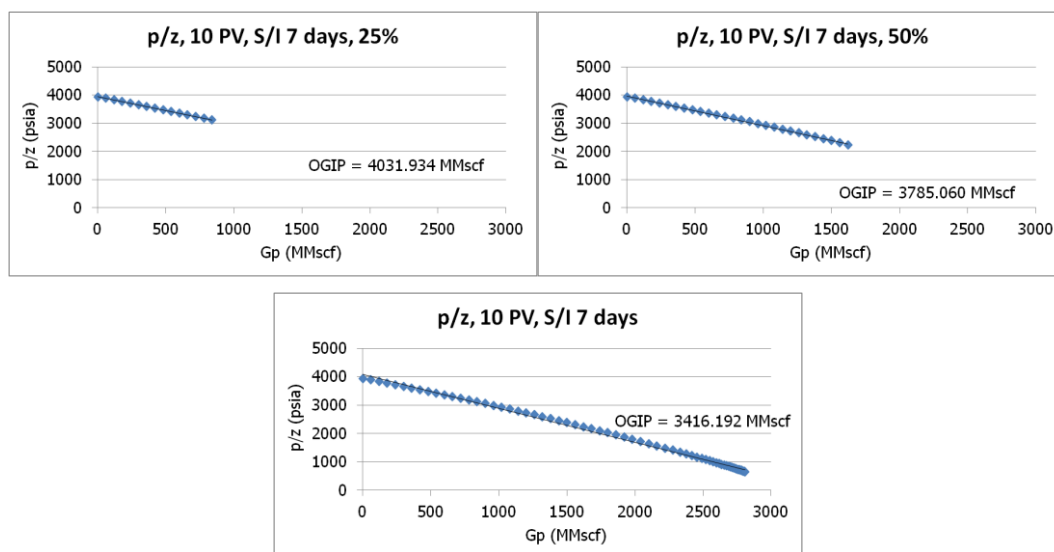


Figure 6.99 p/z versus G_p at 10-PV aquifer size and 7-day shut-in duration for 50 mD reservoir, case 25-27

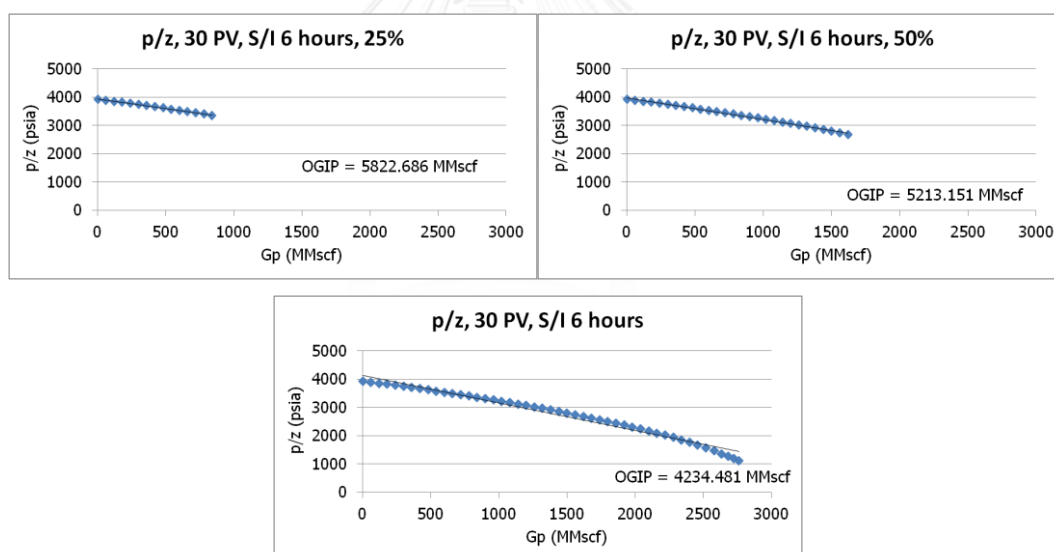


Figure 6.100 p/z versus G_p at 30-PV aquifer size and 6-hour shut-in duration for 50 mD reservoir, case 28-30

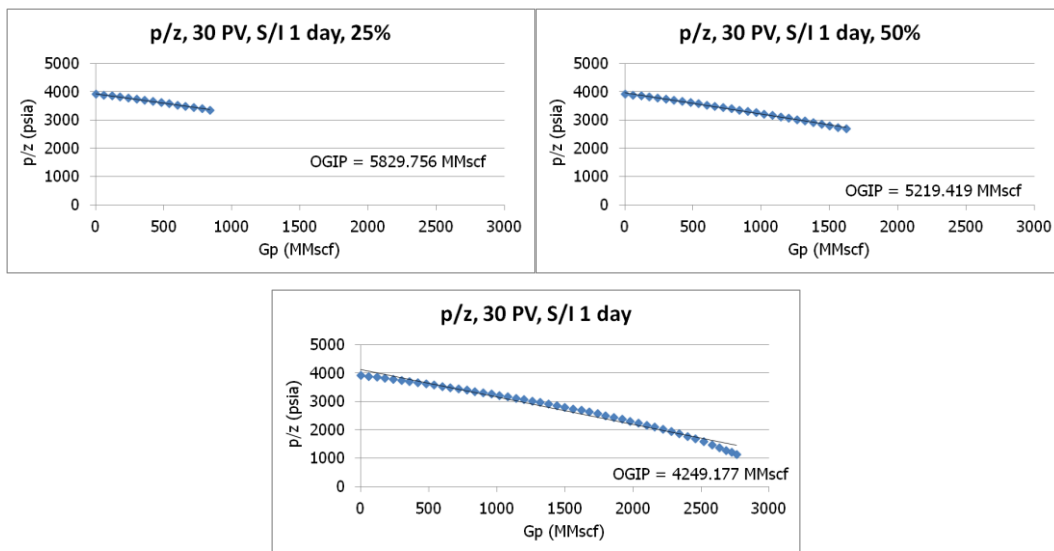


Figure 6.101 p/z versus G_p at 30-PV aquifer size and 1-day shut-in duration for 50 mD reservoir, case 31-33

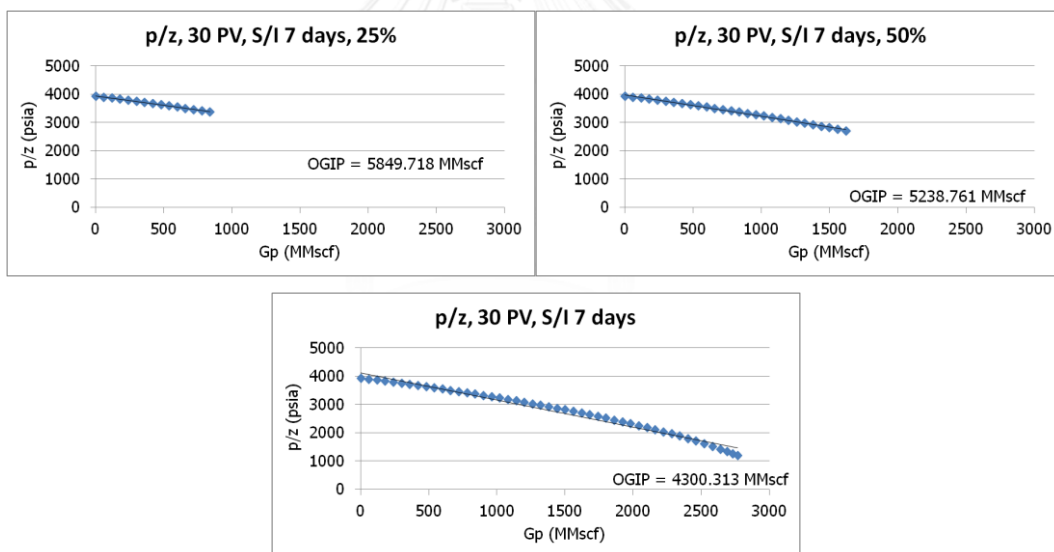


Figure 6.102 p/z versus G_p at 30-PV aquifer size and 7-day shut-in duration for 50 mD reservoir, case 34-36

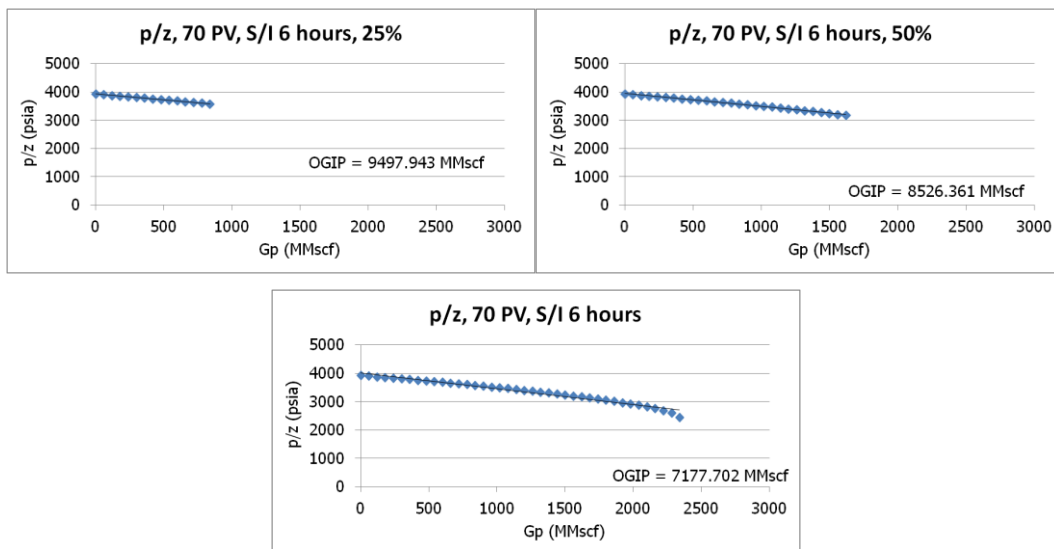


Figure 6.103 p/z versus G_p at 70-PV aquifer size and 6-hour shut-in duration for 50 mD reservoir, case 37-39

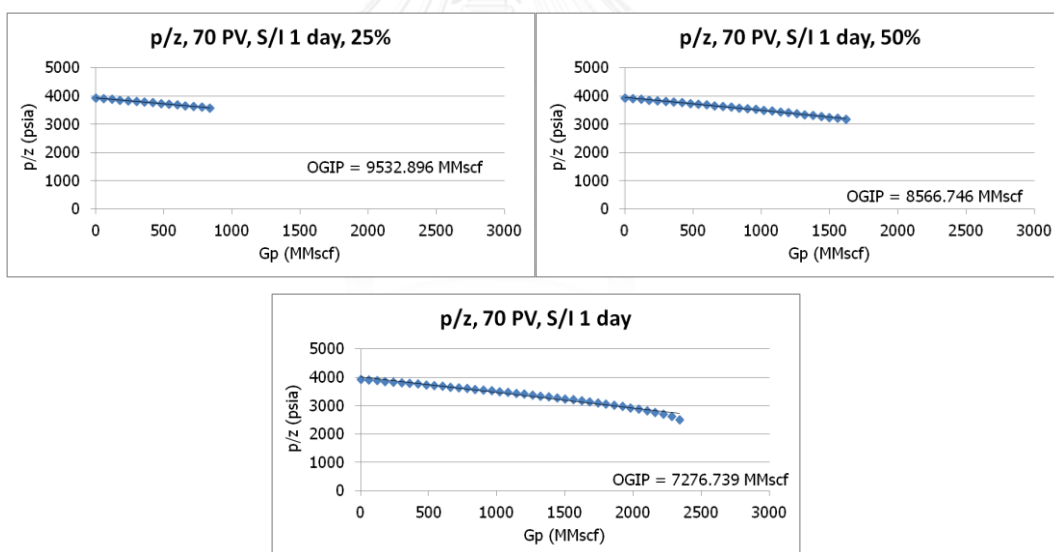


Figure 6.104 p/z versus G_p at 70-PV aquifer size and 1-day shut-in duration for 50 mD reservoir, case 40-42

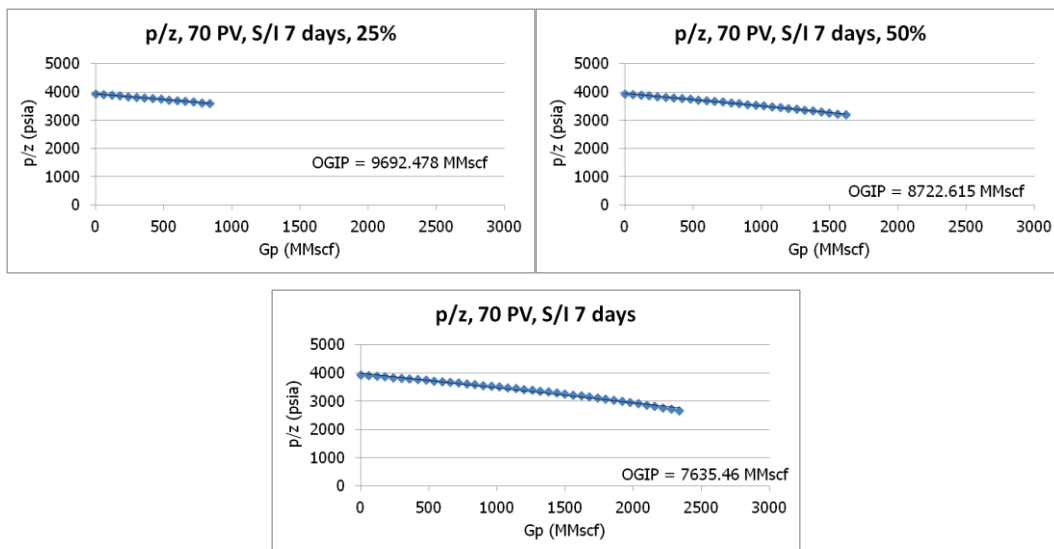


Figure 6.105 p/z versus G_p at 70-PV aquifer size and 7-day shut-in duration for 50 mD reservoir, case 43-45

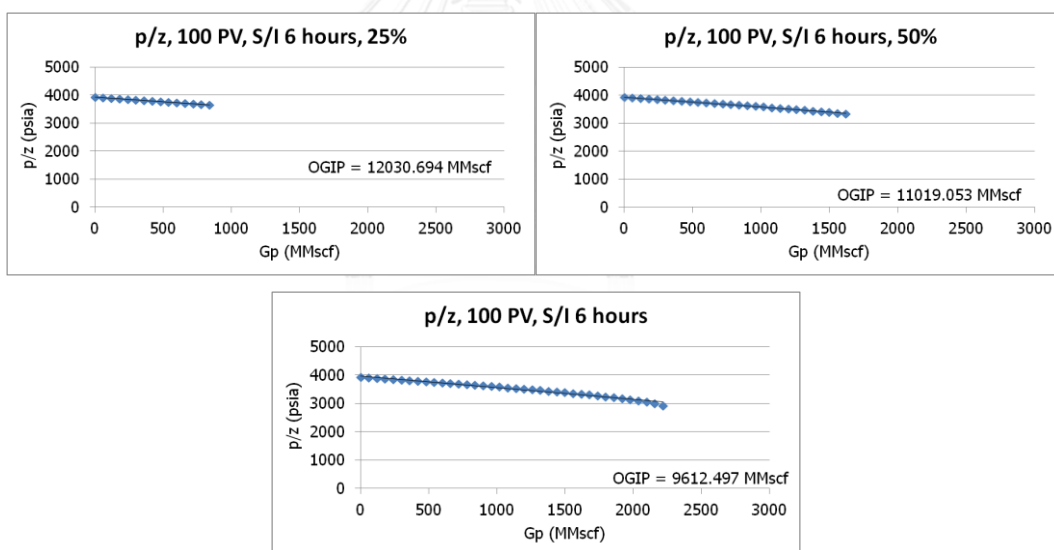


Figure 6.106 p/z versus G_p at 100-PV aquifer size and 6-hour shut-in duration for 50 mD reservoir, case 46-48

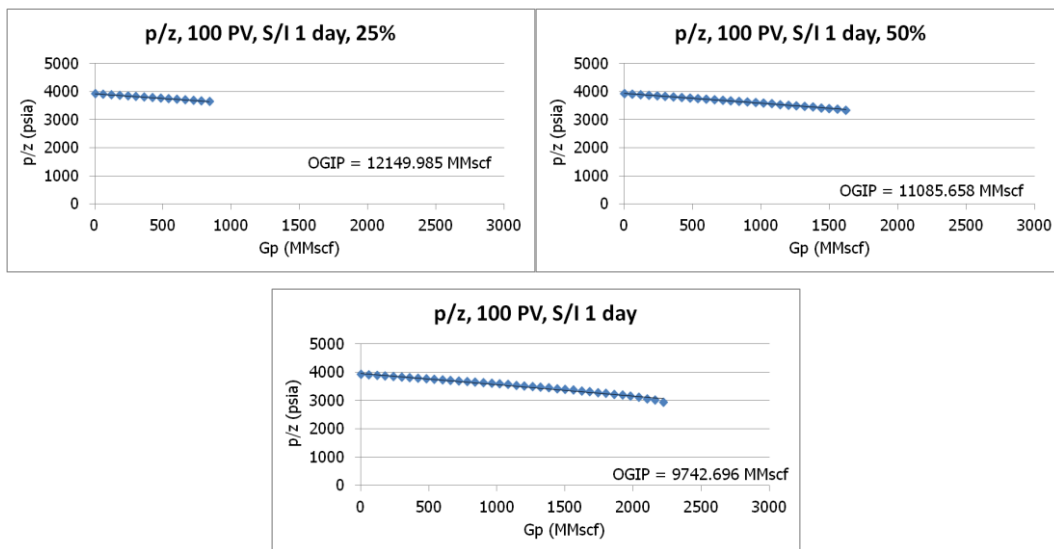


Figure 6.107 p/z versus G_p at 100-PV aquifer size and 1-day shut-in duration for 50 mD reservoir, case 49-51

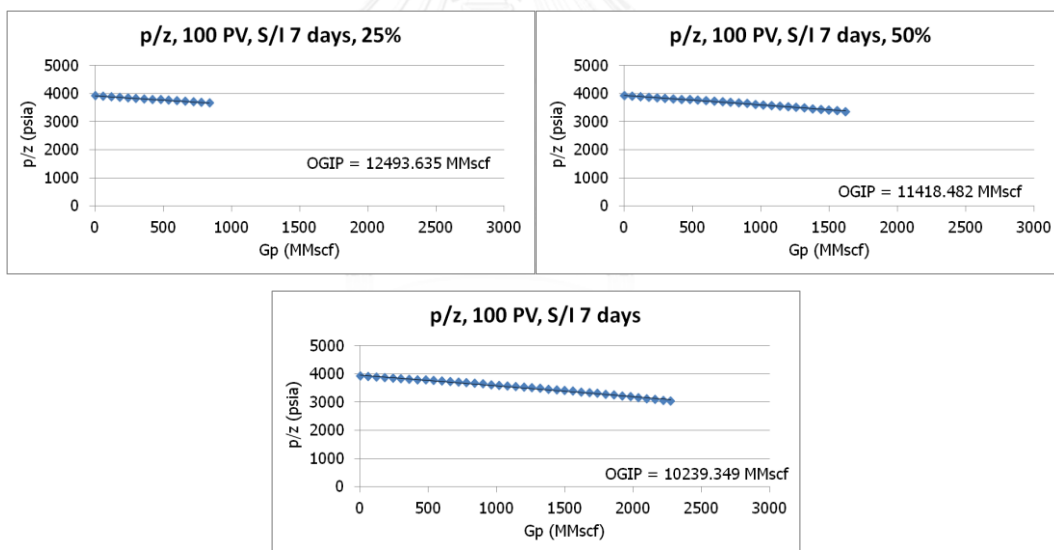


Figure 6.108 p/z versus G_p at 100-PV aquifer size and 7-day shut-in duration for 50 mD reservoir, case 52-54

Figure 6.109 indicates that a higher amount of historical data yields more accurate value of the estimated OGIP for all aquifer sizes and shut-in durations. The reason is the estimated OGIPs from p/z versus G_p plot are always higher than the actual

values as mentioned in Section 6.5 but the convex trends in the late time period make the value of the estimated OGIPs smaller and closer to the actual value.

The more amount of historical data also give the less R-squared value as shown in Table 6.25 because they contain more data in the convex trend. This behavior of the p/z versus G_p plot is aligned with the study of M.Elahmady and R.A. Wattenbarger [1] that the p/z versus G_p plot in some water-drive gas reservoirs show the straight line behavior, especially at the early time.

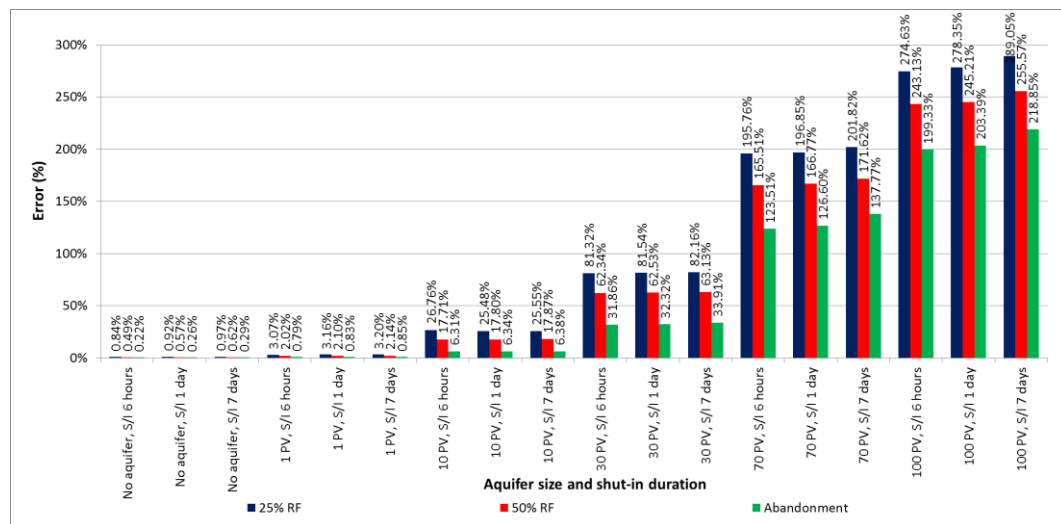


Figure 6.109 Error of estimated OGIP for 50 mD water-drive dry-gas reservoir by p/z versus G_p plot for various amounts of historical data

Table 6.25 The result of OGIP estimation for 50 mD water-drive dry-gas reservoir by p/z versus G_p plot for various amounts of historical data

Case	Aquifer size (PV)	Shut-in duration	Amount of historical data	Estimated OGIP (MMscf)	Error (%)	R-squared
1	0	6 hours	25% RF	3238.157	0.84%	1.0000
2			50% RF	3227.191	0.49%	1.0000
3			Abandonment	3218.519	0.22%	1.0000

Table 6.25 The result of OGIP estimation for 50 mD water-drive dry-gas reservoir by p/z versus G_p plot for various amounts of historical data (continued)

Case	Aquifer size (PV)	Shut-in duration	Amount of historical data	Estimated OGIP (MMscf)	Error (%)	R-squared	
4	0	1 day	25% RF	3240.951	0.92%	1.0000	
5			50% RF	3229.722	0.57%	1.0000	
6			Abandonment	3219.701	0.26%	1.0000	
7		7 days	25% RF	3242.442	0.97%	1.0000	
8			50% RF	3231.199	0.62%	1.0000	
9			Abandonment	3220.58	0.29%	1.0000	
10		1	6 hours	25% RF	3309.837	3.07%	1.0000
11				50% RF	3276.224	2.02%	1.0000
12				Abandonment	3236.663	0.79%	0.9999
13	1 day		25% RF	3312.769	3.16%	1.0000	
14			50% RF	3278.824	2.10%	1.0000	
15			Abandonment	3237.83	0.83%	0.9999	
16	7 days		25% RF	3314.054	3.20%	1.0000	
17			50% RF	3280.083	2.14%	1.0000	
18			Abandonment	3238.505	0.85%	0.9999	
19	10	6 hours	25% RF	4070.531	26.76%	0.9994	
20			50% RF	3780.044	17.71%	0.9986	
21			Abandonment	3413.828	6.31%	0.9966	
22		1 day	25% RF	4029.463	25.48%	0.9994	

Table 6.25 The result of OGIP estimation for 50 mD water-drive dry-gas reservoir by p/z versus G_p plot for various amounts of historical data (continued)

Case	Aquifer size (PV)	Shut-in duration	Amount of historical data	Estimated OGIP (MMscf)	Error (%)	R-squared	
23	10	1 day	50% RF	3782.874	17.80%	0.9986	
24			Abandonment	3414.832	6.34%	0.9965	
25		7 days	25% RF	4031.934	25.55%	0.9994	
26			50% RF	3785.06	17.87%	0.9986	
27			Abandonment	3416.192	6.38%	0.9965	
28		30	6 hours	25% RF	5822.686	81.32%	0.9988
29	50% RF			5213.151	62.34%	0.9959	
30	Abandonment			4234.481	31.86%	0.9763	
31	1 day		25% RF	5829.756	81.54%	0.9988	
32			50% RF	5219.419	62.53%	0.9959	
33			Abandonment	4249.177	32.32%	0.9770	
34			7 days	25% RF	5849.718	82.16%	0.9987
35				50% RF	5238.761	63.13%	0.9959
36				Abandonment	4300.313	33.91%	0.9796
37	70		6 hours	25% RF	9497.943	195.76%	0.9995
38				50% RF	8526.361	165.51%	0.9958
39				Abandonment	7177.702	123.51%	0.9704
40		1 day	25% RF	9532.896	196.85%	0.9994	
41			50% RF	8566.746	166.77%	0.9959	

Table 6.25 The result of OGIP estimation for 50 mD water-drive dry-gas reservoir by p/z versus G_p plot for various amounts of historical data (continued)

Case	Aquifer size (PV)	Shut-in duration	Amount of historical data	Estimated OGIP (MMscf)	Error (%)	R-squared
42	70	1 day	Abandonment	7276.739	126.60%	0.9753
43		7 days	25% RF	9692.478	201.82%	0.9993
44			50% RF	8722.615	171.62%	0.9962
45			Abandonment	7635.46	137.77%	0.9860
46	100	6 hours	25% RF	12030.69	274.63%	0.9991
47			50% RF	11019.05	243.13%	0.9967
48			Abandonment	9612.497	199.33%	0.9799
49		1 day	25% RF	12149.99	278.35%	0.9993
50			50% RF	11085.66	245.21%	0.9966
51			Abandonment	9742.696	203.39%	0.9826
52		7 days	25% RF	12493.64	289.05%	0.9996
53			50% RF	11418.48	255.57%	0.9970
54			Abandonment	10239.35	218.85%	0.9903

The accuracy of OGIP estimation by p/z versus G_p plot are summarized in Table 6.26.

Table 6.26 The accuracy of OGIP estimation for 50 mD water-drive dry-gas reservoir by p/z versus G_p plot for various amounts of historical data

Aquifer size (PV)	Shut-in duration	Amount of historical data	Accuracy
0 and 1	6 hours, 1 day and 7 days	Up to 25% RF, 50% RF and Abandonment	Accurate
10		Up to 25% RF and 50% RF	Not acceptable
		Up to Abandonment	Acceptable
30, 70 and 100		Up to 25% RF, 50% RF and Abandonment	Not acceptable

Accurate: error < 5%, Acceptable: error < 10%, Not acceptable: error ≥ 10%

The aquifer size is required for OGIP estimation by p/z versus G_p plot. If the aquifer size is not larger than 10 PV, the OGIP can be estimated with appropriate amount of historical data as shown in Table 6.26.

6.8.2 p/z versus G_p for 500 mD Water-drive Dry-gas Reservoir

Figure 6.110 to Figure 6.112 Figure 6.59 display p/z versus G_p plots for the case without aquifer while Figure 6.113 to Figure 6.127 represent the p/z versus G_p plots with the estimated OGIP value in 500 mD water-drive dry-gas reservoir for different aquifer sizes, shut-in durations and amounts of historical data.

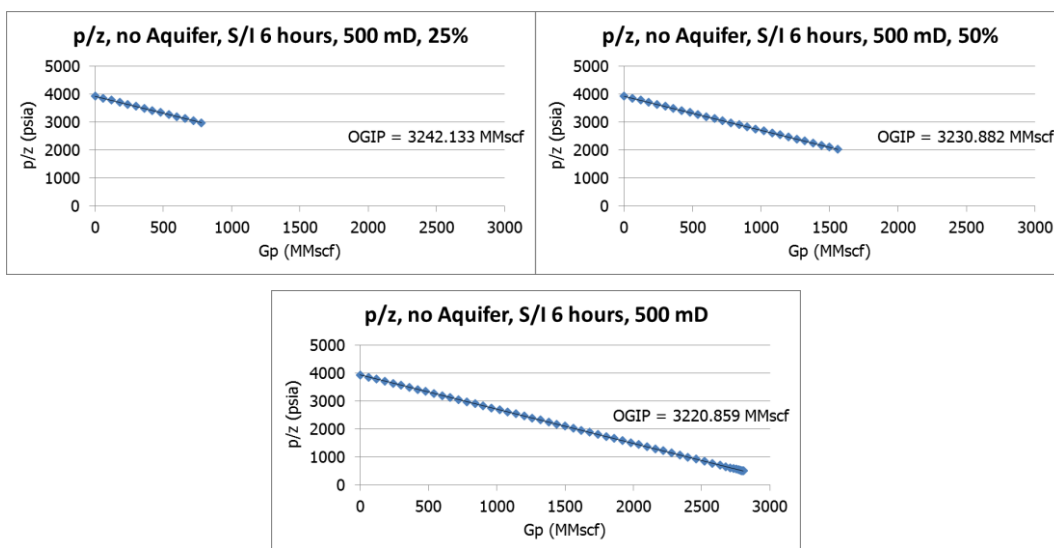


Figure 6.110 p/z versus G_p without aquifer support and 6-hour shut-in duration for 500 mD reservoir, case 1-3

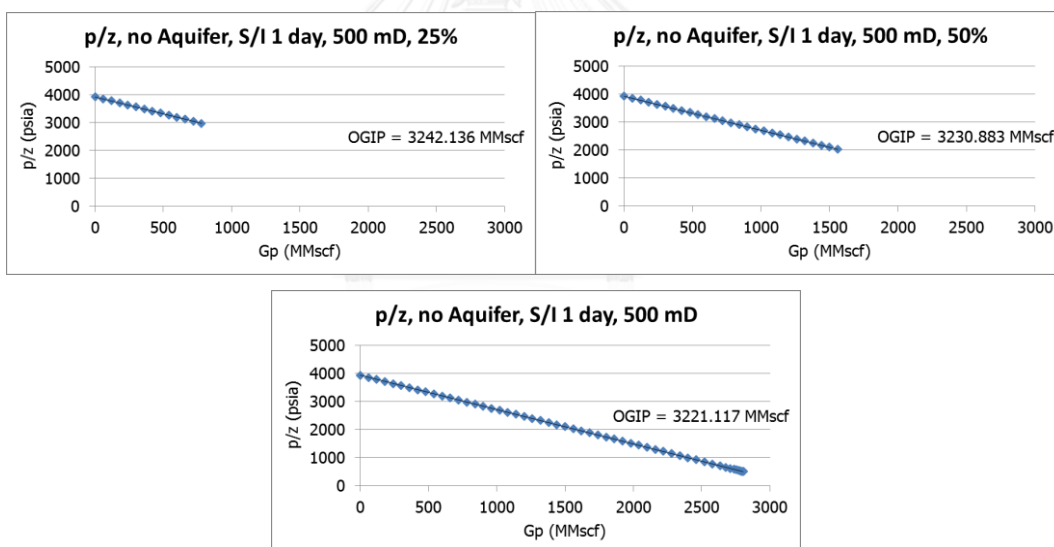


Figure 6.111 p/z versus G_p without aquifer support and 1-day shut-in duration for 500 mD reservoir, case 4-6

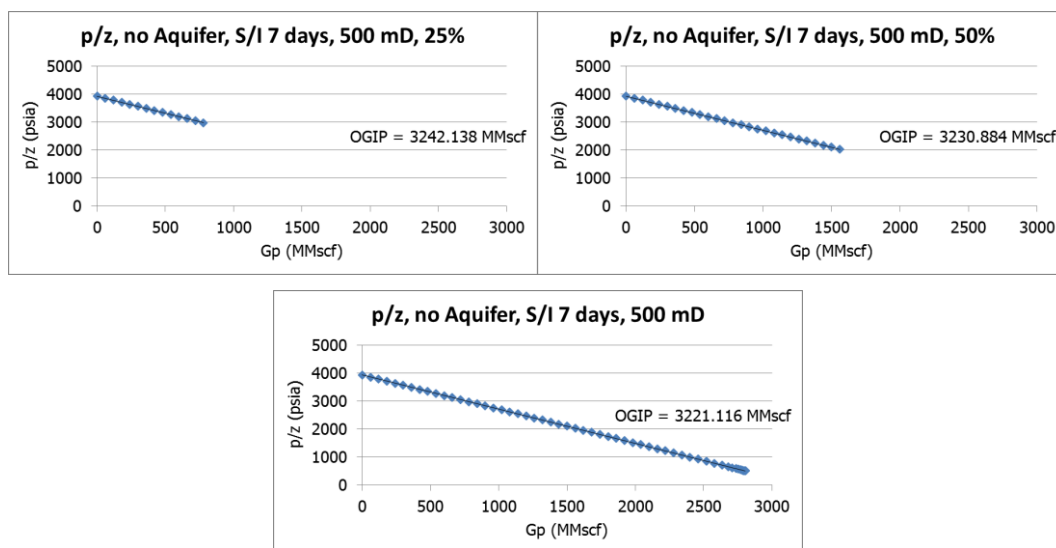


Figure 6.112 p/z versus G_p without aquifer support and 7-days shut-in duration for 500 mD reservoir, case 7-9

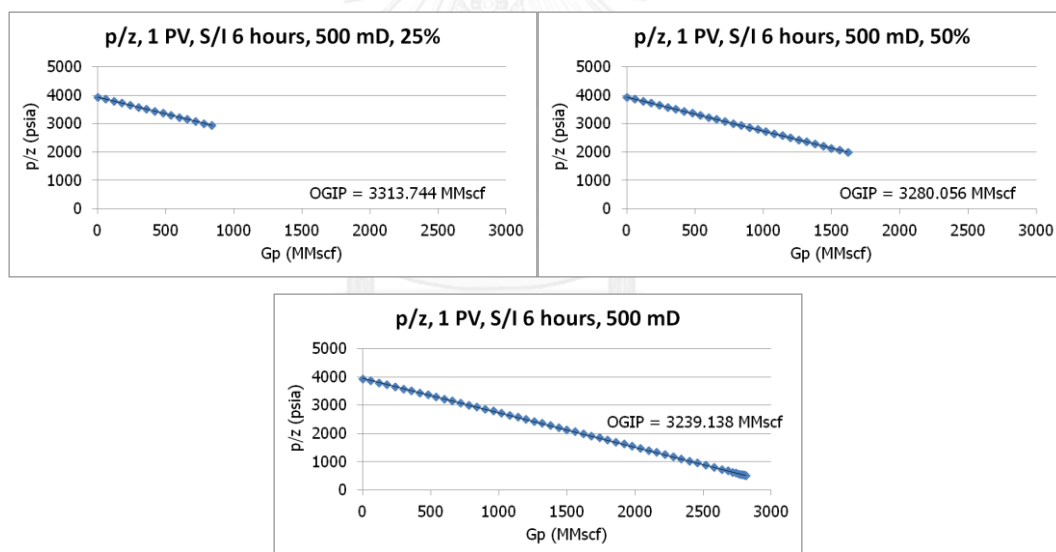


Figure 6.113 p/z versus G_p at 1-PV aquifer size and 6-hour shut-in duration for 500 mD reservoir, case 10-12

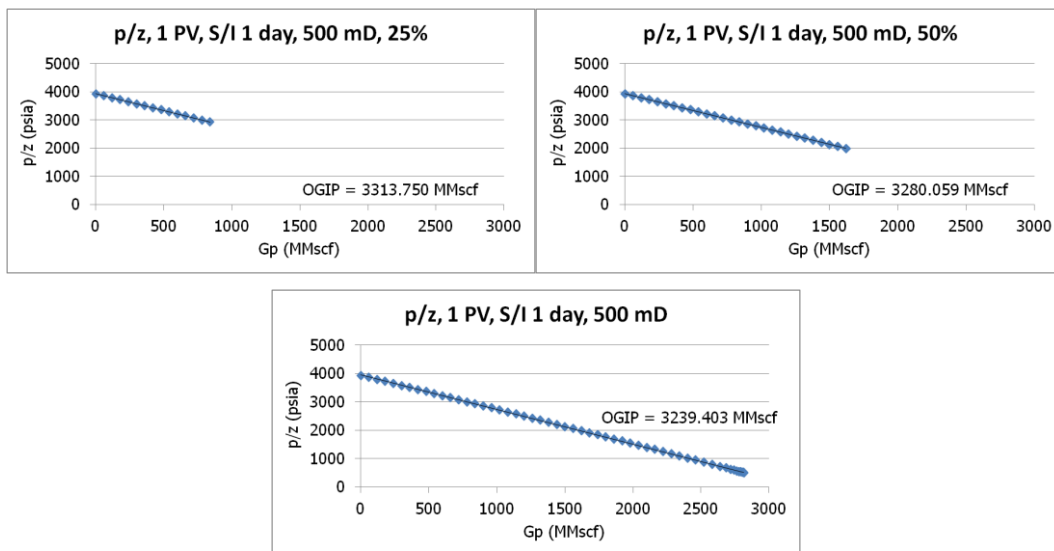


Figure 6.114 p/z versus G_p at 1-PV aquifer size and 1-day shut-in duration for 500 mD reservoir, case 13-15

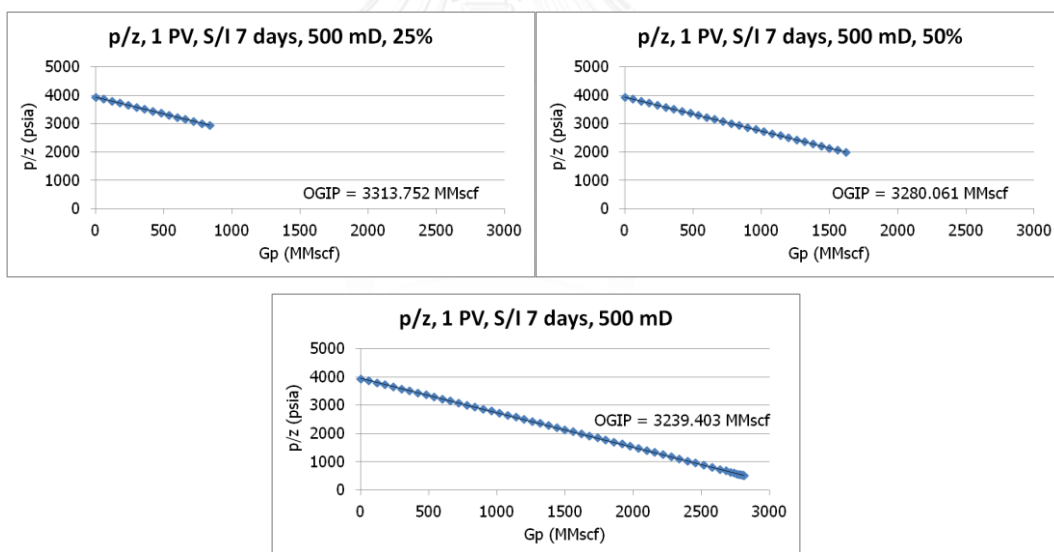


Figure 6.115 p/z versus G_p at 1-PV aquifer size and 7-day shut-in duration for 500 mD reservoir, case 16-18

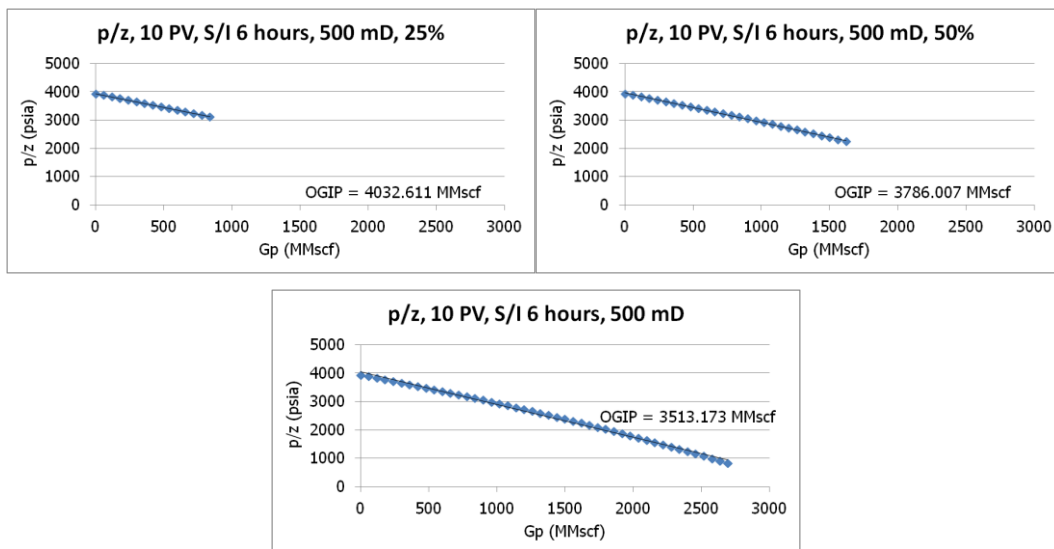


Figure 6.116 p/z versus G_p at 10-PV aquifer size and 6-hour shut-in duration for 500 mD reservoir, case 19-21

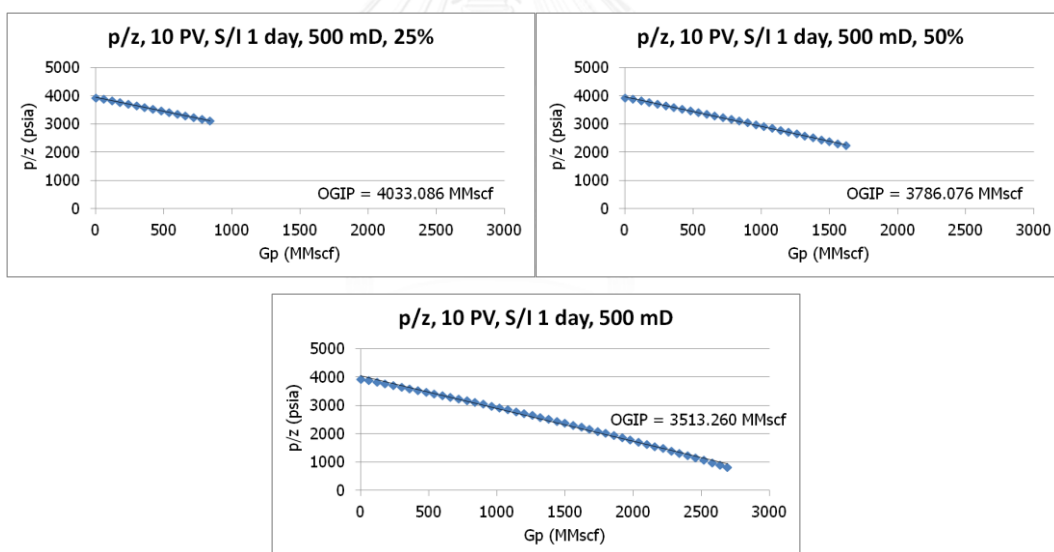


Figure 6.117 p/z versus G_p at 10-PV aquifer size and 1-day shut-in duration for 500 mD reservoir, case 22-24

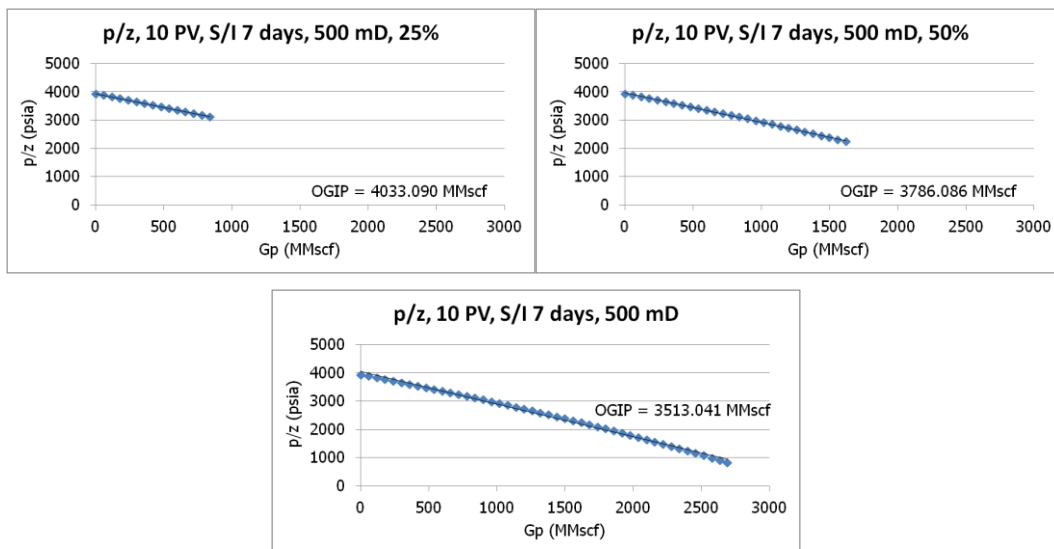


Figure 6.118 p/z versus G_p at 10-PV aquifer size and 7-day shut-in duration for 500 mD reservoir, case 25-27

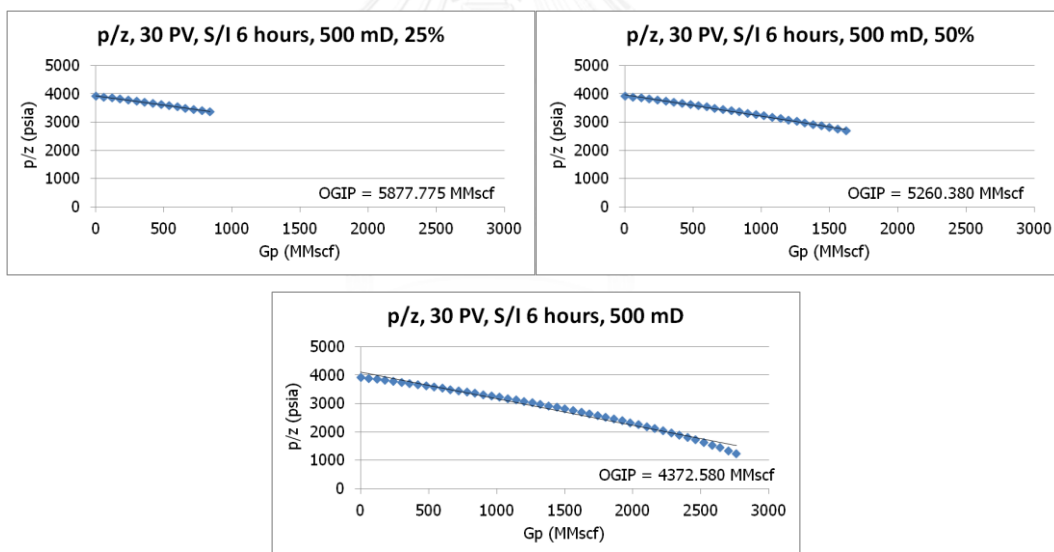


Figure 6.119 p/z versus G_p at 30-PV aquifer size and 6-hour shut-in duration for 500 mD reservoir, case 28-30

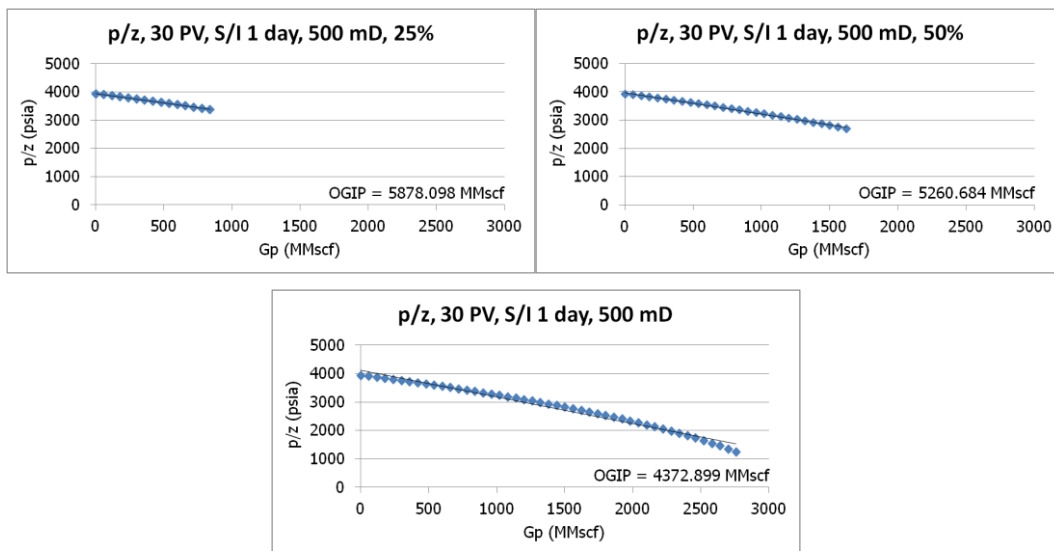


Figure 6.120 p/z versus G_p at 30-PV aquifer size and 1-day shut-in duration for 500 mD reservoir, case 31-33

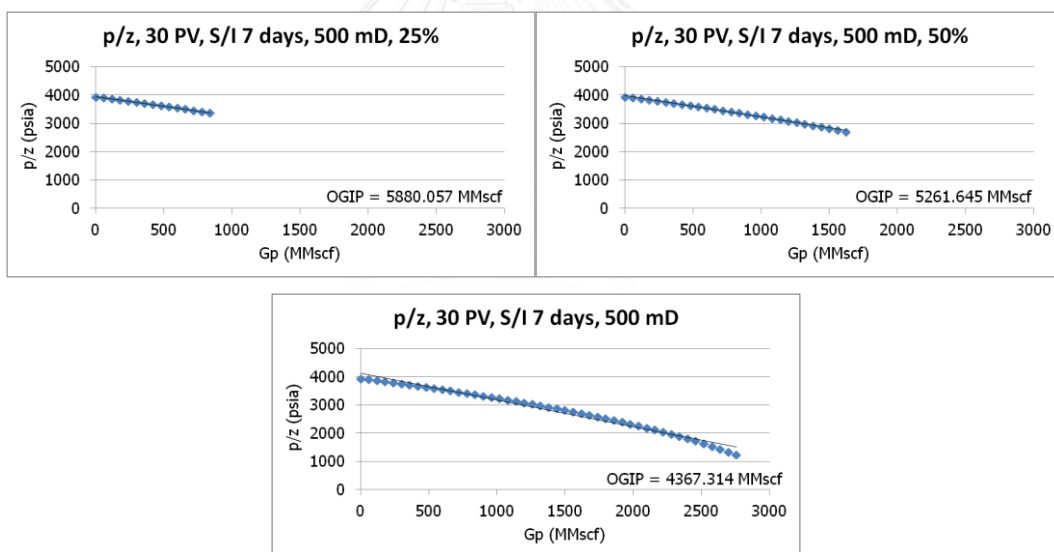


Figure 6.121 p/z versus G_p at 30-PV aquifer size and 7-day shut-in duration for 500 mD reservoir, case 34-36

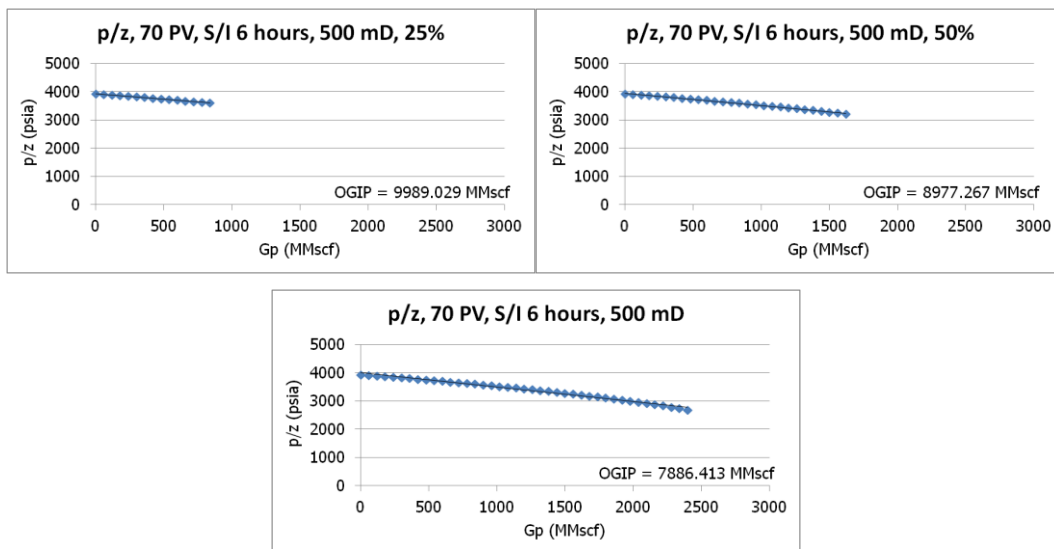


Figure 6.122 p/z versus G_p at 70-PV aquifer size and 6-hour shut-in duration for 500 mD reservoir, case 37-39

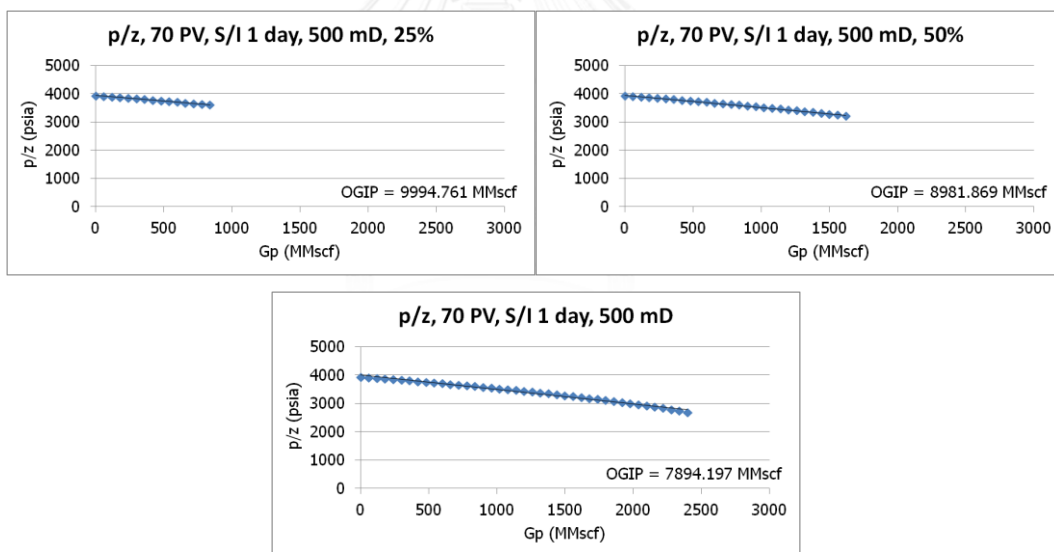


Figure 6.123 p/z versus G_p at 70-PV aquifer size and 1-day shut-in duration for 500 mD reservoir, case 40-42

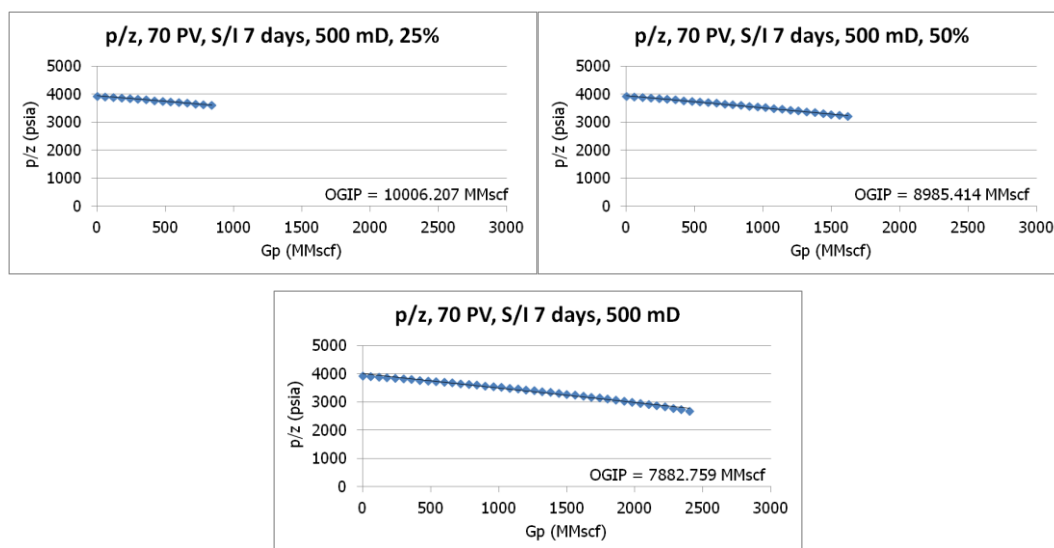


Figure 6.124 p/z versus G_p at 70-PV aquifer size and 7-day shut-in duration for 500 mD reservoir, case 43-45

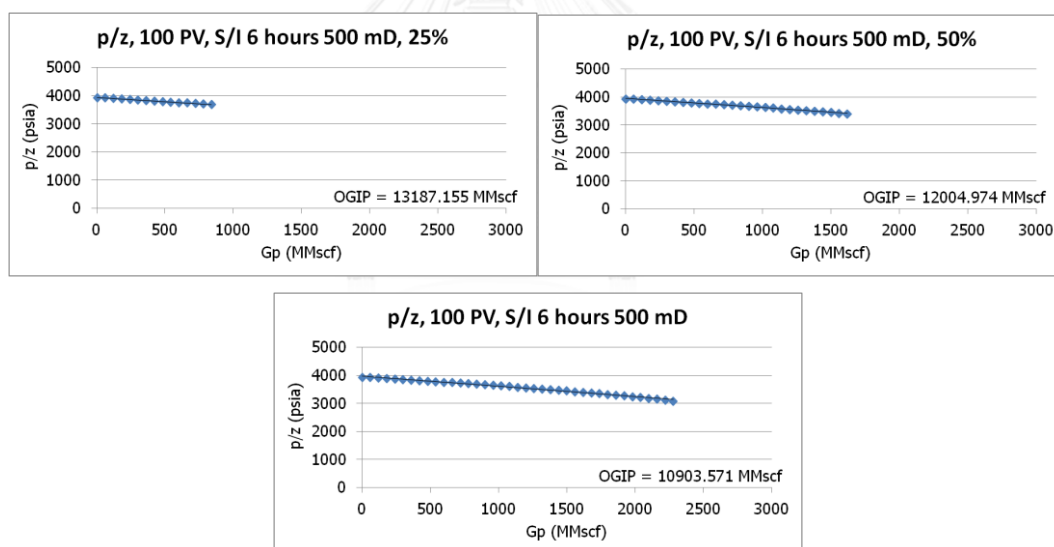


Figure 6.125 p/z versus G_p at 100-PV aquifer size and 6-hour shut-in duration for 500 mD reservoir, case 46-48

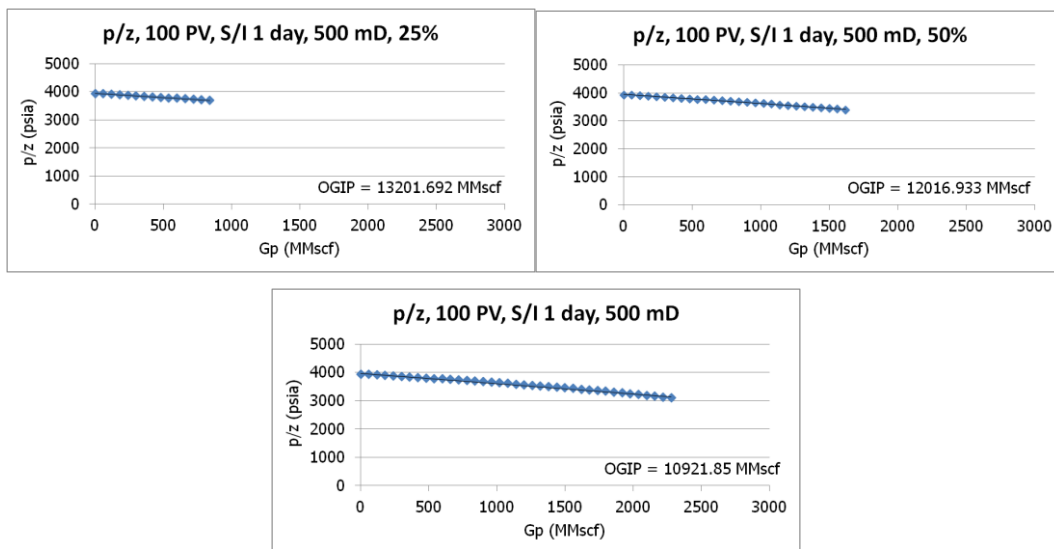


Figure 6.126 p/z versus G_p at 100-PV aquifer size and 1-day shut-in duration for 500 mD reservoir, case 49-51

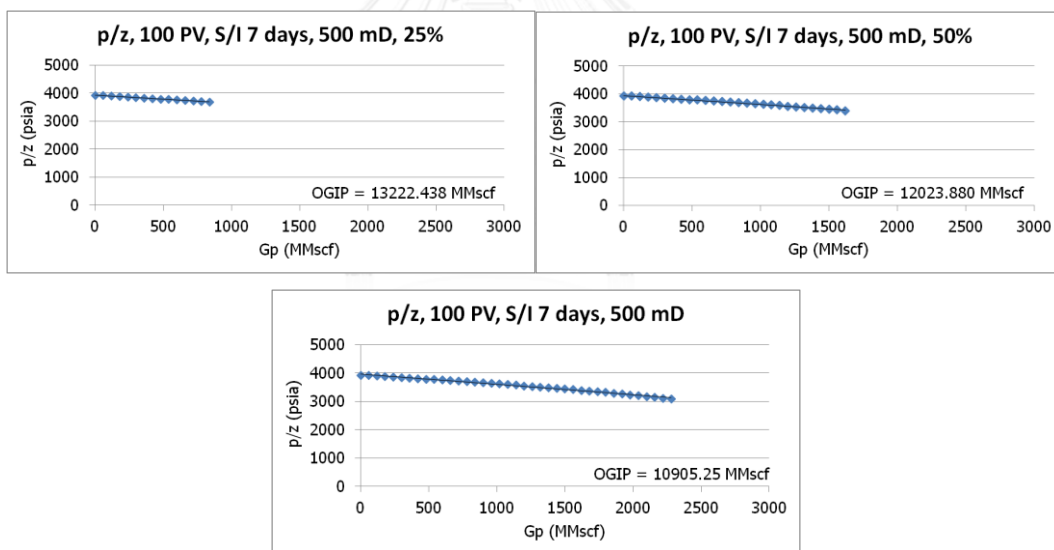


Figure 6.127 p/z versus G_p at 100-PV aquifer size and 7-day shut-in duration for 500 mD reservoir, case 52-54

The result of OGIP estimation for 500 mD reservoir are similar to 50 mD reservoir. A larger amount of historical data yields more accurate value of the estimated OGIP and less R-squared value for all aquifer sizes and shut-in duration cases due to the same reason as in 50 mD reservoir as illustrated in Figure 6.128 and Table 6.27.

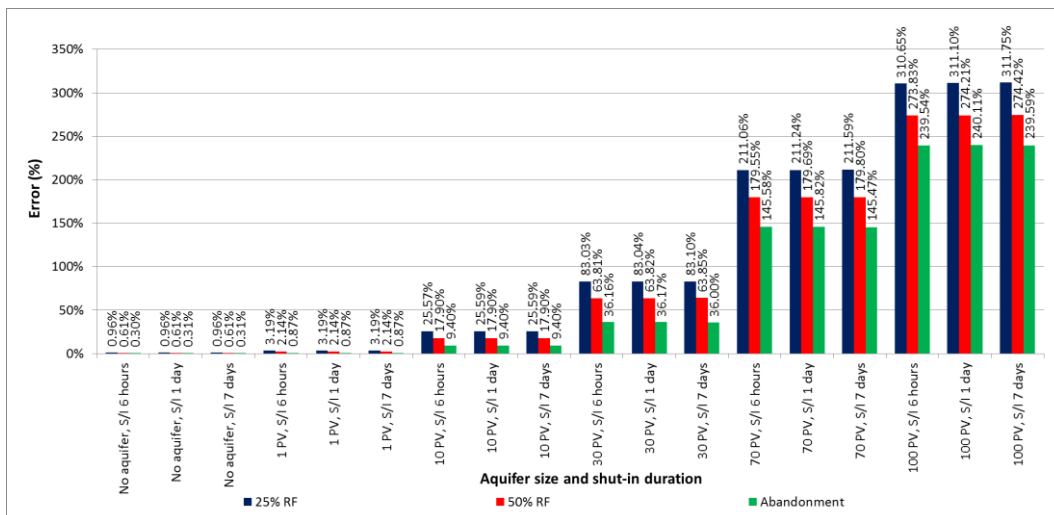


Figure 6.128 Error of estimated OGIP for 500 mD water-drive dry-gas reservoir by p/z versus G_p plot for various amounts of historical data

Table 6.27 The result of OGIP estimation for 500 mD water-drive dry-gas reservoir by p/z versus G_p plot for various amounts of historical

Case	Aquifer size (PV)	Shut-in duration	Amount of historical data	Estimated OGIP (MMscf)	Error (%)	R-squared
1	0	6 hours	25% RF	3242.13	0.96%	1.0000
2			50% RF	3230.88	0.61%	1.0000
3			Abandonment	3220.86	0.30%	1.0000
4		1 day	25% RF	3242.14	0.96%	1.0000
5			50% RF	3230.88	0.61%	1.0000
6			Abandonment	3221.12	0.31%	1.0000
7		7 days	25% RF	3242.14	0.96%	1.0000
8			50% RF	3230.88	0.61%	1.0000
9			Abandonment	3221.12	0.31%	1.0000
10	1	6 hours	25% RF	3313.74	3.19%	1.0000

Table 6.27 The result of OGIP estimation for 500 mD water-drive dry-gas reservoir by p/z versus G_p plot for various amounts of historical (continued)

Case	Aquifer size (PV)	Shut-in duration	Amount of historical data	Estimated OGIP (MMscf)	Error (%)	R-squared
11	1	6 hours	50% RF	3280.06	2.14%	1.0000
12			Abandonment	3239.14	0.87%	0.9999
13		1 day	25% RF	3313.75	3.19%	1.0000
14			50% RF	3280.06	2.14%	1.0000
15			Abandonment	3239.4	0.87%	0.9999
16		7 days	25% RF	3313.75	3.19%	1.0000
17			50% RF	3280.06	2.14%	1.0000
18			Abandonment	3239.4	0.87%	0.9999
19		10	6 hours	25% RF	4032.61	25.57%
20	50% RF			3786.01	17.90%	0.9986
21	Abandonment			3513.17	9.40%	0.9964
22	1 day		25% RF	4033.09	25.59%	0.9994
23			50% RF	3786.08	17.90%	0.9986
24			Abandonment	3513.26	9.40%	0.9964
25	7 days		25% RF	4033.09	25.59%	0.9994
26			50% RF	3786.09	17.90%	0.9986
27			Abandonment	3513.04	9.40%	0.9964
28	30	6 hours	25% RF	5877.78	83.03%	0.9987
29			50% RF	5260.38	63.81%	0.9959

Table 6.27 The result of OGIP estimation for 500 mD water-drive dry-gas reservoir by p/z versus G_p plot for various amounts of historical (continued)

Case	Aquifer size (PV)	Shut-in duration	Amount of historical data	Estimated OGIP (MMscf)	Error (%)	R-squared	
30	30	6 hours	Abandonment	4372.58	36.16%	0.9813	
31		1 day	25% RF	5878.1	83.04%	0.9987	
32			50% RF	5260.68	63.82%	0.9959	
33			Abandonment	4372.9	36.17%	0.9814	
34		7 days	25% RF	5880.06	83.10%	0.9986	
35			50% RF	5261.65	63.85%	0.9959	
36			Abandonment	4367.31	36.00%	0.9812	
37		70	6 hours	25% RF	9989.03	211.06%	0.9987
38				50% RF	8977.27	179.55%	0.9963
39	Abandonment			7886.41	145.58%	0.9880	
40	1 day		25% RF	9994.76	211.24%	0.9986	
41			50% RF	8981.87	179.69%	0.9963	
42			Abandonment	7894.2	145.82%	0.9881	
43	7 days		25% RF	10006.2	211.59%	0.9985	
44			50% RF	8985.41	179.80%	0.9962	
45			Abandonment	7882.76	145.47%	0.9879	
46	100	6 hours	25% RF	13187.2	310.65%	0.9987	
47			50% RF	12005	273.83%	0.9971	
48			Abandonment	10903.6	239.54%	0.9920	

Table 6.27 The result of OGIP estimation for 500 mD water-drive dry-gas reservoir by p/z versus G_p plot for various amounts of historical (continued)

Case	Aquifer size (PV)	Shut-in duration	Amount of historical data	Estimated OGIP (MMscf)	Error (%)	R-squared
49	100	1 day	25% RF	13201.7	311.10%	0.9987
50			50% RF	12016.9	274.21%	0.9972
51			Abandonment	10921.9	240.11%	0.9922
52		7 days	25% RF	13222.4	311.75%	0.9984
53			50% RF	12023.9	274.42%	0.9970
54			Abandonment	10905.3	239.59%	0.9920

The accuracy of OGIP estimation by p/z versus G_p plot for 500 mD reservoir are summarized in Table 6.28. The criteria for accuracy level is same as the one in Section 6.8.1.

Table 6.28 The accuracy of OGIP estimation for 500 mD water-drive dry-gas reservoir by p/z versus G_p plot for various amounts of historical data

Aquifer size (PV)	Shut-in duration	Amount of historical data	Accuracy
0 and 1	6 hours, 1 day and 7 days	Up to 25% RF, 50% RF and Abandonment	Accurate
10		Up to 25% RF and 50% RF	Not acceptable
		Up to Abandonment	Acceptable
30, 70 and 100		Up to 25% RF, 50% RF and Abandonment	Not acceptable

Accurate: error < 5%, Acceptable: error < 10%, Not acceptable: error ≥ 10%

If the aquifer size is not larger than 10 PV, the OGIP can be estimated with appropriate amount of historical data at shown in Table 6.28, similar to 50 mD reservoir in Section 6.8.1.

6.8.3 $(G_p B_g + W_p B_w)/(B_g - B_{gi})$ versus $W_e/(B_g - B_{gi})$ Plot for 50 mD Water-drive Dry-gas Reservoir

Figure 6.129 to Figure 6.143 represent the $(G_p B_g + W_p B_w)/(B_g - B_{gi})$ versus $W_e/(B_g - B_{gi})$ plots with the estimated OGIP value for 50 mD water-drive dry-gas reservoir with different aquifer sizes, shut-in durations and amounts of historical data.

For 1-PV aquifer size, the positive slope trends of $(G_p B_g + W_p B_w)/(B_g - B_{gi})$ versus $W_e/(B_g - B_{gi})$ plot, Figure 6.129 to Figure 6.131, are shown at late times for all shut-in durations. In order to estimate OGIP by applying $(G_p B_g + W_p B_w)/(B_g - B_{gi})$ versus $W_e/(B_g - B_{gi})$ plot, the historical data for almost up to the abandonment condition are needed.

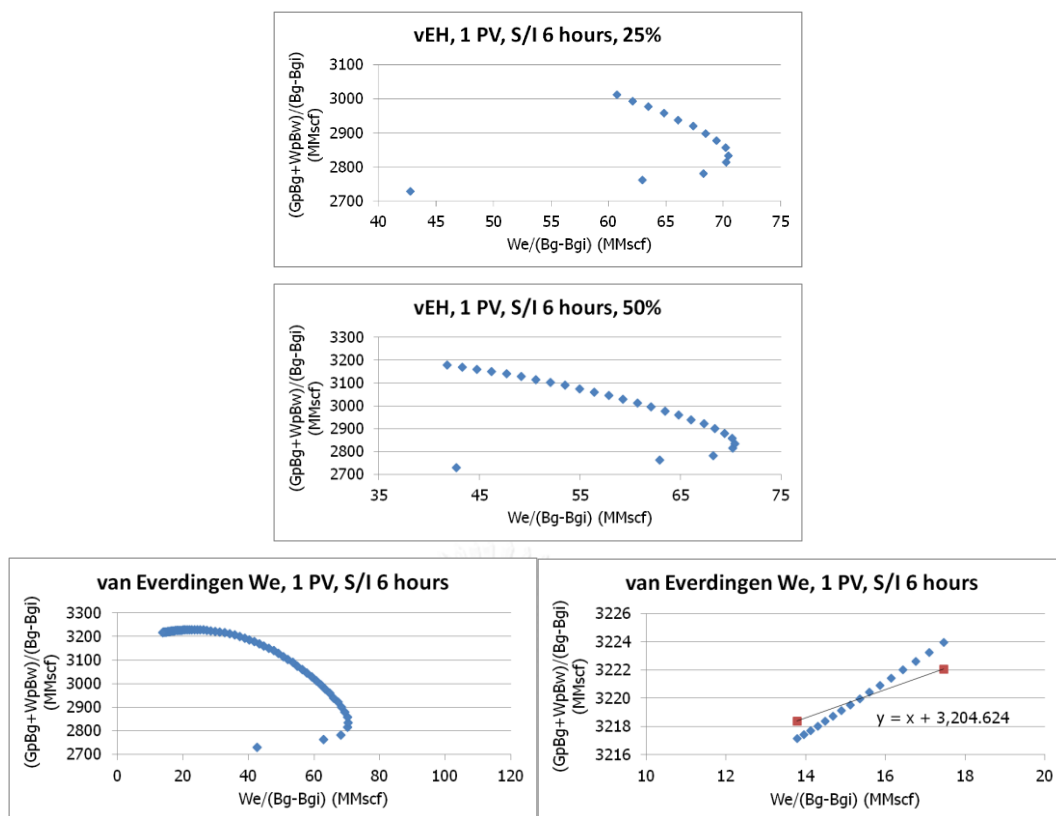


Figure 6.129 $(G_p B_g + W_p B_w) / (B_g - B_{gi})$ versus $W_e / (B_g - B_{gi})$ at 1-PV aquifer size and 6-hour shut-in duration for 50 mD reservoir, case 1-3

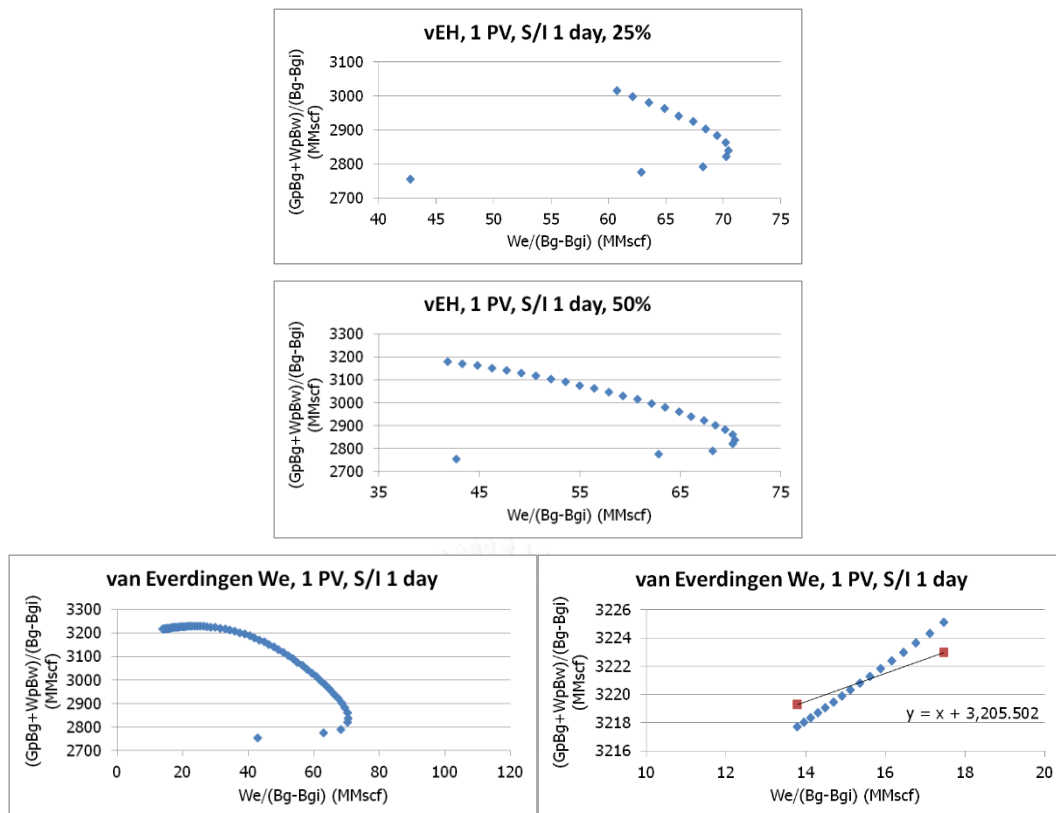


Figure 6.130 $(G_p B_g + W_p B_w) / (B_g - B_{gi})$ versus $W_e / (B_g - B_{gi})$ at 1-PV aquifer size and 1-day shut-in duration for 50 mD reservoir, case 4-6

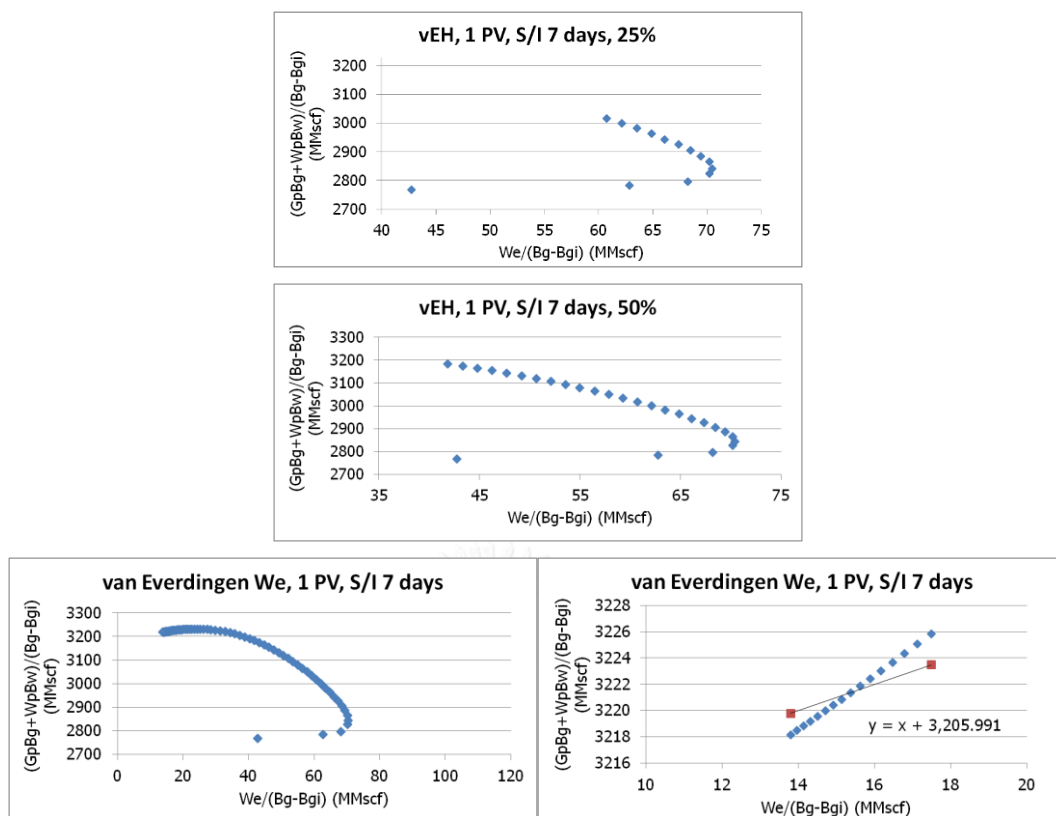


Figure 6.131 $(G_p B_g + W_p B_w)/(B_g - B_{gi})$ versus $W_e/(B_g - B_{gi})$ at 1-PV aquifer size and 7-day shut-in duration for 50 mD reservoir, case 7-9

Table 6.29 The result of OGIP estimation at 1-PV aquifer size for 50 mD water-drive dry-gas reservoir by $(G_p B_g + W_p B_w)/(B_g - B_{gi})$ versus $W_e/(B_g - B_{gi})$ plot for various amounts of historical data

Shut-in duration	Amount of historical data	Estimated OGIP (MMscf)	Error (%)	R-squared
6 hours	Up to 25% RF	Not applicable	Not applicable	Not applicable
	Up to 50% RF	Not applicable	Not applicable	Not applicable

Table 6.29 The result of OGIP estimation at 1-PV aquifer size for 50 mD water-drive dry-gas reservoir by $(G_p B_g + W_p B_w)/(B_g - B_{gi})$ versus $W_e/(B_g - B_{gi})$ plot for various amounts of historical data (continued)

Shut-in duration	Amount of historical data	Estimated OGIP (MMscf)	Error (%)	R-squared
6 hours	Up to abandonment	3204.624	-0.21%	0.7862
1 day	Up to 25% RF	Not applicable	Not applicable	Not applicable
	Up to 50% RF	Not applicable	Not applicable	Not applicable
	Up to abandonment	3205.502	-0.18%	0.7494
7 days	Up to 25% RF	Not applicable	Not applicable	Not applicable
	Up to 50% RF	Not applicable	Not applicable	Not applicable
	Up to abandonment	3205.991	-0.17%	0.7287

In reality, p/z versus G_p plot is more useful than $(G_p B_g + W_p B_w)/(B_g - B_{gi})$ versus $W_e/(B_g - B_{gi})$ plot for OGIP estimation for 1-PV aquifer size. The historical data up to 25% or 50% RF with p/z versus G_p plot can yield the accurate estimated OGIP values with the error around 2% to 3.2% as shown in Figure 6.109.

For 10-PV aquifer size, as shown in Figure 6.132 to Figure 6.134, the slopes of $(G_p B_g + W_p B_w)/(B_g - B_{gi})$ versus $W_e/(B_g - B_{gi})$ plots change from negative to be positive at 45% RF. Thus, the amount of historical data for OGIP estimation at 50% RF is too short, and the plots are not well fitted with a unit slope straight line.

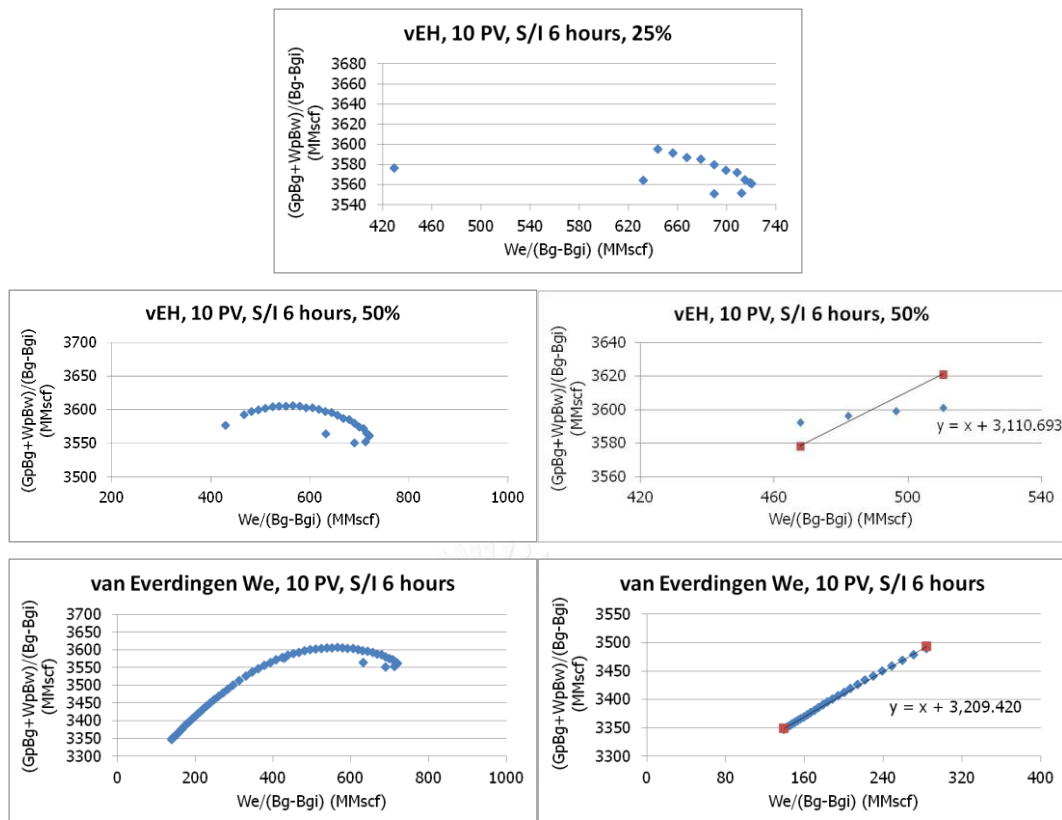


Figure 6.132 $(G_p B_g + W_p B_w) / (B_g - B_{gi})$ versus $W_e / (B_g - B_{gi})$ at 10-PV aquifer size and 6-hour shut-in duration for 50 mD reservoir, case 10-12

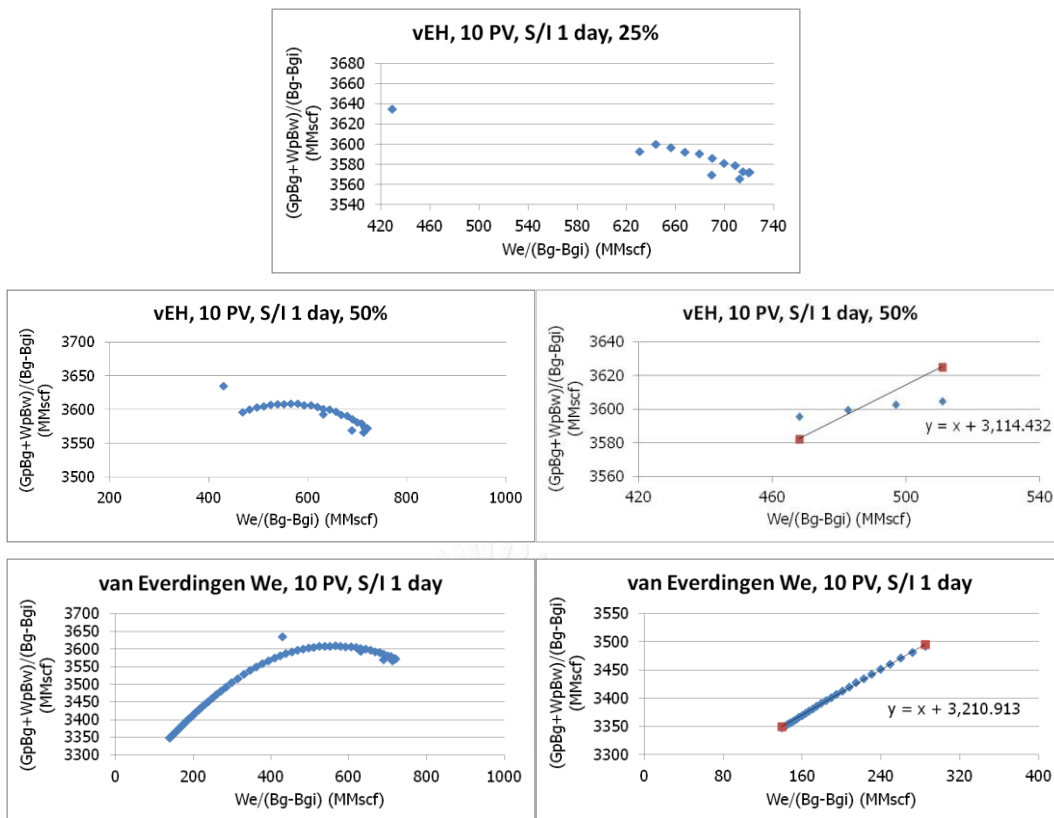


Figure 6.133 $(G_p B_g + W_p B_w) / (B_g - B_{gi})$ versus $W_e / (B_g - B_{gi})$ at 10-PV aquifer size and 1-day shut-in duration for 50 mD reservoir, case 13-15

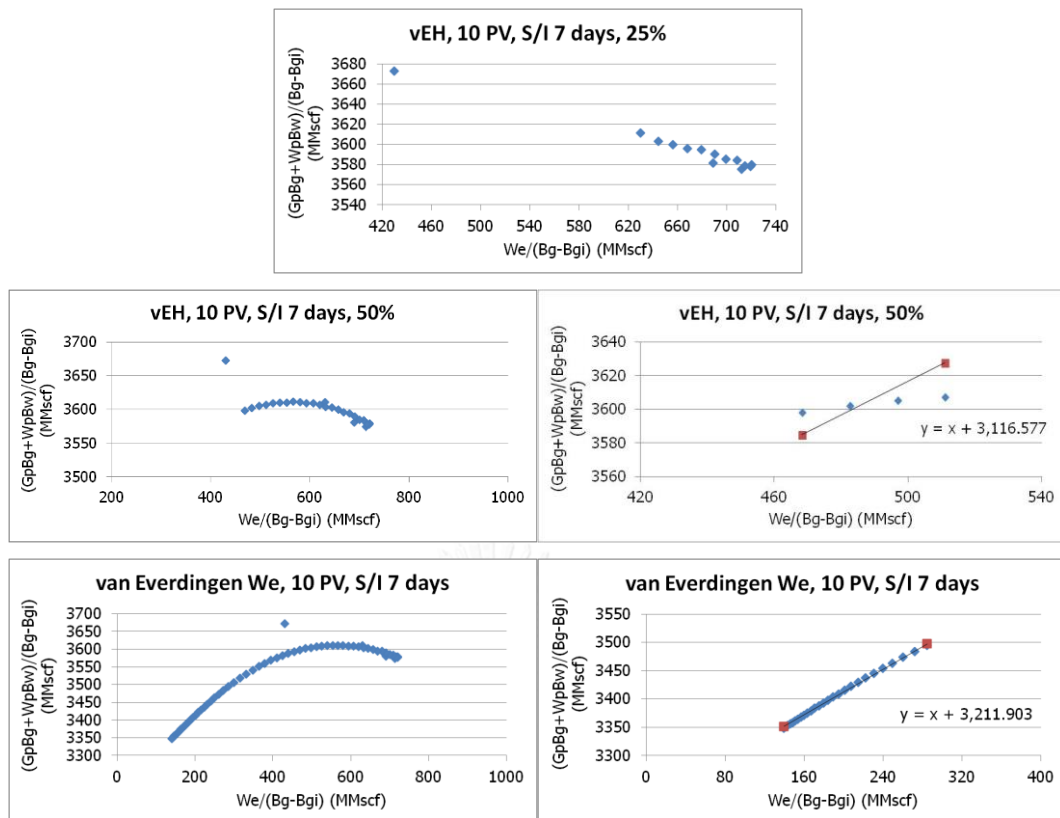


Figure 6.134 $(G_p B_g + W_p B_w) / (B_g - B_{gi})$ versus $W_e / (B_g - B_{gi})$ at 10-PV aquifer size and 7-day shut-in duration for 50 mD reservoir, case 16-18

The slopes of $(G_p B_g + W_p B_w) / (B_g - B_{gi})$ versus $W_e / (B_g - B_{gi})$ plots in 10-PV aquifer size cases approach the value of one as %RF increases. A larger amount of historical data provides more accuracy in OGIP estimation for all shut-in durations.

If the historical data are available only up to 25% RF, the OGIP value cannot be estimated by $(G_p B_g + W_p B_w) / (B_g - B_{gi})$ versus $W_e / (B_g - B_{gi})$ plot for all shut-in durations but can be estimated by p/z versus G_p plot with error around 26% as shown in Figure 6.109.

When the historical data are available for at least 50% RF, the errors of estimated OGIPs from $(G_p B_g + W_p B_w) / (B_g - B_{gi})$ versus $W_e / (B_g - B_{gi})$ plot, lower than -3.13%, are always less than the ones from p/z versus G_p plot, more than 6.31%. The R-squared values of these cases are negative. That means the unit slope straight lines fit the data worse than a horizontal line.

Table 6.30 The result of OGIP estimation at 10-PV aquifer size for 50 mD water-drive dry-gas reservoir by $(G_p B_g + W_p B_w)/(B_g - B_{gi})$ versus $W_e/(B_g - B_{gi})$ plot for various amounts of historical data

Shut-in duration	Amount of historical data	Estimated OGIP (MMscf)	Error (%)	R-squared
6 hours	Up to 25% RF	Not applicable	Not applicable	Not applicable
	Up to 50% RF	3110.693	-3.13%	-13.9665
	Up to abandonment	3209.42	-0.06%	0.9984
1 day	Up to 25% RF	Not applicable	Not applicable	Not applicable
	Up to 50% RF	3114.432	-3.02%	-13.8579
	Up to abandonment	3210.913	-0.01%	0.9984
7 days	Up to 25% RF	Not applicable	Not applicable	Not applicable
	Up to 50% RF	3116.577	-2.95%	-13.7409
	Up to abandonment	3211.903	0.02%	0.9981

For 30-PV aquifer size, the slopes of $(G_p B_g + W_p B_w)/(B_g - B_{gi})$ versus $W_e/(B_g - B_{gi})$ plots become positive since the early time as shown in Figure 6.135 to Figure 6.137. The OGIP values can be estimated by $(G_p B_g + W_p B_w)/(B_g - B_{gi})$ versus $W_e/(B_g - B_{gi})$ plot even the amount of historical data are available up to only 25% RF in all shut-in durations.

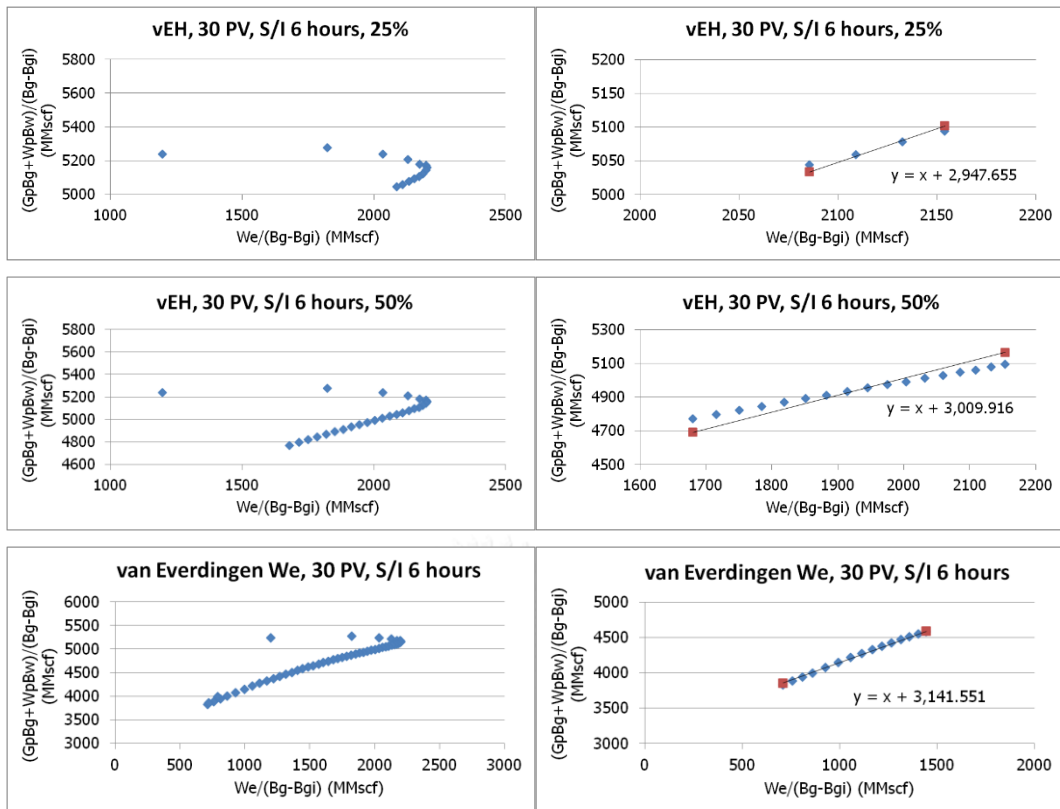


Figure 6.135 $(G_p B_g + W_p B_w) / (B_g - B_{gi})$ versus $W_e / (B_g - B_{gi})$ at 30-PV aquifer size and 6-hour shut-in duration for 50 mD reservoir, case 19-21

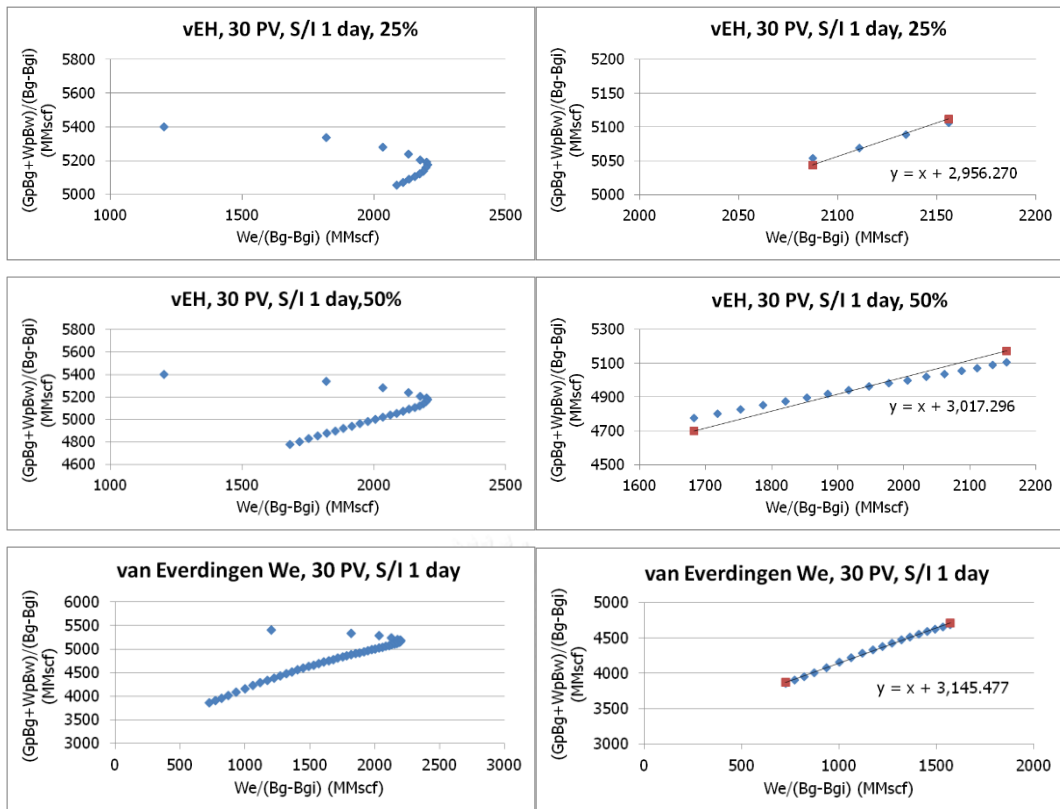


Figure 6.136 $(G_p B_g + W_p B_w) / (B_g - B_{gi})$ versus $W_e / (B_g - B_{gi})$ at 30-PV aquifer size and 1-day shut-in duration for 50 mD reservoir, case 22-24

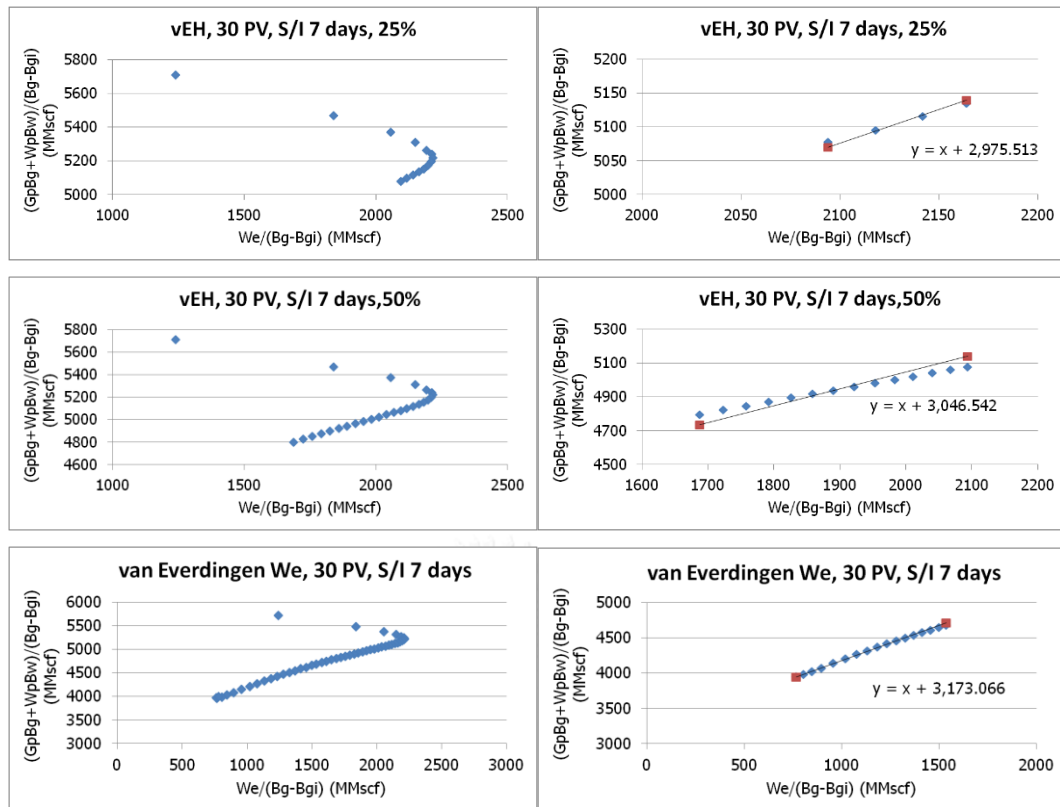


Figure 6.137 $(G_p B_g + W_p B_w) / (B_g - B_{gi})$ versus $W_e / (B_g - B_{gi})$ at 30-PV aquifer size and 7-day shut-in duration for 50 mD reservoir, case 25-27

The slopes of $(G_p B_g + W_p B_w) / (B_g - B_{gi})$ versus $W_e / (B_g - B_{gi})$ plot approach the value of one when %RF increases. The plots are better fitted with a unit slope straight line and yield more accurate estimated OGIP values when more amount of historical data are available as tabulated in Table 6.31.

Table 6.31 The result of OGIP estimation at 30-PV aquifer size for 50 mD water-drive dry-gas reservoir by $(G_p B_g + W_p B_w)/(B_g - B_{gi})$ versus $W_e/(B_g - B_{gi})$ plot for various amounts of historical data

Shut-in duration	Amount of historical data	Estimated OGIP (MMscf)	Error (%)	R-squared
6 hours	Up to 25% RF	2947.655	-8.21%	0.8687
	Up to 50% RF	3009.916	-6.27%	0.7656
	Up to abandonment	3141.551	-2.17%	0.9973
1 day	Up to 25% RF	2956.27	-7.94%	0.8992
	Up to 50% RF	3017.296	-6.04%	0.7852
	Up to abandonment	3145.477	-2.05%	0.9976
7 days	Up to 25% RF	2975.513	-7.34%	0.9473
	Up to 50% RF	3046.542	-5.13%	0.7952
	Up to abandonment	3173.066	-1.19%	0.9970

The errors of estimated OGIPs from $(G_p B_g + W_p B_w)/(B_g - B_{gi})$ versus $W_e/(B_g - B_{gi})$ plot (lower than -8.21%) are less than the ones from p/z versus G_p plot, more than 31.86%, if the historical data is available at least 25% RF as shown in Table 6.25.

For 70-PV aquifer size, $(G_p B_g + W_p B_w)/(B_g - B_{gi})$ versus $W_e/(B_g - B_{gi})$ plot cannot be used for OGIP estimation if the historical data is available only 25% RF for all shut-in durations as shown in Figure 6.138 to Figure 6.140. At 25% RF, $(G_p B_g + W_p B_w)/(B_g - B_{gi})$ versus $W_e/(B_g - B_{gi})$ plot just changes from the early positive slope trend into the main positive slope trend. There are only a few data points in the main positive slope trend, and the slope of these data points is not stable yet.

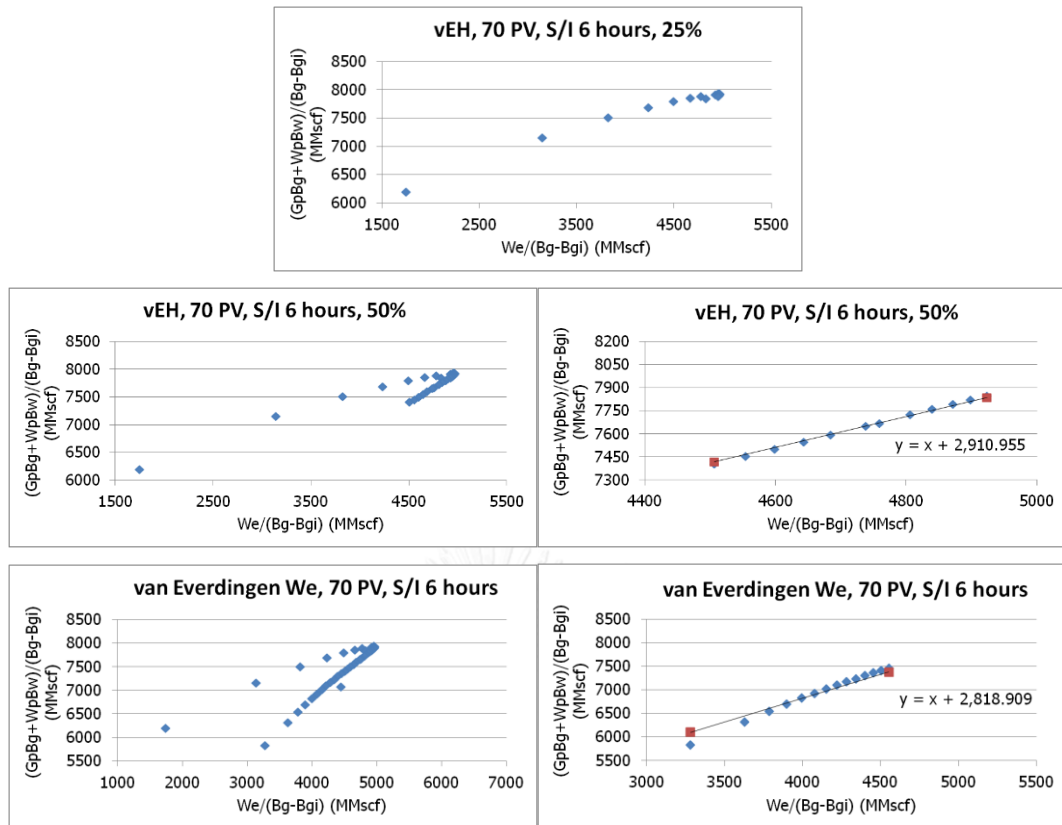


Figure 6.138 $(G_p B_g + W_p B_w) / (B_g - B_{gi})$ versus $W_e / (B_g - B_{gi})$ at 70-PV aquifer size and 6-hour shut-in duration for 50 mD reservoir, case 28-30

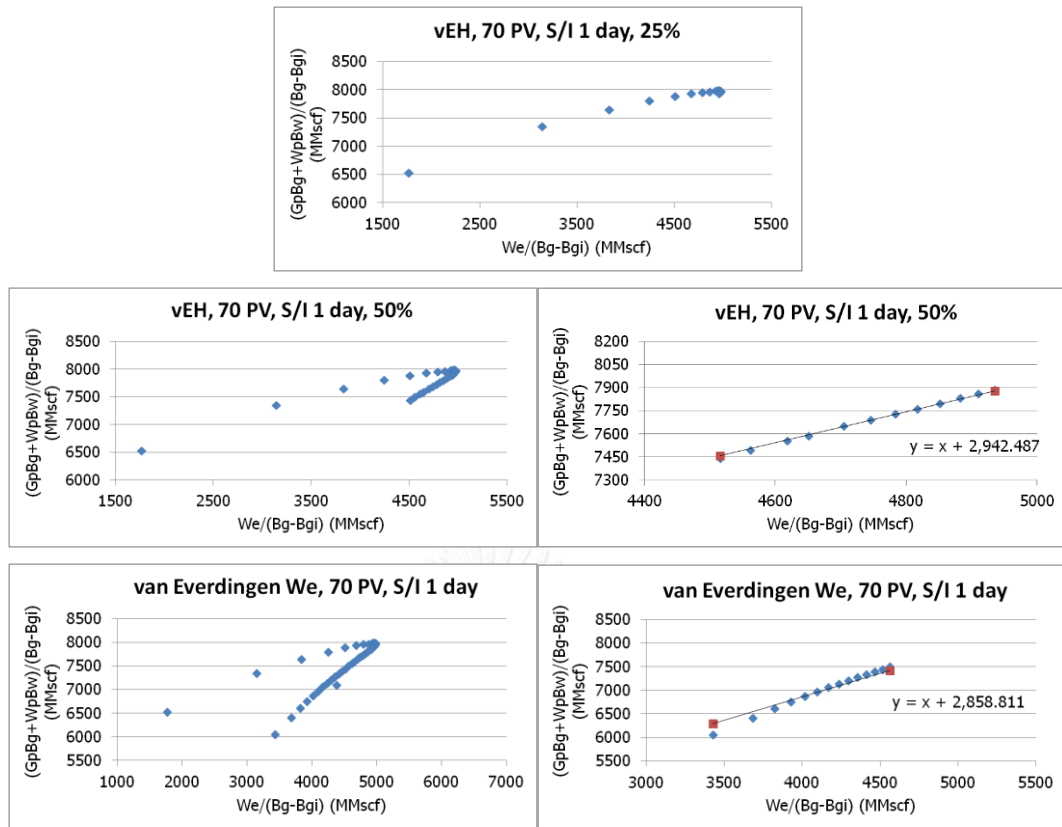


Figure 6.139 $(G_p B_g + W_p B_w) / (B_g - B_{gi})$ versus $W_e / (B_g - B_{gi})$ at 70-PV aquifer size and 1-day shut-in duration for 50 mD reservoir, case 31-33

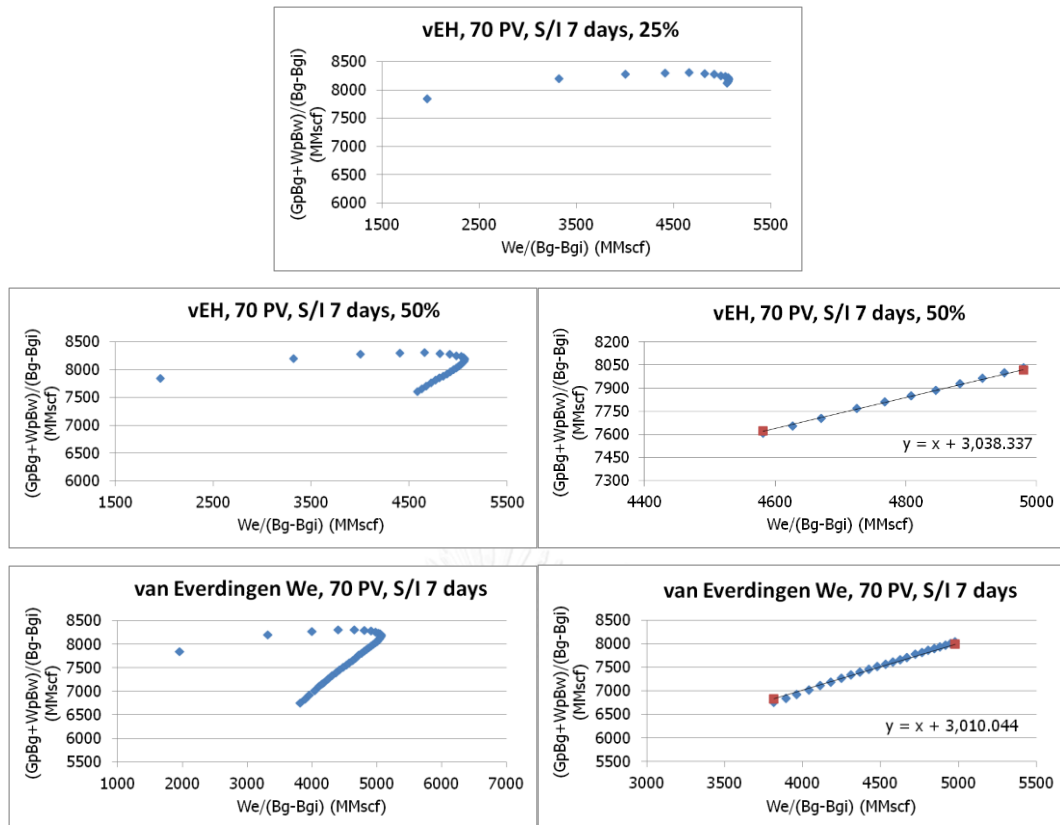


Figure 6.140 $(G_p B_g + W_p B_w)/(B_g - B_{gi})$ versus $W_e/(B_g - B_{gi})$ at 70-PV aquifer size and 7-day shut-in duration for 50 mD reservoir, case 34-36

When the historical data are available up to 50% RF, the OGIP value can be estimated by $(G_p B_g + W_p B_w)/(B_g - B_{gi})$ versus $W_e/(B_g - B_{gi})$ plot since there are enough data points in the main positive slope trend. The estimated OGIPs at 50% RF, -9.35% to -5.39% error, are more accurate than the ones at the abandonment condition, -12.22% to -6.27% error, for all shut-in durations as shown in Table 6.32, because the calculated W_e from van Everdingen & Hurst water influx model is higher than the simulated W_e in the late time as shown in Figure 6.48. The smaller value of W_e , the larger value of estimated OGIP. Since the errors in OGIP estimation in 70-PV aquifer size cases are all negative, the higher estimated OGIP value is more accurate than the lower one.

Table 6.32 The result of OGIP estimation at 70-PV aquifer size for 50 mD water-drive dry-gas reservoir by $(G_p B_g + W_p B_w)/(B_g - B_{gi})$ versus $W_e/(B_g - B_{gi})$ plot for various amounts of historical data

Shut-in duration	Amount of historical data	Estimated OGIP (MMscf)	Error (%)	R-squared
6 hours	Up to 25% RF	Not applicable	Not applicable	Not applicable
	Up to 50% RF	2910.955	-9.35%	0.9952
	Up to abandonment	2818.909	-12.22%	0.9502
1 day	Up to 25% RF	Not applicable	Not applicable	Not applicable
	Up to 50% RF	2942.487	-8.37%	0.9971
	Up to abandonment	2858.811	-10.98%	0.9549
7 days	Up to 25% RF	Not applicable	Not applicable	Not applicable
	Up to 50% RF	3038.337	-5.39%	0.9964
	Up to abandonment	3010.044	-6.27%	0.9917

For 100-PV aquifer size, the behavior of the $(G_p B_g + W_p B_w)/(B_g - B_{gi})$ versus $W_e/(B_g - B_{gi})$ plots as shown in Figure 6.141 to Figure 6.143, are similar with those for 70-PV aquifer size cases. The amount of historical data up to 50% RF is needed in order to estimate the OGIP value by $(G_p B_g + W_p B_w)/(B_g - B_{gi})$ versus $W_e/(B_g - B_{gi})$ plot.

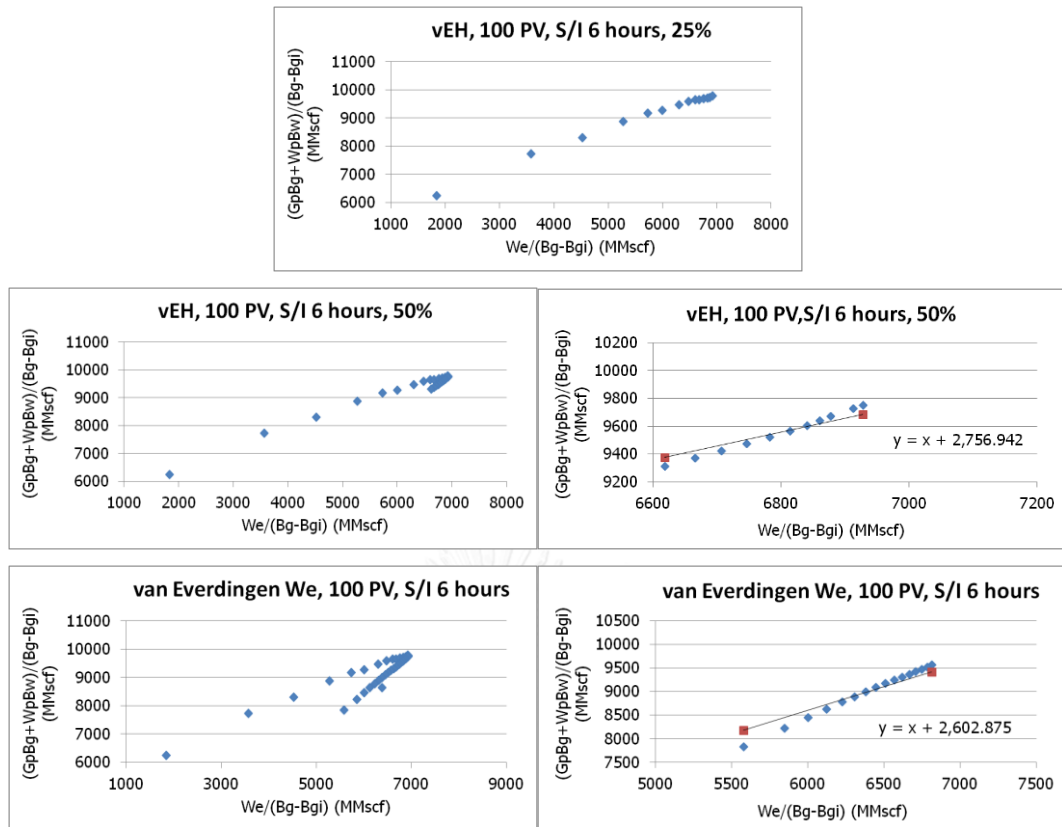


Figure 6.141 $(G_p B_g + W_p B_w)/(B_g - B_{gi})$ versus $We/(Bg-B_{gi})$ at 100-PV aquifer size and 6-hour shut-in duration for 50 mD reservoir, case 37-39

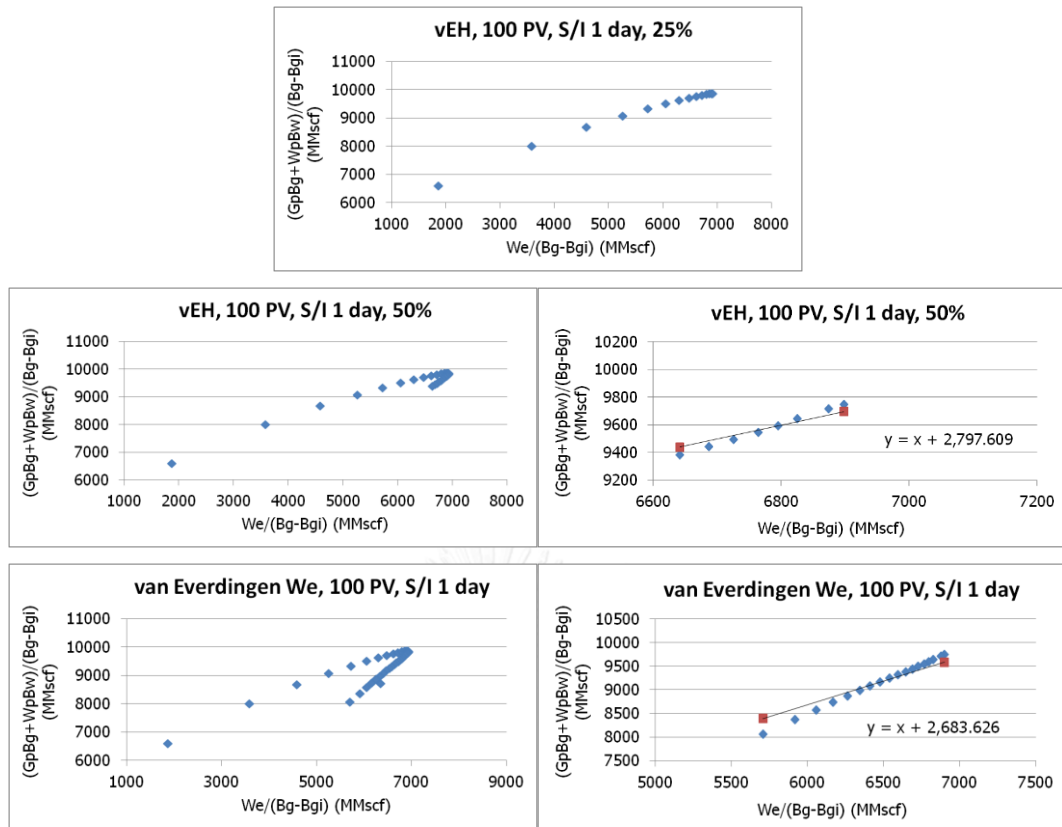


Figure 6.142 $(G_p B_g + W_p B_w) / (B_g - B_{gi})$ versus $W_e / (B_g - B_{gi})$ at 100-PV aquifer size and 1-day shut-in duration for 50 mD reservoir, case 40-42

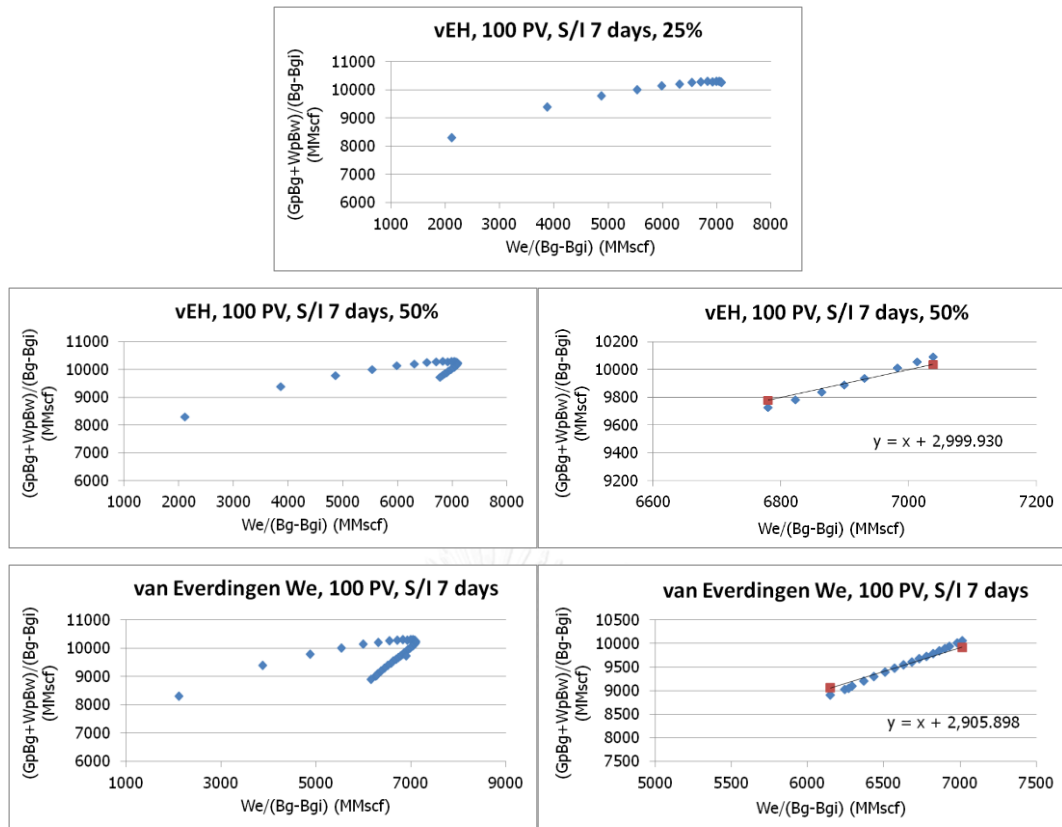


Figure 6.143 $(G_p B_g + W_p B_w) / (B_g - B_{gi})$ versus $W_e / (B_g - B_{gi})$ at 100-PV aquifer size and 7-day shut-in duration for 50 mD reservoir, case 43-45

The estimated OGIPs at 50% RF, -14.15% to -6.58% error, are more accurate than the ones at the abandonment condition, -18.95% to -9.51% error, for all shut-in durations as shown in Table 6.33 due to the same reason as mentioned in 70-PV aquifer size cases.

Table 6.33 The result of OGIP estimation at 100-PV aquifer size for 50 mD water-drive dry-gas reservoir by $(G_p B_g + W_p B_w)/(B_g - B_{gi})$ versus $W_e/(B_g - B_{gi})$ plot for various amounts of historical data

Shut-in duration	Amount of historical data	Estimated OGIP (MMscf)	Error (%)	R-squared
6 hours	Up to 25% RF	Not applicable	Not applicable	Not applicable
	Up to 50% RF	2756.942	-14.15%	0.9083
	Up to abandonment	2602.875	-18.95%	0.9202
1 day	Up to 25% RF	Not applicable	Not applicable	Not applicable
	Up to 50% RF	2797.609	-12.88%	0.9041
	Up to abandonment	2683.626	-16.43%	0.9190
7 days	Up to 25% RF	Not applicable	Not applicable	Not applicable
	Up to 50% RF	2999.93	-6.58%	0.9121
	Up to abandonment	2905.898	-9.51%	0.9398

For small to moderate aquifer size cases (1 PV, 10 PV and 30 PV), more historical data provide more accurate estimated OGIP values as shown in Figure 6.144. For 10-PV and 30-PV aquifer size cases, the later data points can represent the aquifer support behavior better because the reservoir-aquifer system have more time to reach pseudo-steady state as the slope of $(G_p B_g + W_p B_w)/(B_g - B_{gi})$ versus $W_e/(B_g - B_{gi})$ plot approach the value of one at late time. The larger the aquifer size, the earlier the aquifer support. Then, less amount of historical data is required for OGIP estimation by $(G_p B_g + W_p B_w)/(B_g - B_{gi})$ versus $W_e/(B_g - B_{gi})$ plot. Historical data up to almost the abandonment condition are

required in 1-PV aquifer size while the 10-PV and 30-PV aquifer size require only up to 50% RF and 25% RF, respectively.

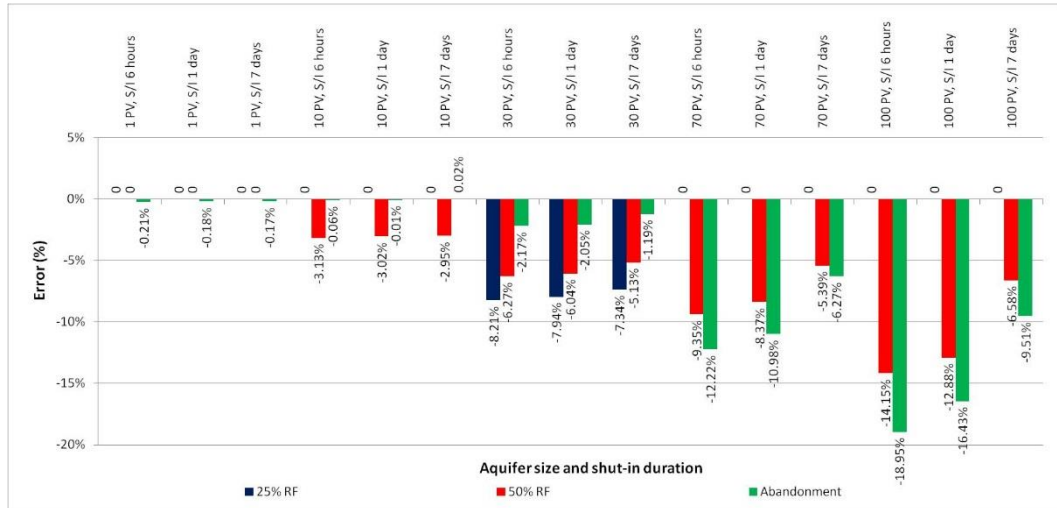


Figure 6.144 Error of estimated OGIP for 50 mD water-drive dry-gas reservoir by $(G_p B_g + W_p B_w)/(B_g - B_{gi})$ versus $W_e/(B_g - B_{gi})$ plot for various amounts of historical data

For large aquifer size cases (70 PV and 100 PV), $(G_p B_g + W_p B_w)/(B_g - B_{gi})$ versus $W_e/(B_g - B_{gi})$ plot cannot be applied for OGIP estimation if the historical data are available up to only 25% RF because the reservoir-aquifer system has not reached pseudo-steady state yet. The $(G_p B_g + W_p B_w)/(B_g - B_{gi})$ versus $W_e/(B_g - B_{gi})$ plots are changing from the early trend into the final trend. The estimated OGIPs from the historical data up to 50% RF are more accurate than the ones from the historical data up to the abandonment condition because of the overestimated W_e in late time as shown in Figure 6.48 and Figure 6.50.

The shut-in duration does not affect the minimum amount of historical data required for OGIP estimation. The effect of shut-in duration on the accuracy of OGIP estimation is the same as those discussed in Section 6.6.

Table 6.34 The result of OGIP estimation for 50 mD water-drive dry-gas reservoir by $(G_p B_g + W_p B_w) / (B_g - B_{gi})$ versus $W_e / (B_g - B_{gi})$ plot for various amounts of historical data

Case	Aquifer size (PV)	Shut-in duration	Amount of historical data	Estimated OGIP (MMscf)	Error (%)	R-squared
1	1	6 hours	25% RF	Not applicable	Not applicable	Not applicable
2			50% RF	Not applicable	Not applicable	Not applicable
3			Abandonment	3204.624	-0.21%	0.7862
4		1 day	25% RF	Not applicable	Not applicable	Not applicable
5			50% RF	Not applicable	Not applicable	Not applicable
6			Abandonment	3205.502	-0.18%	0.7494
7		7 days	25% RF	Not applicable	Not applicable	Not applicable
8			50% RF	Not applicable	Not applicable	Not applicable
9			Abandonment	3205.991	-0.17%	0.7287
10	10	6 hours	25% RF	Not applicable	Not applicable	Not applicable
11			50% RF	3110.693	-3.13%	-13.9665
12			Abandonment	3209.42	-0.06%	0.9984
13		1 day	25% RF	Not applicable	Not applicable	Not applicable

Table 6.34 The result of OGIP estimation for 50 mD water-drive dry-gas reservoir by $(G_p B_g + W_p B_w)/(B_g - B_{gi})$ versus $W_e/(B_g - B_{gi})$ plot for various amounts of historical data

(continued)

Case	Aquifer size (PV)	Shut-in duration	Amount of historical data	Estimated OGIP (MMscf)	Error (%)	R-squared
14	10	1 day	50% RF	3114.432	-3.02%	-13.8579
15			Abandonment	3210.913	-0.01%	0.9984
16		7 days	25% RF	Not applicable	Not applicable	Not applicable
17			50% RF	3116.577	-2.95%	-13.7409
18			Abandonment	3211.903	0.02%	0.9981
19		30	6 hours	25% RF	2947.655	-8.21%
20	50% RF			3009.916	-6.27%	0.7656
21	Abandonment			3141.551	-2.17%	0.9973
22	1 day		25% RF	2956.27	-7.94%	0.8992
23			50% RF	3017.296	-6.04%	0.7852
24			Abandonment	3145.477	-2.05%	0.9976
25	7 days		25% RF	2975.513	-7.34%	0.9473
26			50% RF	3046.542	-5.13%	0.7952
27			Abandonment	3173.066	-1.19%	0.9970
28	70	6 hours	25% RF	Not applicable	Not applicable	Not applicable

Table 6.34 The result of OGIP estimation for 50 mD water-drive dry-gas reservoir by $(G_p B_g + W_p B_w)/(B_g - B_{gi})$ versus $W_e/(B_g - B_{gi})$ plot for various amounts of historical data

(continued)

Case	Aquifer size (PV)	Shut-in duration	Amount of historical data	Estimated OGIP (MMscf)	Error (%)	R-squared	
29	70	6 hours	50% RF	2910.955	-9.35%	0.9952	
30			Abandonment	2818.909	-12.22%	0.9502	
31		1 day	25% RF	Not applicable	Not applicable	Not applicable	
32			50% RF	2942.487	-8.37%	0.9971	
33			Abandonment	2858.811	-10.98%	0.9549	
34		7 days	25% RF	Not applicable	Not applicable	Not applicable	
35			50% RF	3038.337	-5.39%	0.9964	
36			Abandonment	3010.044	-6.27%	0.9917	
37		100	6 hours	25% RF	Not applicable	Not applicable	Not applicable
38				50% RF	2756.942	-14.15%	0.9083
39	Abandonment			2602.875	-18.95%	0.9202	
40	1 day		25% RF	Not applicable	Not applicable	Not applicable	

Table 6.34 The result of OGIP estimation for 50 mD water-drive dry-gas reservoir by $(G_p B_g + W_p B_w)/(B_g - B_{gi})$ versus $W_e/(B_g - B_{gi})$ plot for various amounts of historical data

(continued)

Case	Aquifer size (PV)	Shut-in duration	Amount of historical data	Estimated OGIP (MMscf)	Error (%)	R-squared
41	100	1 day	50% RF	2797.609	-12.88%	0.9041
42			Abandonment	2683.626	-16.43%	0.9190
43		7 days	25% RF	Not applicable	Not applicable	Not applicable
44			50% RF	2999.93	-6.58%	0.9121
45			Abandonment	2905.898	-9.51%	0.9398

The accuracy of OGIP estimation by $(G_p B_g + W_p B_w)/(B_g - B_{gi})$ versus $W_e/(B_g - B_{gi})$ plot for 50 mD reservoir are summarized in Table 6.35. The criteria for accuracy level is same as the one in Section 6.8.1.

Table 6.35 The accuracy of OGIP estimation for 50 mD water-drive dry-gas reservoir by $(G_p B_g + W_p B_w)/(B_g - B_{gi})$ versus $W_e/(B_g - B_{gi})$ plot for various amounts of historical data

Aquifer size (PV)	Amount of historical data	Shut-in duration	Accuracy
1	Up to 25% RF and 50% RF	6 hours, 1 day and 7 days	Not applicable
	Up to Abandonment		Accurate
10	Up to 25% RF		Not applicable

Table 6.35 The accuracy of OGIP estimation for 50 mD water-drive dry-gas reservoir by $(G_p B_g + W_p B_w) / (B_g - B_{gi})$ versus $W_e / (B_g - B_{gi})$ plot for various amounts of historical data

(continued)

Aquifer size (PV)	Amount of historical data	Shut-in duration	Accuracy
10	Up 50% RF and Abandonment	6 hours, 1 day and 7 days	Accurate
30	Up to 25% RF and 50% RF		Acceptable
	Up to Abandonment		Accurate
70	Up to 25% RF		Not applicable
	Up to 50% RF	Acceptable	
	Up to Abandonment	6 hours and 1 day	Not acceptable
		7 days	Acceptable
100	Up to 25% RF	6 hours, 1 day and 7 days	Not applicable
	Up to 50% RF	6 hours and 1 day	Not acceptable
		7 days	Acceptable
		Up to Abandonment	6 hours and 1 day
	7 days		Acceptable

Accurate: error < 5%, Acceptable: error < 10%, Not acceptable: error ≥ 10%

6.8.4 $(G_p B_g + W_p B_w)/(B_g - B_{gi})$ versus $W_e/(B_g - B_{gi})$ Plot for 500 mD Water-drive Dry-gas Reservoir

Figure 6.145 to Figure 6.159 represent the $(G_p B_g + W_p B_w)/(B_g - B_{gi})$ versus $W_e/(B_g - B_{gi})$ plots with the estimated OGIP value for 500 mD water-drive dry-gas reservoir at different aquifer sizes, shut-in durations and amounts of historical data.

For 1-PV aquifer size, from Figure 6.145 to Figure 6.147, $(G_p B_g + W_p B_w)/(B_g - B_{gi})$ versus $W_e/(B_g - B_{gi})$ plots start to have positive slope trend at late times for all shut-in durations. The historical data up to the abandonment condition are required for OGIP estimation by $(G_p B_g + W_p B_w)/(B_g - B_{gi})$ versus $W_e/(B_g - B_{gi})$ plot.

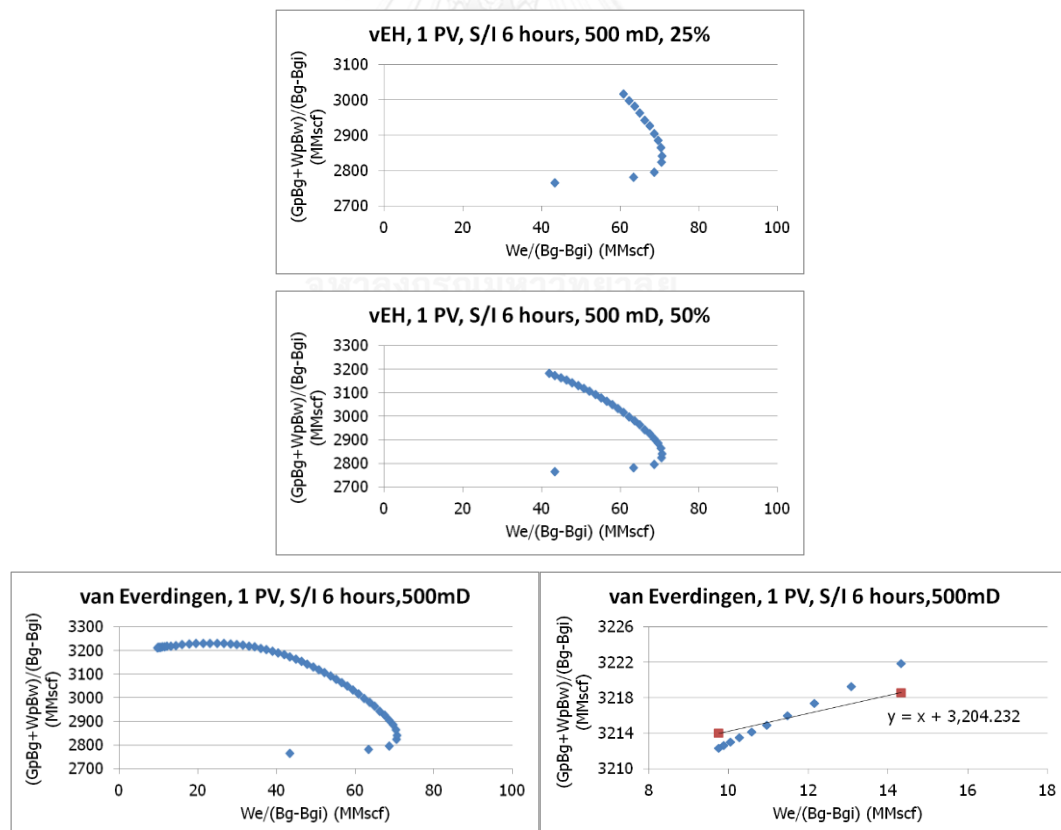


Figure 6.145 $(G_p B_g + W_p B_w)/(B_g - B_{gi})$ versus $W_e/(B_g - B_{gi})$ at 1-PV aquifer size and 6-hour shut-in duration for 500 mD reservoir, case 1-3

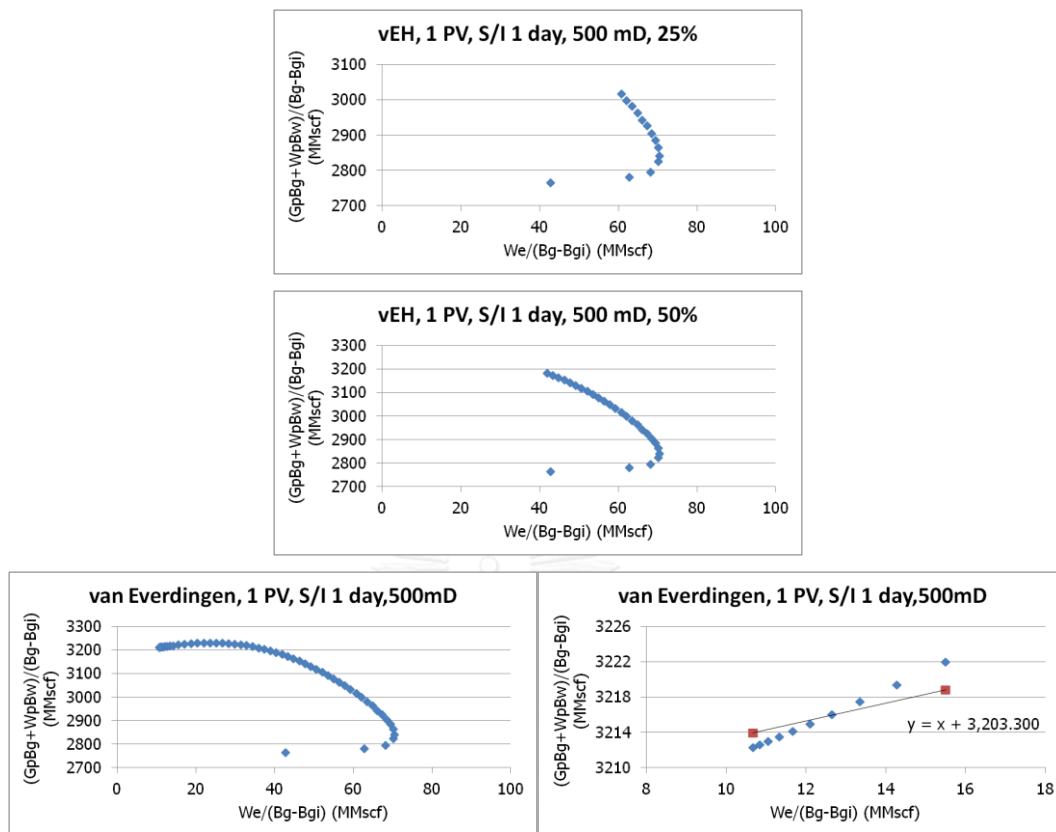


Figure 6.146 $(G_p B_g + W_p B_w) / (B_g - B_{gi})$ versus $W_e / (B_g - B_{gi})$ at 1-PV aquifer size and 1-day shut-in duration for 500 mD reservoir, case 4-6

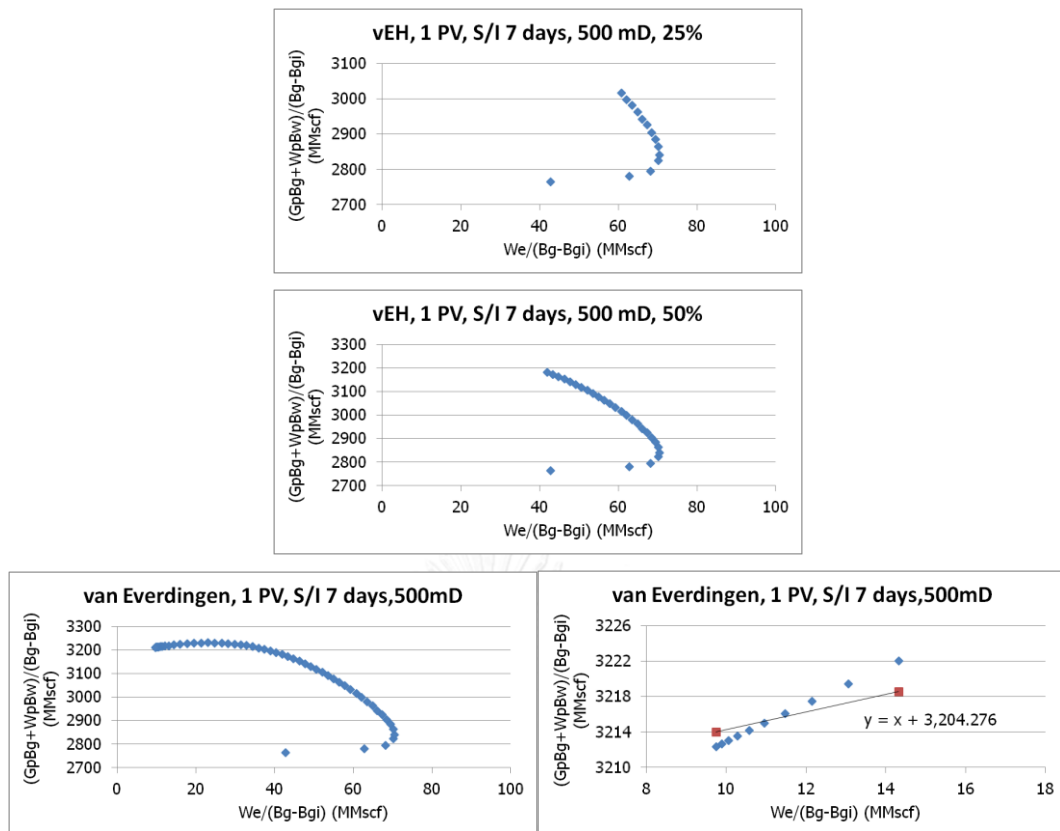


Figure 6.147 $(G_p B_g + W_p B_w) / (B_g - B_{gi})$ versus $W_e / (B_g - B_{gi})$ at 1-PV aquifer size and 7-day shut-in duration for 500 mD reservoir, case 7-9

The p/z versus G_p plot is more practical for OGIP estimation in 1-PV aquifer size cases than $(G_p B_g + W_p B_w) / (B_g - B_{gi})$ versus $W_e / (B_g - B_{gi})$ plot because these two methods provide the accurate estimated OGIPs if the historical data are available up to the abandonment condition but p/z versus G_p plots also provide the estimated OGIPs with error less than 3.19% when the historical data are available for at least 25% RF while $(G_p B_g + W_p B_w) / (B_g - B_{gi})$ versus $W_e / (B_g - B_{gi})$ plots cannot.

Table 6.36 The result of OGIP estimation at 1-PV aquifer size for 500 mD water-drive dry-gas reservoir by $(G_p B_g + W_p B_w)/(B_g - B_{gi})$ versus $W_e/(B_g - B_{gi})$ plot for various amounts of historical data

Shut-in duration	Amount of historical data	Estimated OGIP (MMscf)	Error (%)	R-squared
6 hours	Up to 25% RF	Not applicable	Not applicable	Not applicable
	Up to 50% RF	Not applicable	Not applicable	Not applicable
	Up to abandonment	3204.232	-0.22%	0.7300
1 day	Up to 25% RF	Not applicable	Not applicable	Not applicable
	Up to 50% RF	Not applicable	Not applicable	Not applicable
	Up to abandonment	3203.3	-0.25%	0.7495
7 days	Up to 25% RF	Not applicable	Not applicable	Not applicable
	Up to 50% RF	Not applicable	Not applicable	Not applicable
	Up to abandonment	3204.276	-0.22%	0.7206

For 10-PV aquifer size, the slopes of $(G_p B_g + W_p B_w)/(B_g - B_{gi})$ versus $W_e/(B_g - B_{gi})$ plots change from negative to be positive at 40% RF as shown in Figure 6.148 to Figure 6.150. At 50% RF, $(G_p B_g + W_p B_w)/(B_g - B_{gi})$ versus $W_e/(B_g - B_{gi})$ plot can be used for OGIP estimation but there is not many data points for curve fitting and the plots are not well fitted with a unit slope straight line.

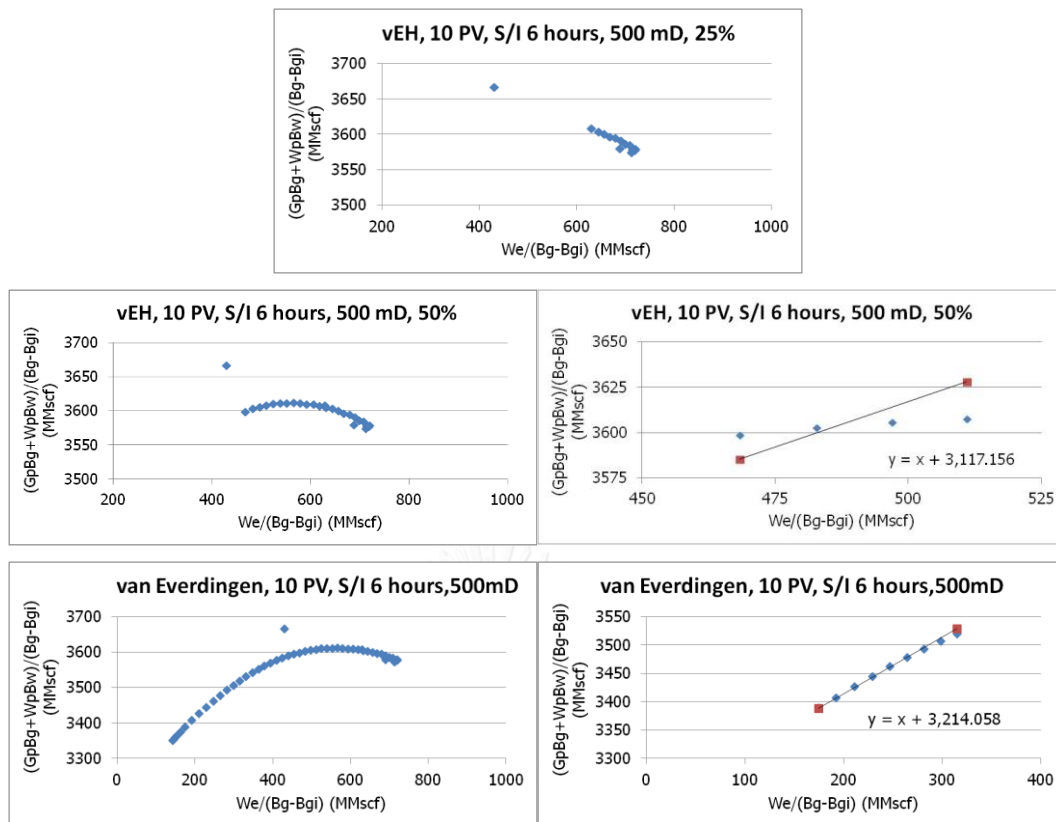


Figure 6.148 $(G_p B_g + W_p B_w) / (B_g - B_{gi})$ versus $W_e / (B_g - B_{gi})$ at 10-PV aquifer size and 6-hour shut-in duration for 500 mD reservoir, case 10-12

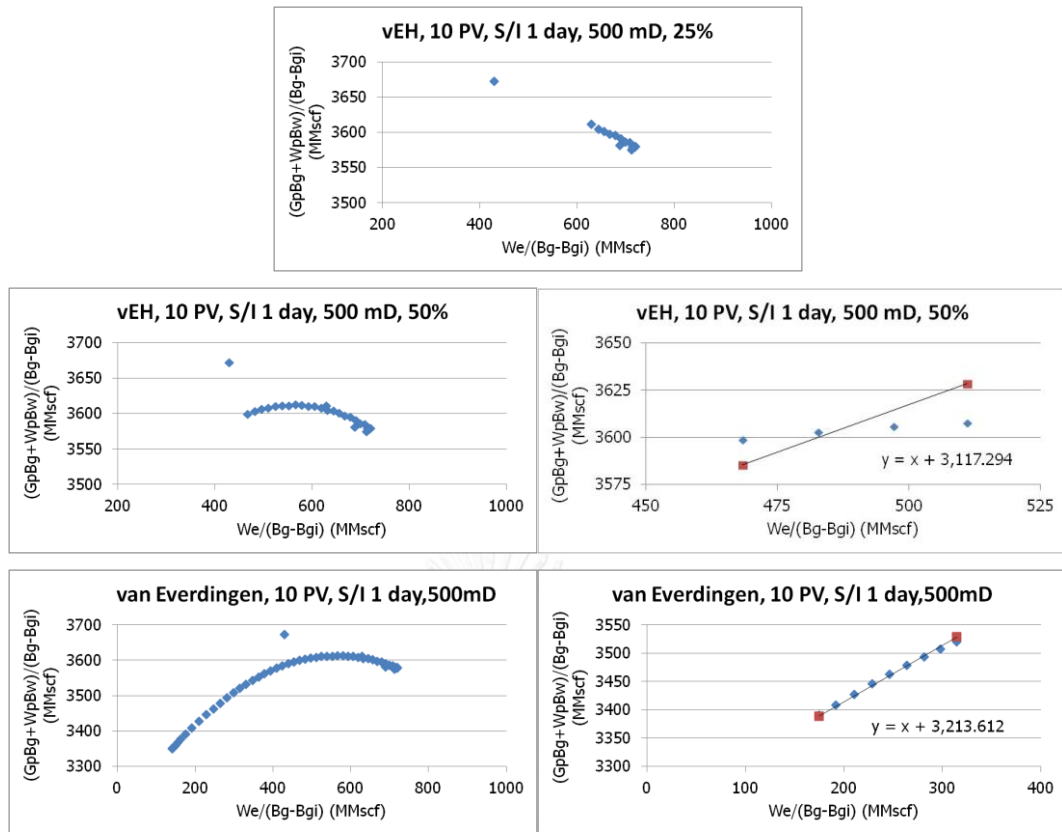


Figure 6.149 $(G_p B_g + W_p B_w) / (B_g - B_{gi})$ versus $W_e / (B_g - B_{gi})$ at 10-PV aquifer size and 1-day shut-in duration for 500 mD reservoir, case 13-15

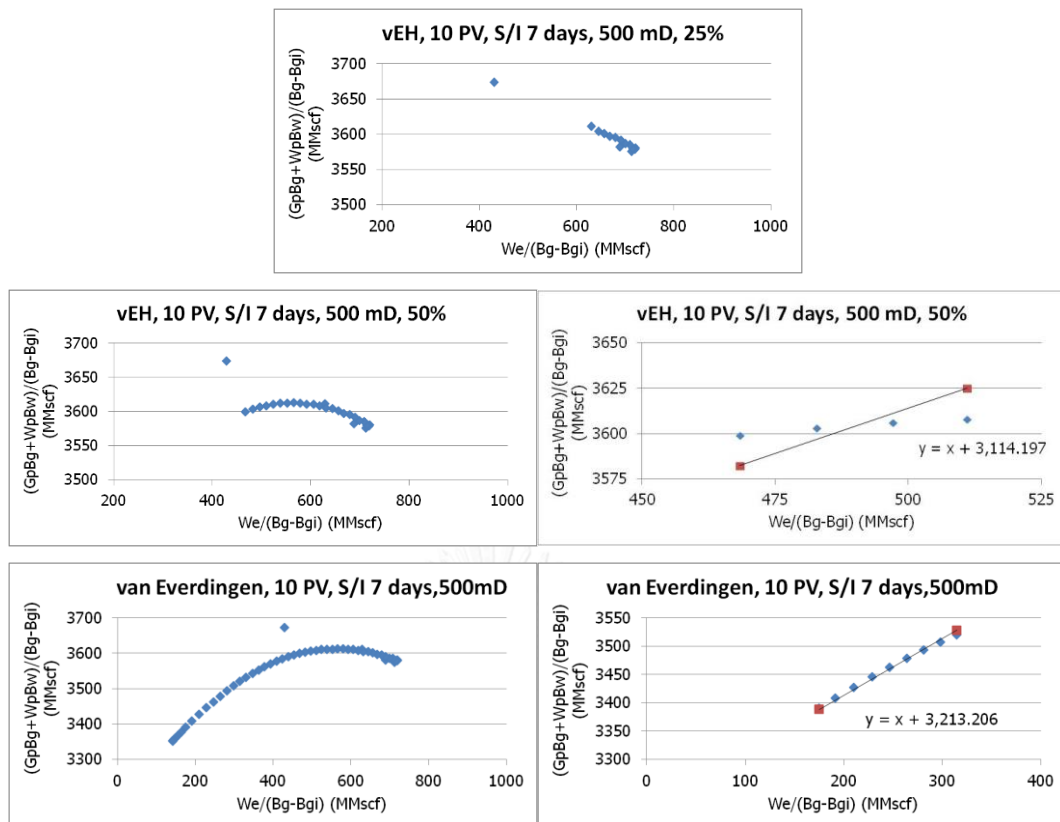


Figure 6.150 $(G_p B_g + W_p B_w)/(B_g - B_{gi})$ versus $W_e/(B_g - B_{gi})$ at 10-PV aquifer size and 7-day shut-in duration for 500 mD reservoir, case 16-18

The slopes of $(G_p B_g + W_p B_w)/(B_g - B_{gi})$ versus $W_e/(B_g - B_{gi})$ plots in 10-PV aquifer size cases approach the value of one at late times then larger amount of historical data can provide more accurate OGIP values for all shut-in durations.

At 25% RF, p/z versus G_p plot can provide the estimated OGIP value with error around 26% as shown in Figure 6.128 but $(G_p B_g + W_p B_w)/(B_g - B_{gi})$ versus $W_e/(B_g - B_{gi})$ plot is not applicable for OGIP estimation.

If the amount of historical data are available for at least 50% RF, the errors of the estimated OGIPs from $(G_p B_g + W_p B_w)/(B_g - B_{gi})$ versus $W_e/(B_g - B_{gi})$ plots are less than - 3.02% as shown in Table 6.37 while those from p/z versus G_p plots are in the range between 9.40% to 17.90%.

Table 6.37 The result of OGIP estimation at 10-PV aquifer size for 500 mD water-drive dry-gas reservoir by $(G_p B_g + W_p B_w)/(B_g - B_{gi})$ versus $W_e/(B_g - B_{gi})$ plot for various amounts of historical data

Shut-in duration	Amount of historical data	Estimated OGIP (MMscf)	Error (%)	R-squared
6 hours	Up to 25% RF	Not applicable	Not applicable	Not applicable
	Up to 50% RF	3117.156	-2.93%	-13.9138
	Up to abandonment	3214.058	0.09%	0.9913
1 day	Up to 25% RF	Not applicable	Not applicable	Not applicable
	Up to 50% RF	3117.294	-2.93%	-13.8164
	Up to abandonment	3213.612	0.07%	0.9917
7 days	Up to 25% RF	Not applicable	Not applicable	Not applicable
	Up to 50% RF	3114.196	-3.02%	-12.9324
	Up to abandonment	3213.206	0.06%	0.9918

For 30-PV aquifer size, $(G_p B_g + W_p B_w)/(B_g - B_{gi})$ versus $W_e/(B_g - B_{gi})$ plots start to have positive slope since early time as shown in Figure 6.151 to Figure 6.153. The historical data up to 25% RF can be used for OGIP estimation by applying $(G_p B_g + W_p B_w)/(B_g - B_{gi})$ versus $W_e/(B_g - B_{gi})$ plot for all shut-in durations.

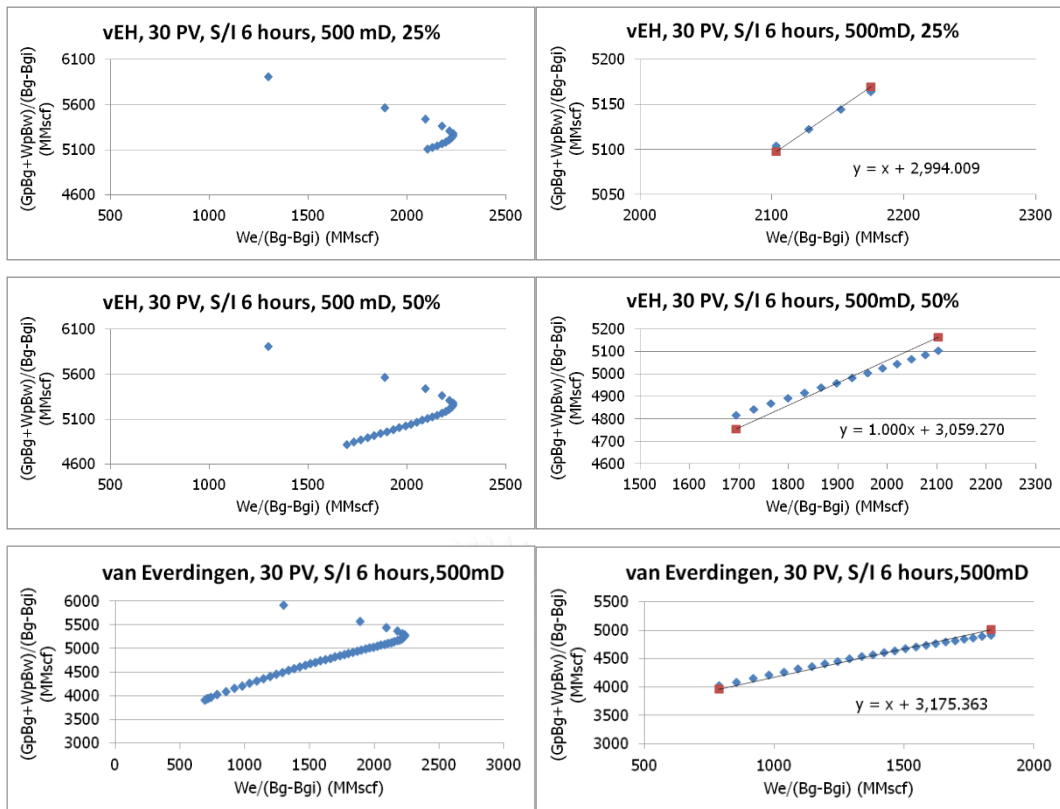


Figure 6.151 $(G_p B_g + W_p B_w) / (B_g - B_{gi})$ versus $W_e / (B_g - B_{gi})$ at 30-PV aquifer size and 6-hour shut-in duration for 500 mD reservoir, case 19-21



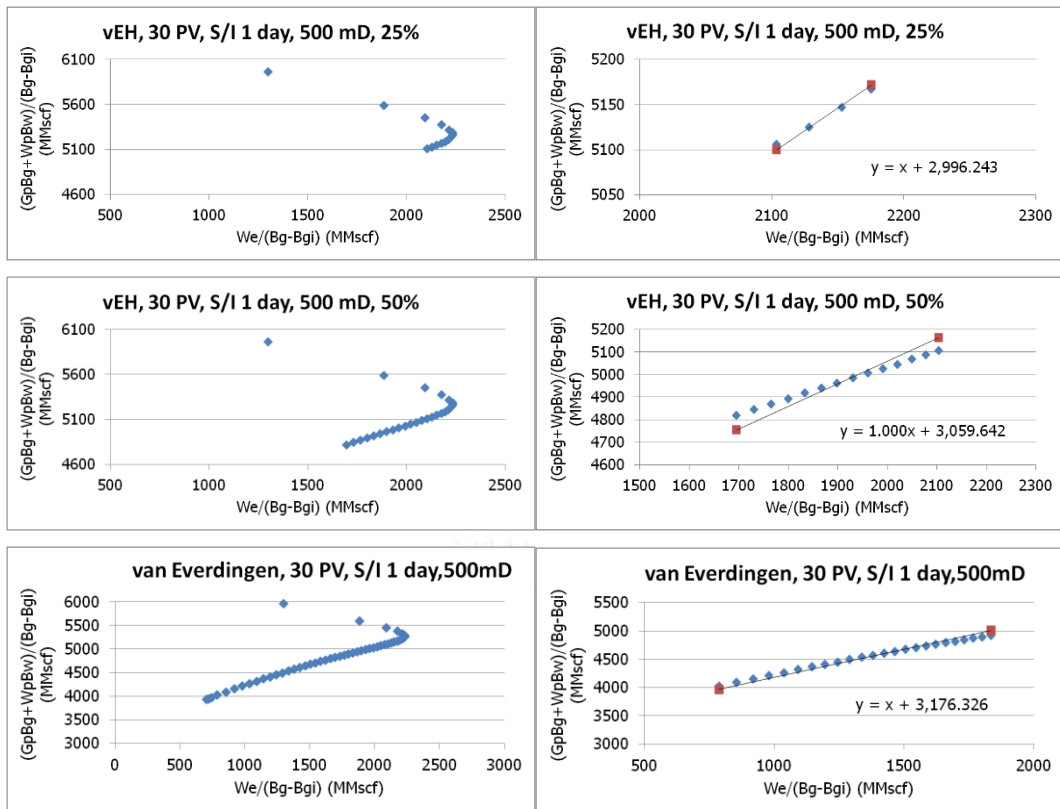


Figure 6.152 $(G_p B_g + W_p B_w) / (B_g - B_{gi})$ versus $W_e / (B_g - B_{gi})$ at 30-PV aquifer size and 1-day shut-in duration for 500 mD reservoir, case 22-24



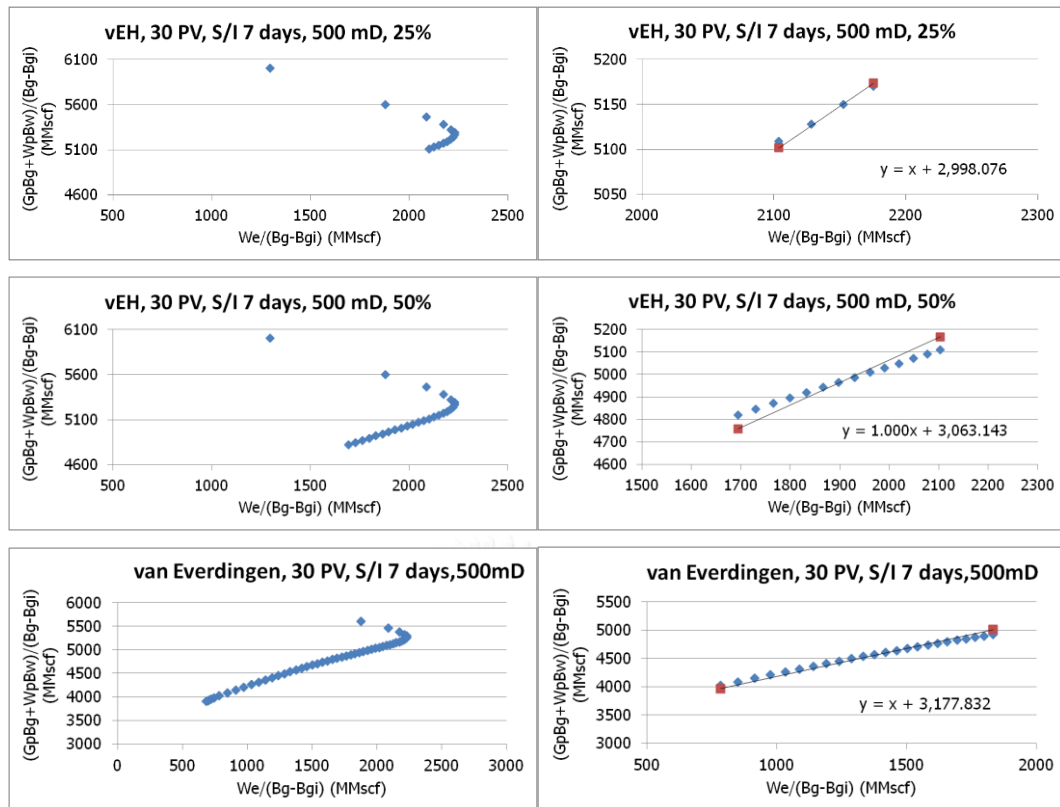


Figure 6.153 $(G_p B_g + W_p B_w)/(B_g - B_{gi})$ versus $W_e/(B_g - B_{gi})$ at 30-PV aquifer size and 7-day shut-in duration for 500 mD reservoir, case 25-27

The plots of $(G_p B_g + W_p B_w)/(B_g - B_{gi})$ versus $W_e/(B_g - B_{gi})$ are fitted better with a unit slope straight line and the accuracy of OGIP estimation become higher when the more historical data are available because the slopes of $(G_p B_g + W_p B_w)/(B_g - B_{gi})$ versus $W_e/(B_g - B_{gi})$ plots approach the value of one in late times.

If the historical data are available at least 25% RF, $(G_p B_g + W_p B_w)/(B_g - B_{gi})$ versus $W_e/(B_g - B_{gi})$ plots always provide more accurate OGIP values, -6.77% to -1.04% error, than p/z versus G_p plots, 36.00% to 83.10% error.

Table 6.38 The result of OGIP estimation at 30-PV aquifer size for 500 mD water-drive dry-gas reservoir by $(G_p B_g + W_p B_w)/(B_g - B_{gi})$ versus $W_e/(B_g - B_{gi})$ plot for various amounts of historical data

Shut-in duration	Amount of historical data	Estimated OGIP (MMscf)	Error (%)	R-squared
6 hours	Up to 25% RF	2994.009	-6.77%	0.9628
	Up to 50% RF	3059.27	-4.73%	0.8133
	Up to abandonment	3175.363	-1.12%	0.9672
1 day	Up to 25% RF	2996.243	-6.70%	0.968
	Up to 50% RF	3059.642	-4.72%	0.8178
	Up to abandonment	3176.326	-1.09%	0.9673
7 days	Up to 25% RF	2998.076	-6.64%	0.9704
	Up to 50% RF	3063.143	-4.61%	0.8224
	Up to abandonment	3177.832	-1.04%	0.9678

For 70-PV aquifer size, the slopes of $(G_p B_g + W_p B_w)/(B_g - B_{gi})$ versus $W_e/(B_g - B_{gi})$ plots for all shut-in durations change from negative to be positive at 19% RF. Then, $(G_p B_g + W_p B_w)/(B_g - B_{gi})$ versus $W_e/(B_g - B_{gi})$ plot can be applied for OGIP estimation when historical data are available only up to 25% RF. The good fitting with a unit slope straight line are shown for all shut-in durations even only a few data points are available for the fitting.

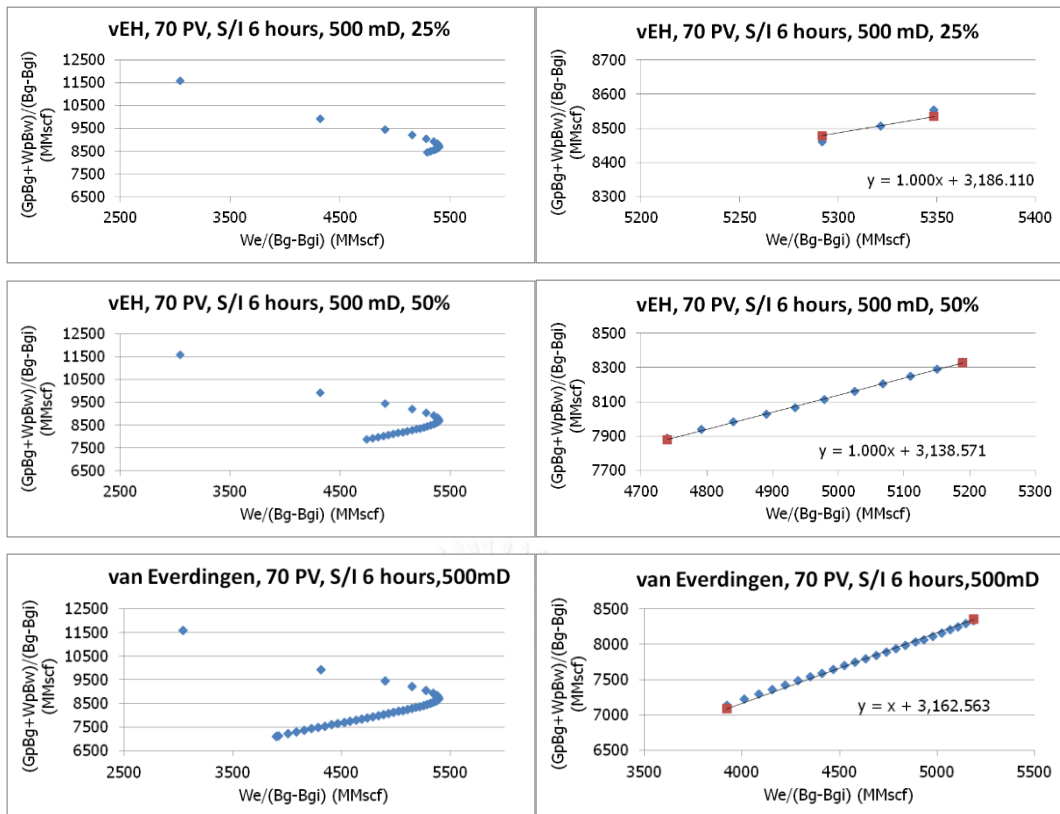


Figure 6.154 $(G_p B_g + W_p B_w) / (B_g - B_{gi})$ versus $W_e / (B_g - B_{gi})$ at 70-PV aquifer size and 6-hour shut-in duration for 500 mD reservoir, case 28-30

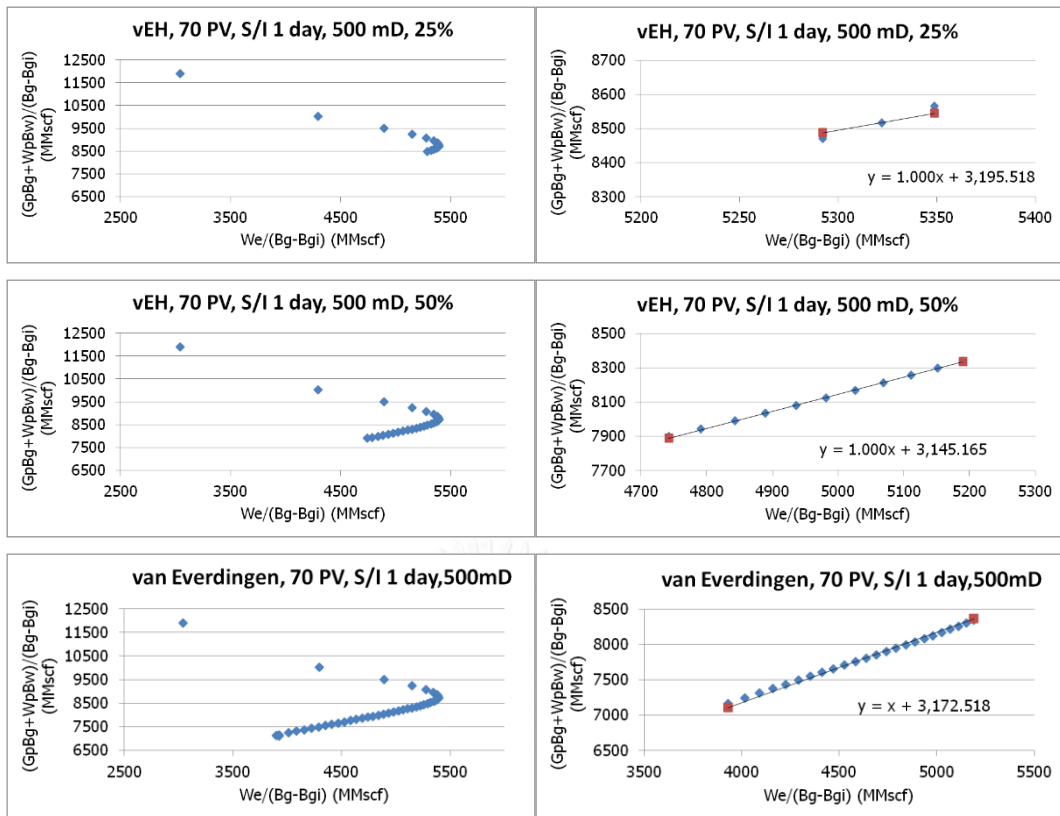


Figure 6.155 $(G_p B_g + W_p B_w) / (B_g - B_{gi})$ versus $W_e / (B_g - B_{gi})$ at 70-PV aquifer size and 1-day shut-in duration for 500 mD reservoir, case 31-33

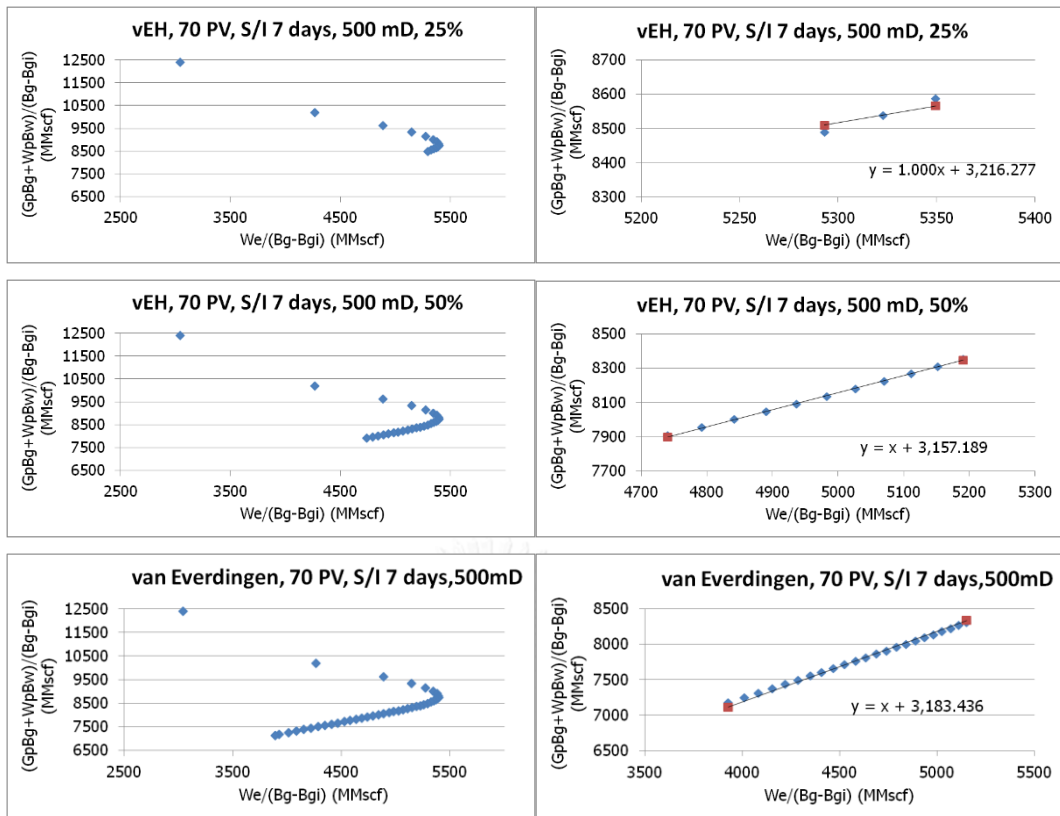


Figure 6.156 $(G_p B_g + W_p B_w) / (B_g - B_{gi})$ versus $W_e / (B_g - B_{gi})$ at 70-PV aquifer size and 7-day shut-in duration for 500 mD reservoir, case 34-36

The estimated OGIP values at 50% RF and those at almost up to the abandonment condition are similar, the differences of errors are less than 1%. These estimated OGIPs are considered to be accurate since the errors are less than 2.3% as shown in Table 6.39.

Table 6.39 The result of OGIP estimation at 70-PV aquifer size for 500 mD water-drive dry-gas reservoir by $(G_p B_g + W_p B_w)/(B_g - B_{gi})$ versus $W_e/(B_g - B_{gi})$ plot for various amounts of historical data

Shut-in duration	Amount of historical data	Estimated OGIP (MMscf)	Error (%)	R-squared
6 hours	Up to 25% RF	3186.11	-0.78%	0.8436
	Up to 50% RF	3138.571	-2.27%	0.9987
	Up to abandonment	3162.563	-1.52%	0.9932
1 day	Up to 25% RF	3195.518	-0.49%	0.8354
	Up to 50% RF	3145.165	-2.06%	0.9989
	Up to abandonment	3172.518	-1.21%	0.9927
7 days	Up to 25% RF	3216.277	0.15%	0.8166
	Up to 50% RF	3157.189	-1.69%	0.9989
	Up to abandonment	3183.436	-0.87%	0.9928

For 100-PV aquifer size, the slopes of $(G_p B_g + W_p B_w)/(B_g - B_{gi})$ versus $W_e/(B_g - B_{gi})$ plots become positive at 21% RF for all shut-in durations. At 25% RF, there are only a couple points of data available for OGIP estimation by $(G_p B_g + W_p B_w)/(B_g - B_{gi})$ versus $W_e/(B_g - B_{gi})$ plots as shown in Figure 6.157 to Figure 6.159. The accuracy of OGIP estimation at 25% RF is not high compare to the other cases for 500 mD reservoir as shown in Figure 6.160, because $(G_p B_g + W_p B_w)/(B_g - B_{gi})$ versus $W_e/(B_g - B_{gi})$ plots just change from negative to positive slope and not stable yet.

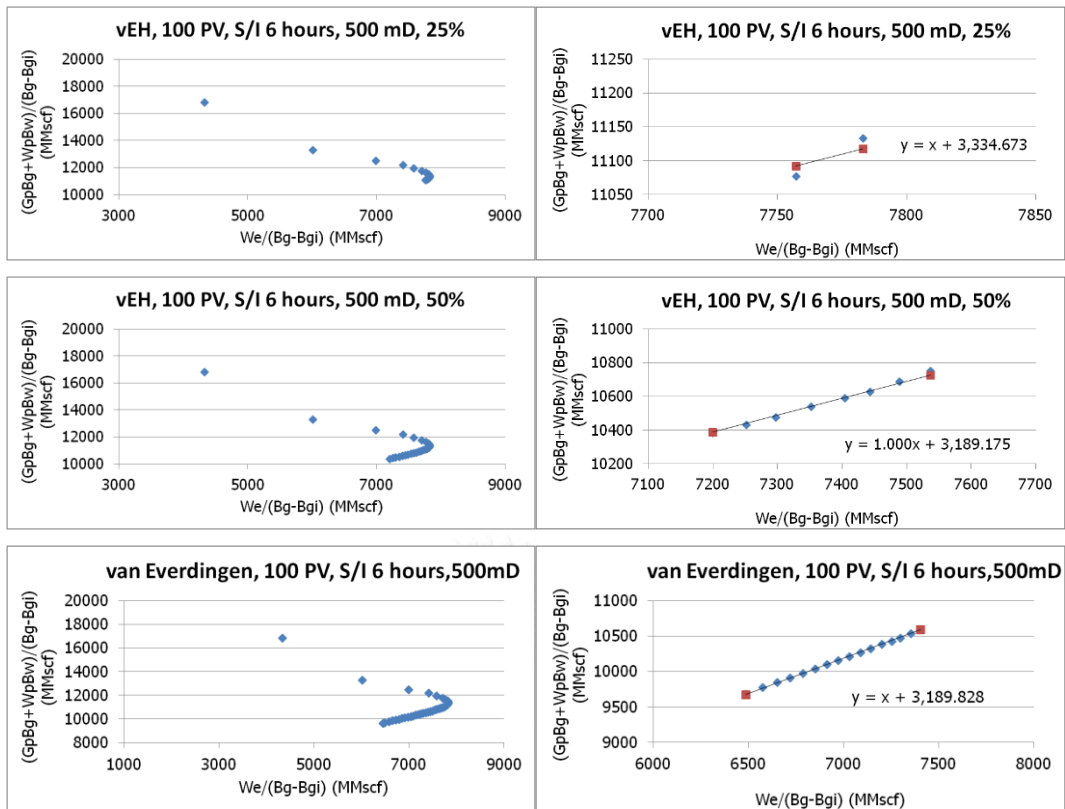


Figure 6.157 $(G_p B_g + W_p B_w) / (B_g - B_{gi})$ versus $W_e / (B_g - B_{gi})$ at 100-PV aquifer size and 6-hour shut-in duration for 500 mD reservoir, case 37-39

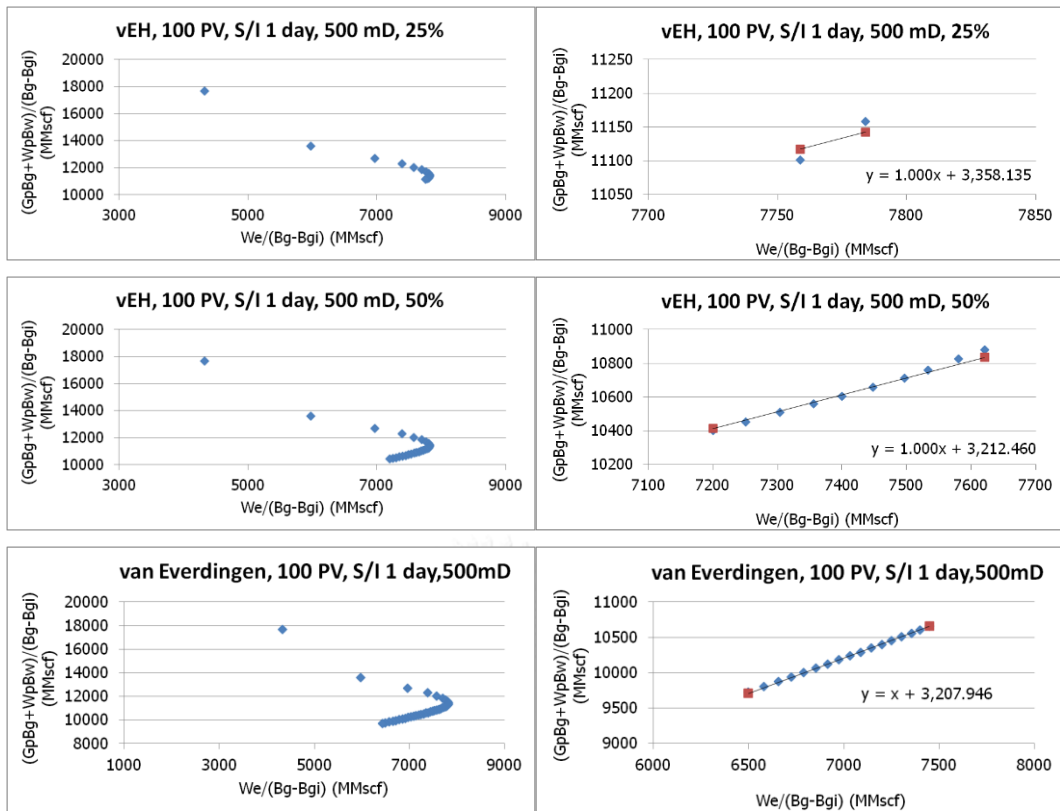


Figure 6.158 $(G_p B_g + W_p B_w) / (B_g - B_{gi})$ versus $W_e / (B_g - B_{gi})$ at 100-PV aquifer size and 1-day shut-in duration for 500 mD reservoir, case 40-42

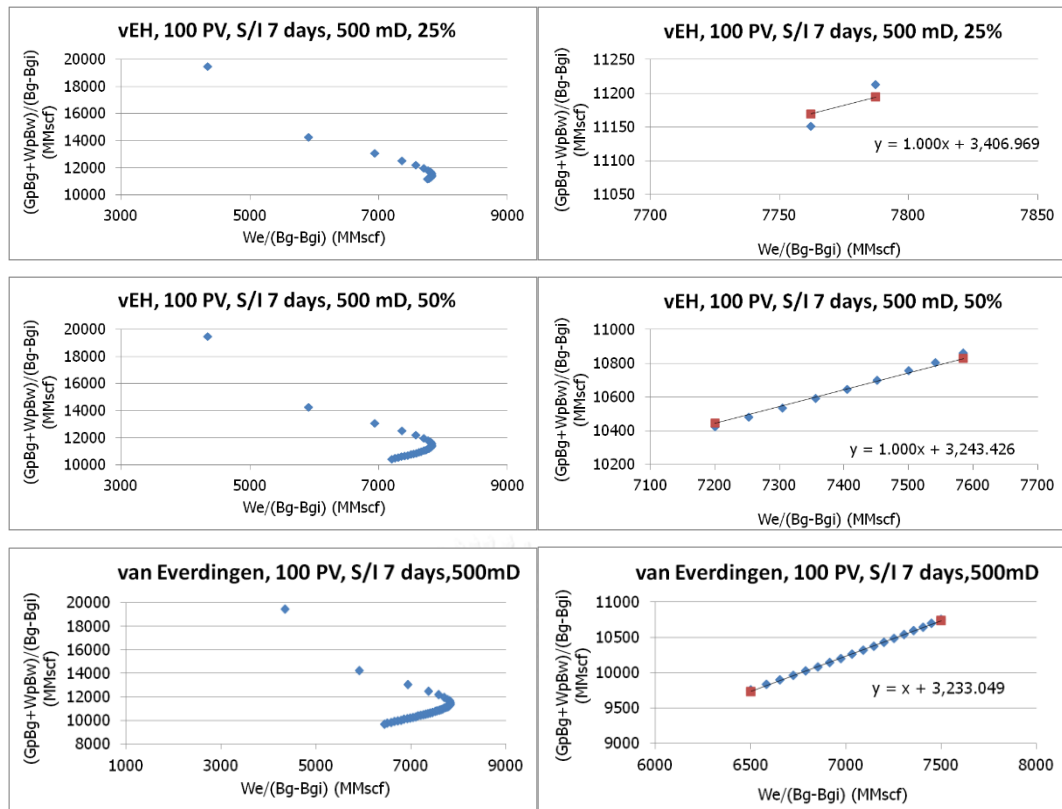


Figure 6.159 $(G_p B_g + W_p B_w) / (B_g - B_{gi})$ versus $W_e / (B_g - B_{gi})$ at 100-PV aquifer size and 7-day shut-in duration for 500 mD reservoir, case 43-45

When the historical data are available for at least 50% RF, the estimated OGIPs are very accurate and very similar, the errors are in the range between -0.69% to 1.00% as shown in Table 6.40.

Table 6.40 The result of OGIP estimation at 100-PV aquifer size for 500 mD water-drive dry-gas reservoir by $(G_p B_g + W_p B_w)/(B_g - B_{gi})$ versus $W_e/(B_g - B_{gi})$ plot for various amounts of historical data

Shut-in duration	Amount of historical data	Estimated OGIP (MMscf)	Error (%)	R-squared
6 hours	Up to 25% RF	3334.673	3.84%	0.7068
	Up to 50% RF	3189.175	-0.69%	0.9904
	Up to abandonment	3189.828	-0.67%	0.9994
1 day	Up to 25% RF	3358.135	4.57%	0.6921
	Up to 50% RF	3212.46	0.04%	0.9832
	Up to abandonment	3207.946	-0.10%	0.9991
7 days	Up to 25% RF	3406.969	6.09%	0.6473
	Up to 50% RF	3243.426	1.00%	0.986
	Up to abandonment	3233.049	0.68%	0.9988

For small to moderate aquifer size cases (1 PV, 10 PV and 30 PV), the behavior of the $(G_p B_g + W_p B_w)/(B_g - B_{gi})$ versus $W_e/(B_g - B_{gi})$ plots for 500 mD reservoir are similar with those for 50 mD reservoir. More historical data provide more accurate estimated OGIP values for all shut-in durations as shown in Figure 6.160 due to the same reason as mentioned in 50 mD reservoir cases. The historical data up to almost the abandonment condition are required in 1-PV aquifer size cases while the 10-PV and 30-PV aquifer size cases require only up to 50% RF and 25% RF, respectively.

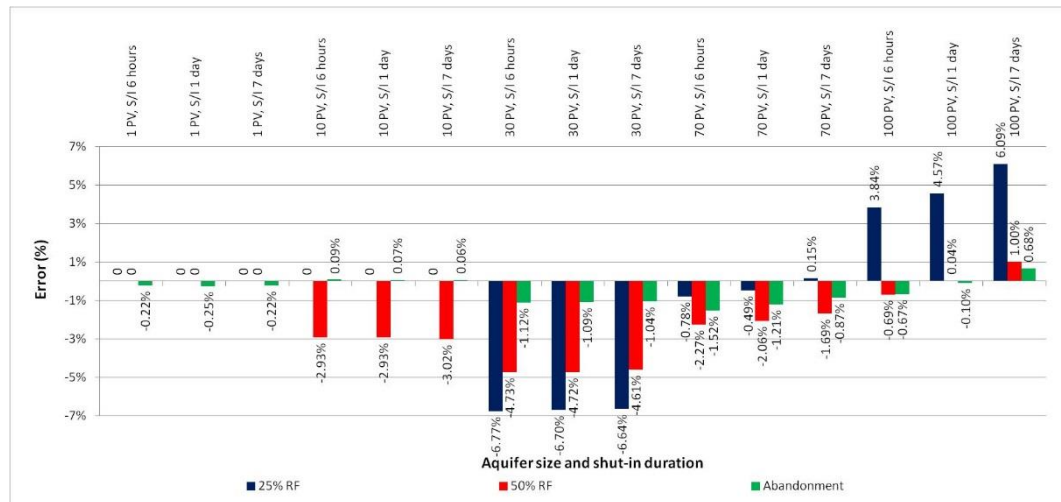


Figure 6.160 Error of estimated OGIP for 500 mD water-drive dry-gas reservoir by $(G_p B_g + W_p B_w)/(B_g - B_{gi})$ versus $W_e/(B_g - B_{gi})$ plot for various amounts of historical data

For large aquifer size cases (70 PV and 100 PV), $(G_p B_g + W_p B_w)/(B_g - B_{gi})$ versus $W_e/(B_g - B_{gi})$ plot can be used for OGIP estimation since the historical data are available up to only 25% RF for all shut-in durations. At 25% RF, there are only a few data points for OGIP estimation since the $(G_p B_g + W_p B_w)/(B_g - B_{gi})$ versus $W_e/(B_g - B_{gi})$ plots just turn into the positive slope trends, the error of the estimated OGIP values are around -0.8% to 0.2% in 70-PV aquifer size cases and 3.8% to 6.1% in 100-PV aquifer size cases. The estimated OGIPs from the historical data up to 50% RF and almost the abandonment condition are very accurate, the errors are in the range between -2.3% to 1% as shown in Figure 6.160.

The shut-in duration has no effect on the minimum amount of historical data required for OGIP estimation.

Table 6.41 The result of OGIP estimation for 500 mD water-drive dry-gas reservoir by $(G_p B_g + W_p B_w)/(B_g - B_{gi})$ versus $W_e/(B_g - B_{gi})$ plot for various amounts of historical data

Case	Aquifer size (PV)	Shut-in duration	Amount of historical data	Estimated OGIP (MMscf)	Error (%)	R-squared
1	1	6 hours	25% RF	Not applicable	Not applicable	Not applicable
2			50% RF	Not applicable	Not applicable	Not applicable
3			Abandonment	3204.232	-0.22%	0.73
4		1 day	25% RF	Not applicable	Not applicable	Not applicable
5			50% RF	Not applicable	Not applicable	Not applicable
6			Abandonment	3203.3	-0.25%	0.7495
7		7 days	25% RF	Not applicable	Not applicable	Not applicable
8			50% RF	Not applicable	Not applicable	Not applicable
9			Abandonment	3204.276	-0.22%	0.7206
10	10	6 hours	25% RF	Not applicable	Not applicable	Not applicable
11			50% RF	3117.156	-2.93%	-13.9138
12			Abandonment	3214.058	0.09%	0.9913

Table 6.41 The result of OGIP estimation for 500 mD water-drive dry-gas reservoir by $(G_p B_g + W_p B_w)/(B_g - B_{gi})$ versus $W_e/(B_g - B_{gi})$ plot for various amounts of historical data (continued)

Case	Aquifer size (PV)	Shut-in duration	Amount of historical data	Estimated OGIP (MMscf)	Error (%)	R-squared
13	10	1 day	25% RF	Not applicable	Not applicable	Not applicable
14			50% RF	3117.294	-2.93%	-13.8164
15			Abandonment	3213.612	0.07%	0.9917
16		7 days	25% RF	Not applicable	Not applicable	Not applicable
17			50% RF	3114.197	-3.02%	-12.9324
18			Abandonment	3213.206	0.06%	0.9918
19	30	6 hours	25% RF	2994.009	-6.77%	0.9628
20			50% RF	3059.27	-4.73%	0.8133
21			Abandonment	3175.363	-1.12%	0.9672
22		1 day	25% RF	2996.243	-6.70%	0.9680
23			50% RF	3059.642	-4.72%	0.8178
24			Abandonment	3176.326	-1.09%	0.9673
25		7 days	25% RF	2998.076	-6.64%	0.9704
26			50% RF	3063.143	-4.61%	0.8224
27			Abandonment	3177.832	-1.04%	0.9678

Table 6.41 The result of OGIP estimation for 500 mD water-drive dry-gas reservoir by $(G_p B_g + W_p B_w)/(B_g - B_{gi})$ versus $W_e/(B_g - B_{gi})$ plot for various amounts of historical data (continued)

Case	Aquifer size (PV)	Shut-in duration	Amount of historical data	Estimated OGIP (MMscf)	Error (%)	R-squared
28	70	6 hours	25% RF	3186.11	-0.78%	0.8436
29			50% RF	3138.571	-2.27%	0.9987
30			Abandonment	3162.563	-1.52%	0.9932
31		1 day	25% RF	3195.518	-0.49%	0.8354
32			50% RF	3145.165	-2.06%	0.9989
33			Abandonment	3172.518	-1.21%	0.9927
34		7 days	25% RF	3216.277	0.15%	0.8166
35			50% RF	3157.189	-1.69%	0.9989
36			Abandonment	3183.436	-0.87%	0.9928
37	100	6 hours	25% RF	3334.673	3.84%	0.7068
38			50% RF	3189.175	-0.69%	0.9904
39			Abandonment	3189.828	-0.67%	0.9994
40		1 day	25% RF	3358.135	4.57%	0.6921
41			50% RF	3212.46	0.04%	0.9832
42			Abandonment	3207.946	-0.10%	0.9991
43		7 days	25% RF	3406.969	6.09%	0.6473
44			50% RF	3243.426	1.00%	0.9860
45			Abandonment	3233.049	0.68%	0.9988

Table 6.42 The accuracy of OGIP estimation for 500 mD water-drive dry-gas reservoir by $(G_p B_g + W_p B_w) / (B_g - B_{gi})$ versus $W_e / (B_g - B_{gi})$ plot for various amounts of historical data

Aquifer size (PV)	Amount of historical data	Shut-in duration	Accuracy	
1	Up to 25% RF and 50% RF	6 hours, 1 day and 7 days	Not applicable	
	Up to Abandonment		Accurate	
10	Up to 25% RF		Not applicable	
	Up 50% RF and Abandonment		Accurate	
30	Up to 25% RF		Acceptable	
	Up 50% RF and Abandonment		Accurate	
70	Up 25% RF, 50% RF and Abandonment		Accurate	
100	Up to 25% RF		6 hours and 1 day	Accurate
			7 days	Acceptable
	Up 50% RF and Abandonment		6 hours, 1 day and 7 days	Accurate

Accurate: error < 5%, Acceptable: error < 10%, Not acceptable: error ≥ 10%

6.9 OGIP Estimation from Unknown Aquifer Size

As shown in previous sections, aquifer size is the parameter that has high impact on the OGIP estimation. Unfortunately, aquifer size is usually unknown in reality. Then, we need to try on different aquifer sizes until a unit slope straight line is seen on $(G_p B_g + W_p B_w) / (B_g - B_{gi})$ versus $W_e / (B_g - B_{gi})$ plot.

The objective of this section is to investigate the feasibility and accuracy of OGIP estimation by applying $(G_p B_g + W_p B_w)/(B_g - B_{gi})$ versus $W_e/(B_g - B_{gi})$ plot with unknown aquifer size for 50 mD and 500 mD reservoir with 1-day shut-in duration for SBHP measurement and historical data up to almost the abandonment condition. Table 6.43 shows the parameters to be studied in this section.

Table 6.43 Parameters to be studied on the feasibility and accuracy of OGIP estimation by $(G_p B_g + W_p B_w)/(B_g - B_{gi})$ versus $W_e/(B_g - B_{gi})$ plot with unknown aquifer size

Case	Permeability (mD)	Actual aquifer size (PV)	Water influx model
1	50	1	Simple model
2			Fetkovich
3			van Everdingen & Hurst
4			Carter & Tracy
5		10	Simple model
6			Fetkovich
7			van Everdingen & Hurst
8			Carter & Tracy
9		30	Simple model
10			Fetkovich
11			van Everdingen & Hurst
12			Carter & Tracy
13		70	Simple model
14			Fetkovich
15			van Everdingen & Hurst

Table 6.43 Parameters to be studied on the feasibility and accuracy of OGIP estimation by $(G_p B_g + W_p B_w)/(B_g - B_{gi})$ versus $W_e/(B_g - B_{gi})$ plot with unknown aquifer size (continued)

Case	Permeability (mD)	Actual aquifer size (PV)	Water influx model
16	50	70	Carter & Tracy
17		100	Simple model
18			Fetkovich
19			van Everdingen & Hurst
20			Carter & Tracy
21	500	1	van Everdingen & Hurst
22		10	
23		30	
24		70	
25		100	

Figure 6.161 to Figure 6.165 represent the plot of the R-squared value and the error in estimated OGIP versus the trial aquifer size and $(G_p B_g + W_p B_w)/(B_g - B_{gi})$ versus $W_e/(B_g - B_{gi})$ plot associated to the best selected estimated aquifer size, the one that yields the maximum R-squared value, for 50 mD water-drive dry-gas reservoir with 1-day shut-in duration having different actual aquifer sizes.

Only the term $W_e/(B_g - B_{gi})$ or x-axis depends on the value of trial aquifer size. The term $(G_p B_g + W_p B_w)/(B_g - B_{gi})$ or y-axis is independent of the trial aquifer size. A larger trial aquifer size causes less slope of $(G_p B_g + W_p B_w)/(B_g - B_{gi})$ versus $W_e/(B_g - B_{gi})$ plot, and the plot shifts to the right. The reason of this behavior is W_e or the numerator of the term $W_e/(B_g - B_{gi})$ increases with trial aquifer size.

For 1-PV actual aquifer size, as illustrated in Figure 6.161, all of the water influx models provide the same estimated aquifer size of 2 PV. From Figure 6.67, the values of the slope of $(G_p B_g + W_p B_w)/(B_g - B_{gi})$ versus $W_e/(B_g - B_{gi})$ plots at the late time from all water influx models are around 2 then the 2-PV estimated aquifer size yield the highest R-squared value.

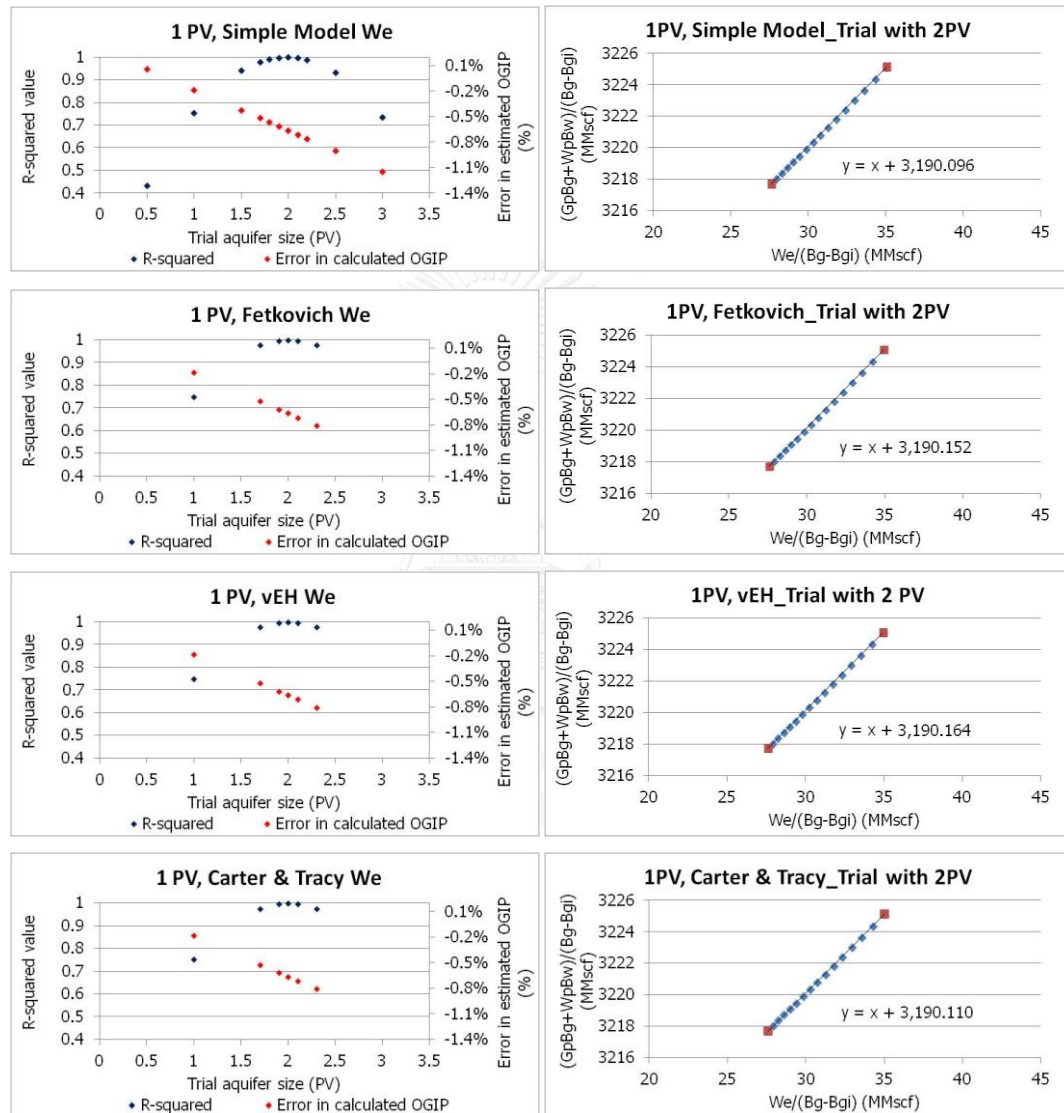


Figure 6.161 Left: R-squared value and error in estimated OGIP

Right: $(G_p B_g + W_p B_w)/(B_g - B_{gi})$ versus $W_e/(B_g - B_{gi})$ at 1-PV aquifer size for 50 mD, case 1-4

The estimated OGIPs from all water influx models are similar because the estimated aquifer size of 2 PV is small. Then, the effect from the different W_e from

different water influx models is small. The estimated OGIPs from the 2-PV estimated aquifer size are slightly lower than the ones from the actual 1-PV aquifer size in Figure 6.67 because the value of aquifer size and OGIP are inversely proportional.

For 10-PV actual aquifer size, Figure 6.162 shows that the estimated aquifer size from all water influx models is 10 PV which is equal to the actual aquifer size. This is because $(G_p B_g + W_p B_w) / (B_g - B_{gi})$ versus $W_e / (B_g - B_{gi})$ plots from the actual aquifer size in Figure 6.70 have the late time slope value equal to one.

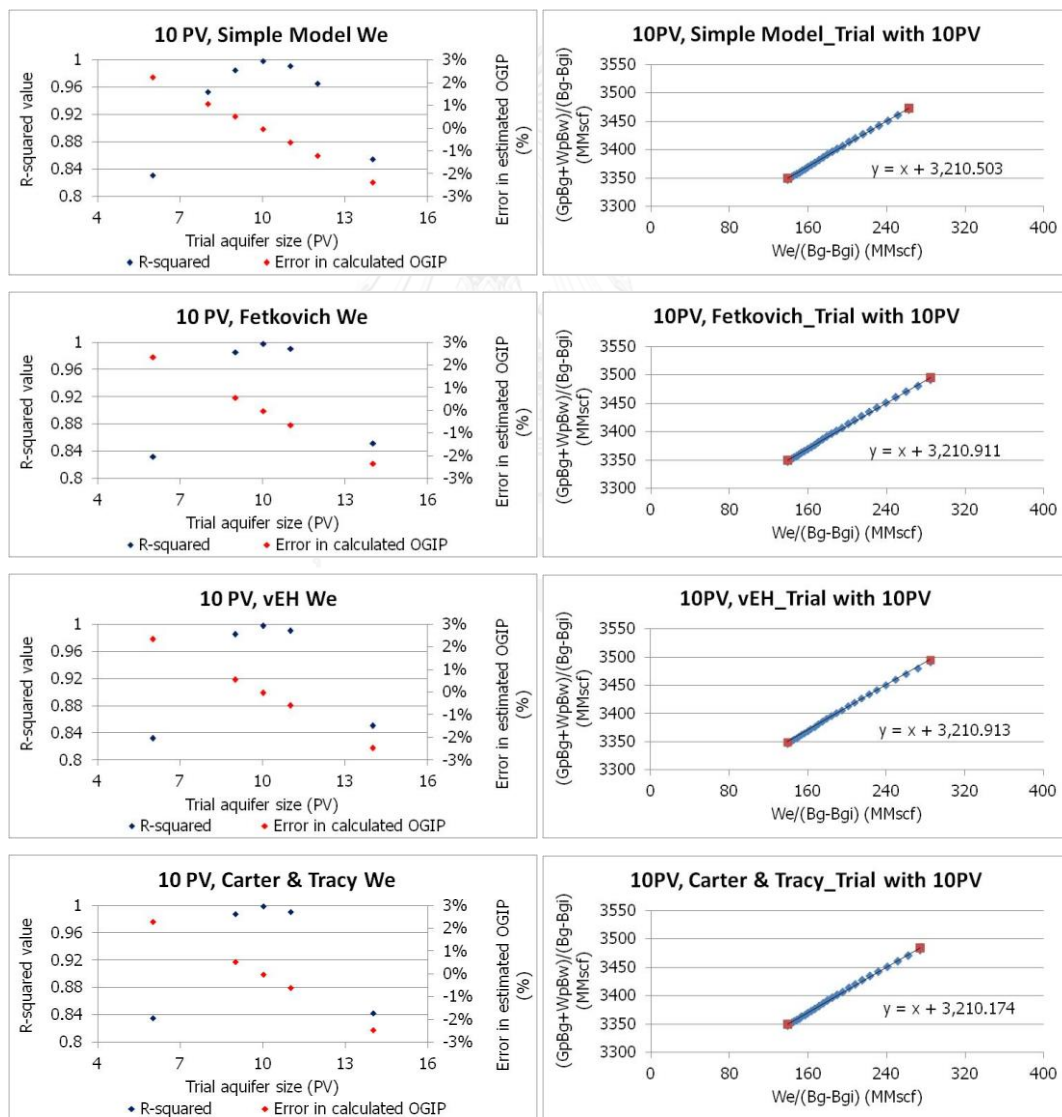


Figure 6.162 Left: R-squared value and error in estimated OGIP
 Right: $(G_p B_g + W_p B_w) / (B_g - B_{gi})$ versus $W_e / (B_g - B_{gi})$ at 10-PV aquifer size for 50 mD, case 5-8

Since the estimated aquifer size is exactly equal to the actual aquifer size in these cases, estimated OGIP values in this case are equal to the ones from the actual aquifer size in Figure 6.70.

For 30-PV actual aquifer size, the estimated aquifer size from simple aquifer model is 29 PV but the remaining water influx model give the same values of 30 PV as depicted in Figure 6.163. The reason that simple aquifer model gives a lower estimated aquifer size than the others is because simple aquifer model always gives higher W_e than other water influx models as shown in Figure 6.46 for the 30-PV aquifer size cases.



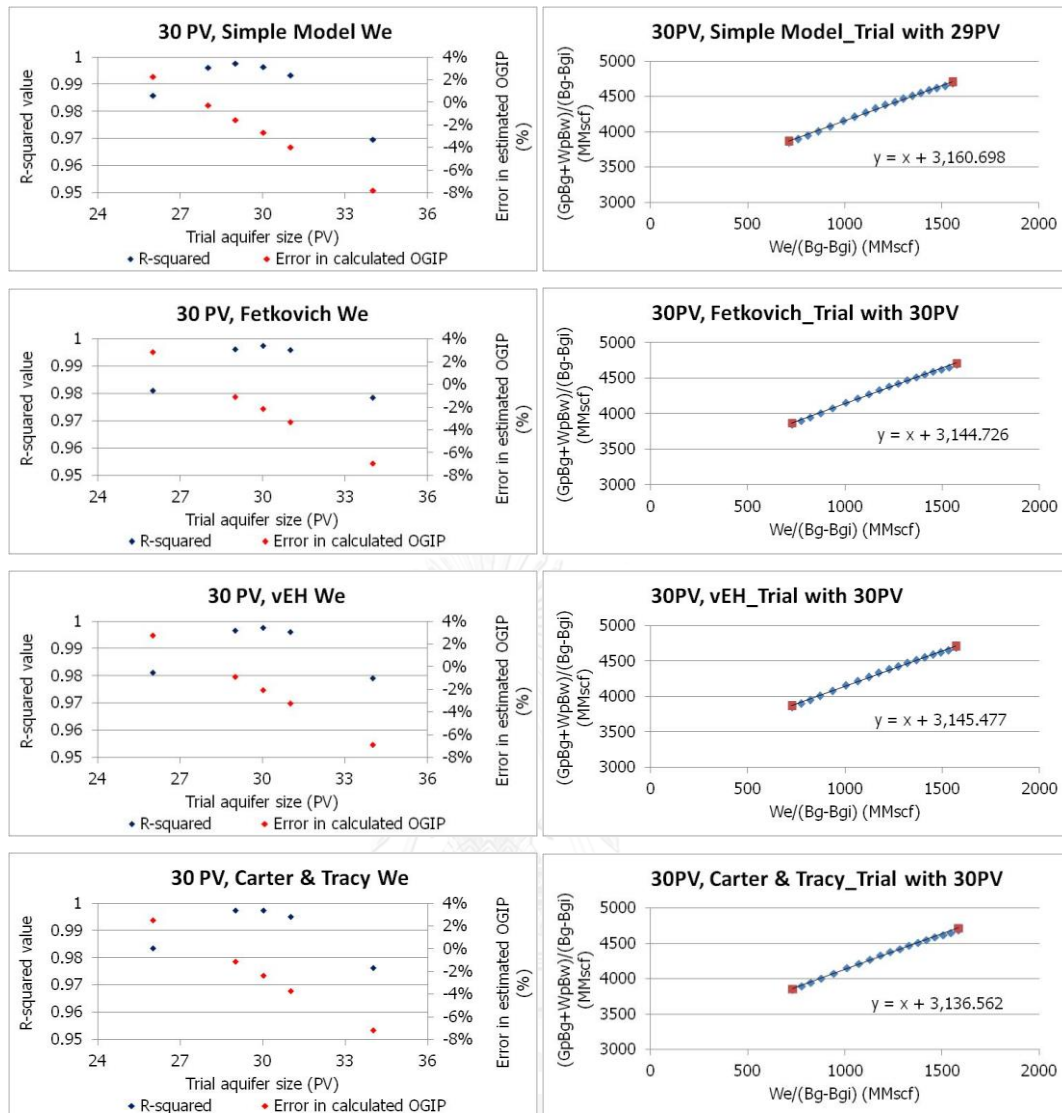


Figure 6.163 Left: R-squared value and error in estimated OGIP

Right: $(G_p B_g + W_p B_w) / (B_g - B_{gi})$ versus $W_e / (B_g - B_{gi})$ at 30-PV aquifer size for 50 mD, case 9-12

For van Everdingen & Hurst, Fetkovich and Carter & Tracy water influx models, the estimated OGIPs from unknown aquifer size in this case are exactly matched with the ones from the actual aquifer size in Figure 6.73 because the estimated aquifer size is equal to the actual aquifer size. The estimated OGIP from simple aquifer model with unknown aquifer size is slightly higher than the one from the actual aquifer size in Figure 6.73 because the estimated aquifer size is slightly lower than the actual one.

For 70-PV actual aquifer size, van Everdingen & Hurst, Fetkovich and Carter & Tracy water influx models give larger estimated aquifer size than the actual one. The reason of this behavior is the slope of $(G_p B_g + W_p B_w) / (B_g - B_{gi})$ versus $W_e / (B_g - B_{gi})$ plots at late times from these water influx models in 70-PV aquifer size cases are higher than one as shown in Figure 6.76. Trial aquifer size process can change only the value of term $W_e / (B_g - B_{gi})$ or x-axis. In order to reduce the slope of $(G_p B_g + W_p B_w) / (B_g - B_{gi})$ versus $W_e / (B_g - B_{gi})$ plots to be one in order to reach the maximum R-squared value, a larger aquifer size is needed. The larger estimated aquifer size yield smaller estimated OGIP as shown in Figure 6.164.



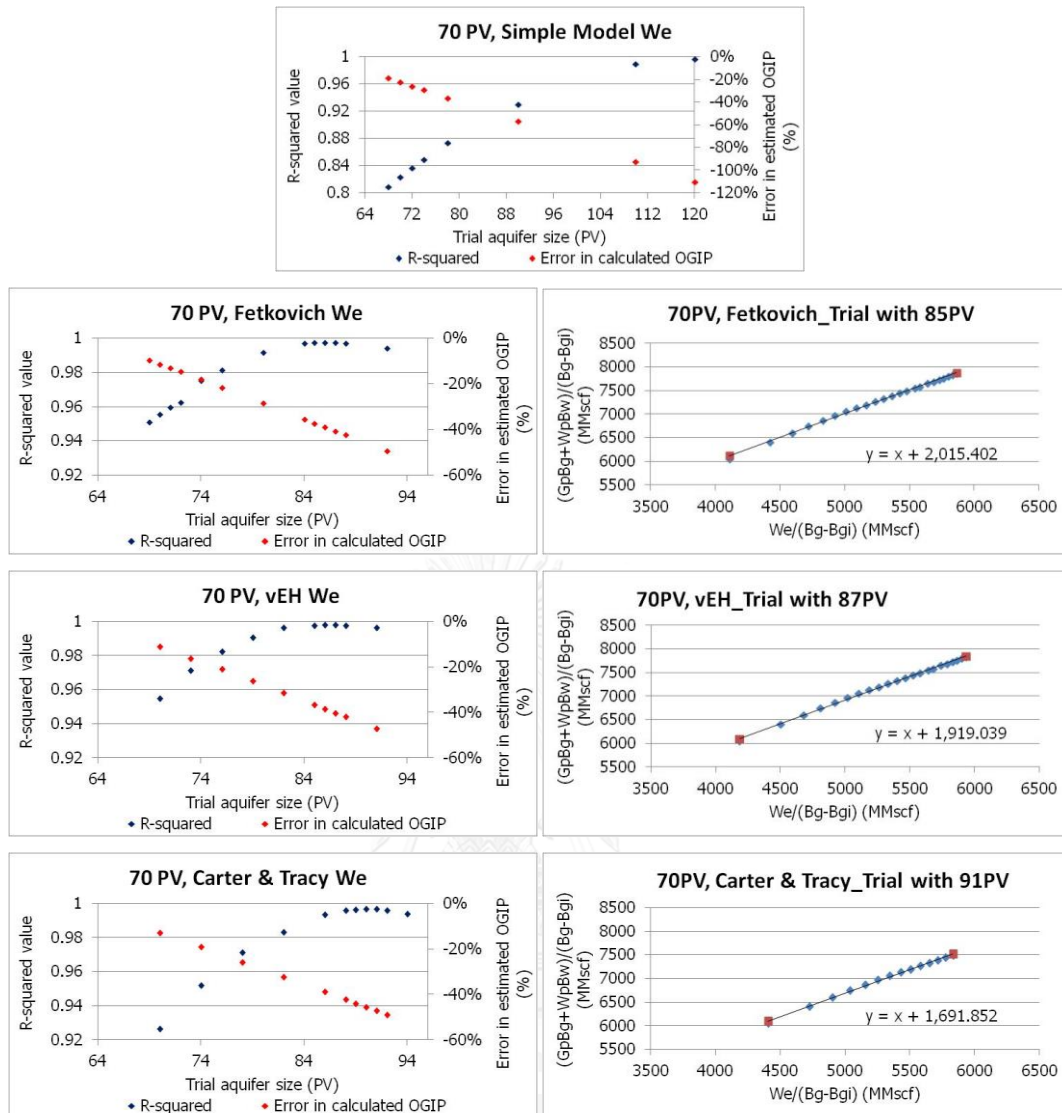


Figure 6.164 Left: R-squared value and error in estimated OGIP

Right: $(G_p B_g + W_p B_w) / (B_g - B_{gi})$ versus $W_e / (B_g - B_{gi})$ at 70-PV aquifer size for 50 mD, case 13-

For simple aquifer model, a larger trial aquifer size gives a higher R-squared value. As the trial aquifer size increases, the estimated OGIP value becomes negative before the maximum R-squared is reached. From Figure 6.76 and Table 6.14, the slope of $(G_p B_g + W_p B_w) / (B_g - B_{gi})$ versus $W_e / (B_g - B_{gi})$ plot from simple aquifer model is much more deviated from one than those from the remaining water influx models. The R-squared value of simple aquifer model is also less than those for other water influx models. A

larger trial aquifer size is needed for simple aquifer model in order to make the slope of $(G_p B_g + W_p B_w)/(B_g - B_{gi})$ versus $W_e/(B_g - B_{gi})$ plot equal to one in order to reach the maximum R-squared value. The estimated OGIP value from simple aquifer model then becomes negative because the trial aquifer size is too large.

For 100-PV actual aquifer size, all of the water influx models cannot be used to estimate the aquifer size and OGIP. All of them show the same behavior as simple aquifer model in 70-PV actual aquifer size case, i.e., the maximum R-squared value cannot be found since the OGIP values become negative. The reason of the behavior is same as mentioned in simple aquifer model in 70-PV actual aquifer size case. Since the slope of $(G_p B_g + W_p B_w)/(B_g - B_{gi})$ versus $W_e/(B_g - B_{gi})$ plot in 100-PV aquifer size cases are more deviated from one than the ones in 70-PV aquifer size cases, as shown in Figure 6.76 and Figure 6.81, a larger trial aquifer size is needed in order to make the slope of $(G_p B_g + W_p B_w)/(B_g - B_{gi})$ versus $W_e/(B_g - B_{gi})$ plot equal to one in order to reach the maximum R-squared value.

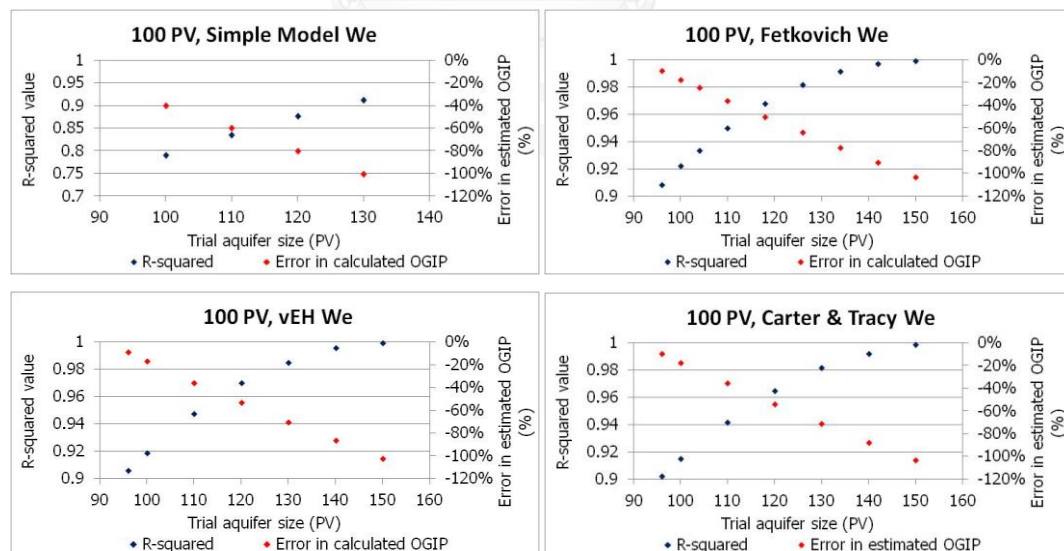


Figure 6.165 R-squared value and error in estimated OGIP at 100-PV aquifer size for 50 mD, case 17-20

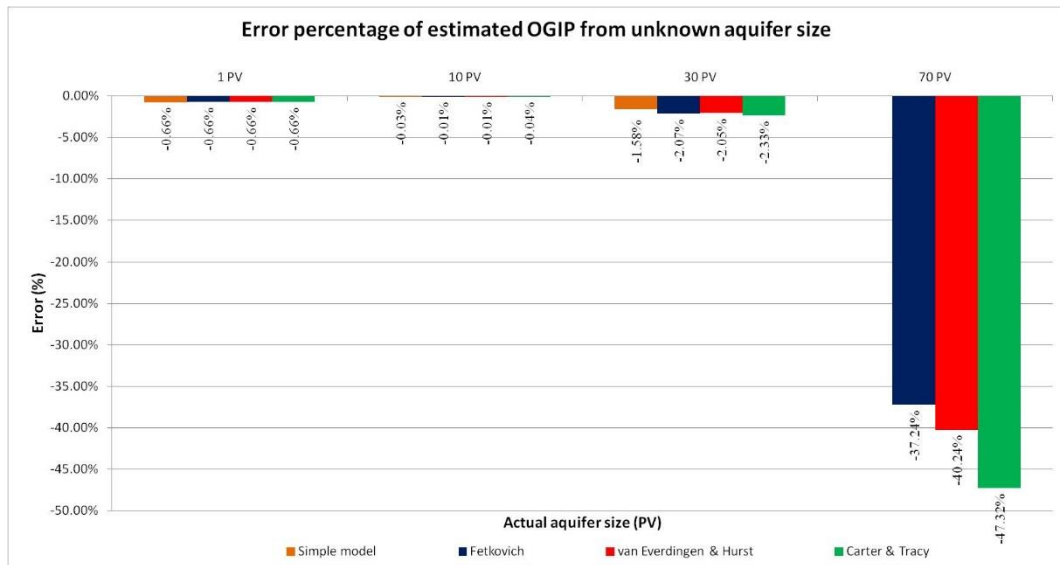


Figure 6.166 Error percentage of estimated OGIP in 50 mD water-drive dry-gas reservoir by $(G_p B_g + W_p B_w) / (B_g - B_{gi})$ versus $W_e / (B_g - B_{gi})$ plot with unknown aquifer size

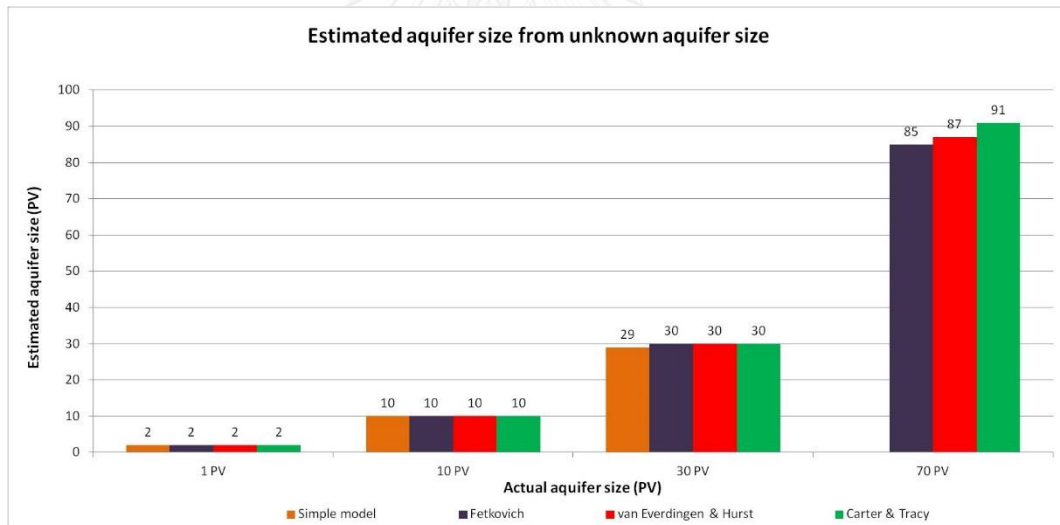


Figure 6.167 Estimated aquifer size in 50 mD water-drive dry-gas reservoir by $(G_p B_g + W_p B_w) / (B_g - B_{gi})$ versus $W_e / (B_g - B_{gi})$ plot with unknown aquifer size

The results of the analysis in this section are summarized in Table 6.44. For 1-PV actual aquifer size, the estimated OGIP values are very accurate because the aquifer support impact is very low. For 10-PV and 30-PV actual aquifer sizes, the estimated OGIPs and aquifer sizes are very accurate because the aquifer support behavior is

obvious and the effect from the error in SBHP is small. For 70-PV and 100-PV actual aquifer sizes, the estimated OGIPs and aquifer sizes are not accurate or even cannot be estimated at all because the effect from the error in SBHP is high.

The effect of water influx model is very small for 1-PV, 10-PV and 30-PV actual aquifer size cases. In 70-PV and 100-PV aquifer size cases, the effect of water influx model is more obvious because the difference in W_e between models is higher.

Table 6.44 The result of OGIP estimation for 50 mD water-drive dry-gas reservoir by $(G_p B_g + W_p B_w) / (B_g - B_{gi})$ versus $W_e / (B_g - B_{gi})$ plot with unknown aquifer size

Case	Actual aquifer size (PV)	Water influx model	Estimated aquifer size (PV)	Error (%)	Estimated OGIP (MMscf)	Error (%)	R-squared
1	1	Simple aquifer model	2	100%	3,190.10	-0.66%	0.999
2		Fetkovich	2	100%	3,190.15	-0.66%	0.999
3		van Everdingen & Hurst	2	100%	3,190.16	-0.66%	0.999
4		Carter & Tracy	2	100%	3,190.11	-0.66%	0.999
5	10	Simple aquifer model	10	0%	3,210.50	-0.03%	0.999

Table 6.44 The result of OGIP estimation for 50 mD water-drive dry-gas reservoir by $(G_p B_g + W_p B_{gw}) / (B_g - B_{gi})$ versus $W_e / (B_g - B_{gi})$ plot with unknown aquifer size (continued)

Case	Actual aquifer size (PV)	Water influx model	Estimated aquifer size (PV)	Error (%)	Estimated OGIP (MMscf)	Error (%)	R-squared
6	10	Fetkovich	10	0%	3,210.91	-0.01%	0.998
7		van Everdingen & Hurst	10	0%	3,210.91	-0.01%	0.998
8		Carter & Tracy	10	0%	3,210.17	-0.04%	0.999
9	30	Simple aquifer model	29	-3%	3,160.70	-1.58%	0.998
10		Fetkovich	30	0%	3,144.73	-2.07%	0.998
11		van Everdingen & Hurst	30	0%	3,145.48	-2.05%	0.998
12		Carter & Tracy	30	0%	3,136.56	-2.33%	0.997
13	70	Simple aquifer model	Not applicable				
14		Fetkovich	85	21%	2,015.40	-37.24%	0.998

Table 6.44 The result of OGIP estimation for 50 mD water-drive dry-gas reservoir by $(G_p B_g + W_p B_{gw}) / (B_g - B_{gi})$ versus $W_e / (B_g - B_{gi})$ plot with unknown aquifer size (continued)

Case	Actual aquifer size (PV)	Water influx model	Estimated aquifer size (PV)	Error (%)	Estimated OGIP (MMscf)	Error (%)	R-squared	
15	70	van Everdingen & Hurst	87	24%	1,919.04	-40.24%	0.998	
16		Carter & Tracy	91	30%	1,691.85	-47.32%	0.997	
17	100	Simple aquifer model	Not applicable					
18		Fetkovich						
19		van Everdingen & Hurst						
20		Carter & Tracy						

Table 6.45 The accuracy of OGIP estimation for 50 mD water-drive dry-gas reservoir by $(G_p B_g + W_p B_w)/(B_g - B_{gi})$ versus $W_e/(B_g - B_{gi})$ plot with unknown aquifer size

Aquifer size (PV)	Water influx model	Accuracy
1, 10 and 30	Simple aquifer model , Fetkovich , van Everdingen & Hurst and Carter & Tracy	Accurate
70	Simple model	Not applicable
	Fetkovich , van Everdingen & Hurst and Carter & Tracy	Not acceptable
100	Simple aquifer model , Fetkovich , van Everdingen & Hurst and Carter & Tracy	Not applicable

Accurate: error < 5%, Acceptable: error < 10%, Not acceptable: error ≥ 10%

Figure 6.168 to Figure 6.172 represent the plot of the R-squared value and the error in estimated OGIP versus the trial aquifer size and $(G_p B_g + W_p B_w)/(B_g - B_{gi})$ versus $W_e/(B_g - B_{gi})$ plot associated to the best selected estimated aquifer size, the one that yields the maximum R-squared value, for 500 mD water-drive dry-gas reservoir with 1-day shut-in duration having different actual aquifer sizes. Only van Everdingen & Hurst water influx model is applied in this section because it yields the most accurate value of estimated OGIP for all aquifer sizes and shut-in durations as shown in Section 6.6.

For 1-PV actual aquifer size, as shown in Figure 6.168, the estimated aquifer size is 2 PV due to the same reason as mentioned in 1-PV actual aquifer size for 50 mD reservoir cases.

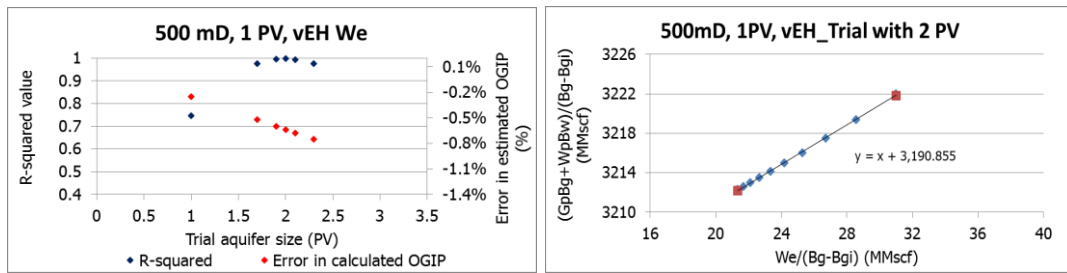


Figure 6.168 Left: R-squared value and error in estimated OGIP
 Right: $(G_p B_g + W_p B_w)/(B_g - B_{gi})$ versus $W_e/(B_g - B_{gi})$ at 1-PV aquifer size for 500 mD, case 21

For 10-PV actual aquifer size, as illustrated in Figure 6.169, the estimated aquifer size is 9 PV, not exactly 10 PV because the late time slope of $(G_p B_g + W_p B_w)/(B_g - B_{gi})$ versus $W_e/(B_g - B_{gi})$ plots from the actual aquifer size in Figure 6.85 is not exactly one. R-squared value is 0.992 as shown in Table 6.22.

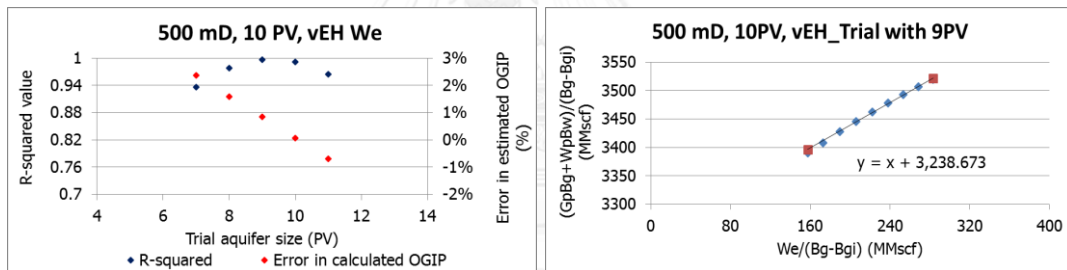


Figure 6.169 Left: R-square value and error in estimated OGIP
 Right: $(G_p B_g + W_p B_w)/(B_g - B_{gi})$ versus $W_e/(B_g - B_{gi})$ at 10-PV aquifer size for 500 mD, case 22

For 30-PV, 70-PV and 100-PV actual aquifer size, as shown in Figure 6.170 to Figure 6.172, the estimated aquifer sizes are not exactly equal to the actual ones due to the same reason as mentioned in 10-PV actual aquifer size case.

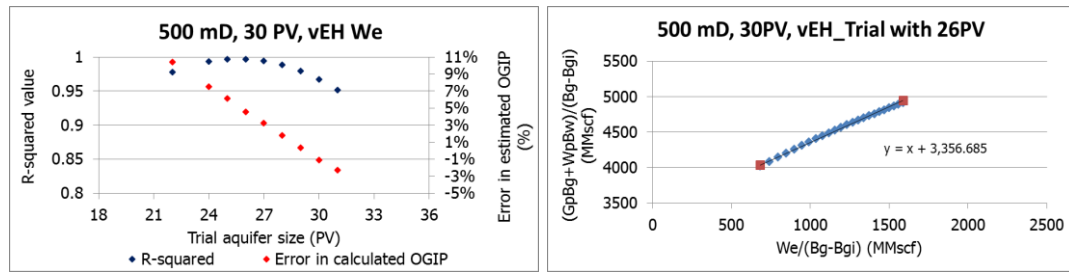


Figure 6.170 Left: R-square value and error in estimated OGIP
 Right: $(G_p B_g + W_p B_w) / (B_g - B_{gi})$ versus $W_e / (B_g - B_{gi})$ at 30-PV aquifer size for 500 mD, case 23

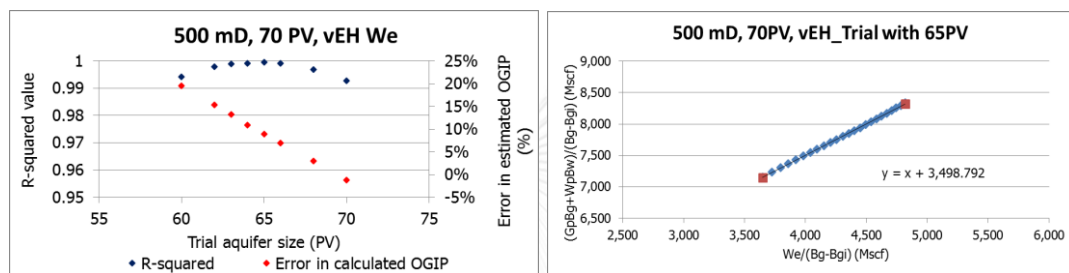


Figure 6.171 Left: R-square value and error in estimated OGIP
 Right: $(G_p B_g + W_p B_w) / (B_g - B_{gi})$ versus $W_e / (B_g - B_{gi})$ at 70-PV aquifer size for 500 mD, case 24

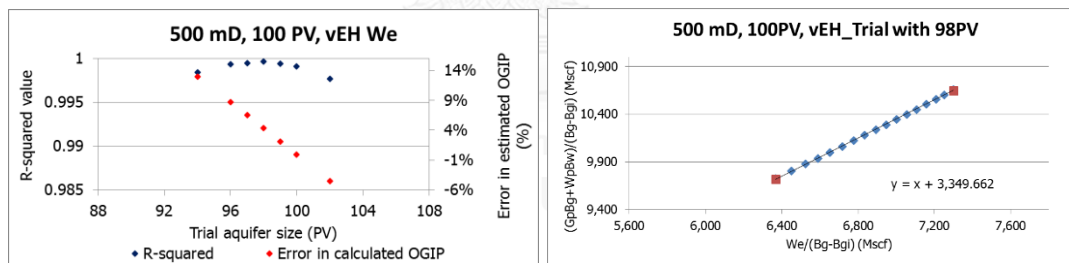


Figure 6.172 Left: R-square value and error in estimated OGIP
 Right: $(G_p B_g + W_p B_w) / (B_g - B_{gi})$ versus $W_e / (B_g - B_{gi})$ at 100-PV aquifer size for 500 mD, case 25

Figure 6.173 shows the values of the estimated aquifer size compared to the actual values. The magnitude of the error increases when the R-squared value in Table 6.22 decreases. The less R-squared value in Table 6.22 indicates that the late time slope of $(G_p B_g + W_p B_w) / (B_g - B_{gi})$ versus $W_e / (B_g - B_{gi})$ plots from the actual aquifer size in Section 6.7 deviates more from one. Thus, the estimated aquifer size needs to be different from the actual one in order to yield the maximum R-squared value.

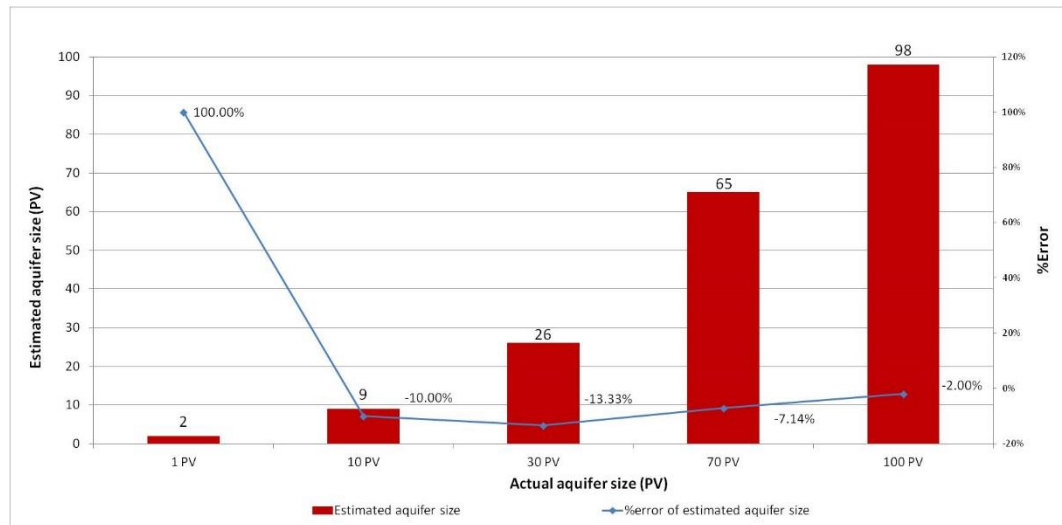


Figure 6.173 Estimated aquifer size and error percentage in 500 mD water-drive dry-gas reservoir by $(G_p B_g + W_p B_w)/(B_g - B_{gi})$ versus $W_e/(B_g - B_{gi})$ plot and van Everdingen & Hurst water influx model with unknown aquifer size

Figure 6.174 and Table 6.46 represent the result of OGIP estimation in this section. The $(G_p B_g + W_p B_w)/(B_g - B_{gi})$ versus $W_e/(B_g - B_{gi})$ plot with van Everdingen & Hurst water influx model is applicable for OGIP estimation with %error less than 10% in all aquifer sizes for 500 mD water-drive dry-gas reservoir when the actual aquifer size is an unknown because the error in SBHP is small.

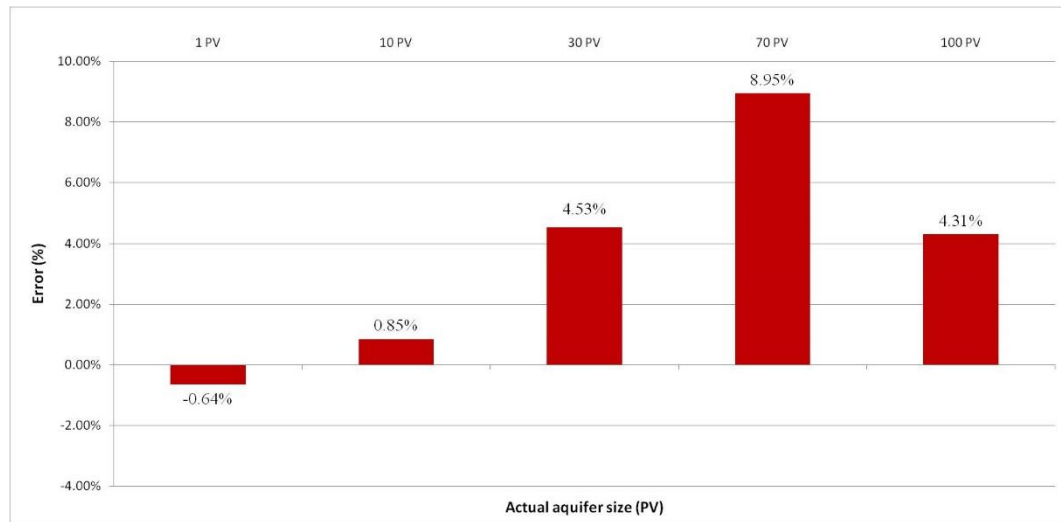


Figure 6.174 Error percentage of estimated OGIP in 500 mD water-drive dry-gas reservoir by $(G_p B_g + W_p B_w) / (B_g - B_{gi})$ versus $W_e / (B_g - B_{gi})$ plot and van Everdingen & Hurst water influx model with unknown aquifer size

Table 6.46 The result of OGIP estimation for 500 mD water-drive dry-gas reservoir by $(G_p B_g + W_p B_w) / (B_g - B_{gi})$ versus $W_e / (B_g - B_{gi})$ plot and van Everdingen & Hurst water influx model with unknown aquifer size

Case	Actual aquifer size (PV)	Estimated aquifer size (PV)	Error (%)	Estimated OGIP (MMscf)	Error (%)	R-squared
21	1	2	100.00%	3,190.86	-0.64%	0.999
22	10	9	-10.00%	3,238.67	0.85%	0.996
23	30	26	-13.33%	3,356.69	4.53%	0.997
24	70	65	-7.14%	3,498.79	8.95%	0.999
25	100	98	-2.00%	3,349.66	4.31%	1.000

Table 6.47 The accuracy of OGIP estimation for 500 mD water-drive dry-gas reservoir by $(G_p B_g + W_p B_w) / (B_g - B_{gi})$ versus $W_e / (B_g - B_{gi})$ plot and van Everdingen & Hurst water influx model with unknown aquifer size

Aquifer size (PV)	Accuracy
1, 10, 30 and 100	Accurate
70	Acceptable

Accurate: error < 5%, Acceptable: error < 10%, Not acceptable: error ≥ 10%



CHAPTER 7

CONCLUSIONS AND RECOMMENDATIONS

7.1 Conclusion

The objectives of this thesis are to evaluate the effect of aquifer size, shut-in duration, permeability, water influx model and amount of historical data on the feasibility and accuracy of OGIP estimation in water-drive dry gas reservoir. The results can be summarized as follows:

(i) Even p/z versus G_p plot is derived from volumetric dry-gas reservoirs but it is also applicable for OGIP estimation in water-drive dry-gas reservoirs with the acceptable %error, less than 10%. If the aquifer sizes are not larger than 10 PV for both 50 mD and 500 mD reservoirs with any shut-in duration between 6 hours to 7 days.

(ii) When $(G_p B_g + W_p B_w) / (B_g - B_{gi})$ versus $W_e / (B_g - B_{gi})$ plot is applied for OGIP estimation for 50 mD water-drive dry-gas reservoirs, the aquifer size, water influx model and shut-in duration have impacts on the accuracy of the estimated OGIP. The aquifer size has the highest impact. If the aquifer size is not larger than 30 PV, %error of the estimated OGIP is always less than 3% with any shut-in duration between 6 hours to 7 days and any of the studied water influx models. For 70-PV and 100-PV aquifer sizes, only Fetkovich, van Everdingen & Hurst and Carter & Tracy water influx models are applicable with shut-in duration 7 days to yield the acceptable estimated OGIP, %error less than 10%. For 500 mD water-drive dry-gas reservoirs, the impact of aquifer size and shut-in duration are less than those in 50 mD cases, van Everdingen & Hurst water influx model can be applied for all studied aquifer sizes and shut-in durations to yield the estimated OGIP which %error less than 1.6%.

(iii) The amount of historical data has big impact on the feasibility and accuracy of OGIP estimation in water-drive dry-gas reservoirs from both p/z versus G_p and $(G_p B_g + W_p B_w) / (B_g - B_{gi})$ versus $W_e / (B_g - B_{gi})$ plots.

(iv) For p/z versus G_p plot, the amount of historical data affects on the accuracy. A larger amount of historical data yields more accurate OGIP for all aquifer sizes and shut-in durations for both 50 mD and 500 mD water-drive dry-gas reservoirs. For 10-PV aquifer size, the amount of historical data up to the abandonment is needed in order to limit the error of OGIP estimation to be less than 10% for all shut-in durations while the amount of historical data up to only 25% RF is enough for 1-PV aquifer size.

(v) For $(G_p B_g + W_p B_w)/(B_g - B_{gi})$ versus $W_e/(B_g - B_{gi})$ plot, the amount of historical data affects accuracy of OGIP estimation. For 1-PV, 10-PV and 30-PV aquifer sizes, the larger aquifer size, the less amount of required historical data for OGIP estimation and the larger amount of historical data, the more accurate of OGIP estimation for all shut-in durations for both 50 mD and 500 mD water-drive dry-gas reservoirs. The amount of historical data up to the abandonment, 50% RF and 25% RF are required for 1-PV, 10-PV and 30-PV aquifer sizes, respectively. For 70-PV and 100-PV aquifer sizes, the amount of historical data up to 50% RF and 25% RF are required for OGIP estimation for 50 mD and 500 mD water-drive dry-gas reservoirs, respectively.

(vi) When the amount of historical data are available up to the abandonment but the aquifer size is unknown, $(G_p B_g + W_p B_w)/(B_g - B_{gi})$ versus $W_e/(B_g - B_{gi})$ plot can be applied with simple aquifer model, Fetkovich, van Everdingen & Hurst and Carter & Tracy water influx model for OGIP estimation in 50 mD water-drive dry-gas reservoirs if the aquifer size is not larger than 30 PV. For 500 mD water-drive dry-gas reservoirs, $(G_p B_g + W_p B_w)/(B_g - B_{gi})$ versus $W_e/(B_g - B_{gi})$ plot can be applied with van Everdingen & Hurst water influx model for OGIP estimation with unknown aquifer size for all studied aquifer sizes.

7.2 Recommendation

It is recommended that further study in multiple-layered gas reservoirs should be conducted since most of the gas wells in the Gulf of Thailand penetrate more than one reservoir per well and the production strategy is usually commingled production.

REFERENCES

1. Elahmady, M. and R.A. Wattenbarger, *A Straight Line p/z Plot is Possible in Waterdrive Gas Reservoirs*. Society of Petroleum Engineers.
2. Van Everdingen, A.F. and W. Hurst, *The Application of the Laplace Transformation to Flow Problems in Reservoirs*.
3. Fetkovich, M.J., *A Simplified Approach to Water Influx Calculations-Finite Aquifer Systems*.
4. Carter, R.D. and G.W. Tracy, *An Improved Method for Calculating Water Influx*. Society of Petroleum Engineers.
5. Klins, M.A., A.J. Bouchard, and C.L. Cable, *A Polynomial Approach to the van Everdingen-Hurst Dimensionless Variables for Water Encroachment*.
6. Abdul-Majeed, G.H. and J.R. Al-Assal, *Graphical Method For Estimating Original Gas In-Place in Water Drive Gas Reservoirs*. Society of Petroleum Engineers.
7. Vega, L. and R.A. Wattenbarger, *New Approach for Simultaneous Determination of the and Aquifer Performance with No Prior Knowledge of Aquifer Properties and Geometry*. Society of Petroleum Engineers.
8. Chen, T.-L., Y.-L. Chen, and Z.-S. Lin, *Determination Of The Original-Gas-In-Place And Aquifer Properties In A Water-Drive Reservoir By Optimization Technique*. Society of Petroleum Engineers.
9. Gajdica, R.J., R.A. Wattenbarger, and R.A. Startzman, *A New Method of Matching Aquifer Performance and Determining Original Gas in Place*.
10. Bhuiyan, M.H., A. Chamorro, and R. Sachdeva, *Determination of OHIP and Aquifer Constant Without Prior Knowledge of Aquifer Models*. Society of Petroleum Engineers.
11. Cole, F.W., *Reservoir Engineering Manual*. 1969, Houston: Gulf Publishing Co.
12. Dake, L.P., *The Practice of Reservoir Engineering*. 1994, Amsterdam: Elsevier.



APPENDICES

จุฬาลงกรณ์มหาวิทยาลัย
CHULALONGKORN UNIVERSITY

APPENDIX A: Reservoir Model Construction by ECLIPSE 100

A-1 Case Definition

Simulator:	Black oil
Model dimensions:	Number of cells in x direction 50
	Number of cells in y direction 30
	Number of cells in z direction 21
Grid type:	Radial
Geometry type:	Block centred
Oil-gas-water option:	Gas and water

A-2 Grid

Active grid block:	1 for box x, y, z – 1:50, 1:30, 1:21
	0 for box x, y, z – 31:50, 1:30, 1:21
	0 for box x, y, z – 1:50, 1:30, 11:21
Permeability:	x permeability 50 mD
	y permeability 50 mD
	z permeability 5 mD
Porosity:	0.2
x grid block size:	30 ft for box x, y, z – 1:50, 1:30, 1:21
y grid block size:	12 deg for box x, y, z – 1:50, 1:30, 1:21
z grid block size:	5 ft for box x, y, z – 1:50, 1:30, 1:21

Depths of top faces: 6000 ft for box x, y, z – 1:50, 1:30, 1:1

A-3 PVT

Fluid densities at surface conditions: Oil density 49.99914 lb/ft³

Water density 62.42797 lb/ft³

Gas density 0.04369958 lb/ft³

Water properties:

Reference pressure (Pref) 3500 psia

Water FVF at Pref 1.020998 rb/stb

Water compressibility $3.06298 \times 10^{-6} \text{ psi}^{-1}$

Water viscosity at Pref 0.3018746 cp

Water viscosibility $3.928482 \times 10^{-6} \text{ psi}^{-1}$

Rock properties:

Reference pressure 3500 psia

Rock compressibility $1.529896 \times 10^{-6} \text{ psi}^{-1}$

Dry-gas PVT properties (no vapourised oil)

Pressure (psia)	FVF (rb/Mscf)	Viscosity (cp)
600.00	5.24135	0.01382
768.42	4.03452	0.01407
936.84	3.26483	0.01436
1105.26	2.73275	0.01468
1273.68	2.34431	0.01503
1442.11	2.04941	0.01542
1610.53	1.81892	0.01584
1778.95	1.63469	0.01628
1947.37	1.48484	0.01676
2115.79	1.36123	0.01726
2284.21	1.25807	0.01778
2452.63	1.17115	0.01833
2621.05	1.09727	0.01889
2789.47	1.03401	0.01946
2957.89	0.97947	0.02004
3114.16	0.93533	0.02059
3294.74	0.89080	0.02122
3500.00	0.84715	0.02194
3631.58	0.82243	0.02240
3800.00	0.79396	0.02298

A-4 SCAL

Gas saturation functions

S_g	k_{rg}	P_c (psia)
0.000	0.0000	0
0.200	0.0000	0
0.244	0.0011	0
0.289	0.0088	0
0.333	0.0296	0
0.378	0.0702	0
0.422	0.1372	0
0.467	0.2370	0
0.511	0.3764	0
0.556	0.5619	0
0.600	0.8000	0

Water saturation functions

S_w	k_{rw}	P_c (psia)
0.400	0.0000	0
0.444	0.0001	0
0.489	0.0010	0
0.533	0.0049	0
0.578	0.0156	0
0.622	0.0381	0
0.667	0.0790	0
0.711	0.1464	0
0.756	0.2497	0
0.800	0.4000	0
1.000	1.0000	0

A-5 Initialization

Initial pressure: 3500 psia for box x, y, z - 1:50, 1:30, 1:21

Initial water saturation: 0.4 for box x, y, z - 1:50, 1:30, 1:21

Aquifer: Fetkovich aquifer

Datum depth: 6000 ft

Initial pressure: 3500 psia

Total compressibility: $4.592876 \times 10^{-6} \text{ psi}^{-1}$

Initial volume: 4532297 stb for 1 PV

45322966 stb for 10 PV

	135968897 stb for 30 PV
	317260759 stb for 70 PV
	453229655 stb for 100 PV
Productivity index:	169.18086 stb/day.psi for 1 PV
	130.60235 stb/day.psi for 10 PV
	60.63496 stb/day.psi for 30 PV
	42.446914 stb/day.psi for 70 PV
	37.644526 stb/day.psi for 100 PV
Aquifer connection data:	Lower i = 30, Upper i = 30
	Lower j = 1, Upper j = 30
	Lower k = 1, Upper k = 10
	Connection face i+

A-6 Schedule

Well specification

Well:	P1
i location:	1
j location:	1
Preferred phase:	Gas
Inflow equation:	STD
Automatic shut-in instruction:	SHUT
Crossflow:	Yes
Density calculation:	SEG

Well connection data

Well:	P1
k Upper:	1
k Lower:	10
Open/shut flag:	OPEN
Well bore ID:	0.358 ft
Skin factor:	0
Direction:	Z

Production well control

Well:	P1
Open/shut flag:	OPEN
Control:	GRAT
Gas rate:	2000 Mscf/day
THP target:	400 psia
VFP pressure table:	1 (Detail in Appendix B)

Production vertical flow performance

VFP table number:	1 (Detail in Appendix B)
Datum depth:	6000 ft
Flow rate definition:	GAS
Water fraction definition:	WGR
Gas fraction definition:	OGR
Fixed pressure definition:	THP
Table units:	FIELD
Tabulated quantity definition:	BHP

APPENDIX B: PROSPER Input Data for Reservoir Model

B-1 System summary

Fluid:	Dry and wet gas
Method:	Black oil
Separator:	Single-stage separator
Hydrates:	Disable warning
Water viscosity:	Use default correlation
Water vapour:	No calculations
Flow type:	Tubing flow
Well type:	Producer
Predict:	Pressure and temperature (offshore)
Model:	Rough approximation
Range:	Full system
Output:	Show calculating data
Well completion type:	Cased hole
Gravel pack:	no
Inflow type:	Single branch

B-2 PVT input data

Gas gravity:	0.7
Separator pressure:	400 psig

Condensate to gas ratio:	0 stb/MMscf
Condensate gravity:	45 API
Water to gas ratio:	100 stb/MMscf
Water salinity:	100000 ppm
Mole percent H ₂ S:	0%
Mole percent CO ₂ :	0%
Mole percent N ₂ :	0%
Correlation of gas viscosity:	Lee et al.

B-3 Deviation survey

Measured depth:	0, 6000 ft
True vertical depth:	0, 6000 ft
Angle:	0, 0 degree

B-4 Downhole equipment

Type	Measured depth (ft)	Tubing ID (inches)	Tubing roughness (inches)
Xmas Tree	0		
Tubing	6000	2.441	0.0006

B-5 Geothermal gradient

Formation measured depth (ft)	Formation temperature (deg F)
0	80
6000	200

Overall heat transfer coefficient: 8 BTU/h/ft²/°F

B-6 Average heat capacities

Cp oil: 0.53 BTU/lb/°F

Cp gas: 0.51 BTU/lb/°F

Cp water: 1 BTU/lb/°F

B-7 VLP calculation

Top node pressure: 200 psig

Water gas ratio: 100 stb/MMscf

Condensate gas ratio: 0 stb/MMscf

Surface equipment correlation: Beggs and Brill

Vertical lift correlation: Gray

Fist node: Xmas tree 0 ft

Last node: Tubing 6000 ft

Tubing head pressure (psia)	Water gas ratio (stb/MMscf)
399.7	0
745.8	111.11
1091.9	222.22
1438	333.33
1784.1	444.44
2130.3	555.56
2476.4	666.67
2822.5	777.78
3168.6	888.89
3514.7	1000



VITA

Miss Chonlada Jungjaroensin was born on July 16th, 1985 in Bangkok, Thailand. She received her Bachelor degree in Chemical Engineering from Faculty of Engineering, Chulalongkorn University in 2009. She has worked as a petroleum engineer at Chevron since graduation. She started her study in the Master degree in Petroleum Engineering at the Department of Mining and Petroleum Engineering, Faculty of Engineering, Chulalongkorn University since the academic year 2011.

